Novel Findings about the Role of Glial Cells in Retinal Function, Disease, and Therapy

Dissertation

zur Erlangung des Grades eines
Doktors der Naturwissenschaften

der Mathematisch-Naturwissenschaftlichen Fakultät
und
der Medizinischen Fakultät
der Eberhard-Karls-Universität Tübingen

vorgelegt
von

Kirsten Anika Wunderlich
aus Bremen, Deutschland

Januar - 2014

Tag der mündlichen Prüfung:	28.10.2014
Dekan der Math.-Nat. Fakultät:	Prof. Dr. W. Rosenstiel
Dekan der Medizinischen Fakultät:	Prof. Dr. I. B. Autenrieth
1. Berichterstatter:	Prof. Dr. E. Zrenner
2. Berichterstatter:	Prof. Dr. B. Wissinger
Prüfungskommission:	Prof. Dr. E. Zrenner
	Prof. Dr. B. Wissinger
	PD Dr. E. Küppers
	Dr. M. Kukley

I hereby declare that I have produced the work entitled: Novel Findings about the Role of Glial Cells in Retinal Function, Disease, and Therapy",submitted for the award of a doctorate, on my own (without external help), have used only the sources and aids indicated and have marked passages included from other works, whether verbatim or in content, as such. I swear upon oath that these statements are true and that I have not concealed anything. I am aware that making a false declaration under oath is punishable by a term of imprisonment of up to three years or by a fine.

Tübingen, _____ _____

Date Signature

In Gedenken an Josef,

einen meiner besten Freunde

Annotations

The present thesis is written in a cumulative manner. It includes the following four manuscripts:

Chapter 4.1: Wunderlich et al.: “Retinal functional alterations in mice lacking the intermediate filament proteins glial fibrillary acidic protein (GFAP) and vimentin” (manuscript);

Chapter 4.2: Wunderlich et al.: “The inability to produce glial fibrillary acidic protein (GFAP) and vimentin does not protect photoreceptors in a genetic model of degeneration” (manuscript);

Chapter 4.3: Wunderlich et al., 2010: “Altered expression of metallothionein-I and -II and their receptor megalin in inherited photoreceptor degeneration”;

Chapter 4.4: Sancho-Pelluz et al., 2008: “Sialoadhesin expression in intact degenerating retinas and following transplantation”.

Chapters 4.3 and 4.4 have already been published in the ARVO journal Investigative Ophthalmology & Visual Science. Chapters 4.1 and 4.2 are included as manuscripts. The results of the four studies are summarized in chapter 4 before each manuscript.

Major parts of the experimental work were performed at the University of Lund, in the Institute of Clinical Sciences, Division of Ophthalmology, in Lund, Sweden, under the supervision of Dr. Maria Thereza Perez. The ERG experiments were carried out in collaboration with project partners at the Center for Ophthalmology, Institute for Ophthalmic Research of the University of Tübingen, Germany, within the EARN-RET agreement between the Medical Faculty of the University of Tübingen and the Medical Faculty at the University of Lund. The microarray analysis was carried out by partners at the Institute de la Vision in Paris, France, within the EU EVI-GenoRet program.

Contents

1. Introduction

Our senses determine how we perceive the world, and accordingly, how we can act and live in it. For us humans, sight is the dominant sense, and the ability to see has a great impact on the quality of life. Blindness is a substantial obstacle to leading an economically and socially independent life. Inherited degenerations of the retina are an important cause of blindness. So far, there is no known cure, and most of the diverse underlying disease mechanisms are not well understood yet. Many studies suggest a role for secondary reactive changes mediated by the retinal glial cells (macroglia and microglia) in the progression of retinal cell dysfunction and loss. With this thesis, I want to provide new insights into the role of glial cells during retinal function, disease and therapy. Specifically, I focused:

i. on the glial intermediate filament proteins glial fibrillary acidic protein (**GFAP**) and **vimentin** and their potential impact on retinal function (chapter 4.1) and on the progression of retinal degeneration (chapter 4.2);

ii. on the putative neuroprotective proteins **metallothionein-I and -II,** which are expressed by activated retinal glial cells (chapter 4.3);

iii. and on the cell adhesion protein **sialoadhesin**, which is expressed by a subset of retinal microglia after intraocular transplantation of neonatal retinal cells in wild-type mice and in a mouse model for retinal degeneration (chapter 4.4).

In the following chapters, I will first give an introduction to the human sensory system, particularly the eye with the retina and common forms of neurodegeneration with the emphasis on retinal degenerations, before I present the methodologies with which I have approached my projects. Since the model animals of choice were rats and mice, I will point out major differences between man and rodent, where appropriate. The outcome of my studies is described in the four papers/manuscripts that are included in this thesis (chapter 4).

1.1 Sensory systems

Parts of the nervous system are specialized to detect physical or chemical input from the environment. These sensory systems consist of receptors that transform a stimulus into a neuronal signal (stimulus transduction) and neuronal pathways that conduct the information to the perceptive region of the brain. Further processing may lead to conscious awareness (sensation).

Sensory receptors are either specialized endings of neurons that initiate action potentials upon stimulation (e.g. the chemosensory receptors of the olfactory receptor neurons), or separate cells that synapse with afferent neurons (e.g., the hair cells of the inner ear and the photoreceptor cells in the retina). Each receptor is specific to a certain type and intensity range of stimulus but might react in its typical manner even by nonspecific stimuli with high intensity; we see stars after strong pressure on the eye for example. The magnitude of a stimulus is represented by a graded receptor potential that results in different action potential frequencies, depending on stimulus strength, summation of several receptor responses, and receptor sensitivity. Adaptation to a constant stimulus might decrease the receptor sensitivity (Smith, 2008).

The five classical senses in humans were already mentioned by Aristotle: smell, taste, touch, hearing and vision. In the following, the latter will be explained in more detail.

1.2 General anatomy of the eye

The eye functions as an optical system, collecting light from the surrounding and focusing it onto the light-sensitive retina in the back of the eyeball. A pigmented circular muscle, the iris, controls the diameter of its central aperture called pupil, and thereby the amount of incident light. The iris and the anterior chamber in front of it are covered by the transparent cornea. In terrestrial animals, the curved cornea is the strongest refractive element. To ensure transparency, the cornea is avascular. Instead it is provided with oxygen through the tear film on the outside. At the inner surface, the cornea is nourished by diffusion from the aqueous humor in the anterior chamber, the main purpose of which is to keep a steady pressure for a rounded surface. The cornea borders on a tough fibrous continuation of the *dura mater*, namely the sclera, which supports the shape of the eyeball and prevents light passage from the side. In the posterior chamber, behind the iris, lies the biconvex crystalline lens (Wormstone and Wride, 2011). The lens has only about half the refractive power of the cornea. But, as opposed to the fixed curvature of the cornea, the shape of the human lens can be changed by the action of the ciliary muscles in order to focus the incoming light from various distances to the photoreceptors in the retina (accommodation). The lenses of rodents become proportionally much bigger than human lenses and are less flexible. UV-light can pass through the lenses of mice and rats (Henriksson et al., 2010), while human lenses filter all wavelengths except light of the visible range (Bova et al., 1999; reviewed in Gouras and Ekesten, 2004). This may have to be considered when extrapolating functional studies on mice to humans. The space between the lens and the back of the eye is filled with vitreous

humor that holds the actual light-sensitive tissue in place: the retina (http://webvision.med.utah.edu/). See figure 1 for a schematic overview of the eye:

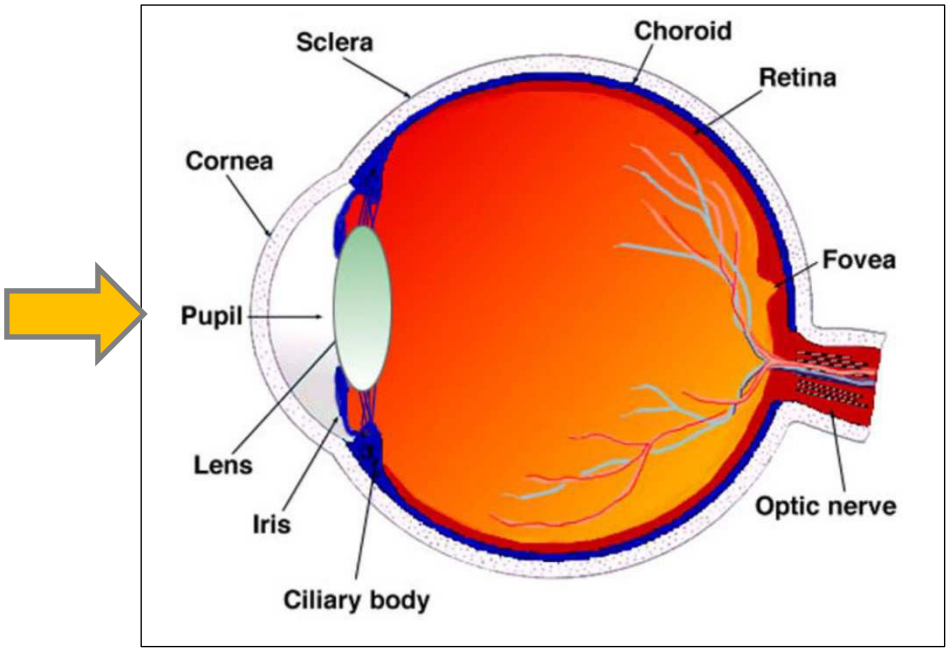

Figure 1: A schematic section through a human eye. (Reproduced from www.webvision.med.utah.edu). Light would hit the eye at the cornea from the left side (yellow arrow), pass through the pupil and the lens and eventually reach the retina in the back of the eye.

1.3 The retina

The thin neural retina is part of the brain, having derived from invaginations of the anterior neuroectoderm during embryogenesis. It is specialized to convert light into electrical signals that are transmitted via the optic nerve to the brain. The vertebrate retina is distinctly structured into three cellular (nuclear) layers that are separated by synaptic (plexiform) layers. The light-sensitive photoreceptor cells are situated in the outermost layer of the retina; hence incoming light has to pass the inner layers first:

the inner limiting membrane (ILM) that separates the vitreous body from the retina

the nerve fiber layer (NFL)

the ganglion cell layer (GCL)

the inner nuclear layer (INL)

the outer plexiform layer (OPL)

and the outer nuclear layer (ONL)

Apically, the photoreceptors interconnect with the retinal pigment epithelium (RPE), a single cell layer just behind the neural retina (Kolb et al., 2001; http://webvision.med.utah.edu/).

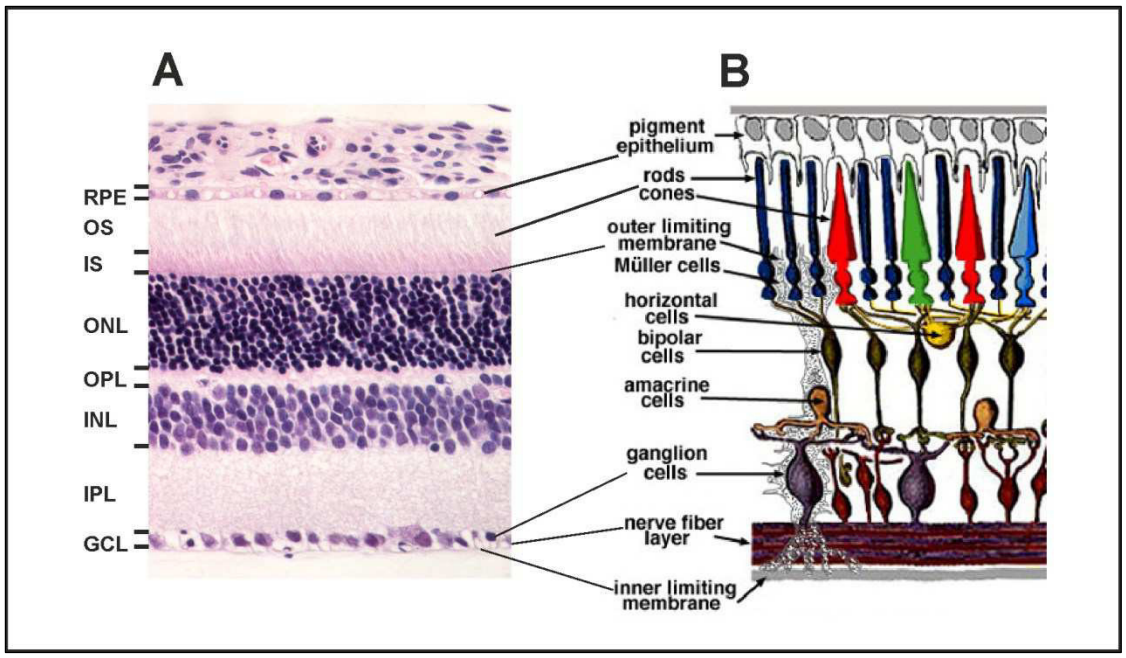

Figure 2: (A) Light micrograph of a rat retinal section stained with hematoxilin and eosin. (B) Schematic section through a human retina.

The inner limiting membrane that separates the vitreous body from the retina is made by astrocytes and Müller cell endfeet. Astrocyte cell bodies and processes are mainly located in the nerve fiber layer. Moreover, the nerve fiber layer consists of axons from retinal ganglion cells that converge at the optic disc into the optic nerve. The cell bodies of the ganglion cells are located in the ganglion cell layer (GCL) together with cell bodies of displaced amacrine cells. In the inner plexiform layer (IPL), ganglion cells get input from bipolar cells. Additionally, horizontal interactions with amacrine cells take place. Bipolar cells and most amacrine cells have their cell bodies in the inner nuclear layer (INL), as well as horizontal cells and interplexiform cells. Also Müller glial cells that vertically span the whole retina have their cell bodies in the INL (note the Müller cell in the scheme; it is drawn in gray on the left side. Photoreceptors, the vertically oriented bipolar cells, and horizontal cells synapse in the outer plexiform layer (OPL). The photoreceptors have their cell bodies with the nucleus in the outer nuclear layer (ONL). Most of the cell organelles are located in the inner segments beyond the outer limiting membrane (OLM), which is formed by connections between apical Müller cell processes and the photoreceptor cells. The thin connecting cilium (CC) connects the inner segment (IS) with the outer segment (OS) of the photoreceptor. Apically, the outer segments interconnect with the retinal pigment epithelium (RPE), a single cell layer just behind the neural retina. (Scheme reproduced from http://webvision.med.utah.edu/)

1.4 Retinal neurons

Photoreceptor cells are specialized to convert light into neuronal signals. Signal integration begins already in the post-photoreceptor neurons in the retina, when these signals are transmitted via **bipolar cells** to the output neurons of the retina, the **ganglion cells**. A certain degree of preliminary processing takes place through modulation by **horizontal**, **amacrine**, and **interplexiform cells**. Final processing takes place in the visual cortex, in the posterior pole of the occipital lobe (Kolb et al., 2001; Smith, 2008).

1.4.1 Photoreceptors

Photoreceptors are highly polarized neurons. Their axons synapse with the next order neurons in the outer plexiform layer. Photoreceptor somata are located in the outer nuclear layer. The apical end of a photoreceptor beyond the outer limiting membrane, which is formed by connections between apical Müller cell processes and the photoreceptor cells, consists of an inner and an outer segment. A thin connecting cilium connects the inner segment with the outer segment of the photoreceptor. Most of the cell organelles are located in the inner segment, most importantly the Golgi apparatus and large numbers of mitochondria that are important for the metabolically highly active photoreceptor cell. Phototransduction, on the other hand, takes place in the outer segment. The outer segment is filled with stacks of invaginated membranes, which carry the photo-active pigment molecules and other transduction components.

Two types of photoreceptors exist in the vertebrate retina: rods and cones. In humans, most of the cones are concentrated in the rod-free central fovea within the *macula lutea*, whereas the periphery is particularly rich in rods. In mice, the cones, which comprise approximately 1% of the photoreceptors, are distributed evenly (Jeon et al., 1998). Rods have thin and long segments, and their membrane disc stacks are detached from the outer membrane. They contain the visual pigment rhodopsin and are very sensitive and reactive under dim light conditions. Rhodopsin is therefore used as a marker protein for rod photoreceptor cells (Hicks and Barnstable, 1987: Hicks and Molday, 1986; chapter 4.1 and 4.2 of this thesis). The shorter, conically shaped cones respond only to brighter stimuli but are faster to react and recover. Cones are responsible for visual acuity. The membrane discs of cones stay connected to the outer membrane. They contain different cone opsins that respond to distinct wavelengths thereby enabling color vision. Humans are typically trichromatic, which means that they have three different kinds of cones: S-cones (**S**hort wavelength) have a response maximum in the blue light, M-cones (**M**edium wavelength) in the green, and L-cones (**L**ong wavelength) in the red range. Mice and rats are dichromatic. They have cones that are

sensitive for middle-wavelength light and cones that respond to UV light (Jacobs et al., 1991).

1.4.2 Bipolar cells

Bipolar cells transmit the signals from rod and cone photoreceptors to the ganglion cells. One rod-driven and 11 cone-driven bipolar cell types have been discovered so far that can be divided into two groups: ON-bipolar cells and OFF-bipolar cells. ON-bipolar cells depolarize upon a light stimulus, while OFF-bipolar cells hyperpolarize under the same conditions, but depolarize recognizing dark areas on a light background. Both, ON- and OFF-bipolar cells can express rapidly or slowly inactivating glutamate receptors, so additional distinctions between sustained and transient bipolar cells can be made. Further differentiation can be made according to their diverse connectivity to photoreceptors and postsynaptic targets. Cone bipolar cells synapse directly with ganglion cells, whereas rod bipolar cells transmit their signals first to amacrine cells that connect to cone bipolar cells or form a feedback-loop back to the rods. An antibody against the protein kinase C (PKC), which has been shown to be expressed by rod bipolar cells, was employed to identify the latter in chapter 4.1 (Ruether et al., 2010; Wässle and Boycott, 1991). Stainings with an antibody against recoverin were performed to mark a subset of cone bipolar cells (and photoreceptors)(Dizhoor et al., 1991; Milam et al., 1993). Most bipolar cells contact several cones, being described as diffuse bipolar cells, but in the primate macula, the special midget bipolar cells receive input from only one cone, each contributing to the high visual resolution of this area. (reviewed in: Kolb et al., 2001; Masland, 2012: http://webvision.med.utah.edu/).

1.4.3 Ganglion cells

The final output neurons of the retina are the ganglion cells. Their axons converge to form the optic nerve that transmits the signals from the intermediate neurons via action potentials to the brain. Numerous distinct ganglion cell types have been discovered that differ from each other e.g., by molecular and electrophysiological properties or morphology like dendritic arborization. Some ganglion cells have very wide receptive fields, while others, like the midget ganglion cell, might receive signals from as little as one single midget bipolar cell allowing a high resolution one-to-one signal transmission. Again, ON-center and OFF-center cells constitute two basic types of ganglion cells, being excited by brighter (ON) or darker (OFF) stimuli than the mean background. Ganglion cells integrate the opposing signals of center and surrounding allowing the perception of forms, color, contrast, and directional movement (Kolb et al., 2001; Masland, 2012; http://webvision.med.utah.edu/; Jacobs et al., 2004; Lyubarsky et al., 1999). A subpopulation of ganglion cells is also photosensitive. They

contain the pigment melanopsin and are involved in the pupillary light reflex and daily adjustment of the circadian rhythm but do not participate in image formation (Hattar et al., 2002; Provencio et al., 2000).

1.4.4 Horizontal cells

A lot of signal processing takes place in the different layers of the retina. The first lateral processing of the visual signals is carried out by horizontal cells. The cell bodies of horizontal cells are situated in the inner nuclear layer, next to the outer plexiform layer, where they interconnect the photoreceptor terminals in both, a feedback and a feed-forward manner. Two types of horizontal cells exist, though a third type is discussed for some species. One type is connecting both, rods via the axons and cones via the dendrites, whereas the second type synapses with cones only. Horizontal cells receive input from many photoreceptors, covering a large receptive field. The receptive field becomes even larger through gap junction connections between different horizontal cells. One of the main functions of this modulation is to shape adaptational responses to light intensity changes (Kolb et al., 2001; Masland, 2012; http://webvision.med.utah.edu/).

1.4.5 Amacrine cells

The third type of interneurons in the INL are amacrine cells that have their cell bodies at the inner border of the INL or in the ganglion cell layer (displaced amacrine cells). Approximately 30 different amacrine cell types can be distinguished, mainly by their size and stratification pattern, and so far, many of their functions are not understood yet (Masland, 2012). The different amacrine cells are often divided into three major groups: the wide-field, medium-field, and narrow-field amacrine cells. The probably best known type, the narrow-field AII amacrine cell, transmits the signals of many rod bipolar cells to cone bipolar cells, which then pass it on to the ganglion cells. This classical rod pathway increases the light sensitivity to a degree that enables the detection of the absorption of a single photon (Wässle, 2004). AII cells express the calcium-binding proteins parvalbumin and calbindin, which were therefore used as marker proteins in chapter 4.1 and 4.2 (Haverkamp and Wässle, 2000; Wässle et al., 1995). The wide-field A17 cell collects even input from thousands of rod-driven bipolar cells and forms feedback loops back to the rod bipolar terminals. Amacrine cells mostly release inhibitory neurotransmitters such as GABA (e.g. A17) and glycine (e.g. AII) but also other neuroactive substances, which may diffuse longer distances across the retina (Masland, 2012). Most amacrine cells are axonless, lack obvious polarity, and often interconnect via gap junctions. It is suggested that the strength of the electrical coupling is dependent on the level of background light (Hartveit and Veruki, 2012). Amacrine cells seem

to be involved in center-surround interactions, reciprocal inhibitions between the ON- and OFF-pathways, periphery effects and direction-selective light responses (Wässle, 2004).

1.4.6 Interplexiform cells

Most vertebrate retinas have a fourth type of interneuron: the interplexiform cell. Interplexiform cells link the two plexiform layers; they receive input from amacrine cells in the inner plexiform layer and have synaptic output upon the neurons of the outer plexiform layer. So far, not much is known about their exact function (Kolb et al., 2001; http://webvision.med.utah.edu/).

1.5 Phototransduction

The visual pigment, integrated in the membranes of the photoreceptor outer segments, is composed of the transmembrane protein opsin and retinal, a derivative of vitamin A. When a photon hits the chromophore, it converts from the isoform 11-cis-retinal to an all-trans form inducing conformational changes in the opsin (bleaching). The activated opsin promotes the dissociation of the GTP-binding alpha-subunit of transducin, which in turn activates the cGMP-phosphodiesterase that catalyzes the conversion of cGMP to 5´-GMP. Thus, dark-adapted photoreceptors have very high levels of cGMP that keep membrane-bound cGMP-gated cation channels open. This leads to an influx of mainly Na^+, but also Ca^{2+}. Accordingly, photoreceptors are constantly depolarized in the dark and release the neurotransmitter glutamate. Since one single photon can stimulate several hundreds of cGMP-phosphodiesterases with this cascade, cGMP levels decrease significantly upon light stimulation, and the cation channels close, causing hyperpolarization of the photoreceptor cells, and diminishing levels of released glutamate (http://webvision.med.utah.edu/).

Mutations in components of the phototransduction chain often lead to retinal degenerations. A deletion in the beta-subunit of the cGMP-phosphodiesterase, for example, is causative for the photoreceptor degeneration retinitis pigmentosa in patients (McLaughlin et al., 1995) and mice (Bowes et al., 1990; Chang et al., 2002). The retinal degeneration (*rd*) 1 mouse, carrying a nonsense-mutation in the relevant gene, is therefore often used as a model organism to study causes, consequences and possible therapies for this devastating group of diseases. Likewise, in chapter 4.2, 4.3, and 4.4 included in this thesis, *rd1* mice were employed as one model of choice.

The regeneration of the visual pigment after photoexcitation occurs partly in the photoreceptor cells but involves the adjacent tissue as well: the all-trans-retinal separates from the opsin protein and is reduced to all-trans-retinol within the outer segment before

being released from the cell. With the help of the carrier molecule interphotoreceptor retinoid-binding protein (IRBP), all-trans-retinol is transferred through the extracellular compartment to the retinal pigment epithelium, where the 11-cis-retinal isoform is restored involving different proteins, including e.g. the cellular retinal-binding protein (CRALBP), which was used as a marker for retinal pigment epithelium and Müller glia cells in chapter 4.1 and 4.3 in this thesis. Blood-derived all-trans-retinol can also be fed into the visual cycle. The recycled 11-cis-retinal moves back to the photoreceptor, again chaperoned by IRBP, and is re-conjugated to opsin to newly form a light sensitive visual pigment. Rod photoreceptors rely completely on this retinal pigment epithelium-dependent rod visual cycle, whereas cone photoreceptors can additionally use 11-cis-retinol provided from Müller cells, which is, however, still much less characterized (Saari, 2012).

1.6 Non-neuronal cells

1.6.1 Retinal pigment epithelium

The retinal pigment epithelium is a single cell layer of flattened, hexagonal, melanin-pigmented epithelium between the neural retina and the choroid. The melanin granules in the retinal pigment epithelium absorb abundant photons preventing blurred images by reflecting light strays. With tight junctions between its cells, the epithelium is part of the blood-retina-barrier, controlling the entry of nutrients, e.g., glucose and retinol, from the choroidal vasculature behind it. In the reverse direction, the epithelium transports water, ions and metabolic end products from the subretinal space to the blood (reviewed in (Strauss, 2005)). Furthermore, the retinal pigment epithelium interacts structurally and functionally with photoreceptors and is important for the maintenance of visual function (see above). With their apical processes, one retinal pigment epithelial cell envelopes the photoreceptor outer segments of approximately 20 to 30 photoreceptor cells in the human retina (Gao and Hollyfield, 1992). New membrane discs are constantly added at the base of the photoreceptor outer segments, pushing the older discs towards the distal end where they are shed from the tip. The retinal pigment epithelial cells phagocytose those photoreceptor outer segment discs and digest them by lysis. Shedding of rod discs mostly happens at light onset, whereas cone outer segment pieces are mainly shed at light offset (Strauss, 2005). A mutation in the *Mertk* gene that leads to the failure of disc uptake and consequently of phagocytosis is the basis for retinal degeneration in a group of patients (Gal et al., 2000) and in the RCS (Royal College of Surgeons) rat (D'Cruz et al., 2000), one of the examined animal models in chapter 4.3 of this thesis. Many growth factors that are important during development and maintenance of the retina and the choroidal vasculature are secreted by

the retinal pigment epithelium (Strauss, 2005). It expresses the metal-binding proteins metallothionein-I and -II (Oliver et al., 1992; chapter 4.3). Last but not least, the retinal pigment epithelium contributes to the immune defense of the retina by innate and adaptive immunity mechanisms, expressing Toll-like receptors, complement components, major histocompatibility complex (MHC) class I and II molecules, and a variety of cytokines, just as macrophages and dendritic retinal pigment epithelial do (Detrick and Hooks, 2010). During the cause of several diseases, activated cells may also proliferate and migrate (Li et al., 2007; reviewed in (Schraermeyer and Heimann, 1999).

1.6.2 Retinal glia

Approximately ten times more glial cells than neurons exist in the central nervous system. Glial cells support neurons structurally and metabolically, but also interact actively with neurons and vasculature, the retinal pigment epithelium, and each other. There are three different types of glia in the vascularized retina: microglia, radial Müller cells, and astrocytes (reviewed in Bringmann et al., 2006; Newman, 2009).

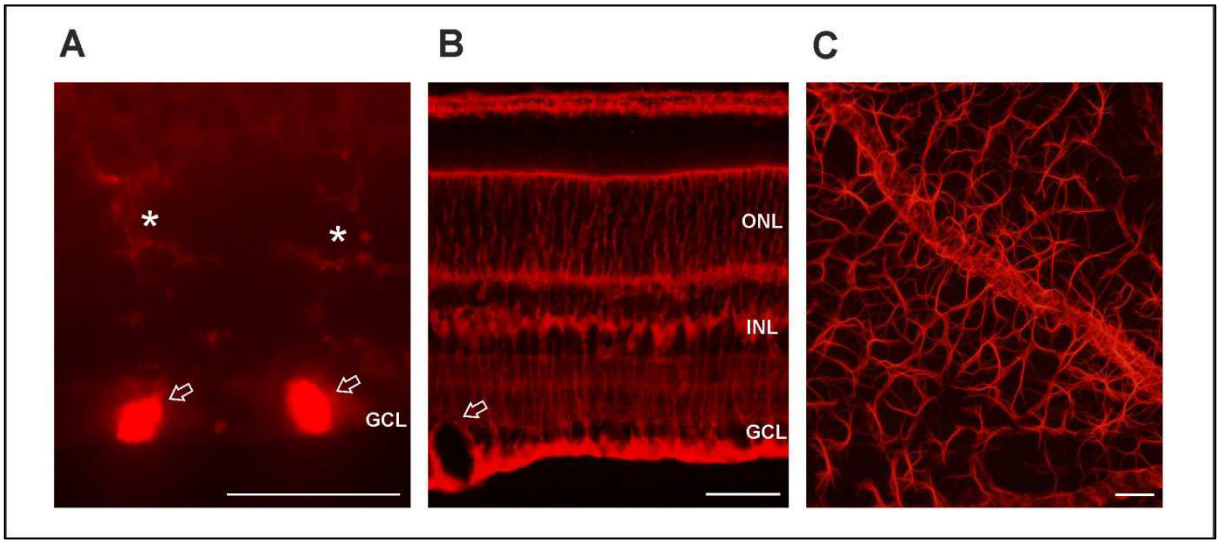

Figure 3: Retinal glia cells. (A) Two ramified **microglia** cells (asterisks) in the inner plexiform layer of a PN42 RCS (Royal College of Surgeons) rat stained with isolectin B4 (IB4), which also labels vessels (arrowhead). **(B)** Section of a PN28 mouse retina stained for the **Müller cell** marker cellular retinal-binding protein (CRALBP). Müller cell somata are located in the middle of the inner nuclear layer (INL). Müller cell processes span from the inner limiting membrane at the inner surface of the retina to the outer limiting membrane, which is located apically of the outer nuclear layer (ONL). Note how the Müller cell end feet coat a vessel (arrowhead) in the ganglion cell layer (GCL). **(C) Astrocytes** in the nerve fiber layer of a flat-mounted PN35 mouse retina stained with a fluorophore-conjugated antibody

against the glial fibrillary acidic protein (GFAP). Astrocytes grow in close association with vessels. Scalebar: 50 µm.

1.6.3 Microglia

An important part in the local host defense is carried out by retinal microglia. Microglia are of hematopoietic origin and invade the retina during development. In the healthy rodent retina, the ramified microglia reside in the inner retinal layers, mainly in the inner plexiform layer. Human retinal microglia are distributed in all retinal layers (reviewed in (Chen et al., 2002). Resting microglia are structurally very dynamic, constantly monitoring the surrounding area with their long, highly mobile protrusions (reviewed in Karlstetter et al., 2010; Langmann, 2007). Invading microorganisms, injury, and degeneration rapidly activate microglial cells. They change to a more amoeboid shape with only few branched processes, divide and migrate to the place of insult, where they phagocytose debris and release a range of cytokines and chemokines, initiating both inflammatory processes and tissue repair (reviewed in Chen et al., 2002; Karlstetter et al., 2010). Neurons that die by apoptosis during normal retinal development are also phagocytosed by microglia (Newman 2009). The expression of metallothionein-I and -II (see chapter 1.11.2) in retinal microglia was examined in chapter 4.3. In chapter 4.4, the expression pattern of sialoadhesin (see chapter 1.11.3) was assessed in healthy and degenerating retinas as well as after intraocular transplantation of neonatal retinal cells. Several surface proteins are commonly used as marker proteins for microglia, as for instances CD11b (in chapter 4.3 and 4.4), the isolectin IB4 (chapter 4.3), and tomato lectin (chapter 4.3) (reviewed in (Langmann, 2007)).

1.6.4 Radial glia: Müller cells

The principal macroglial cells of the retina are the Müller cells, discovered and first described by the anatomist Heinrich Müller in 1851 (Müller, 1851). Their cell bodies are located in the middle region of the inner nuclear layer, and their distal and proximal processes span almost the entire thickness of the retina, thereby providing structural support and limiting the width of the retina. The apical villi restrict the retina at the outer limiting membrane, and the so-called endfeet, enlarged structures at the vitreous side, form the inner limiting membrane together with astrocytes (Newman, 2009). The geometry of Müller cells, with conical endfeet and elongated cell shape, oriented in the direction of the passing light, facilitates image transfer through the retina with minimal loss and distortion. Thereby, Müller cells act as optical fibers (Franze et al., 2007). Like astrocyte endfeet, Müller cell endfeet coat the retinal vessels in the nerve fiber layer and, additionally, also within the retina, mediating neurovascular coupling, a signaling process to adjust the blood flow to the activity-dependent oxygen needs of the

retina (Newman, 2009). Furthermore, glial endfeet support the blood-retina barrier that isolates the retina and restricts uncontrolled passage of water and solutes (reviewed in (Bringmann et al., 2006)). Fine secondary processes of the Müller cells contact every retinal cell and fill out all space that is left by neurons and vessels. This allows for the close interactions between Müller cells and neurons.

Müller cells most probably participate in the recycling of photopigments from the photoreceptors (reviewed in Wang and Kefalov, 2009; Wang and Kefalov, 2011)). They metabolize glucose and provide the resulting lactate/pyruvate to the photoreceptors (Bringmann et al., 2006; Poitry et al., 2000; Poitry-Yamate et al., 1995). Rapid uptake of glutamate through high affinity **gl**utamate-**as**partate **t**ransporters (**GLAST**) ensures a low glutamate concentration in the extracellular space. Thus, neuronal signals are terminated quickly, and any glutamate excitotoxicity is prevented. Other neurotransmitters, like GABA and glycine, are also removed by Müller cells. Glutamate is processed in several different ways. The glutamine synthetase (**GS**) uses ammonia to recycle glutamine, and this neurotransmitter precursor is provided back to the neurons (Bringmann et al., 2009; Matsui et al., 1999). Both, GLAST and GS are commonly used as Müller cell markers (see also chapter 4.1, 4.2, and 4.3 of this thesis. The glutathione synthetase converts glutamate, cysteine, and glycine to glutathione. Glutathione is an antioxidant that protects the retina against oxidative damage. Müller cells influence neuronal signaling not only by rapid neurotransmitter uptake, recycling and provision of neurotransmitter precursors, but also by releasing glutamate and other substances, which modulate excitability (Bringmann et al., 2006; Newman and Zahs, 1998).

Müller cells contain bundles of intermediate filaments made of **vimentin** and glial fibrillary acidic protein (**GFAP**) (see chapter 1.11.1), though the latter is expressed only at very low levels unless the glial cells get activated. GFAP and vimentin are therefore often used as markers for activated glia/gliosis, as e.g., in chapter 4.3. The effect of intermediate filament-deficiency on normal retinal function as well as on the progression of retinal degeneration was examined in chapter 4.1 and chapter 4.2, respectively.

Müller cells produce numerous neurotrophic factors and cytokines that act on neurons: such as basic fibroblast growth factor (bFGF), brain-derived neurotrophic factor (BDNF), nerve growth factor (NGF), neurotrophin-3, neurotrophin-4, and glial cell line-derived neurotrophic factor (GDNF) (Bringmann et al., 2006; Newman, 2009; Wahlin et al., 2000). The putatively neuroprotective protein metallothionein is also expressed by Müller cells (Gerhardinger et al., 2005; Wunderlich et al., 2010), see also chapter 4.3.

Important for neuronal function and excitability are parameters like pH, water and ion concentration in the extracellular space. Müller cells are important players in maintaining homeostasis through several acid/base transport systems, water channels (e.g., aquaporins, **AQP**) and ion channels (e.g., inwardly rectifying potassium channels, **Kir**) (reviewed in (Bringmann et al., 2006; Newman, 2009)). The expression of the two latter was examined in healthy and degenerating retinas of mice lacking the intermediate filaments GFAP and vimentin (chapter 4.1 and 4.2).

1.6.5 Astrocytes

The typical macroglial cells of the nervous system are astrocytes. Astrocytes have a flat, almost two-dimensional, star-like shape. They contain much of the intermediate filament glial fibrillary acidic protein (GFAP), which is therefore often used as a marker for astrocytes. During retinal development, the astrocytes migrate through the optic nerve head into the retina, forming a framework for the retinal vasculature that develops shortly after. They stay mostly restricted to the nerve fiber layer and in close contact to the blood vessels. Species with no retinal circulation, e.g., guinea pigs, do not have retinal astrocytes (Newman, 2009).

1.7 Blood supply

The retina is metabolically highly active and has the highest oxygen consumption per unit weight of any tissue. Thus, a sufficient blood supply is very important, and a minimal interference with the passing light has to be ensured. The outer retina is therefore indirectly nourished by the choroid behind the retinal pigment epithelium, while the retinal vasculature supplies the inner two thirds. Except for the central fovea, which is avascular to facilitate high acuity vision, and a small avascular rim at the very periphery of the retina, the human as well as murine and rat retinas are completely vascularized (holangiotic), whereas the retinas of some animals, like the rabbit, are only partly vascularized and rely more on nutritive support from the choroid. During development, a third vessel network, the transient hyaloid vasculature, supplies the lens and the retina. All ocular vessels originate from a branch of the internal carotid artery, namely the ophthalmic artery (reviewed in Kur et al., 2012).

1.7.1 The choroid

The choroid consists of three vascular layers delimited by the Bruch's membrane towards the retinal pigment epithelium and the suprachoroidea on the outer surface attached to the sclera. The choroidal capillaries are fenestrated with especially large pores enabling a high permeability. Aside from supplying the outer retina, the choroid is also involved in thermoregulation, modulation of intraocular pressure, and adjustment of the position of the

retina by changes in choroidal thickness (reviewed in Nickla and Wallman, 2010). In contrast to the retinal vessels, the smooth muscles of the choroidal circulation are innervated by sympathetic and parasympathetic nerves (reviewed in Kur et al., 2012; Nickla and Wallman, 2010; Saint-Geniez and D'Amore, 2004).

1.7.2 The retinal vasculature

The retinal blood vessels branch off the central retinal artery, which enters the retina through the optic nerve, and are organized in two interconnecting planar networks. During retinal development, astrocytes spread from the optic nerve head towards the peripheral retina, guiding the outgrowth of a superficial plexus located in the nerve fiber layer and ganglion cell layer. Subsequently, a deeper plexus between the inner nuclear layer and outer plexiform layer develops, sprouting from the primary plexus. The venous system is similarly arranged, with the central retinal vein leaving the retina along the optic nerve again. Astrocyte-derived vascular endothelial growth factor (VEGF) is thought to play a key role in the vascular development; however, recent studies have demonstrated that retinal vessels can form independently of VEGF (Weidemann et al., 2010). Still, the temporal and spatial distributions point to a relationship during development. Astrocytes and Müller glia stay in close contact with the retinal vessels, controlling their distribution and, as mentioned above, contributing to the tight blood-retina-barrier (reviewed in Kur et al., 2012; Riva et al., 2011; Saint-Geniez and D'Amore, 2004).

1.7.3 The hyaloid vasculature

The retinal vascular network is fully mature only after birth. During retinal development, prior to the formation of the retinal vessel net, the lens and the developing inner retina are supported by the hyaloidal vasculature. The hyaloid artery enters the eye cup through the embryonic fissures, branches into the vitreous humor as the *vasa hyaloidea propria*, and ensheaths the lens. The main vessels branch over the lens surface, forming a dense capillary network, the so-called *tunica vasculosa lentis* At the anterior margin of the optic cup, the capillary network merges into the annular vessel, a loop of the hyaloid artery, and connects to the choroidal system, which accomplishes the venous drain, since the hyaloidal system consists only of arteries. From the annular vessel, the *tunica vasculosa lentis* spreads over the anterior sector of the lens forming the pupillary membrane. Since the fully developed lens has a very low metabolism, it can be nourished by diffusion from the aqueous and the vitreous humor alone. The hyaloidal vessels therefore regress before birth in humans and within the first three postnatal weeks in mice (Ito and Yoshioka, 1999). Defective hyaloid retraction may lead to different eye pathologies (Saint-Geniez and D'Amore, 2004).

1.8 Neurodegeneration

The progressive loss of neuronal function and integrity of a specific subpopulation of neurons is called neurodegeneration (Przedborski et al., 2003). The different diseases of this large and very heterogeneous group are usually categorized based on the affected localization and/or the dominant clinical symptoms. Within the central nervous system, many neurodegenerative diseases affect also the retina. Recent studies suggest that the retina is affected in mouse models of Alzheimer's disease as well as in human patients, affecting especially the ganglion cells, the optic nerve, and the vasculature. This fact could become important as there is so far no possibility for an early and accurate diagnosis of Alzheimer's disease in living patients (reviewed in Chiu et al., 2012; Guo et al., 2010). In Parkinson's disease, there is evidence for visual disturbances regarding visual acuity, contrast sensitivity, color vision, and motion perception, as well as visual hallucinations (Archibald et al., 2009). Disrupted retinal structure and function, especially of the dopaminergic neurons, is probably responsible for such problems, additionally to malfunctioning cortical processing (Archibald et al., 2009). Visual impairments, specifically on the level of the retina, are being discussed for Huntington's disease as well (Helmlinger et al., 2002; O'Donnell et al., 2008; Paulus et al., 1993; Petrasch-Parwez et al., 2005). Much better explored are the visual deficits during the course of spinocerebellar ataxias 7 (SCA 7). The retinal degeneration starts with cone photoreceptor loss in the central fovea, but spreads over the whole retina as the disease progresses and eventually also affects rod photoreceptors and the inner retina leading to complete blindness (Aleman et al., 2002; Michalik et al., 2004; Hugosson et al., 2009).

Many neuronal degenerations affect the retina specifically:

1.9 Retinal degeneration

1.9.1 Predominance

According to the World Health Organization (WHO), about 39 million people were estimated to be blind in 2010 (http://www.who.int/blindness/en/). While infectious diseases and operable cataracts are major causes of vision loss in economically less developed areas of the world, retinal degenerations take the lead in the most industrialized countries. However, the specific prevalence may vary greatly, e.g., by ethnicity. One major risk factor for retinal degenerations is aging; about 82% of the blind are over 50 years old (http://www.who.int/blindness/en/).

1.9.2 Glaucoma

Second to cataract, glaucoma is the leading cause of blindness worldwide (Resnikoff et al., 2004). Glaucoma is the term that describes disorders with a distinct type of optic nerve damage that leads to irreversible defects of the visual field. It is characterized by the progressive loss of retinal ganglion cells and their axons, leading to changes in the optic disc that are visible on fundus examinations. A major risk factor for glaucoma is elevated intraocular pressure (IOP) (Caprioli and Varma, 2011). Normally, the IOP stays steady as a result of a balanced rate of aqueous humor formation and fluid removal. In many glaucoma patients, this homeostasis is disturbed. But glaucoma may also occur despite normal IOP. Recent studies suggest an involvement of hypoxia, oxidative stress, excitotoxicity, and autoimmune processes in the pathogenesis (reviewed in (Rieck, 2013)). Glaucoma may lead to blindness, and so far there is no cure known. However, lowering the IOP may stop or slow the progression in some cases (reviewed in (Caprioli and Varma, 2011)).

1.9.3 Age related macular degeneration

Age-related macular degeneration (AMD) is another leading cause of blindness, especially in the elderly of European descent. The prevalence among people over the age of 75 is 1:4 (Klein et al., 2004; van Leeuwen et al., 2003). The immune system seems to be involved in the disposition for the disease, as specific haplotypes for certain components of the complement system have an increased or decreased risk for developing AMD (Hageman et al., 2005; Haines et al., 2005). A hallmark of AMD is the formation of drusen - subretinal, extracellular deposits that are composed of glycoproteins and lipids - in the Bruch’s membrane of the macula. A limited number of small drusen in the peripheral retina is normal in the aged eye, but greater number, size, and confluency are common risk factors for AMD (Klein et al., 2004; reviewed in Katta et al., 2009 and Coleman et al., 2008). Other features of the disease are structural changes of the Bruch's membrane, lipofuscin accumulation in the retinal pigment epithelium, and geographic atrophy in the macular region (Coleman et al., 2008). The retinal pigment epithelium is affected most, but big parts of the outer nuclear layer degenerate progressively as well, which leads to the irreversible loss of central vision. In the late stage of the disease, AMD is commonly divided into the 'dry' and the 'wet' form. Approximately 10-20% of the patients develop wet AMD. Wet AMD is the more severe form due to choroidal neovascularization that enters the subretinal space, where leaking, scarring, and possible retinal detachment cause the majority of the cases of legal blindness in AMD. The neovascularization in the wet form is treated with thermal photocoagulation,

photodynamic therapy, and anti-angiogenic (anti-VEGF) therapy (reviewed in Coleman et al., 2008 and Joussen and Bornfeld, 2009). So far, there is no cure for dry AMD.

1.9.4 Diabetic retinopathy

In industrialized countries, the most common cause of visual impairment in people of working-age is diabetic retinopathy (reviewed in Heng et al., 2013). Approximately 40% of diabetic people show signs of diabetic retinopathy; one third of them suffer from vision-threatening conditions (Cheung et al., 2010; Heng et al., 2013). Primarily, diabetic retinopathy is defined as a vascular complication: impaired retinal vessel walls and changed blood properties during diabetes may cause capillary occlusions and pathologically higher permeability that lead to ischemia and blood leakage in the retina (Jackson and Barber, 2010; Kollias and Ulbig, 2010). The local hypoxia leads to elevated levels of vascular endothelial growth factor (VEGF) and other growth factors, which in turn stimulate neovascularization in the proliferative form of diabetic retinopathy (Kollias and Ulbig, 2010). Similarly to wet AMD, diabetic retinopathy is thus mostly treated by photocoagulation and anti-angiogenic (anti-VEGF) and anti-inflammatory therapy (Heng et al., 2013; Heng et al., 2013). Nevertheless, diabetic retinopathy is not a mere micro-vascular disease but also leads to retinal neurodegeneration and dysfunction, as well as glial activation, in parallel, if not before the onset of vascular changes (Antonetti et al., 2012; Johnson et al., 2013). It is thus currently debated which is the initial cause and what is consequence (Heng et al., 2013). Numerous interconnected biochemical mechanisms seem to be involved in the pathogenesis, including oxidative stress, protein kinase C (PKC) activation, differentially regulated cellular metabolism, signaling and release of growth factors (Cheung et al., 2010; Heng et al., 2013). However, the exact molecular connection between altered blood sugar levels and the appearance of neurovascular changes remains elusive (Heng et al., 2013).

1.9.5 Pigmentary retinopathies (retinitis pigmentosa)

The term ***retinitis pigmentosa*** refers to a heterogeneous group of inherited retinal degenerations that is characterized by a progressive and irreversible loss of rod photoreceptor cells, followed by cone cell death. Later in the disease, other cell types may degenerate as well, and vessel abnormalities may occur. Disease onset and progression can vary substantially. In some cases, retinitis pigmentosa is first noticed during childhood and advances over several decades. Usually, the first symptom is night blindness, followed by progressive vision loss from the periphery towards the center in daylight as well, reduced visual acuity, and loss of cones, eventually leading to complete blindness. Fundus examinations show retinal pigment deposits, starting in the periphery.

Electroretinogram (ERG) measurements can reveal altered photoreceptor responses regarding amplitudes and latencies even in childhood, before the first symptoms are noticed (Hamel, 2006)(Hartong et al., 2006). To date, more than 60 genes have been identified at which mutations cause retinitis pigmentosa (RETNET database, http://www.sph.uth.tmc.edu/retnet/sum-dis.htm#B-diseases; information retrieved in November 2013). Mutations that lead to retinitis pigmentosa are primarily mutations in rod-specific genes, many of them in the *rhodopsin gene* (Athanasiou et al., 2013) or other proteins involved in phototransduction (reviewed in (Delyfer et al., 2004)). Further disease-causing genes encode for structural proteins, transcription factors, proteins involved in intracellular transport, signaling, photoreceptor differentiation, and many more. But also genes specific to other cell types, e.g., RPE cells, and even ubiquitously expressed genes may cause retinitis pigmentosa. The prevalence of non syndromic retinitis pigmentosa is about 1:4,000 (Hamel, 2006).

Around one quarter of the retinitis pigmentosa cases are not restricted to the eye but are part of a syndrome. Overall, there are over 30 different syndromes in which retinitis pigmentosa is part of the disease. The most frequent one is the **human Usher syndrome,** in which retinitis pigmentosa occurs along with hearing impairment, and sometimes balance difficulties (Wolfrum, 2011). Around 5% of retinitis pigmentosa patients suffer from the **Bardet-Biedl syndrome**, where retinitis pigmentosa is often associated with obesity, cognitive impairment, polydactyly, hypogenitalism, and renal disease (Hamel, 2006; Hartong et al., 2006).

1.9.6 Pigmentary retinopathies (cone rod dystrophy)

With a prevalence of 1:40,000, the **cone rod dystrophy** is much rarer than retinitis pigmentosa, but the disease progression is more rapid and severe, leading much faster to legal blindness (Hamel, 2007). Retinal pigment deposits are primarily found in the macular region. The primary cone photoreceptor cell degeneration is followed by the loss of rods. Thus, the first symptoms are a decrease in the visual acuity, central scotomas, color vision deficiency, and photophobia. Night blindness, loss of peripheral vision, and vessel attenuations occur later. Early during the disease, the electroretinogram (ERG) displays delayed photopic responses, in later stages the response amplitudes decrease dramatically. Most cone rod dystrophies are non-syndromic, but they may also be associated with some syndromes, such as the Bardet-Biedl syndrome or SCA7 (Hamel, 2007).

1.9.7 Leber congenital amaurosis (LCA)

Approximately 5% of all hereditary retinopathy cases are based on Leber congenical amaurosis (LCA), the most severe infantile onset retinal dystrophy (Chung and Traboulsi, 2009). Caused by a variety of recessive single-gene defects, LCA is characterized by very low visual acuity, severely reduced ERG signals of either rods, cones, or both, nystagmus, absent pupillary responses and photophobia (Chung and Traboulsi, 2009)(Estrada-Cuzcano et al., 2012)(Hamel, 2007). The relatively mild form of LCA, caused by gene defects in the retinal pigment epithelium-specific protein 65 kDa (RPE65), was the first retina degeneration that was approached with gene-based therapy in humans (Chung and Traboulsi, 2009).

1.10 Cell death mechanisms

Numerous mutations in a variety of genes encoding for very different protein families may cause neurodegeneration, including retinal degenerations (RETNET database, http://www.sph.uth.tmc.edu/retnet/). Although the disease-causing mutations are often known, the downstream events leading to cell death remain most often obscure. Yet, many disease processes converge on common cell death mechanisms. Some well-described cell death concepts are programmed cell death mechanisms, such as apoptosis and autophagy, which are regulated by intracellular, energy-consuming (signaling) cascades, or necrosis, a more passive event resulting in autolysis and inflammatory responses, most often also affecting the surrounding tissue.

1.10.1 Apoptosis

Apoptosis, the best-described cell-death mechanism, is morphologically characterized by condensation of the nucleus, membrane blebbing, reduction of cellular volume, rounding-up and budding of the cell, and finally engulfment by phagocytic cells before leakage of any cell contents (Martin and Henry, 2013; Murakami et al., 2011; Murakami et al., 2013; Sancho-Pelluz et al., 2008). Any damage of neighboring tissue and inflammation is avoided during this well-regulated cell removal - be it during development or due to cellular damage. Classically, the biochemical changes are mediated by activated caspases, a family of cysteine proteases, and for a long time, caspase-driven apoptosis has been thought to be the relevant mechanism of cell death in retinal dystrophies (Leist and Jäättelä, 2001; Lohr et al., 2006). However, apoptosis during retinal degeneration may also occur independently of caspase activation (Doonan et al., 2003).

1.10.2 Autophagy

There is evidence that autophagy contributes to a second form of programmed cell death that is distinct from apoptosis. Autophagy is defined by the lack of cellular condensation and fragmentation but the formation of double- or multimembrane vacuoles (autophagosomes) that fuse with lysosomes forming autolysosomes. This is where the content, cytoplasmic material and organelles, is degraded (Murakami et al., 2013). Yet, autophagy also seems to be important for cell survival as it regulates the cellular homeostasis by removing dysfunctional organelles and proteins and thereby providing recycled energy (Murakami et al., 2013). While it is clear that autophagy takes place during retinal degeneration, especially when apoptosis is prevented, its role in either promoting or protecting against cell death remains elusive (Murakami et al., 2013).

1.10.3 Necrosis

Several studies have shown that both autophagy and apoptosis are linked to necrosis (Murakami et al., 2013; Sancho-Pelluz et al., 2008). Features of necrosis are swelling of cytoplasm and organelles, thus an increasing cellular volume, along with plasma membrane rupture, which leads to the release of cellular content, often causing inflammation (Murakami et al., 2011). Usually, necrosis is a reaction to external factors. Although earlier thought to be purely passive, necrosis has now been shown to involve regulated signal transduction pathways as well (Murakami et al., 2011). This programmed necrosis is called **necroptosis** (Murakami et al., 2011).

The predominant cell death patterns might change during different stages of the disease. In fact, the various mechanisms are not necessarily separated events but may have overlapping features or occur in combination in the degenerating retina (Sancho-Pelluz et al., 2008; Trifunović et al., 2012; Wright et al., 2010).

1.10.4 Cellular stress factors

With its unique structure and highly specialized physiology, the retina has to be finely tuned to integrate function and survival. Many stress factors are able to disturb this balance towards photoreceptor cell death, especially when mutations make the cells even more vulnerable, no matter whether the mutations affect photoreceptor specific genes or disturb more general functions (Wright et al., 2010). The above mentioned cell death mechanisms are tightly controlled by signaling pathways, either promoting or preventing cell death. Factors triggering pro-apoptotic cascades include excitotoxicity, mitochondrial dysfunction, endoplasmatic reticulum (ER) stress, and oxidative stress (Jing et al., 2012).

1.10.5 Misfolded proteins

Major stressors are misfolded proteins. Protein synthesis is a complex process during which approximately one third of the synthesized proteins is not folded correctly even under normal circumstances (Schubert et al., 2000). The continuous shedding and replacement of photoreceptor discs requires a very high protein turnover. Mutations that lead to misfolded proteins (e.g., many rhodopsin mutations) challenge the cell's quality control mechanisms even more (Athanasiou et al., 2013). Many mechanisms have evolved to avoid or remove misfolded proteins that could affect normal function. Accumulation of misfolded proteins in the endoplasmatic reticulum triggers the unfolded protein response (UPR), which leads to inhibition of protein synthesis and increased protein folding capacity and degradation, respectively (Athanasiou et al., 2013). The endoplasmatic reticulum associated degradation acts in three steps: recognition of the misfolded proteins, retrotranslocation into the cytosol, and degradation through the ubiquitin proteasome system. However, the UPR has been shown to occur even independently of protein misfolding in retinal degenerations and is thus discussed to be a common process, activated as a response to degenerative events (Athanasiou et al., 2013). If the endoplasmatic reticulum stress remains despite counteractive efforts, cell death may be induced actively. Prolonged UPR can generate reactive oxygen species, which in turn affects the functionality of the ER (Haynes et al., 2004).

1.10.6 Oxidative stress

Oxidative stress occurs when the generation of reactive oxygen species (ROS), such as singlet oxygen, superoxide and hydrogen peroxide, as well as reactive nitrogen species, exceeds the capacity of the cell's counter mechanisms, ultimately harming the cell, because high concentrations of ROS mediate damage to lipids and membranes, proteins, and nucleic acids (reviewed in (Valko et al., 2007)). ROS are normal byproducts of the mitochondrial respiratory chain (Valko et al., 2007). The retina, one of the tissues in the body with the highest metabolic activity, a large oxygen gradient between the different layers, and very high membrane content in the photoreceptor outer segments, is particularly vulnerable to oxidative damage. Excessive ROS in photoreceptors may also originate from the exposure to light in the presence of abundant photosensitizing molecules like retinoids (Sun and Nathans, 2001; reviewed in Athanasiou et al., 2013 and Wright et al., 2010) and decline of energy utilization and resulting hyperoxia during retinal degeneration (Wright et al., 2010). Indeed, it could be shown that oxidative damage occurs during the course of retinal degeneration (Sanz et al., 2007; chapter 4.3), in parallel with a downregulation of defense systems (Ahuja

et al., 2005; Ahuja-Jensen et al., 2007). Under normal conditions, the effects of harmful ROS are counterbalanced by repair mechanisms, antioxidant enzymes such as glutathione-S-transferase and glutathione peroxidase, and non-enzymatic antioxidants. Among the latter are metallothioneins (Ruttkay-Nedecky et al., 2013), which were the focus of chapter 4.3 of the present thesis.

1.11 Secondary reactive changes

Normal development and survival of retinal cells rely on an equilibrium of pro- and anti-survival factors. In the case of retinal degenerations, this balance tips over towards cell death. Most frequently, photoreceptors and ganglion cells are the primary targets. Although the disease-causing mutations might affect only one single type of cells, the neighboring cells are likely to be affected by the new situation. This is the reason why retinitis pigmentosa, for example, is leading to legal blindness: the cones die secondarily, possibly due to lack of structural (Hewitt et al., 1990) or trophic support (Faktorovich et al., 1990; Léveillard et al., 2004) by the rods or to hyperoxia associated with oxidative stress (Komeima et al., 2006; Shen et al., 2005). Furthermore, remodeling and degeneration of third order neurons occasionally takes place (Gargini et al., 2007; Strettoi et al., 2002). At the same time, secondary reactions occur, in the vulnerable cells themselves, but also in the non-neuronal elements of the retina: vasculature, retinal pigment epithelial cells, macroglia, and microglia.

Some of the vessel alterations, i.e. **vascular occlusions** and **neovascularization**, are already mentioned above (chapter diabetic retinopathy, chapter AMD). As a result of several retinal diseases, e.g. proliferative diabetic retinopathy and AMD, as well as breakdown of the blood-retina-barrier, **retinal pigment epithelium** cells can get activated. Activated retinal pigment epithelium cells can reenter the cell cycle, proliferate and migrate (Hiscott et al., 1999; Miller et al., 1986). They react to changes of certain cytokine levels, such as TNF-α, IL-1β, and IFNγ by altered secretion of a variety of chemokines, cytokines, and extracellular matrix proteins (Shi et al., 2008). The levels of some cytokines, as for example TGF-β, regulate the expression of antigen-presenting molecules and thus the inflammatory **reactivity of microglia** (D'Orazio and Niederkorn, 1998; Paglinawan et al., 2003; reviewed in Langmann, 2007). Activated microglia change shape, divide and migrate. Several studies have shown that activation of microglia and recruitment of macrophages from the circulation are associated with retinal degeneration (Roque et al., 1996; Zeiss and Johnson, 2004; see also chapter 4.4). *In vivo* studies, in which neurons were cultured in microglia-conditioned medium, supported the hypothesis that microglia activation may induce neuronal cell death (Roque et al., 1999).

There is a constant reciprocal signaling also between microglia and macroglia in the retina. Typical reactive changes of the two macroglial cell types in the retina, **astrocytes** and **Müller cells**, include increase in the expression of the intermediate filament proteins glial fibrillary acidic protein and vimentin (Ekström et al., 1988; reviewed in Bringmann et al., 2006 and Bringmann et al., 2009), but also alterations in Müller-cell specific proteins, such as glutamine synthetase, inwardly rectifying potassium channels and aquaporins (reviewed in Bringmann et al., 2006). These features may lead to dysregulation of the homeostases in the extracellular space, possibly adding to the cell stress of the dying neurons and their primarily unaffected neighbors. Many of the gliotic features also correspond to immature Müller cells. And indeed are activated Müller cells thought to de-differentiate before proliferation and migration (reviewed in Bringmann et al., 2006).

Many of the above changes may be detrimental and contribute to the disease progression, others may promote survival and repair, e.g., by production of anti-oxidants, trophic factors, various cytokines, metallothionein, etc. In any case, they are likely to influence putative treatments.

1.11.1 Intermediate filament proteins

Intermediate filaments are intermediate in size (≈10 nm on a cross-section) between actin filaments (6-7 nm) and microtubules (23-25 nm). The expression of the intermediate filament proteins glial fibrillary acidic protein (**GFAP**) and **vimentin** is activation stage- and age-dependent (Pekny and Lane, 2007; Szeverenyi et al., 2008). Both these structural elements of the glial cytoskeleton are very conserved between species (Lewis et al., 1984; Wood et al., 1989), and were thus expected to play very important roles during development and the function of adult glial cells.

Surprisingly, the in different laboratories independently developed mice deficient for either GFAP (Gomi et al., 1995; Liedtke et al., 1996; McCall et al., 1996; Pekny et al., 1995), vimentin (Colucci-Guyon et al., 1994) or even both (Giménez Y Ribotta et al., 2000; Pekny et al., 1999) not only survived, but did not show any obvious alteration in development, anatomy, histology, glial cell number and distribution, viability, behavior, or any other abnormal phenotype other than not having any normal amounts of intermediate filaments in their glia (Galou et al., 1997; Wilhelmsson et al., 2004). Although in aged $GFAP^{-/-}$ mice, dysmyelination and locally higher permeability of the blood brain barrier becomes apparent, and the prevalence of mice that develop a hydrocephalus rises (Liedtke et al., 1996). Moreover, mice deficient for vimentin display abnormal Bergmann glia and Purkinje cells, as well as an impaired motor coordination (Colucci-Guyon et al., 1999). No other possible

compensatory filament like e.g., nestin seems to be induced (Liedtke et al., 1996; McCall et al., 1996).

Mutations in the gene encoding GFAP lead to the fatal Alexander disease that is characterized by diffuse demyelination and protein aggregations in astrocytes (Mignot et al., 2004; Quinlan et al., 2007). Similar cellular inclusions are seen in mice that transgenically overexpress GFAP (Eng et al., 1998; Messing et al., 1998). Very strong GFAP overexpression will even lead to the death of the animals within the first weeks after birth (Messing et al., 1998).

Overexpression of vimentin disturbs normal lens development in mice (Capetanaki et al., 1989), and a connection between vimentin mutations and dominant cataract formation has been postulated in humans as well (Müller et al., 2009).

Many studies have been carried out to examine the role of intermediate filament proteins during glial cell reactivity, a process that is usually accompanied by characteristic up-regulation of GFAP and vimentin. So, it has, for instance, been shown that astrocytes in $GFAP^{-/-}$ $Vim^{-/-}$ mice are less reactive in response to injury than those of wildtype mice in the sense that they become less hypertrophic and do not upregulate endothelin B receptors (Wilhelmsson et al., 2004). The degeneration early after the injury is more severe, but the recovery later is far better (Wilhelmsson et al., 2004).

Similarly, there is a less gliotic response to retinal detachment in the eye, which includes less glial scar formation and better recovery (Nakazawa et al., 2007; Verardo et al., 2008).

Rather little is known, however, about the functions of intermediate filament proteins in the unchallenged, healthy state.

1.11.2 Metallothionein

Neuroinflammation, injury, oxidative stress, and several other insults have been shown to induce upregulation of the cysteine-rich, metal-binding proteins metallothioneins in brain tissue. Metallothioneins exists in four major isoforms: Metallothionein-I, -II, -III, and -IV. Most tissues ubiquitously express Metallothionein-I and -II, including the central nervous system, while metallothionein-III and -IV are restricted to a few specific tissues (reviewed in West et al., 2008). Altered levels of metallothionein have been observed during the course of several neurological diseases, including Alzheimer's disease, amyotrophic lateral sclerosis, and multiple sclerosis (West et al., 2008). Metallothionein-I and -II are structurally and functionally almost indistinguishable and are thus often referred to as a single entity (metallothionein-I+II; chapter 4.3). The low-molecular-mass (6-7 kDa) proteins bind and release both essential and

toxic metals and seem to play important roles in protection against metal toxicity, zinc absorption and homeostasis, and to exhibit redox capacity (reviewed in (Coyle et al., 2002; Haq et al., 2003; Ruttkay-Nedecky et al., 2013; West et al., 2008). Increased levels of metallothionein-II mRNA and protein have been shown in different experimental models of retinal degeneration induced by intense light (Chen et al., 2004; Chen et al., 2004) or intravitreal injection of excitotoxic N-Methyl-D-Aspartate (NMDA) (Suemori et al., 2006), as well as after hypoxic preconditioning (Thiersch et al., 2008), and mechanical damage (Vázquez-Chona et al., 2004). Lower zinc levels and metallothionein synthesis, on the other hand, have been reported in cynomolgus monkeys and human patients with age-related macular degeneration (AMD) (Nicolas et al., 1996; Sato et al., 2000). Thus, one focus of chapter 4.3 was to evaluate the expression pattern of metallothionein-I+II in the retinas of different rodent models of retinal degeneration.

Metallothioneins potentially have neuroprotective functions since cell loss after NMDA application is increased in metallothionein-deficient mice (Suemori et al., 2006), and direct and indirect up-regulation of metallothionein in the retinal pigment epithelium has been shown to contribute to protect the cells against oxidative damage (Lu et al., 2002; reviewed in West et al., 2008). Further studies have shown that metallothionein seem to regulate also neuronal survival in a paracrine manner, being released by astrocytes and taken up by retinal ganglion cells *in vitro* (Chung et al., 2008; Fitzgerald et al., 2007). The release of metallothionein seems to take place in a non-classical, still selective manner (reviewed in Lynes et al., 2006), whilst uptake might be mediated through interaction with megalin, a member of the low-density lipoprotein receptor (LDLR) family (Ambjörn et al., 2008; Leung et al., 2012).

In chapter 4.3, a potential interaction between metallothionein-I+II and megalin was examined with the *in situ* proximity ligation assay.

1.11.3 Sialoadhesin

Sialoadhesin (alternative names: CD169 or Siglec-1, formerly Ser-4), a member of the sialic acid-binding Ig-like lectin (Siglec) family, is a macrophage-restricted cell-adhesion molecule (reviewed in Martinez-Pomares and Gordon, 2012). Under normal conditions, high levels of sialoadhesin are found on subsets of macrophages in secondary lymphoid tissues, such as the marginal zone of the spleen and the perifollicular zones of lymphoid tissues (Crocker and Gordon, 1986). Sialoadhesin can also be expressed by inflammatory macrophages and has been shown to mediate adhesion of macrophages to e.g., T cells, neutrophils, or other activated macrophages (Crocker et al., 1995). In mice, microglia/macrophages need to have

been in contact with serum in order to express sialoadhesin (Crocker et al., 1988). Accordingly, sialoadhesin expressing microglia in the central nervous system imply an impaired blood-brain barrier (Perry et al., 1992). Sialoadhesin has been shown to support immunoregulating functions influencing T-cell behavior in a pro-inflammatory manner (Wu et al., 2009). Recent publications have shown that sialoadhesin positive macrophages play an important role in enforced viral replication, thereby activating adaptive immunity (Honke et al., 2012). Sialoadhesin seems to participate in the recognition and discrimination of pathogens versus 'self' (reviewed in Klaas and Crocker, 2012).

In the eye, sialoadhesin has been shown to be expressed by macrophages following experimental autoimmune uveoretinitis, contributing to the inflammatory response triggered in this model (Jiang et al., 1999; Jiang et al., 2006). Sialoadhesin was reported to be present in retinal microglia/macrophages also in a model of photoreceptor degeneration, which has been suggested to indicate a breakdown of the blood-retina barrier (Hughes et al., 2003).

In chapter 4.4, the expression of sialoadhesin in healthy and degenerating mouse retinas was assessed, as well as after intraocular transplantation of neonatal retinal cells.

2. Aim of the thesis

More than 200 identified genes have so far been found to be associated with inherited retinal degenerations (RETNET database, http://www.sph.uth.tmc.edu/retnet/sum-dis.htm#B-diseases; information retrieved in November 2013). Despite the progress in elucidating the genetic background, little is known about the exact mechanisms of photoreceptor degeneration, and no effective treatments are yet available. Recent studies suggest a role for secondary reactive changes mediated by glial cells in the progression of retinal cell loss (Caicedo et al., 2005; Joussen et al., 2004; Nakazawa et al., 2006).

The aim of this thesis was to examine some of the dynamics of reactive changes and how these affect the progression of photoreceptor cell degeneration in several models of human retinal degeneration. The analysis of reactive changes focused primarily on those mediated by the retinal glial cells (macroglia and microglia). An understanding of the nature of these changes and how they may be controlled is critical for the improvement of clinical treatments aimed at preserving photoreceptor cell function and vision.

The key goals of this thesis were

a) to first characterize the role of the type III intermediate filament proteins GFAP and vimentin, typically highly upregulated during reactive gliosis, in normal physiology in healthy mouse retinas (chapter 4.1);
b) to investigate the potential impact of GFAP and vimentin on the progression of retinal degeneration in a mouse model for retinitis pigmentosa (chapter 4.2);
c) to evaluate the temporal and spatial expression pattern of the putative neuroprotective metallothionein-I+II and their potential interaction with the low-density lipoprotein receptor megalin in retinal glia of three different rodent models of retinal degeneration (chapter 4.3);
d) to examine the expression of the macrophage-restricted cell-adhesion molecule sialoadhesin in healthy and degenerating mouse retinas, as well as after intraocular transplantation of neonatal retinal cells (chapter 4.4).

3. Methods

The following chapter presents the methods that I have employed in the studies described in this thesis. These methods were mainly aiming at the analysis of the retinal morphology in different rodent models of photoreceptor degeneration and at the quantification as well as spatial/temporal expression patterns of RNA and proteins, respectively. The exact details can be found in each individual chapter and in previous publications. Methods performed by the co-authors, as for example full-field electroretinography (chapter 4.1 and 4.2), microarray analysis (chapter 4.3), and transplantation of neonatal retinal tissue (chapter 4.4), are described in the according studies (see Authors' contributions).

3.1 Ethics/Animals

To date, there is no cure for retinal degenerative diseases such as retinitis pigmentosa. Profound knowledge of the biological mechanisms behind disease development, progression and treatment impact is crucial, and animal models are still indispensable for many investigations. Rodents are often the animals of choice, and a number of models with spontaneous or genetically engineered mutations exist that are representative for human forms of the disease. Some retinal degenerations (rd) have been found in natural populations of mice numbered from rd1 to rd16, based on the order of their discovery (Fletcher et al., 2011). Because of the heterogeneous nature of retinitis pigmentosa, several different rodent models were used in this thesis. In chapter 4.2, 4.3, and 4.4, rd1 mice were included.

In the rd1 mouse, a mutation in the β-subunit of the rod *cGMP-phosphodiesterase* gene (*Pde6b*) causes a rapid degeneration of rods within less than two weeks after opening their eyes (Bowes et al., 1990). This fast degeneration allows an easy evaluation of cell death at different time points. A major drawback is, however, that the course of the disease overlaps with the normal developmental cell death and the photoreceptors never fully mature before dying (Fletcher et al., 2011; Sancho-Pelluz et al., 2008).

Mice homozygous for a null mutation in the *Prph*2 gene ($Prph2^{Rd2}$) encoding peripherin, the so-called retinal degeneration slow (rds) mice, were evaluated in chapter 4.3 and 4.4. Due to the lack of this structural protein, the photoreceptors of these mice do not develop outer segments and die over a period of several months (Sanyal and Jansen, 1981). Therefore, rather few photoreceptors are lost at a time, making assessments of cell death events at different stages difficult.

In the Royal College of Surgeons (RCS) rat, photoreceptors degenerate during the first 3 months after birth although the primary defect is not in a photoreceptor-specific gene. The

underlying mutation in the *Mertk* gene prevents the retinal pigment epithelium from taking up shed photoreceptor outer segment discs, which leads to the accumulation of debris in the subretinal space (D'Cruz et al., 2000).

The possibility to knockout specific genes in mice enables investigations on the functional role of the encoded proteins. In chapter 4.1 and 4.2, mice lacking GFAP (*GFAP*$^{-/-}$), vimentin (*Vim*$^{-/-}$), or both (*GFAP*$^{-/-}$*Vim*$^{-/-}$) were used to examine the role of these glial intermediate filaments on retinal function, and the progression of retinal degeneration in rd1 mice. Sialoadhesin-deficient mice were examined in chapter 4.3.

The animals were bred on homozygous backgrounds and kept on a 12-hour light-dark cycle with no limitation of food or water. All experiments were performed with the approval of the local committee for animal experimentation and ethics. Animals were killed with carbon dioxide and their eyes were quickly enucleated for further processing. Handling of animals was in accordance with the ARVO Statement for the Use of Animals in Ophthalmic and Vision Research.

3.2 Genotyping

The DNA for genotyping was extracted as follows: pieces of tail or ear were broken up and lipids and proteins partly digested by addition of a lysis buffer containing detergents and proteinase (100 µg/ml proteinase K in 100 mM Tris pH 8.5, 5 mM EDTA, 0,2% SDS, 200mM NaCl) at 55°C overnight. Chelation of divalent ions, such as Mg^{2+} and Ca^{2+}, by EDTA prevented DNase activity. The solution was vortexed, and the supernatant with the released DNA was transferred to an equal amount of isopropanol. The DNA precipitated and formed a pellet that was washed with 70% ethanol before being resuspended in 80 µl water and stored at -20°C.

Polymerase chain reaction (PCR) was used to genotype the animals. The purpose of a PCR is the selective amplification of a specific DNA region through repetitive cycles of DNA-melting by heating up to approximately 94–98°C, annealing of specific primers complementary to the DNA target region on each strand at lower temperatures (50-65°C), and elongation catalyzed by polymerase close to its optimal activity temperature (70-75°C). Temperature settings and buffer compositions were optimized for each primer set. The PCR products can be separated by size with agarose gel electrophoresis. The ethidium bromide in the gel intercalates into nucleic acids and makes them visible under UV-light.

3.3 Quantitative Real-Time PCR

Quantitative real-time PCR (q-RT-PCR) is a technique used to quantify the amount of DNA in a sample. It is based on the same principle as a conventional PCR, but the fluorescent signal derived from a dye such as SYBR green that binds to double stranded DNA is measured after each cycle. The signal strength is proportional to the amount of product. Since the number of target DNA-copies ideally doubles in each cycle, comparison to standard curves and/or other samples allows conclusions about the initial absolute or relative amount of DNA template. This method is often used to make predictions about gene expression. To do so, the mRNA is first converted to its complementary DNA (cDNA) by the enzyme reverse transcriptase and can then be amplified as described above. The retinas for q-RT-PCR examination in chapter 4.3 were removed through a slit in the cornea immediately after the animals were killed, snap frozen separately in liquid nitrogen, and stored at -80°C until further processing. The RNA was isolated following the manual of the utilized RNeasy MiniKit (Qiagen, Hilden, Germany), including a DNase treatment step to remove any contamination of genomic DNA.

3.4 Western blot analysis

Evaluation of gene expression permits only predictions about the actual levels of resulting protein as translation and degradation efficiency have to be considered. A Western blot (WB) analysis allows quantitative evaluation of protein expression itself. Proteins are denatured when heated in homogenizing buffer containing detergents like sodium dodecyl sulfate (SDS) and further reduced to their primary structures by strong reducing agents as dithiothreitol (DTT) in the buffer, in which they are loaded onto a polyacrylamide gel. SDS denatures proteins and covers them with a negative charge, so once an electrical current is applied they move through the pores of the gel and are separated according to their size. A current perpendicular to the gel transfers the proteins to a polyvinylidene fluoride transfer (PVDF) membrane. After a blocking step, the membrane (blot) is incubated with a primary antibody that is later detected by a secondary antibody conjugated to horseradish peroxidase. This enzyme cleaves a chemiluminescent substrate producing a signal that can be detected on a photographic film. The relative amount of protein can be analyzed by comparison of the light intensities/the sizes and densities of the bands on the film. In chapter 4.1 and 4.2, expression levels of several glial and neuronal proteins from wildtype retinas (control) and retinas from GFAP/vimentin knockout mice were compared.

3.5 Immunohistochemistry

Immunohistochemistry allows for qualitative assessments about the localization of a protein within a tissue. For the immunohistochemical studies in this thesis, enucleated eyes were fixed in 4% paraformaldehyde in Sörensen's buffer at 4°C for 2 hours. After several rinses with the same buffer and ensuing cryo-protection with increasing concentrations of sucrose in the buffer, the eyes were embedded in an albumin-gelatin medium and frozen. Cryostat sections of 12 µm thickness were collected on gelatin/chrome alum-coated glass slides and stored at -20°C until further processing. Thawed and air-dried sections were preincubated in blocking solution [Tris-buffered saline (TBS) or Phosphate-buffered saline (PBS) containing bovine serum albumin (BSA) and normal serum corresponding to the species in which the secondary antibody was made] for 60-90 minutes at room temperature to prevent unspecific binding of the antibodies. Incubation with primary antiserum was performed overnight at 4°C. In case the primary antibody was not directly conjugated to a fluorescent label, a fluorophore-conjugated secondary antibody was utilized after several washing steps and applied for 60-90 minutes at room temperature or a biotinylated secondary antibody was used, followed by washing steps and labeling with CY3-conjugated streptavidin. Since more than one secondary antibody carrying the fluorophore binds to the primary antibody, a weak signal can be enhanced. Moreover, the biotinylated secondary antibodies provide even more docking sites for dye-labeled streptavidin, which results in further signal enhancement. Washed sections were mounted with an antifading medium (Vectashield, Vector Laboratories, Burlingame, CA, USA), examined with a fluorescence microscope (Axiophot, Carl Zeiss Meditec, Inc., Oberkochen, Germany), and documented with an Axiocam camera with the associated software (Axiovision 4.2, Carl Zeiss Meditec). Incubation times were prolonged when whole flat mounted retinas were stained.

Specificity controls were performed by either omitting the primary antibody, by preincubating it with the according peptide, by staining tissue from animals that do not express the particular protein, or by western blot analyses. In papers 4 and 5, a number of co-stainings with the antibodies of interest and known cellular markers were performed to establish which cell type expresses the proteins of interest (e.g., metallothionein-I and –II; sialoadhesin).

3.6 Proximity ligation assay

In order to make predictions about possible protein-protein interactions, it is necessary to show that the relevant proteins are located in close proximity. The proximity ligation assay (PLA) visualizes molecules that are at least as close as 40 nm from each other. The applied primary antibodies, which are raised in different species, are recognized by the according

secondary antibodies tagged with complementary oligonucleotides (PLA probes). Following hybridization, ligation, and a rolling circle DNA amplification step, the product is labeled with a complementary DNA linker conjugated to a fluorophore. This method was applied according to the manufacturer's instructions to visualize the co-localization of metallothionein-I+II and megalin in the mouse retina *in situ* and described in more detail in chapter 4.3.

3.7 Lectin staining

Lectins are proteins that bind to specific sugar moieties. A number of lectins have been found to have strong affinities to specific tissues or cell structures and are therefore often used as markers for those. Many lectins require calcium for binding. So, incubation with lectins was performed in a buffer containing $CaCl_2$ (300 mM NaCl, 100 µM $CaCl_2$, and 10 mM HEPES, pH 7.5).

Microglia and vessels were stained with isolection B4 (IB4) and tomato-lectin in chapter 4.3. The lectin peanut agglutinin (PNA) was used as a cone photoreceptor marker in chapter 4.1 and 4.2.

3.8 Oxidative stress-/damage-assay

Above a certain threshold, free radicals cannot be handled by the cells and may cause damage to proteins, lipids and DNA (see Oxidative stress). Oxidized nucleotides are products of oxidative DNA damage. Avidin has been found to bind to 8-oxodeoxyguanosine (and 8-oxoguanine) with high specificity. In chapter 4.3, avidin was used as a marker for oxidatively damaged DNA on retinal sections. Sections were incubated for one hour at room temperature with Texas Red- or Alexa Fluor 488-conjugated avidin (10 µg/ml in PBS-T-BSA, Molecular Probes Inc., OR, USA).

3.9 TUNEL-assay

Programmed cell death, such as apoptosis, is associated with DNA fragmentation in its last phase. Endogenous endonucleases break up the DNA into short fragments of regular size. In the TUNEL-assay (**T**erminal deoxynucleotidyl transferase d**U**TP **N**ick **E**nd **L**abeling = TUNEL), the enzyme “terminal deoxynucleotidyl transferase” catalizes the addition of labeled dUTPs (deoxyuridine triphosphate) to free nick ends of the DNA fragments. TUNEL-staining was used for detection of dying cells in chapter 4.1 and 4.3. The enzyme solutions of the *In Situ* Cell Death Detection Kit (TMR red, Roche Diagnostics, Mannheim, Germany) were diluted as described in detail in the according chapter (4.1 and 4.3) and applied to the

sections for 45 minutes at 37°C. The reaction was stopped by several washes with cold PBS before mounting with antifading solution. However, the results have to be interpreted with caution: although traditionally used to identify apoptotic cell death, the TUNEL assay fails to discriminate between different types of (programmed) cell death (Grasl-Kraupp et al., 1995).

3.10 Hematoxylin and eosin staining

Some eyes in chapter 4.1 and 4.3 were fixed in Bouin's solution (Sigma, Saint Louis, USA) at 4°C overnight, dehydrated in ethanol of increasing concentrations and xylene, embedded in paraffin and cut into 4-5 µm sections. Prior to morphological examination under the light microscope, the sections were stained with hematoxylin and eosin to stain nuclei and surrounding structures, respectively.

4. Results

Manuscripts/publications

4.1 Retinal functional alterations in mice lacking the intermediate filament proteins glial fibrillary acidic protein (GFAP) and vimentin
Manuscript

4.2 The inability to produce glial fibrillary acidic protein (GFAP) and vimentin does not protect photoreceptors in a genetic model of degeneration
Manuscript

4.3 Altered expression of metallothionein-I and -II and their receptor megalin in inherited photoreceptor degeneration
Invest Ophthalmol Vis Sci. 2010 Sep;51(9):4809-20.

4.4 Sialoadhesin expression in intact degenerating retinas and following transplantation
Invest Ophthalmol Vis Sci. 2008 Dec;49(12):5602-10.

4.1 Retinal functional alterations in mice lacking the intermediate filament proteins glial fibrillary acidic protein (GFAP) and vimentin

Manuscript

Summary

Gliotic astrocytes and Müller cells undergo characteristic morphological and biochemical changes, such as increased expression of the intermediate filament proteins glial fibrillary acidic protein (GFAP) and vimentin ((Ekström et al., 1988); reviewed in (Bringmann et al., 2006; Bringmann et al., 2009). The inability of astrocytes to produce GFAP and vimentin was shown to have a positive effect on neurite outgrowth and cell survival in co-cultured neurons (Menet et al., 2001). GFAP and vimentin deficient mice have been studied extensively to gain more knowledge about the function of astrocytic intermediate filaments in response to different insults (Eliasson et al., 1999). However, little is known about the role of those intermediate filaments in normal retinal physiology.

In chapter 4.1, retinal function of knockout mice for GFAP, vimentin or both was assessed by electroretinography (ERG; performed by Naoyuki Tanimoto, Tübingen), and the expression patterns of different neuronal and glial proteins were analyzed by means of immunohistochemistry and western blot.

The ERG analyses revealed distinct alterations in the scotopic responses of GFAP-vimentin double knockout, but not the single-knockout mice, compared to wildtype controls. While the comparison of all four mouse lines did not indicate any measurable differences in the photoreceptoral responses (a-waves), the scotopic b-wave amplitudes were significantly increased and returned much more slowly to baseline in double-knockout animals than in wildtype or single-knockout mice. These alterations seem to mainly involve the rod pathways, since no differences could be observed under photopic conditions. However, when measuring the responses to a series of flashes (flicker), the situation reversed: at frequencies above 5 Hz, which are usually attributed to the cone system, flicker responses in *GFAP*$^{-/-}$*Vim*$^{-/-}$ mice were smaller than those in wildtype mice. It is possible that very minor defects in the cone system could only be observed after continuous repetitive stimuli.

The main source of the b-wave is the depolarization of bipolar cells (Lei and Perlman, 1999). Since the a-wave was not altered, the higher b-waves were most likely not a response to higher input from photoreceptors but rather emerged on the post-photoreceptor level.

No obvious morphological differences could explain the ERG results. All retinal layers displayed the same overall thickness in all genotypes, and no abnormal cell death could be

detected. Likewise, the evaluation of the retinal expression of different established neuronal marker proteins did not result in any detectable differences between the four groups. The number and distribution of rod and cone photoreceptors, bipolar, ganglion, horizontal and amacrine cells tested was comparable in all four mouse lines.

Since GFAP and vimentin are glial intermediate filaments, it appeared likely that the expression of other glial proteins is altered. Indeed, although the number of Müller cells seemed comparable in *GFAP*$^{-/-}$*Vim*$^{-/-}$ and wildtype mice, indicated by similar expression levels of the Müller cell markers SOX-9 and cellular retinaldehyde binding protein (CRALBP), some proteins involved in fundamental glial functions were differentially expressed in the different genotypes. Of the two proteins involved in glutamate homeostasis that were examined, the glutamate aspartate transporter (GLAST) appeared slightly higher expressed in *GFAP*$^{-/-}$*Vim*$^{-/-}$ compared to wildtype mice, whereas glutamine synthetase (GS) levels were clearly reduced. Both proteins were found to be expressed in all retinal layers in association with Müller cell processes. The protein levels of the water channel aquaporin 4 (AQP4) increased with age in both, double-knockout and wildtype mouse retinas, but no major difference could be observed between the two in terms of protein expression level or distribution along the Müller cells. The levels of the inwardly rectifying potassium (Kir) channels Kir2.1 and Kir4.1, on the other hand, were considerably lower in mice lacking GFAP and vimentin or vimentin only. GFAP single knockout mice resembled the wildtype phenotype. An overall reduction of the Müller cell staining of Kir2.1 could be observed on retinal sections of *GFAP*$^{-/-}$*Vim*$^{-/-}$ and *Vim*$^{-/-}$ mice, while the reduction in Kir4.1 expression was particularly reduced in the proximal Müller cell processes. Kir channels are important for the potassium homeostasis of the extracellular space to ensure proper neuronal functionality. Müller cells are responsible for the so-called potassium siphoning, the uptake of extracellular potassium and its release into vessels, subretinal space and vitreous (Kofuji et al., 2002)(Newman, 1993). The resulting ion current is supposedly responsible for the slow and small negative-going PIII component of the ERG, by which Müller cells are thought to modulate the b-wave (Frishman, 2006). Inactivation of Kir4.1 channels has indeed been shown to diminish the PIII response and to increase the intraretinal b-wave in eyecup preparations (Kofuji et al., 2000)(Wu et al., 2004). The disturbed Kir channel expression and localization could thus possibly underlie in parts the functional abnormalities observed in *GFAP*$^{-/-}$*Vim*$^{-/-}$ mice. However, vimentin single knockout mice displayed similar disturbances in Kir channel expression, although their ERG responses did not significantly deviate from the controls. It remains to be evaluated, which role the lack of GFAP plays to produce the functional phenotype in the double-knockout animals.

Retinal functional alterations in mice lacking the intermediate filament proteins glial fibrillary acidic protein (GFAP) and vimentin

*KA Wunderlich[1,2,3], N Tanimoto[3], M Pekny[4,5], E Zrenner[3], MW Seeliger[3], M-T Perez[1,6 *]*

[1] Institute of Clinical Sciences, Division of Ophthalmology, Lund University, Lund, Sweden

[2]Graduate School of Cellular & Molecular Neuroscience, University of Tübingen, Tübingen, Germany

[3]Institute for Ophthalmic Research, University of Tübingen, Tübingen, Germany

[4]Center for Brain Repair and Rehabilitation, Dept. of Clinical Neuroscience and Rehabilitation, Institute of Neuroscience and Physiology, Sahlgrenska Academy at the University of Gothenburg, Gothenburg, Sweden

[5]Florey Institute of Neuroscience and Mental Health, Parkville, Victoria, Australia

[6]Dept. of Ophthalmology, University of Copenhagen, Glostrup Hospital, Glostrup, Denmark

Running title: GFAP and vimentin in mouse retinal function

Key words: retina, GFAP, vimentin, IF, electroretinogram, ERG, b-wave, PIII, potassium, Kir4.1, Kir2.1, GLAST, GS, knockout, intermediate filaments, cerebellum, mouse

Word count:

Abstract: 235
Introduction: 622
Materials and Methods: 926
Results: 2131
Discussion: 2783
Figure Legends: 1214
Tables: 443
References: 2350
Total: 10704

[*] **Corresponding author:**

Maria-Thereza Perez
Inst. Clinical Sciences, Ophthalmology
Lund University
BMC B11, Klinikgatan 26
226 84 LUND, Sweden
tel. (+46) 46 2220772
E-mail: maria_thereza.perez@med.lu.se

ABSTRACT

Activation of retinal glial cells following damage is attenuated in mice lacking intermediate filament (IF) proteins glial fibrillary acidic protein (GFAP) and vimentin. However, it is not known what impact the absence of GFAP and vimentin has on the function of the normal retina. In the present study, we performed full-field electroretinograms (ERG) and, by using western blot and immunohistochemical analyses, assessed the expression of several neuronal and glial retinal markers in mice deficient for GFAP (*GFAP*$^{-/-}$), vimentin (*Vim*$^{-/-}$) or both GFAP and vimetin (*GFAP*$^{-/-}$*Vim*$^{-/-}$). We show that the levels of glutamine synthetase and of inwardly rectifying potassium (K^+) channels, 2.1 (Kir2.1) and 4.1 (Kir4.1), between postnatal days (PN) 14 and 60, were lower in *GFAP*$^{-/-}$*Vim*$^{-/-}$ mice compared to wild-type. ERG analysis at PN60 showed comparable photoreceptoral responses (a-wave) for all genotypes under dark- and light-adapted conditions. The latency and ascending edge of the b-wave were also unaffected. However, the amplitude of the b-wave was increased under mesopic conditions in *GFAP*$^{-/-}$*Vim*$^{-/-}$ mice and its return to baseline was significantly delayed. These results suggest that the rod system is affected, as no alterations were noted in the cone system under photopic conditions. The decreased levels of K^+ channels may explain, at least in part, the ERG abnormalities observed. This study provides evidence that GFAP and vimentin deficiency affects normal retinal physiology.

INTRODUCTION

Intermediate filament (IF) proteins, known also as nanofilaments, constitute a diverse family of proteins encoded by at least 70 genes in the human genome (Szeverenyi et al., 2008). They are intermediate in size (≈10 nm on a cross-section) between actin filaments (6-7 nm) and microtubules (23-25 nm). Expression of IF proteins is tissue- and cell-specific and for some of them also activation stage- and age-dependent (Pekny and Lane, 2007; Szeverenyi et al., 2008).

In the retina, glial fibrillary acidic protein (GFAP) and vimentin (Vim) are expressed by the two macroglial cell types: astrocytes and Müller cells. Astrocytes are found in vascularized retinas and are restricted to the innermost retinal layers where they assume a characteristic star-shaped or bipolar morphology. Müller cells have their cell bodies in the middle of the retina and radial processes that span almost the entire thickness of the retina, reaching from the inner limiting membrane on the vitreal side of the retina, where their proximal processes terminate in funnel-shaped endfeet, to the outer limiting membrane, where their apical processes contact photoreceptors and each other (reviewed in Newman, 2009).

The levels of GFAP and vimentin expression in retinal glia vary, depending on the species and developmental stage (reviewed in Lewis and Fisher, 2003; Fischer et al., 2010). In the adult healthy mouse retina, astrocytes express detectable levels of GFAP, whereas vimentin is observed predominately in the inner portion of the Müller cells (Lewis and Fisher, 2003). Glial cells are activated under all pathological conditions affecting the retina, such as retinal detachment (Lewis et al., 2010), photo-toxic insult (Iandiev et al., 2008), uveitis (Eberhardt et al., 2011), diabetic retinopathy (Kumar and Zhuo 2010), inherited retinal degeneration (Wunderlich et al., 2010), stick injury, retinal ischemia (Hirrlinger et al., 2010; Lu et al., 2011; Rehak et al., 2009), etc. During activation, these cells can proliferate, migrate, change shape, and up-regulate the synthesis of a large number of molecules, such as cytokines and trophic factors (reviewed in Lewis and Fisher, 2003; Bringmann et al., 2006). In this process, the expression of GFAP and vimentin is increased, and these IF proteins are therefore commonly used as early cellular markers for retinal reactive gliosis.

Insight into which functions GFAP and vimentin have in the retina under pathological conditions has been gained from studies of mice devoid of GFAP and vimentin (*GFAP*$^{-/-}$*Vim*$^{-/-}$). The absence of these IF proteins in Müller cells was shown to lead to an abnormal response of the retinal vasculature to ischemia, namely decreased ability of newly formed blood vessels to traverse the inner limiting membrane (Lundkvist et al., 2004). In contrast to wild-type mice, the retinas of *GFAP*$^{-/-}$*Vim*$^{-/-}$ mice showed also attenuated reactive gliosis after neural grafting, retinal ischemia and retinal detachment (Kinouchi et al., 2003;

Nakazawa et al., 2007; Verardo et al., 2008; Lu et al., 2011), supported robust neural integration from retinal transplants (Kinouchi et al., 2003), and showed less prominent monocyte infiltration and photoreceptor degeneration induced by retinal detachment (Nakazawa et al., 2007). Unchallenged retinas of *GFAP*$^{-/-}$*Vim*$^{-/-}$ mice, on the other hand, did not exhibit differences in the distribution or morphology of astrocytes and Müller cells (Kinouchi et al., 2003; Lundkvist et al., 2004) or any other abnormality, except when subjected to mechanical stress, revealing that these IF proteins were important for maintaining the mechanical integrity of Müller-cell endfeet and of the innermost retinal layers (Lundkvist et al., 2004).

The present study was performed with the objective of examining whether and how the lack of GFAP and vimentin might affect the function of the normal, unchallenged retina. For this purpose, an analysis of retinal responses to light stimuli was performed along with a screening of retinal cell-type specific markers.

MATERIALS AND METHODS

Animals

Mice on a mixed C57BL/129 genetic background with null mutations in the GFAP and/or Vim loci (Colucci-Guyon et al., 1994; Pekny et al., 1995; Eliasson et al., 1999; Pekny et al., 1999) and age-matched controls were examined: (i) wildtype mice (*GFAP*$^{+/+}$*Vim*$^{+/+}$, WT); (ii) single-knockout mice: *GFAP*$^{+/+}$*Vim*$^{-/-}$ (*Vim*$^{-/-}$) and *GFAP*$^{-/-}$*Vim*$^{+/+}$ (*GFAP*$^{-/-}$); and (iii) double-knockout mice (*GFAP*$^{-/-}$*Vim*$^{-/-}$, dKO). Mice of various postnatal (PN) ages (ranging from PN0 to PN278) were included in the study. The animals were kept on a 12-hour light-dark cycle, with free access to food and water. They were handled according to the guidelines set by the ARVO statement for the use of animals in Ophthalmic and Vision Research, and all experiments were approved by the local animal experimentation ethics committee.

Electroretinographic Analysis

To test whether the lack of GFAP and/or vimentin affects *in vivo* retinal function, electroretinograms (ERGs) were recorded binocularly from wildtype, *Vim*$^{-/-}$, *GFAP*$^{-/-}$ and *GFAP*$^{-/-}$*Vim*$^{-/-}$ mice at the age of 8 weeks, as described previously (Tanimoto et al., 2009; Tanimoto et al., 2013). Mice were dark-adapted overnight and anesthetized using ketamine (66.7 mg/kg body weight) and xylazine (11.7 mg/kg body weight). The pupils were dilated and single-flash ERG responses were obtained under dark-adapted and light-adapted (with a background illumination of 30 cd/m^2 starting 10 min before recording) conditions. Single white-flash stimuli ranged from –4 to 1.5 log cd s/m^2 under dark-adapted and from –2 to 1.5 log cd s/m^2 under light-adapted conditions, divided into ten and eight steps, respectively. Ten

responses were averaged with inter-stimulus intervals of 5 s (for –4 to –0.5 log cd s/m^2) or 17 s (for 0 to 1.5 log cd s/m^2). Responses to trains of flashes (flicker) for a fixed intensity (0.5 log cd s/m^2; the International Society for Clinical Electrophysiology of Vision standard flash intensity (Marmor et al., 2004) with varying frequency (0.5, 1, 2, 3, 5, 7, 10, 12, 15, 18, 20 and 30 Hz) were obtained under dark-adapted conditions. Flicker responses were averaged either 20 times (for 0.5 to 3 Hz) or 30 times (for 5 Hz and above). Bandpass filter cutoff frequencies were 0.3 and 300 Hz for all ERG recordings. The ERG equipment consisted of a Ganzfeld bowl, a direct current amplifier, and a PC-based control and recording unit (Multiliner Vision; VIASYS Healthcare GmbH, Hoechberg, Germany).

Western blotting

Wildtype, single- and double-knockout mice (PN7 to PN60) were killed with carbon dioxide and the eyes quickly enucleated. Retinas were quickly isolated through a corneal incision and were homogenized. Retinal proteins (10 µg or 20 µg) were separated on 10-15% SDS-polyacrylamide gels and semi-dry-blotted onto Immobilon polyvinylidene fluoride transfer membranes (Millipore, Billerica, MA, USA). Membranes were blocked with 5% non-fat dry milk and subsequently incubated with primary antibodies (see Tables 1 and 2 for list of antibodies used, dilutions, and suppliers), rinsed, incubated with peroxidase-conjugated secondary antibodies, and washed. The reaction was visualized by enhanced chemiluminescence (ECL) using an ECL Western Blotting detection kit (Amersham Biosciences, Sweden). Protein levels were compared between wildtype and single- or double-knockout mice of the same age. The level of tubulin or of glyceraldehyde-3-phosphate dehydrogenase (GAPDH) in each sample was used as an internal loading control. Additionally, a western blot for Kir4.1 was performed to compare the levels of expression in the cerebellum of PN60 wildtype and *GFAP*$^{-/-}$*Vim*$^{-/-}$ mice (2.5 µg protein).

Morphological analysis

Mice were killed with carbon dioxide and the eyes quickly enucleated and immersed for 24 hours in Bouin's solution (Sigma, Saint Louis, USA) or 4% paraformaldehyde (PFA) in 0.1M Sörensen's buffer (28 mM NaH_2PO_4 and 72 mM $NaHPO_4$; pH 7.2). After rinsing and dehydrating, the eyes were embedded in paraffin and sectioned (4-5µm). Sections were collected on glass slides and counterstained with hematoxylin and eosin.

Immunohistochemistry

Eyes from PN0-60 and PN278 mice were fixed in 4% paraformaldehyde in Sörensen's buffer (0.1 M; pH 7.2) for two hours at 4°C, rinsed, cryoprotected, embedded, and frozen, as

described in detail in (Wunderlich et al., 2010). Sections (12 µm) were obtained on a cryostat, air-dried, and stored at -20°C until further processing. For immunohistochemical analysis, retinal sections were blocked with PBS containing Triton-X (0.25%) and BSA (1%) (PBS-TB), and the corresponding normal serum (5%) at room temperature for one hour. This was followed by overnight incubation at 4°C with the primary antiserum, diluted in PBS-TB containing 2% normal serum. The primary antibodies and lectin used, dilutions, and suppliers are listed in Table 1. Following washes with PBS, sections were incubated with secondary antibodies (Table 2). Stained sections were mounted with an anti-fading medium (VECTASHIELD®, Vector Laboratories, CA, USA) and examined with a fluorescence microscope (Axiophot, Carl Zeiss Meditec, Inc., Germany). Images were taken with a digital camera and accompanying software (Axiovision 4.2, Carl Zeiss Meditec) using the same illumination and acquisition settings for all sections processed with the same antibody. Negative controls were included in which the primary antibody was omitted.

TUNEL assay

The occurrence of dying retinal cells was analyzed with a terminal deoxynucleotidyl transferase dUTP nick end-labeling (TUNEL) assay, employing the *In Situ* Cell Death Detection Kit, TMR red (Roche Diagnostics, Mannheim, Germany). The enzyme solution and the labeling solution were diluted 1:9 and 1:4, respectively. The two were mixed 1:4.44 immediately before application to the cryostat sections, which were incubated for 45 minutes at 37°C. The reaction was thereafter stopped by three washes with cold PBS before mounting with VECTASHIELD®. The sections were examined with a fluorescence microscope, as described above.

RESULTS

Electroretinographic (ERG) Analysis

To investigate retinal function in wildtype, *Vim*$^{-/-}$, *GFAP*$^{-/-}$, and *GFAP*$^{-/-}$*Vim*$^{-/-}$ mice, we performed ERG recordings *in vivo*. Full-field ERG is a mass response of transient electrical activity of the entire retina to light stimulation, but importantly, functionality of certain retinal cells types can be assessed by varying stimulus intensity, stimulus frequency, and brightness of static background light.

Figure 1 shows representative single flash ERG traces from each genotype recorded under dark-adapted conditions. The negative deflection that appears directly after light stimulation onset (time 0) at intensities brighter than -2 log cd s/m^2 corresponds to the a-wave, which is initiated by the activity of rod photoreceptor cells. The whole activation phase

of the rod outer segments is visible, when it saturates at high stimulus intensities, such as 1.0 and 1.5 log cd s/m^2, as the response reaches its peak before the onset of the following positive deflection (b-wave). A comparison of all four mouse lines showed no difference in the dark-adapted single flash a-wave up to the highest intensity of the protocol (Fig. 1A), indicating that the lack of GFAP and/or vimentin had no measurable effect on the photoreceptoral responses.

The single-flash ERG b-wave is evoked by both the rod and the cone systems depending on the ERG paradigm, i.e. responses at stimulus intensities up to -2 log cd s/m^2 under dark-adapted conditions are generated exclusively by the rod system (scotopic conditions), whereas at stimulus intensities brighter than -2 log cd s/m^2 under dark-adapted conditions by both systems (mesopic conditions), and at any stimulus intensity under light-adapted conditions usually by the cone system (photopic conditions). Under all three recording conditions, *Vim*$^{-/-}$ and *GFAP*$^{-/-}$ mice showed comparable responses to those in wildtype mice (Fig. 1A, 1B, 1D), indicating that the output signals from rod and cone photoreceptors as well as the responsiveness of both types of depolarising bipolar cells were not affected by a lack of vimentin or GFAP. In contrast, *GFAP*$^{-/-}$*Vim*$^{-/-}$ mice showed some b-wave changes under mesopic conditions of the dark-adapted single flash ERG (Fig. 1A, 1C, 1D). Whereas the a-wave and the ascending edge of the b-wave were unchanged (Fig. 1C), the top of the *GFAP*$^{-/-}$*Vim*$^{-/-}$ b-wave was enhanced [*i.e.,* larger b-wave amplitude (Fig. 1D)], which was accompanied by an alteration of the trailing edge of the b-wave. In wildtype, *Vim*$^{-/-}$, and *GFAP*$^{-/-}$ mice, the shape of the trailing edge was concave, whereas in *GFAP*$^{-/-}$*Vim*$^{-/-}$ mice this concavity became less prominent, particularly at high stimulus intensities (Fig. 1A, 1C). As a result, the light-evoked responses of *GFAP*$^{-/-}$*Vim*$^{-/-}$ mice returned to baseline much more slowly than those in the other mice.

Additionally, we examined the ability of wildtype and *Vim*$^{-/-}$*GFAP*$^{-/-}$ mice to respond to train of flashes (flicker) by performing a dark-adapted flicker ERG frequency series at a fixed mesopic intensity [0.5 log cd*s/m^2; the International Society for Clinical Electrophysiology of Vision standard flash intensity (Marmor et al., 2004)], which provides an overview of the functionality of both photoreceptor systems without using any background light (Tanimoto et al., 2009; Tanimoto et al., 2013). In this protocol, the responses are dominated by the rod system up to about 3 Hz and by the cone system at 5 Hz and higher frequencies. The phenotype of *GFAP*$^{-/-}$*Vim*$^{-/-}$ mice detected at 0.5 Hz in the flicker ERG was similar to that observed in the dark-adapted single-flash ERG, *i.e.,* the negative-going response (a-wave analogue) and the onset and the initial part of the positive-going response (b-wave analogue) were normal in *GFAP*$^{-/-}$*Vim*$^{-/-}$ mice, whereas the top and the trailing edge of the positive-going response were enhanced [Fig. 1E, 1F (top), 1G (blue shading)], and consequently, the

responses in *GFAP*$^{-/-}$*Vim*$^{-/-}$ mice returned to baseline slower than those in wildtype mice. With increasing stimulus frequency, the response amplitude became smaller in wildtype mice due to shorter intervals of flicker stimuli. This amplitude decline was much faster in *GFAP*$^{-/-}$*Vim*$^{-/-}$ mice, and therefore, the situation reversed, *i.e.,* flicker responses in *GFAP*$^{-/-}$*Vim*$^{-/-}$ mice were smaller than those in wildtype mice at 5 Hz and above [Fig. 1E, 1F (bottom), 1G (red shading)], and the *GFAP*$^{-/-}$*Vim*$^{-/-}$ retina could not resolve the flickering stimulus at 30 Hz. Here, we found notable amplitude reductions in the frequency range usually attributed to the cone system (Tanimoto et al., 2009).

Morphology and TUNEL staining

No obvious morphological differences were noted between the different genotypes in hematoxylin-eosin stained sections (Fig. 2A, 2B). The same overall thickness was observed for all the specific retinal layers, except that in *GFAP*$^{-/-}$*Vim*$^{-/-}$ mice, the vitreal margin of the retina and, at times, the ganglion cell layer appeared separated from the rest of the retina in some places. TUNEL staining was observed sporadically in a very small number of cells in the outer nuclear layer in the first postnatal week and in the inner nuclear layer from PN14-21 in both, wildtype and knockout animals. No aberrant cell death was noted in *GFAP*$^{-/-}$*Vim*$^{-/-}$ mouse retinas at any of the time points examined (not shown).

Analysis of retinal proteins

Although no differences were observed between wildtype and *GFAP*$^{-/-}$*Vim*$^{-/-}$ mice with regards to the general morphology, we found, as described above, that the retinal response to light stimuli were altered in the latter. To evaluate whether the lack of IFs caused alterations in the distribution of a specific retinal cell type, an immunohistochemical analysis using several well-established cell markers was performed. For some of the proteins, an estimate of the relative levels present in retinal homogenates was, in addition, performed by using western blotting. In both cases, retinal samples were obtained from animals of various ages, although the images depicting protein localization show PN60 retinas, unless specified otherwise. In the latter, the distribution of most markers analyzed agreed with that described in previous reports (references are provided in Table 1).

Neuronal markers

Apart from the occasional disruption of the innermost retina in some *GFAP*$^{-/-}$*Vim*$^{-/-}$ mice, ganglion cells appeared labeled with the transcription factor Brn3a (Fig. 2C, 2D) and the neuron-specific nuclear protein NeuN (Fig. 2E, 2F) in all specimens analyzed. NeuN labeled also a few cells in the inner part of the inner nuclear layer (Fig. 2E, 2F). The calcium-binding

proteins parvalbumin and calbindin were detected in cell bodies with the position of amacrine cells and, in addition, weakly in a few cells in the ganglion cell layer (Fig. 2G, 2H; 2I, 2J). Several horizontal cells were also positive for calbindin in both wildtype and double-knockout mice (Fig. 2I, 2J).

Upon absorption of light by the rods, these cells hyperpolarize. This leads to a reduction in glutamate release by the rods and a consequent deactivation of metabotropic glutamate receptors (mGluR6) sitting on the contacting bipolar cells, which then depolarize (rod ON-bipolar cells) (Ruether et al., 2010). Our functional analysis revealed an increase in the amplitude of the b-wave (which originates from depolarizing bipolar cells) under mesopic conditions of the dark-adapted single-flash ERG (*i.e.,* with contribution from both, the rod and cone systems), but not under photopic conditions. Using an antibody against protein kinase C alpha (PKC-α), we examined whether there were differences in the distribution of rod bipolar cells or in their morphology. In both genotypes, immunostaining was observed in the cell body and in processes extending towards the outer and inner plexiform layers with no apparent differences (Fig. 2K, 2L). The western blot analysis of PKC-α expression showed also similar levels of the protein in the retinas of wildtype and *GFAP*$^{-/-}$*Vim*$^{-/-}$ mice (Fig. 4).

Staining for recoverin, a small Ca^{2+}-binding protein, resulted in labeling of a small subpopulation of cells located in the outer half of the inner nuclear layer, which are likely to correspond to cone bipolar cells (Fig. 2M, 2N). Immunoreactivity was detected also in the inner plexifom layer, next to the inner nuclear layer. In addition, strong labeling of photoreceptors including their inner and outer segments, cell bodies, and terminals in the outer plexifom layer was observed. Again, no discernable differences were noted between the two genotypes.

The distribution of other markers associated with photoreceptors showed also the same pattern, in both wildtype and *GFAP*$^{-/-}$*Vim*$^{-/-}$ mice. Immunolabeling with an antibody against dystrophin resulted in a distinct punctate staining in the outer plexiform layer (Fig. 2O, 2P) and is likely to correspond to photoreceptor terminals. In both, wildtype and *GFAP*$^{-/-}$*Vim*$^{-/-}$ mouse retinas, the rod outer segments were densely immunopositive for the rod-specific visual pigment rhodopsin, while the cell bodies showed a much weaker labeling, as expected for healthy, differentiated rod photoreceptors (Fig. 2Q, 2R). Fluorophore-conjugated peanut agglutinin (PNA), a carbohydrate-specific lectin that selectively binds to the surface of cones, was detected in the synaptic pedicles at the level of the outer plexiform layer and the inner and the outer segments of cones (Fig. 2S, 2T). Small variations were noted in the same section, but no consistent differences could be seen between wildtype and *GFAP*$^{-/-}$*Vim*$^{-/-}$ mice.

Glial markers

We have screened for several proteins that can be used to identify glial Müller cells and/or are involved in some of the main functions of these cells, such as regeneration of visual pigment and homeostasis of potassium, water and glutamate. Cellular retinaldehyde binding protein (CRALBP), which participates in the processing of visual retinoids, was expressed in the retinal pigment epithelium (not shown) and in the Müller cells, from their endfeet at the inner limiting membrane to the outer limiting membrane, including their cell bodies in the inner nuclear layer (Fig. 3A, 3B). In Fig. 3B, there appears to be a reduced CRALBP expression in the proximal processes of the Müller cells; this figure illustrates also the disruption of the vitreal surface occasionally seen in the *GFAP*$^{-/-}$*Vim*$^{-/-}$ mice. These observations were, however, not consistent, and western blot analysis also did not show any differences in the levels of CRALBP between the two genotypes (Fig. 4). Antibodies against the HMG-box transcription factor Sox-9 recognized the protein in the nuclei of Müller cells in retinas of mice older than PN14 (Fig. 3C, 3D) and in the retinal pigment epithelium (not shown). Neither the distribution nor the levels (Fig. 4) of Sox-9 were found to be different in *GFAP*$^{-/-}$*Vim*$^{-/-}$ mouse retinas compared to their wildtype controls.

Two proteins involved in glutamate homeostasis were analyzed: the glutamate aspartate transporter (GLAST) and glutamine synthetase (GS), which participate in glutamate metabolism. GLAST immunoreactivity was found in all retinal layers in association with Müller cell processes (Fig. 3E, 3F) and a similar distribution was observed with GS (Fig. 3G, 3H). However, while the expression of GLAST appeared slightly increased in *GFAP*$^{-/-}$*Vim*$^{-/-}$ mice, GS levels were found to be reduced (Fig. 4).

Moreover, we have examined the distribution and level of expression of the water channel aquaporin 4 (AQP4). The immunolabeling pattern resembled that of GLAST and GS with no obvious differences noted between the two genotypes (Fig. 3I, 3J). In western blots, it was seen that AQP4 protein levels increased steadily with age and a second band of ~60 kDa, which may represent a dimeric form of AQP4, was found at PN60 (Fig. 4). No differences were noted between wildtype and *GFAP*$^{-/-}$*Vim*$^{-/-}$ mice in the levels of AQP4 in younger ages. However, at PN60, a slight reduction in the levels of the monomeric form (~32 kDa) and an increase in the levels of the putative dimeric form were observed in *GFAP*$^{-/-}$*Vim*$^{-/-}$ mice (Fig. 4).

Distinct differences were noted in the levels of the inwardly rectifying potassium (Kir) channels, Kir2.1 and Kir4.1. Immunostaining corresponding to Kir2.1 was observed mainly in the proximal processes of Müller cells and in cell bodies in the inner nuclear layer and ganglion cell layer (Fig. 3K-3R), starting at around PN14. Kir4.1 labeling was, in addition, found at the level of the outer limiting membrane, in Müller cell distal processes and endfeet

and in association with retinal vessels both at PN21 (Fig. 3M, 3N) and at PN60 (Fig. 3O, 3P). In retinas of *GFAP*$^{-/-}$*Vim*$^{-/-}$ mice, an overall reduction of Kir2.1 was noted (Fig. 3K, 3L). Likewise, a reduction in Kir4.1 was observed, particularly in the proximal Müller cell processes, which appeared less intensely labeled (Fig. 3L, 3N, 3P). Kir4.1 immunoreactivity was reduced in the same manner in vimentin single-knockout mice (Fig. 3R), but not in GFAP single knockouts (Fig. 3Q). Kir4.1-staining remained very strong until at least PN278, and the difference between wildtype and *GFAP*$^{-/-}$*Vim*$^{-/-}$ mouse retinas was still observed (data not shown). In western blots, the expression of the two potassium channels was seen to increase with age in both wildtype and *GFAP*$^{-/-}$*Vim*$^{-/-}$ mice (Fig 5A). This analysis revealed also a clearly decreased expression of Kir2.1 and Kir4.1 in retinas of the double-knockout mice as compared to the wildtype (Fig. 5A). Kir4.1 expression was also analyzed in lysates of cerebellum and we found that levels were similarly reduced in PN60 *GFAP*$^{-/-}$*Vim*$^{-/-}$ mice compared with wildtype controls (Fig. 5B).

DISCUSSION

Mature retinal glial cells respond to structural and metabolic disruptions of normal neuron-glia interactions with a massive and relatively fast up-regulation of GFAP and vimentin (Lewis et al., 1989), increased synthesis of several other glia-associated proteins (Wunderlich et al., 2010; Roesch et al., 2012) and increased stiffness of Müller cells (Lu et al., 2011), resulting in astroglial activation and reactive gliosis (Pekny and Nilsson, 2005; Pekny and Lane, 2007).

Previous studies have shown that the lack of astrocyte IFs attenuates the responses of astroglial cells to stress (Pekny et al., 1999, Wilhelmsson et al., 2004; Li et al., 2008), but the unchallenged retinas of *GFAP*$^{-/-}$*Vim*$^{-/-}$ mice exhibit a normal morphology (Kinouchi et al., 2003; Lundkvist et al., 2004; Verardo et al., 2008). This was confirmed in the present study, where we noted that the overall structure of the retina was similar in *GFAP*$^{-/-}$*, Vim*$^{-/-}$, *GFAP*$^{-/-}$ *Vim*$^{-/-}$, and wildtype mice. There were no signs of degeneration, and TUNEL staining showed the same pattern and degree of developmental cell death in all genotypes and a comparable number of occasional positive cells in the older ages (data not shown). Nevertheless, we observed that the innermost layer of the retina appeared sheared off from the rest of the retina in many places, especially in young animals. Earlier studies have also reported on such a phenomenon and it was concluded that the retina was most likely intact before enucleation and processing of the tissue, and that the shearing was due to mechanical stress inflicted during tissue handling (Kinouchi et al., 2003, Lundkvist et al., 2004; Verardo et al., 2008). Such a lower resistance to mechanical stress is not surprising as different studies have shown that mechanical properties of astroglial cells, such as stiffness and elasticity, depend on the amount of IFs (Eckes et al., 1998; Lu et al., 2011).

When characterizing control animals for retinal transplantation studies, the retinal function of *GFAP*$^{-/-}$*Vim*$^{-/-}$ mice was previously described as being normal as well (Kinouchi et al., 2003); nevertheless these experiments were not the primary focus of that study. In our more extensive ERG analysis, we found that the lack of GFAP and vimentin does affect the electrophysiological responses of the healthy retina to light stimuli. We have shown that the amplitude of the mesopic b-wave was increased in *GFAP*$^{-/-}$*Vim*$^{-/-}$ mice while the a-wave was unchanged. We argue that this functional phenotype was due only to the rod system (in spite of the fact that alterations were noted under mesopic conditions), since there were no similar functional alterations of the cone system responses under photopic conditions. We found that the ERG responses to flicker stimulations were similarly altered in *GFAP*$^{-/-}$*Vim*$^{-/-}$ mice, where the top and the trailing edge of the positive-going response (b-wave analogue) were increased and its return to the baseline slowed down. With increasing stimulus frequency, however, the responses of *GFAP*$^{-/-}$*Vim*$^{-/-}$ mice became smaller than those of wildtype mice. The decline in amplitude occurred in the frequency range usually attributed to the cone system (Tanimoto et al., 2009). Since there was no notable alteration in cone system responses in the light-adapted single-flash ERG, there are at least two possible interpretations for this functional phenotype in *GFAP*$^{-/-}$*Vim*$^{-/-}$ mice: 1) the cone system functionality was not strongly affected, therefore, the alteration could be detected only during continuous repetitive stimuli but not after a single stimulation; 2) neurons of the cone system were normal, but the cone system signaling was disturbed, as the retinal network (including cone pathways) became saturated due to the prolonged photoresponses of the rod system (for a similar situation, see Seeliger et al., 2011). In this study, we could not discriminate between these two possibilities, since it is, to our knowledge, not possible by changing the ERG recording parameters.

The main source of the b-wave is depolarizing bipolar cells (*i.e.,* rod bipolar cells and ON cone bipolar cells) and increases in amplitude could occur if the output from rods and cones and/or their responsiveness is increased. We found that the distribution and level of expression of some of the proteins involved in the rod and cone pathways were comparable in wildtype and *GFAP*$^{-/-}$*Vim*$^{-/-}$ mice.

Müller cells also contribute to the b-wave by generating slow and small negative-going signals (slow PIII), which are usually masked by the large positive-going signals from depolarising bipolar cells (Frishman, 2006). In order to assess whether GFAP and/or vimentin deficiency had an effect on the size of the Müller cell population, we analyzed the expression of Sox-9 and of CRALBP. Sox-9, a member of the SRY-related HMG-box (Sox) gene family of transcription factors, is expressed in the retina in progenitor cells and in Müller cells (Muto et al., 2009). This expression is regulated by Notch signaling and promotes

differentiation of Müller cells at the expense of rod photoreceptors, such that a reduction in Sox-9 levels leads to the specification of a lower number of Müller cells and an increase in the number of rods (Muto et al., 2009). Most recently, we demonstrated markedly reduced Notch signaling capacity in astrocytes derived from *GFAP*$^{-/-}$*Vim*$^{-/-}$ mice (Wilhelmsson et al., 2012). In the present study, we found a similar level of Sox-9 expression between PN7 and PN60 in the retinas of wildtype and of *GFAP*$^{-/-}$*Vim*$^{-/-}$ mice, suggesting that the lack of these IF proteins did not affect the number of Müller cells. Moreover, we did not find that the amplitude of the scotopic a-wave (reflecting rod activity) was increased in *GFAP*$^{-/-}$*Vim*$^{-/-}$ animals, which could be expected if these animals had an increased number of rods cells.

CRALBP is a retinoid-binding cytosolic protein involved in the regeneration of cone visual pigment and is expressed in the retinal pigment epithelium (RPE) and in Müller cells from their apical microvilli to the endfeet (Bunt-Milam and Saari, 1983; Collery et al., 2008). The procedure used to harvest the retinas for western blot analysis could potentially yield variable amounts of RPE contamination. Further, as mentioned above, we observed a localized reduced resistance of the inner retinal surface of *GFAP*$^{-/-}$*Vim*$^{-/-}$ mice to mechanical stress. It is thus possible that a fraction of the proteins normally present in the Müller cell endfeet was lost in some places during dissection of the retinas. Yet, our analysis showed no differences in the amounts of CRALBP between the different genotypes, further indicating that the size of the Müller cell population was not affected by the lack of GFAP and vimentin.

The functional abnormalities observed in the present study in *GFAP*$^{-/-}$*Vim*$^{-/-}$ mice seem therefore likely to reflect changes in synaptic transmission or homeostatic changes, rather than alterations in cell numbers. We found in the present study a reduction in the expression of the inwardly rectifying potassium (K^+) channels Kir2.1 and Kir4.1 in *GFAP*$^{-/-}$*Vim*$^{-/-}$ mouse retinas. These channels are found in Müller cells and are important for the regulation of extracellular K^+ concentrations, allowing entry or exit of K^+ depending on their specific distribution along the cell membrane and on the K^+ levels generated by neuronal activation (Newman, 1993; Kofuji et al., 2002). Light absorption by the photoreceptors initiates a series of events that result in reduced extracellular K^+ concentration in the subretinal space and increased concentrations at the level of the outer and inner plexiform layers. These changes in extracellular K^+ trigger changes in the membrane potential of the Müller cells, which, through activation of Kir channels, clear the extracellular K^+, redirecting it to the vitreous and to the circulation. This is mediated mainly by Kir4.1 channels that are abundant in the endfeet and perivascular processes of the Müller cells, in a mechanism of spatial buffering denominated K^+ siphoning (Newman and Reichenbach, 1996; Kofuji and Newman, 2004). In addition, Kir2.1 channels, which are more homogeneously distributed along the Müller cell, and Kir4.1/Kir5.1 heterotetrameric channels are believed to mediate K^+ influx at the level of

the synaptic layers (Kofuji et al., 2002; Ishii et al., 2003). We did not observe Kir5.1 expression in retinal glia cells (not shown), so the focus of our observations was on Kir2.1 and Kir4.1.

We found, by western blot analysis, a clear reduction in Kir2.1 levels in *GFAP*$^{-/-}$*Vim*$^{-/-}$ mice mainly at the later time points examined (PN21 and PN60) whereas the reduction in Kir4.1 levels was detectable already at PN14. In tissue sections, a small general decrease in Kir2.1 immunostaining was seen while Kir4.1 expression was significantly reduced mainly in the inner retina. The latter was noted also in *Vim*$^{-/-}$ mice, but not in *GFAP*$^{-/-}$ mice. It seems thus that the absence of vimentin is sufficient to affect the number and/or the distribution of certain Kir channels in Müller cells. In any case, this could lead to an insufficient clearance of extracellular K^+ and an insufficient spatial buffering of this ion.

Reduced expression and/or mislocation of Kir4.1 are observed in several pathologic conditions affecting the retina, such as diabetes (Pannicke et al., 2006), detachment (Bringmann et al., 2007), or ischemia (Hirrlinger et al., 2010). However, in these conditions, the alterations in Kir4.1 channels occur in association with increased expression of GFAP and vimentin and various degrees of neuronal damage, which is not the case with the double-knockout mice analyzed here. A total inactivation of Kir4.1 channels in an otherwise intact mouse retina has been achieved by a targeted disruption of the Kir4.1 gene (Kofuji et al., 2000). In these animals, Müller cells displayed normal morphology and glutamine synthetase expression but their resting membrane potential was significantly depolarized and K^+ conductance markedly reduced. It was also found that the light-induced slow PIII response of the ERG was completely absent.

Under normal conditions, the light-evoked hyperpolarization of photoreceptors reduces the extracellular K^+ concentration in the subretinal space. This triggers K^+ fluxes through Müller cells (the negative-going slow PIII response) and a positive-going response of the retinal pigment epithelium, which is counteracted by PIII. Using an eyecup preparation, Kofuji et al. (2000) showed that the intraretinal b-wave amplitude was increased in retinas of Kir4.1 knockout mice, which was attributed to the loss of the slow PIII (Kofuji et al., 2000). The same effect was observed following addition of Ba^{2+} to block the K^+ channels on Müller cells in preparations of normal mouse retinas, confirming that the PIII component is the result of currents produced in these cells (Kofuji et al., 2000). Homozygous Kir4.1 knockout mice die during the first postnatal weeks before retinal development is complete, so that the effects observed in our study at 8 weeks of age cannot be studied in these animals. Nevertheless, similar results were obtained in older animals, heterozygous for the Kir4.1 deletion (Wu et al., 2004). Kir4.1 channels have been found also in the retinal pigment epithelium (Rehak et al., 2009). The contribution of these cells to total Kir4.1 levels could not be appreciated in our

western blots as the retinas were dissected free of RPE, but no differences were noted in this layer by immunocytochemistry in cross sections obtained between wildtype and *GFAP*$^{-/-}$*Vim*$^{-/-}$ mice. The b-wave alterations observed in the present study in *GFAP*$^{-/-}$*Vim*$^{-/-}$ mice (increased amplitude and prolonged decay) are thus likely to have resulted from a reduction in the number (and possibly abnormal distribution) of K^+ channels on Müller cells.

The most significant protein expression alterations observed in the present study in *GFAP*$^{-/-}$*Vim*$^{-/-}$ mice were also noted in *Vim*$^{-/-}$ mice, but not in *GFAP*$^{-/-}$ mice, indicating that vimentin plays a more crucial role. Further, while GFAP builds abnormal IF bundles in *Vim*$^{-/-}$ astrocytes, vimentin cannot form IFs on its own (Eliasson et al., 1999), with consequences predicted to go beyond a mere alteration of the mechanical properties of the cell. Vimentin appears to be an organizer of many important proteins associated with cell-cell adhesion, migration, and cell signaling (reviewed in Ivaska et al., 2007). It has been suggested to be involved in the organization of cell membrane complexes (reviewed in Ivaska et al., 2007) and seems to influence the localization and activity of sodium/glucose cotransporter in membrane rafts (Runembert et al., 2002). Vimentin binds also to phosphorylated extracellular signal-regulated kinases 1 and 2 (ERK1/2), regulating the intracellular translocation of these MAP kinases (MAPK; Perlson et al., 2005). It has been shown that while bound to vimentin, ERK kinase activity is maintained, as the association of ERK1/2 with vimentin prevents their dephosphorylation (Perlson et al., 2006). The inability to produce vimentin could thus affect processes that rely on ERK activation. In the retina, ERK-mediated signaling takes place in ganglion cells and in Müller cells, mediating *e.g.,* the action of several trophic factors and cytokines as well as proliferation and at least some of the responses of Müller cells to mechanical stress (Wahlin et al., 2000; Geller et al., 2001; Cheng et al., 2002; Azadi et al., 2007; Fischer et al., 2009; Lindqvist et al., 2010). We could not find any differences in the distribution or levels of the neuronal markers probed. These results suggest that if the levels of phosphorylated ERK1/2 were indeed reduced in the retina of *GFAP*$^{-/-}$*Vim*$^{-/-}$ mice, the effect is not sufficient to affect the proliferation/differentiation of the Müller cells or the level of trophic support provided by these cells during development.

As mentioned above, a reduction in the expression of Kir2.1 and Kir4.1 channels has been observed in conditions where IFs are up-regulated. In the present study, we also found a reduction, despite the inability of the cells to form IFs. These observations suggest that regulation of Kir2.1- and Kir4.1-expression can occur independently of the presence or amounts of IFs. However, a direct or indirect role for vimentin in the intracellular translocation of Kir2.1 and Kir4.1 may not be ruled out. Dystrophin-associated protein complexes are supposed to integrate Kir4.1 into protein complexes at the cell membrane. The water-channel AQP4 is often connected to these complexes as well; a functional coupling of Kir4.1

and AQP was debated but seems to be disproved in most cases (Connors and Kofuji, 2006; Ruiz-Ederra et al., 2007; Fort et al., 2008; Zhang and Verkman, 2008; Satz et al., 2009; Sene et al., 2009). Our results seem to support that there is at least no functional coupling, as the levels of Kir4.1, but not AQP4, were reduced in the *GFAP*$^{-/-}$*Vim*$^{-/-}$ mouse retinas. We could not detect glial dystrophin expression, but rather a punctuate staining in the outer plexiform layer, localized most likely at the photoreceptor terminals. Further, patients with Duchenne and Becker muscular dystrophy, caused by mutations in the gene coding dystrophin have attenuated, rather than increased, ERG b-waves (Satz et al., 2009; Cibis et al., 1993; Pillers et al., 1999). It appears thus that the alterations observed in *GFAP*$^{-/-}$*Vim*$^{-/-}$ mice cannot be explained by abnormal dystrophin expression.

Further, vimentin is highly expressed by many cell types during development. The morphology and expression of several cell specific markers appeared normal in *Vim*$^{-/-}$ and *GFAP*$^{-/-}$*Vim*$^{-/-}$ mice, suggesting that lack of vimentin had no major impact on the development of the retina. However, we cannot exclude the possibility that the maturation of the Müller cells was somewhat delayed or impaired in these animals. It has been shown that the amplitude of the inward K^+ currents in Müller cells is dependent on the degree of differentiation of these cells (reviewed in Bringmann et al., 2006). Amplitudes thus increase in an age-dependent manner, supported by an increasing number of K^+ channels. In the present study, we show that the expression of Kir2.1 and Kir4.1 gradually increased along with age in both wildtype and in *GFAP*$^{-/-}$*Vim*$^{-/-}$ mice, but that the increase rate was lower in the latter, which could suggest that Müller cells were somewhat less mature in these animals.

In summary, we have shown that the amplitude of the mesopic b-wave is increased in *GFAP*$^{-/-}$*Vim*$^{-/-}$ mice and that the levels of the inwardly rectifying K^+ channels, Kir2.1 and Kir4.1 are decreased, which may explain, at least in part, the electrophysiological findings. However, the possibility that other factors, not directly related to the level or distribution of Kir4.1 channels, may contribute to the alterations observed can not be excluded. Especially, since we observed a clear Kir2.1- and Kir4.1-reduction also in vimentin single knockouts, while their b-wave showed only a slight tendency towards higher amplitude. We found also a reduced expression of Kir4.1 in association with the retinal vasculature, at least in the earlier ages. The functional alterations seen in the retinas of *GFAP*$^{-/-}$*Vim*$^{-/-}$ mice could therefore be the result of a combination of different factors. Nevertheless, our observations indicate that the expression of intermediate filament proteins (in particular vimentin) is required for normal retinal function. Further, we found that Kir4.1 levels were reduced also in the cerebellum of *GFAP*$^{-/-}$*Vim*$^{-/-}$ mice, suggesting that the inability to produce IF proteins and IFs may result in functional abnormalities also in this part of the CNS.

FIGURE LEGENDS

Figure 1. Functional characterization of wildtype (*GFAP*$^{+/+}$*Vim*$^{+/+}$, WT), *Vim*$^{-/-}$, *GFAP*$^{-/-}$, and *GFAP*$^{-/-}$*Vim*$^{-/-}$ mice *in vivo* by electroretinography (ERG). **(A, B)** Representative single flash ERG recordings from WT (black), *Vim*$^{-/-}$ (blue), *GFAP*$^{-/-}$ (green), and *GFAP*$^{-/-}$*Vim*$^{-/-}$ (red) mice (age 8 weeks) for increasing stimulus intensity under dark-adapted **(A)** and light-adapted **(B)** conditions. **(C)** Overlay of the response traces of WT (black) and *GFAP*$^{-/-}$*Vim*$^{-/-}$ (red) mice from **(A)** (left) and **(B)** (right). **(D)** Box-and-whisker plot of dark-adapted (DA) and light-adapted (LA) single flash b-wave amplitudes in WT (black), *Vim*$^{-/-}$ (blue), *GFAP*$^{-/-}$ (green), and *GFAP*$^{-/-}$*Vim*$^{-/-}$ (red) mice. The top and the trailing edge of the *GFAP*$^{-/-}$*Vim*$^{-/-}$ b-wave was increased at middle and high stimulus intensities under dark-adapted conditions, resulting in a delayed return of the light-evoked responses to baseline. **(E)** Representative flicker ERG frequency series from WT (black) and *GFAP*$^{-/-}$*Vim*$^{-/-}$ (red) mice at a flash intensity of 0.5 log cd s/m^2 under dark-adapted conditions. **(F)** Overlay of the response traces of WT (black) and *GFAP*$^{-/-}$*Vim*$^{-/-}$ (red) mice from **(E)**. **(G)** Top: Box-and-whisker plot of flicker ERG response amplitudes in WT (black) and *GFAP*$^{-/-}$*Vim*$^{-/-}$ (red) mice. Bottom: difference of median amplitudes (*GFAP*$^{-/-}$*Vim*$^{-/-}$ median amplitude – WT median amplitude, for each stimulus frequency). Whereas the *GFAP*$^{-/-}$*Vim*$^{-/-}$ flicker responses were larger than the WT responses at low stimulus frequencies (blue shading), they decrease much faster with increasing stimulus frequency and became smaller at 5 Hz and above (red shading). In all quantitative plots **(D, G)**, boxes indicate the 25% and 75% quantile range, whiskers indicate the 5% and 95% quantiles, and the asterisks indicate the median of the data. WT (n=4), *Vim*$^{-/-}$ (n=6), *GFAP*$^{-/-}$ (n=6), *GFAP*$^{-/-}$*Vim*$^{-/-}$ (n=6).

Figure 2. Retinal structure and localization of neuronal markers in wildtype mice (*GFAP*$^{+/+}$*Vim*$^{+/+}$, WT) and in *GFAP*$^{-/-}$*Vim*$^{-/-}$ mice (double-knockout mice, dKO). **(A, B)** Cryostat sections of retinas at PN60 stained with hematoxylin and eosin (H&E). The retinas of WT **(A)** and dKO **(B)** mice both show a clearly stratified structure with all layers of comparable thickness. **(C-T)** Stainings with well-established cell marker proteins did not reveal any obvious differences in the distributions of the specific neuronal cell types in retinas of WT and dKO: **(C, D)** Brn3a staining in the nuclei of ganglion cells in GCL. **(E, F)** NeuN staining in ganglion cells, a few amacrine cells in the INL and displaced amacrine cells in the GCL. **(G, H)** Parvalbumin (Parvalb) staining in some amacrine cells. **(I, J)** Calbindin (Calb) staining in horizontal cells in the INL and some amacrine cells. **(K, L)** Protein kinase C alpha (PKC) staining in rod ON-bipolar cells in the INL and their processes in the OPL and IPL. **(M, N)** Recoverin (Recov) staining in photoreceptors and cone bipolar cells. **(O, P)** Punctate

dystrophin labeling in the OPL. **(Q, R)** Rhodopsin (Rho) staining in the outer segments of rod photoreceptor cells. **(S, T)** Peanut agglutinin (PNA) staining in cone segments. ONL, outer nuclear layer; OPL, outer plexiform layer; INL, inner nuclear layer; IPL, inner plexiform layer; GCL, ganglion cell layer. Scale bar, µm.

Figure 3. Localization of glial proteins in the different genotypes. **(A, B)** Cellular retinaldehyde binding protein (CRALBP) staining was observed in Müller glial cell bodies and processes extending from the outer to the inner limiting membranes in both wildtype (*GFAP*$^{+/+}$*Vim*$^{+/+}$, WT) and *GFAP*$^{-/-}$*Vim*$^{-/-}$ mice (dKO). **(C-D)** The SRY-box 9 (SOX9) protein was detected in the nuclei of Müller cells in the INL of both genotypes. **(E, F)** The glutamate aspartate transporter (GLAST) was found in Müller cells and in their radial processes as well as in the OPL and IPL. No obvious differences between WT and dKO could be observed. **(G, H)** The distribution of glutamine synthetase (GS) appeared similar in WT and dKO mice, except that in the latter staining of the Müller cell radial processes was somewhat weaker. **(I, J)** Aquaporin 4 (AQP4) staining was found in Müller cells, with particularly prominent labeling associated with vessels. **(K, L)** Müller cell bodies and processes were positive for the inwardly rectifying potassium (Kir) channel Kir2.1. The distribution was comparable in both genotypes, the dKO having a slightly weaker overall fluorescence intensity. **(M-R)** In WT **(M** and **O)**, immunostaining with an antibody against Kir4.1 produced a distinct Müller cell labeling within the retina at the level of the outer and inner limiting membranes and in association with vessels. In dKO mice **(N, P)**, the staining in the proximal processes of Müller cells was clearly reduced. Retinas of *GFAP*$^{-/-}$-single-knockout mice **(Q**, GFAP**)** showed a similar distribution pattern as the WT, whereas Kir4.1 staining in *Vim*$^{-/-}$-single-KO mice **(R**, vim**)** resembled that of *GFAP*$^{-/-}$*Vim*$^{-/-}$ mice. **(M**, **N)** PN21, all other PN60. Note also that the inner border of the retina was disrupted in some places in GFAP$^{+/+}$Vim$^{+/+}$ (double-knockout, dKO) mice (*). ONL, outer nuclear layer; OPL, outer plexiform layer; INL, inner nuclear layer; IPL, inner plexiform layer; GCL, ganglion cell layer. Scale bar, µm.

Figure 4. Expression levels of different proteins in the retinas of wildtype (*GFAP*$^{+/+}$*Vim*$^{+/+}$, WT) and *GFAP*$^{-/-}$*Vim*$^{-/-}$ mice (double-knockout mice, dKO) at different ages. **(A)** The levels of protein kinase alpha (PKC) expressed by retinal bipolar cells, and the glial proteins cellular retinaldehyde-binding protein (CRALBP), SRY-box 9 (SOX9), glutamate aspartate transporter (GLAST), glutamine synthetase (GS), and aquaporin 4 (AQP4) were compared between *GFAP*$^{+/+}$*Vim*$^{+/+}$ (WT) and *GFAP*$^{-/-}$*Vim*$^{-/-}$ mice (dKO) at different ages: PN (postnatal day) 7, PN14, PN21, and PN60. The housekeeping proteins glyceraldehyde-3-phosphate dehydrogenase (GAPDH) and tubulin served as loading controls. From PN14 and onwards, PKC showed an equally strong expression in both genotypes. The levels of CRALBP did not

change with age or genotype. An equally sized protein band of SOX9 was observed in all ages and genotypes. A second, weaker band appeared from PN21 and onwards. The levels of GLAST increased with age, being first detectable at PN14. No GS expression could be observed by PN7, but from PN14 and onwards, increasing levels were detected. GS expression was found to be higher in wildtype (WT) than in *GFAP*$^{-/-}$*Vim*$^{-/-}$ mice. The expression of AQP4 (~32 kDa) increased with age in both genotypes, starting with non-detectable levels at PN7. A second band of ~60 kDa was also detected at PN60. At this age, the levels of the ~32 kDa band were reduced and those of the ~60 kDa band were increased in *GFAP*$^{-/-}$*Vim*$^{-/-}$ mice. 10 µg of protein pooled from 3-5 retinas from different animals were loaded to each lane, except for PKC and for AQP4 at PN7 and PN14, where 20 µg of protein were loaded.

Figure 5. Expression levels of the inwardly rectifying potassium channels Kir2.1 and Kir4.1 in retinas and cerebellum of wildtype (WT) and GFAP$^{-/-}$Vim$^{-/-}$ mice (double-knockout mice, dKO) at different ages. **(A)** The expression levels of Kir2.1 (top) increased with age in both *GFAP*$^{+/+}$*Vim*$^{+/+}$ (WT) and *GFAP*$^{-/-}$*Vim*$^{-/-}$ mice (dKO), but expression was lower in dKO at PN21 and PN60. Expression of Kir4.1 (bottom) was not detectable at PN7, but increased with age. Kir4.1 levels were lower in the dKO than in age-matched WT mice. 10 µg of protein pooled from 3-5 retinas from different animals were loaded to each lane. **(B)** Kir4.1 expression is lower also in the cerebellum of dKO animals compared to WT animals. 7.5 µg of protein obtained from a mouse cerebellum (PN60) were loaded to each lane.

TABLE 1. Primary antibodies and lectin used in the study.

Lectin/Antibody	Host	Dilution (IHC)	Dilution (WB)	Company
AQP4	Rabbit	1:800	1:3,000 1:4,500	Sigma-Aldrich, St Louis, MO, USA
Brn3a	Goat	1:200	-	Santa Cruz Biotechnology, USA
Calbindin	Mouse	1:200	-	Sigma-Aldrich, St Louis, MO, USA
Cellular retinaldehyde-binding protein (CRALBP)	Rabbit	1:5,000	1:30,000	Kind gift from J. C. Saari, University of Washington, Seattle, USA
Dystrophin	Mouse	1:20	-	Leica Biosystems (Novocastra) Newcastle Upon Tyne, UK
Glial fibrillary acidic protein (GFAP)	Rabbit	1:1500	-	DAKO A/S, Glostrup, Denmark
Glial fibrillary acidic protein (GFAP) (cy3-conjugated)	Mouse	1:100	-	Sigma-Aldrich, St Louis, MO, USA
Glutamate aspartate transporter (GLAST)				
Glutamine synthetase (GS)	Mouse	1:2,000	1:25,000	BD Biosciences, Franklin Lakes, NJ, USA
Glyceraldehyde-3-phosphate dehydrogenase (GAPDH)	Rabbit	-	1:2,000	Abcam, Cambridge, UK
Kir2.1 (KCNJ2)	Rabbit	1:500	1:400	Sigma-Aldrich, St Louis, MO, USA
	Rabbit	1:100	1:400	Alomone Labs Ltd., Jerusalem, Israel
Kir4.1 (KCNJ10)	Mouse	1:200	1:400	Sigma-Aldrich, St Louis, MO, USA
	Rabbit	1:1,000	1:500	Alomone Labs Ltd., Jerusalem, Israel
NeuN	Mouse	1:100	-	Millipore, Billerica, MA, USA
Parvalbumin				
Peanut agglutinin (PNA) - lectin	-	1:500	-	Vector Laboratories, Burlingame, CA, USA
Protein kinase C-α (PKC-α)	Mouse	1:200	1:200	Nordic BioSite, Täby, Sweden
Recoverin	Rabbit	1:12,000	-	Millipore, Billerica, MA, USA
Rhodopsin (clone RET-P1)	Mouse	1:400	-	Millipore, Billerica, MA, USA
Sox-9	Rabbit	1:500	1:500	Millipore, Billerica, MA, USA
Tubulin	Mouse	-	1:20,000	Abcam, Cambridge, UK
Vimentin				

AQP4 = Nagelhus et al., 1999; Brn3a = Quina et al., 2005; Calbindin = Haverkamp and Wässle, 2000; CRALBP = Bunt-Milam and Saari, 1983; Dystrophin = Wersinger et al., 2011; GFAP = Sarthy and Huang, 1991; GLAST = Derouiche et al., 2005; GS = Derouiche et al., 2005; GAPDH = ; Kir2.1, Kir4.1 = Kofuji et al., 2002; NeuN = Mullen et al., 1992; Parvalbumin = PNA = Blanks and Johnson, 1984; PKC-α = Ruether et al., 2010; Recoverin = Milam et al., 1993; Rhodopsin = Hicks and Molday, 1986; Sox-9 = Muto et al., 2009; Vimentin = Lewis and Fisher, 2003.

TABLE 2. Secondary antibodies used in the study.

Antibody	Host	Dilution	Company
Anti-guinea pig	Goat	1:200	Sigma-Aldrich, St Louis, MO, USA
Anti-guinea pig (peroxidase-conjugated)	Goat	-	Jackson Immunoresearch, Westgrove, PA, USA
Anti-mouse (Alexa Fluor®488-conjugated)	Goat	1:200	Invitrogen Ltd., Paisley, UK
Anti-mouse (DyLight™549-conjugated)	Donkey	1:400	Jackson Immunoresearch, Westgrove, PA, USA
Anti-mouse (peroxidase-conjugated)	Goat	-	Jackson Immunoresearch, Westgrove, PA, USA
Anti-mouse (Texas Red®-conjugated)	Donkey	1:200	Jackson Immunoresearch, Westgrove, PA, USA
Anti-rabbit (Alexa Fluor®488-conjugated)	Goat	1:200	Invitrogen Ltd., Paisley, UK
Anti-rabbit (Alexa Fluor®594-conjugated)	Goat	1:200	Invitrogen Ltd., Paisley, UK
Anti-rabbit (DyLight™488-conjugated)	Donkey	1:400	Jackson Immunoresearch, Westgrove, PA, USA
Anti-rabbit (peroxidase-conjugated)	Goat	-	Nordic BioSite, Täby, Sweden
Anti-rabbit (Texas Red®-conjugated)	Donkey	1:200	Jackson Immunoresearch, Westgrove, PA, USA

REFERENCES

Azadi S, Johnson LE, Paquet-Durand F, Perez MT, Zhang Y, Ekström PA, van Veen T. CNTF+BDNF treatment and neuroprotective pathways in the rd1 mouse retina. Brain Res. 2007 Jan 19;1129(1):116-29.

Blanks JC, Johnson LV. Specific binding of peanut lectin to a class of retinal photoreceptor cells. a species comparison. Invest Ophthalmol Vis Sci. 1984 May;25(5):546-57.

Bringmann A, Pannicke T, Grosche J, Francke M, Wiedemann P, Skatchkov SN, Osborne NN, Reichenbach A. Müller cells in the healthy and diseased retina. Prog Retin Eye Res. 2006 Jul;25(4):397-424.

Bringmann A, Iandiev I, Pannicke T, Wurm A, Bühner E, Reichenbach A, Wiedemann P, Uhlmann S. Porcine Müller glial cells increase expression of BKCa channels in retinal detachment. Curr Eye Res. 2007 Feb;32(2):143-51.

Bunt-Milam AH, Saari JC. Immunocytochemical localization of two retinoid-binding proteins in vertebrate retina. J Cell Biol. 1983 Sep;97(3):703-12.

Cheng L, Sapieha P, Kittlerova P, Hauswirth WW, Di Polo A. TrkB gene transfer protects retinal ganglion cells from axotomy-induced death in vivo. J Neurosci. 2002 May 15;22(10):3977-86.

Cibis GW, Fitzgerald KM, Harris DJ, Rothberg PG, Rupani M. The effects of dystrophin gene mutations on the ERG in mice and humans. Invest Ophthalmol Vis Sci. 1993 Dec;34(13):3646-52.

Collery R, McLoughlin S, Vendrell V, Finnegan J, Crabb JW, Saari JC, Kennedy BN. Duplication and divergence of zebrafish CRALBP genes uncovers novel role for RPE- and Muller-CRALBP in cone vision. Invest Ophthalmol Vis Sci. 2008 Sep;49(9):3812-20.

Colucci-Guyon E, Portier MM, Dunia I, Paulin D, Pournin S, Babinet C. Mice lacking vimentin develop and reproduce without an obvious phenotype. Cell. 1994 Nov 18;79(4):679-94.

Connors NC, Kofuji P. Potassium channel Kir4.1 macromolecular complex in retinal glial cells. Glia. 2006 Jan 15;53(2):124-31.

Derouiche A, Rauen T. Coincidence of L-glutamate/L-aspartate transporter (GLAST) and glutamine synthetase (GS) immunoreactions in retinal glia: evidence for coupling of GLAST and GS in transmitter clearance. J Neurosci Res 1995; 42:131-43.

Eberhardt C, Amann B, Feuchtinger A, Hauck SM, Deeg CA. Differential expression of inwardly rectifying K+ channels and aquaporins 4 and 5 in autoimmune uveitis indicates misbalance in Müller glial cell-dependent ion and water homeostasis. Glia. 2011 May;59(5):697-707.

Eckes B, Dogic D, Colucci-Guyon E, Wang N, Maniotis A, Ingber D, Merckling A, Langa F, Aumailley M, Delouvée A, Koteliansky V, Babinet C, Krieg T. Impaired mechanical stability, migration and contractile capacity in vimentin-deficient fibroblasts. J Cell Sci. 1998 Jul;111 (Pt 13):1897-907

Eliasson C, Sahlgren C, Berthold CH, Stakeberg J, Celis JE, Betsholtz C, Eriksson JE, Pekny M. Intermediate filament protein partnership in astrocytes. J Biol Chem. 1999 Aug 20;274(34):23996-4006.

Fischer AJ, Scott MA, Ritchey ER, Sherwood P. Mitogen-activated protein kinase-signaling regulates the ability of Müller glia to proliferate and protect retinal neurons against excitotoxicity. Glia. 2009 Nov 1;57(14):1538-52.

Fischer AJ, Zelinka C, Scott MA. Heterogeneity of glia in the retina and optic nerve of birds and mammals. PLoS One. 2010. 5: e10774.

Fort PE, Sene A, Pannicke T, Roux MJ, Forster V, Mornet D, Nudel U, Yaffe D, Reichenbach A, Sahel JA, Rendon A. Kir4.1 and AQP4 associate with Dp71- and utrophin-DAPs complexes in specific and defined microdomains of Müller retinal glial cell membrane. Glia. 2008 Apr 15;56(6):597-610.

Frishman LJ (2006) Origins of the electroretinogram. In: Principles and practice of clinical electrophysiology of vision, 2nd edn. (Heckenlively JR and Arden GB, eds), pp 139-183, Massachusetts: The MIT press.

Geller SF, Lewis GP, Fisher SK. FGFR1, signaling, and AP-1 expression after retinal detachment: reactive Müller and RPE cells. Invest Ophthalmol Vis Sci. 2001 May;42(6):1363-9

Haverkamp S, Wässle H. Immunocytochemical analysis of the mouse retina.J Comp Neurol. 2000;424:1-23.

Hicks D, Molday RS. Differential immunogold-dextran labeling of bovine and frog rod and cone cells using monoclonal antibodies against bovine rhodopsin. Exp Eye Res. 1986;42:55-71.

Hirrlinger PG, Ulbricht E, Iandiev I, Reichenbach A, Pannicke T. Alterations in protein expression and membrane properties during Müller cell gliosis in a murine model of transient retinal ischemia. Neurosci Lett. 2010 Mar 12;472(1):73-8.

Iandiev I, Wurm A, Hollborn M, Wiedemann P, Grimm C, Remé CE, Reichenbach A, Pannicke T, Bringmann A. Müller cell response to blue light injury of the rat retina. Invest Ophthalmol Vis Sci. 2008 Aug;49(8):3559-67.

Ishii M, Fujita A, Iwai K, Kusaka S, Higashi K, Inanobe A, Hibino H, Kurachi Y. Differential expression and distribution of Kir5.1 and Kir4.1 inwardly rectifying K+ channels in retina. Am J Physiol Cell Physiol. 2003 Aug;285(2):C260-7.

Ivaska J, Pallari HM, Nevo J, Eriksson JE. Novel functions of vimentin in cell adhesion, migration, and signaling. Exp Cell Res. 2007 Jun 10;313(10):2050-62.

Kinouchi R, Takeda M, Yang L, Wilhelmsson U, Lundkvist A, Pekny M, Chen DF. Robust neural integration from retinal transplants in mice deficient in gfap and vimentin. Nat Neurosci. 2003 Aug;6(8):863-8.

Kofuji P, Ceelen P, Zahs KR, Surbeck LW, Lester HA, Newman EA. Genetic inactivation of an inwardly rectifying potassium channel (Kir4.1 subunit) in mice: phenotypic impact in retina. J Neurosci. 2000 Aug 1;20(15):5733-40.

Kofuji P, Biedermann B, Siddharthan V, Raap M, Iandiev I, Milenkovic I, Thomzig A, Veh RW, Bringmann A, Reichenbach A. Kir potassium channel subunit expression in retinal glial cells: implications for spatial potassium buffering. Glia. 2002 Sep;39(3):292-303.

Kofuji P, Newman EA. Potassium buffering in the central nervous system. Neuroscience. 2004;129(4):1045-56.

Kumar S, Zhuo L. Longitudinal in vivo imaging of retinal gliosis in a diabetic mouse model. Exp Eye Res. 2010 Oct;91(4):530-6.

Lewis GP, Fisher SK. Up-regulation of glial fibrillary acidic protein in response to retinal injury: its potential role in glial remodeling and a comparison to vimentin expression. Int Rev Cytol. 2003; 230:263-290.

Lewis GP, Chapin EA, Luna G, Linberg KA, Fisher SK. The fate of müller's glia following experimental retinal detachment: nuclear migration, cell division, and subretinal glial scar formation. Mol Vis. 2010 Jul 15;16:1361-72.

Li L, Lundkvist A, Andersson D, Wilhelmsson U, Nagai N, Pardo AC, Nodin C, Ståhlberg A, Aprico K, Larsson K, Yabe T, Moons L, Fotheringham A, Davies I, Carmeliet P, Schwartz JP, Pekna M, Kubista M, Blomstrand F, Maragakis N, Nilsson M, Pekny M. Protective role of reactive astrocytes in brain ischemia. J Cereb Blood Flow Metab. 2008 Mar;28(3):468-81.

Lindqvist N, Liu Q, Zajadacz J, Franze K, Reichenbach A. Retinal glial (Müller) cells: sensing and responding to tissue stretch. Invest Ophthalmol Vis Sci. 2010 Mar;51(3):1683-90.

Lundkvist A, Reichenbach A, Betsholtz C, Carmeliet P, Wolburg H, Pekny M. Under stress, the absence of intermediate filaments from Müller cells in the retina has structural and functional consequences. J Cell Sci. 2004 Jul 15;117(Pt 16):3481-8.

Lu YB, Iandiev I, Hollborn M, Körber N, Ulbricht E, Hirrlinger PG, Pannicke T, Wei EQ, Bringmann A, Wolburg H, Wilhelmsson U, Pekny M, Wiedemann P, Reichenbach A, Käs JA. Reactive glial cells: increased stiffness correlates with increased intermediate filament expression. FASEB J. 2011 Feb;25(2):624-31.

Marmor MF, Holder GE, Seeliger MW, Yamamoto S (2004) Standard for clinical electroretinography (2004 update). Doc Ophthalmol. 2004 Mar;108(2):107-14.

Milam AH, Dacey DM, Dizhoor AM. Recoverin immunoreactivity in mammalian cone bipolar cells. Vis Neurosci. 1993;10:1-12.

Mullen RJ, Buck CR, Smith AM: NeuN, a neuronal specific nuclear protein in vertebrates. Development 1992;116:201-11.

Muto A, Iida A, Satoh S, Watanabe S. The group E Sox genes Sox8 and Sox9 are regulated by Notch signaling and are required for Müller glial cell development in mouse retina. Exp Eye Res. 2009 Oct;89(4):549-58.

Nagelhus EA, Horio Y, Inanobe A, Fujita A, Haug FM, Nielsen S, Kurachi Y, Ottersen OP. Immunogold evidence suggests that coupling of K+ siphoning and water transport in rat

retinal Müller cells is mediated by a coenrichment of Kir4.1 and AQP4 in specific membrane domains. Glia. 1999;26:47-54.

Nakazawa T, Takeda M, Lewis GP, Cho K, Jiao J, Wilhelmsson U, Fisher SK, Pekny M, Chen DF, Miller JW. Attenuated glial reactions and photoreceptor degeneration after retinal detachment in mice deficient in glial fibrillary acidic protein and vimentin. Invest Ophthalmol Vis Sci. 2007 Jun;48(6):2760-8.

Newman EA. Inward-rectifying potassium channels in retinal glial (Müller) cells. J Neurosci. 1993 Aug;13(8):3333-45.

Newman E, Reichenbach A. The Müller cell: a functional element of the retina. Trends Neurosci. 1996 Aug;19(8):307-12.

Newman E. (2009) Retinal glia. In: Encyclopedia of neuroscience. Squire L (ed.). pp. 225-232.

Pannicke T, Iandiev I, Wurm A, Uckermann O, vom Hagen F, Reichenbach A, Wiedemann P, Hammes HP, Bringmann A. Diabetes alters osmotic swelling characteristics and membrane conductance of glial cells in rat retina. Diabetes. 2006 Mar;55(3):633-9.

Pekny M, Levéen P, Pekna M, Eliasson C, Berthold CH, Westermark B, Betsholtz C. Mice lacking glial fibrillary acidic protein display astrocytes devoid of intermediate filaments but develop and reproduce normally. EMBO J. 1995 Apr 18;14(8):1590-8.

Pekny M, Johansson CB, Eliasson C, Stakeberg J, Wallén A, Perlmann T, Lendahl U, Betsholtz C, Berthold CH, Frisén J. Abnormal reaction to central nervous system injury in mice lacking glial fibrillary acidic protein and vimentin. J Cell Biol. 1999 May 3;145(3):503-14.

Perlson E, Hanz S, Ben-Yaakov K, Segal-Ruder Y, Seger R, Fainzilber M. Vimentin-dependent spatial translocation of an activated MAP kinase in injured nerve. Neuron. 2005 Mar 3;45(5):715-26.

Pekny M, Nilsson M. Astrocyte activation and reactive gliosis. Glia. 2005 Jun;50(4):427-34.

Pekny M, Lane EB. Intermediate filaments and stress. Exp Cell Res. 2007 Jun 10;313(10):2244-54.

Perlson E, Michaelevski I, Kowalsman N, Ben-Yaakov K, Shaked M, Seger R, Eisenstein M, Fainzilber M. Vimentin binding to phosphorylated Erk sterically hinders enzymatic dephosphorylation of the kinase. J Mol Biol. 2006 Dec 15;364(5):938-44.

Pillers DA, Fitzgerald KM, Duncan NM, Rash SM, White RA, Dwinnell SJ, Powell BR, Schnur RE, Ray PN, Cibis GW, Weleber RG. Duchenne/Becker muscular dystrophy: correlation of phenotype by electroretinography with sites of dystrophin mutations. Hum Genet. 1999 Jul-Aug;105(1-2):2-9.

Quina LA, Pak W, Lanier J, Banwait P, Gratwick K, Liu Y, et al. Brn3a-Expressing Retinal Ganglion Cells Project Specifically to Thalamocortical and Collicular Visual Pathways. J Neurosci. 2005;25:11595-604.

Rehak M, Hollborn M, Iandiev I, Pannicke T, Karl A, Wurm A, Kohen L, Reichenbach A, Wiedemann P, Bringmann A. Retinal gene expression and Müller cell responses after branch retinal vein occlusion in the rat. Invest Ophthalmol Vis Sci. 2009 May;50(5):2359-67.

Roesch K, Stadler MB, Cepko CL. Gene expression changes within Müller glial cells in retinitis pigmentosa. Mol Vis. 2012;18:1197-214.

Ruether K, Feigenspan A, Pirngruber J, Leitges M, Baehr W, Strauss O. PKC{alpha} is essential for the proper activation and termination of rod bipolar cell response. Invest Ophthalmol Vis Sci. 2010 Nov;51(11):6051-8.

Ruiz-Ederra J, Zhang H, Verkman AS. Evidence against functional interaction between aquaporin-4 water channels and Kir4.1 potassium channels in retinal Müller cells. J Biol Chem. 2007 Jul 27;282(30):21866-72.

Runembert I, Queffeulou G, Federici P, Vrtovsnik F, Colucci-Guyon E, Babinet C, Briand P, Trugnan G, Friedlander G, Terzi F. Vimentin affects localization and activity of sodium-glucose cotransporter SGLT1 in membrane rafts. J Cell Sci. 2002 Feb 15;115(Pt 4):713-24.

Sarthy PV, Fu M, Huang J. Developmental expression of the glial fibrillary acidic protein (GFAP) gene in the mouse retina. Cell Mol Neurobiol. 1991;11:623–37.

Satz JS, Philp AR, Nguyen H, Kusano H, Lee J, Turk R, Riker MJ, Hernández J, Weiss RM, Anderson MG, Mullins RF, Moore SA, Stone EM, Campbell KP. Visual impairment in the absence of dystroglycan. J Neurosci. 2009 Oct 21;29(42):13136-46.

Seeliger MW, Grimm C, Ståhlberg F, Friedburg C, Jaissle G, Zrenner E, Guo H, Remé CE, Humphries P, Hofmann F, Biel M, Fariss RN, Redmond TM, Wenzel A. New views on rpe65 deficiency: the rod system is the source of vision in a mouse model of leber congenital amaurosis. Nat Genet. 2001 Sep;29(1):70-4.

Seeliger MW, Brombas A, Weiler R, Humphries P, Knop G, Tanimoto N, Müller F. Modulation of rod photoreceptor output by HCN1 channels is essential for regular mesopic cone vision. Nat Commun. 2011 Nov 8;2:532.

Sene A, Tadayoni R, Pannicke T, Wurm A, El Mathari B, Benard R, Roux MJ, Yaffe D, Mornet D, Reichenbach A, Sahel JA, Rendon A. Functional implication of Dp71 in osmoregulation and vascular permeability of the retina. PLoS One. 2009 Oct 7;4(10):e7329.

Szeverenyi I, Cassidy AJ, Chung CW, Lee BTK, Common JEA, Ogg SC, Chen H, Sim SY, Goh WLP, Ng KW, Simpson JA, Chee LL, Eng GH, Li B, Lunny DP, Chuon D, Venkatesh A, Khoo KH, McLean WHI, Lim YP, Lane EB. The human intermediate filament database: comprehensive information on a gene family involved in many human diseases. Hum Mutat. 2008 Mar;29(3):351-60.

Tanimoto N, Muehlfriedel RL, Fischer MD, Fahl E, Humphries P, Biel M, Seeliger MW. Vision tests in the mouse: functional phenotyping with electroretinography. Front Biosci (Landmark Ed). 2009 Jan 1;14:2730-7.

Tanimoto N, Sothilingam V, Seeliger MW. (2013) Functional phenotyping of mouse models with ERG. In: Methods in Molecular Biology, Vol. 935: Retinal Degeneration: Methods and Protocols (Weber BH and Langmann T, eds.), pp 69-78, New York: Humana Press.

Verardo MR, Lewis GP, Takeda M, Linberg KA, Byun J, Luna G, Wilhelmsson U, Pekny M, Chen D, Fisher SK. Abnormal reactivity of muller cells after retinal detachment in mice deficient in gfap and vimentin. Invest Ophthalmol Vis Sci. 2008 Aug;49(8):3659-65.

Wahlin KJ, Campochiaro PA, Zack DJ, Adler R. Neurotrophic factors cause activation of intracellular signaling pathways in Müller cells and other cells of the inner retina, but not photoreceptors. Invest Ophthalmol Vis Sci. 2000 Mar;41(3):927-36.

Wersinger E, Bordais A, Schwab Y, Sene A, Bénard R, Alunni V, Sahel JA, Rendon A, Roux MJ. Reevaluation of dystrophin localization in the mouse retina. Invest Ophthalmol Vis Sci. 2011 Oct 7;52(11):7901-8.

Wilhelmsson U, Li L, Pekna M, Berthold CH, Blom S, Eliasson C, Renner O, Bushong E, Ellisman M, Morgan TE, Pekny M. Absence of glial fibrillary acidic protein and vimentin prevents hypertrophy of astrocytic processes and improves post-traumatic regeneration. J Neurosci. 2004 May 26;24(21):5016-21.

Wilhelmsson U, Faiz M, de Pablo Y, Sjöqvist M, Andersson D, Widestrand A, Potokar M, Stenovec M, Smith PL, Shinjyo N, Pekny T, Zorec R, Ståhlberg A, Pekna M, Sahlgren C, Pekny M. Astrocytes negatively regulate neurogenesis through the Jagged1-mediated Notch pathway. Stem Cells. 2012 Oct;30(10):2320-9.

Wu J, Marmorstein AD, Kofuji P, Peachey NS. Contribution of Kir4.1 to the mouse electroretinogram. Mol Vis. 2004 Sep 1;10:650-4.

Wunderlich KA, Leveillard T, Penkowa M, Zrenner E, Perez MT. Altered expression of metallothionein-I and -II and their receptor megalin in inherited photoreceptor degeneration. Invest Ophthalmol Vis Sci. 2010 Sep;51(9):4809-20.

Zhang H, Verkman AS. Aquaporin-4 independent Kir4.1 K+ channel function in brain glial cells. Mol Cell Neurosci. 2008 Jan;37(1):1-10.

Figures:

Figure 1

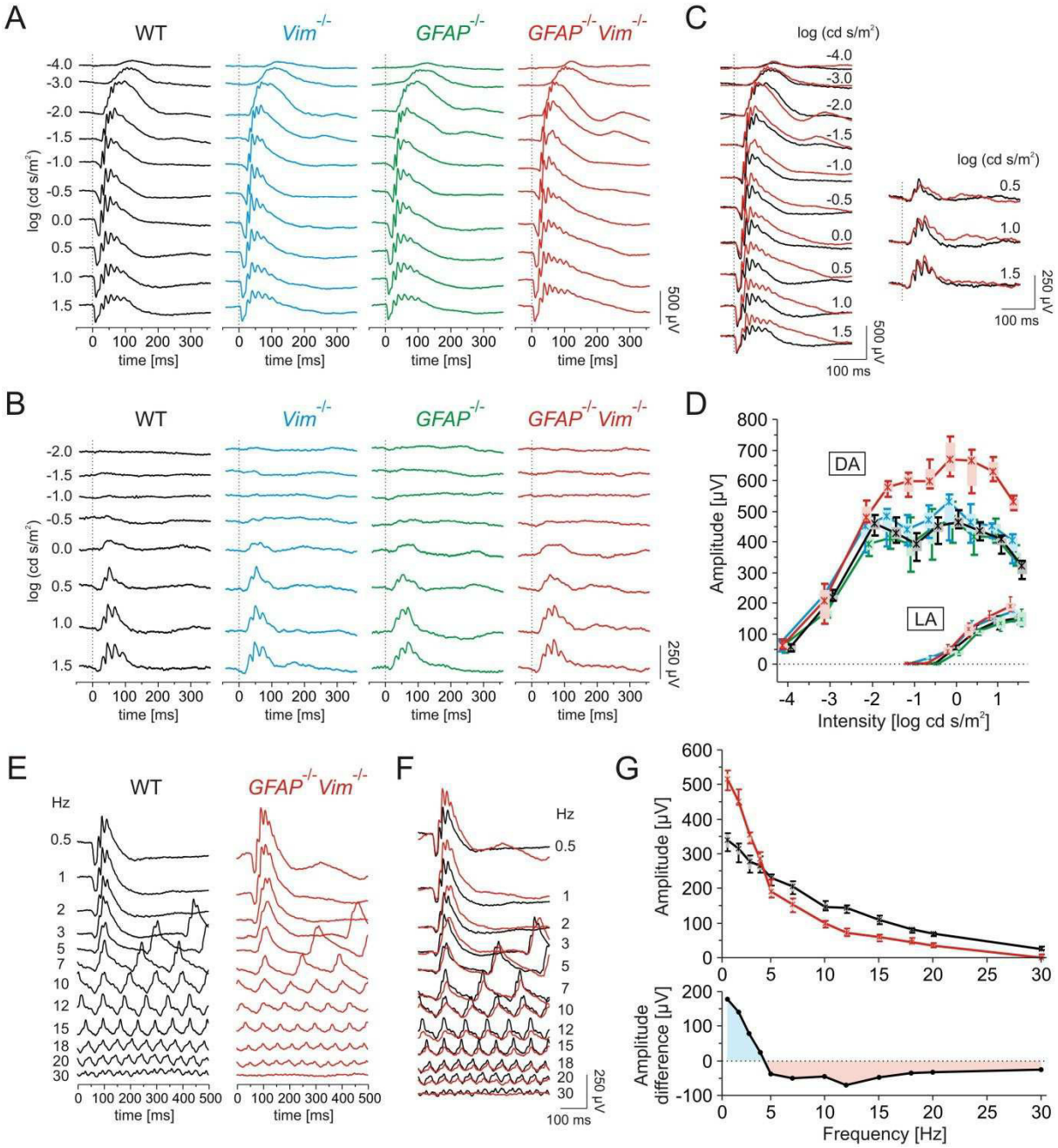

Figure 2

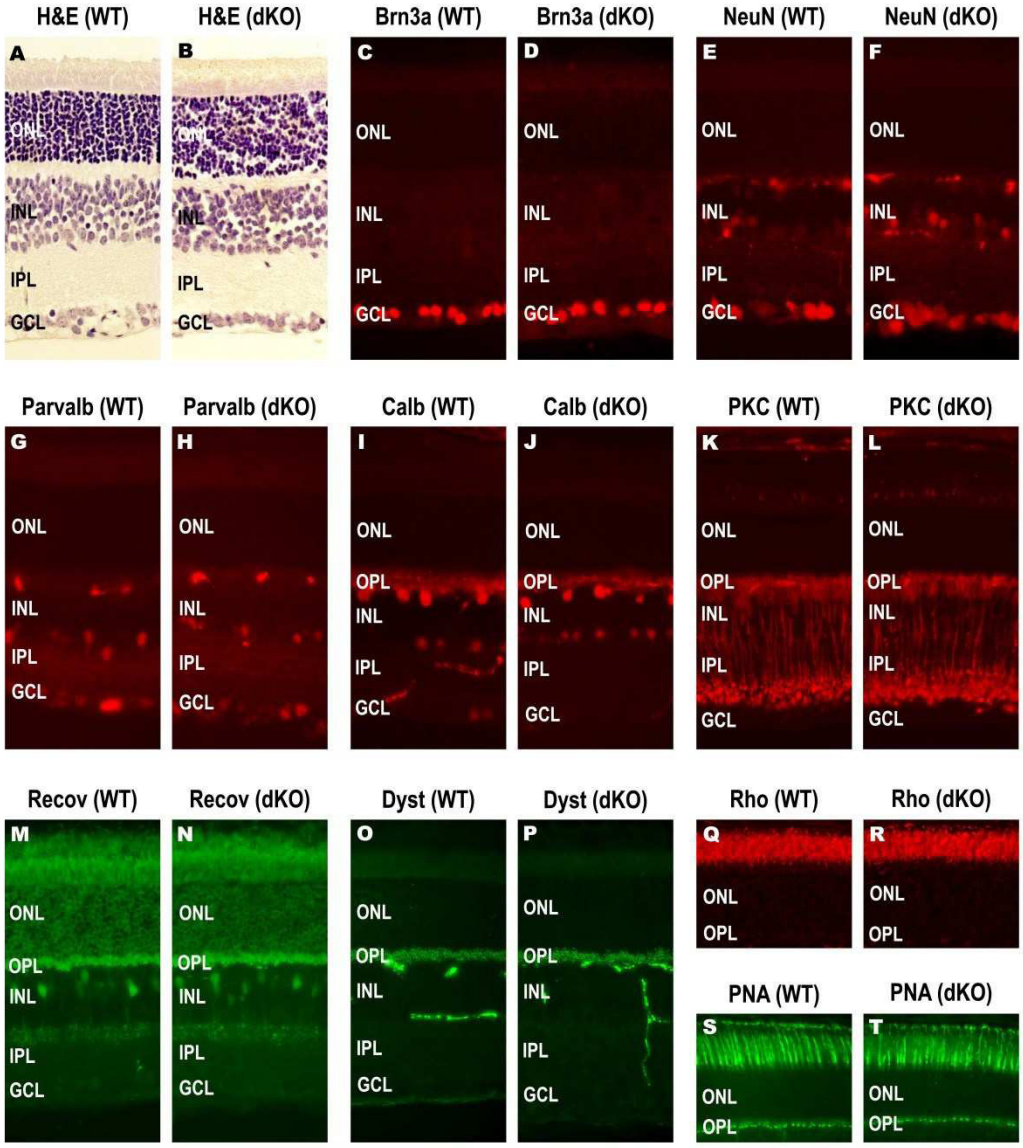
H&E (WT)
H&E (dKO)
Brn3a (WT)
Brn3a (dKO)
NeuN (WT)
NeuN (dKO)
A
B
C
D
E
F
ONL
INL
IPL
GCL
Parvalb (WT)
Parvalb (dKO)
Calb (WT)
Calb (dKO)
PKC (WT)
PKC (dKO)
G
H
I
J
K
L
OPL
Recov (WT)
Recov (dKO)
Dyst (WT)
Dyst (dKO)
Rho (WT)
Rho (dKO)
M
N
O
P
Q
R
PNA (WT)
PNA (dKO)
S
T

Figure 3

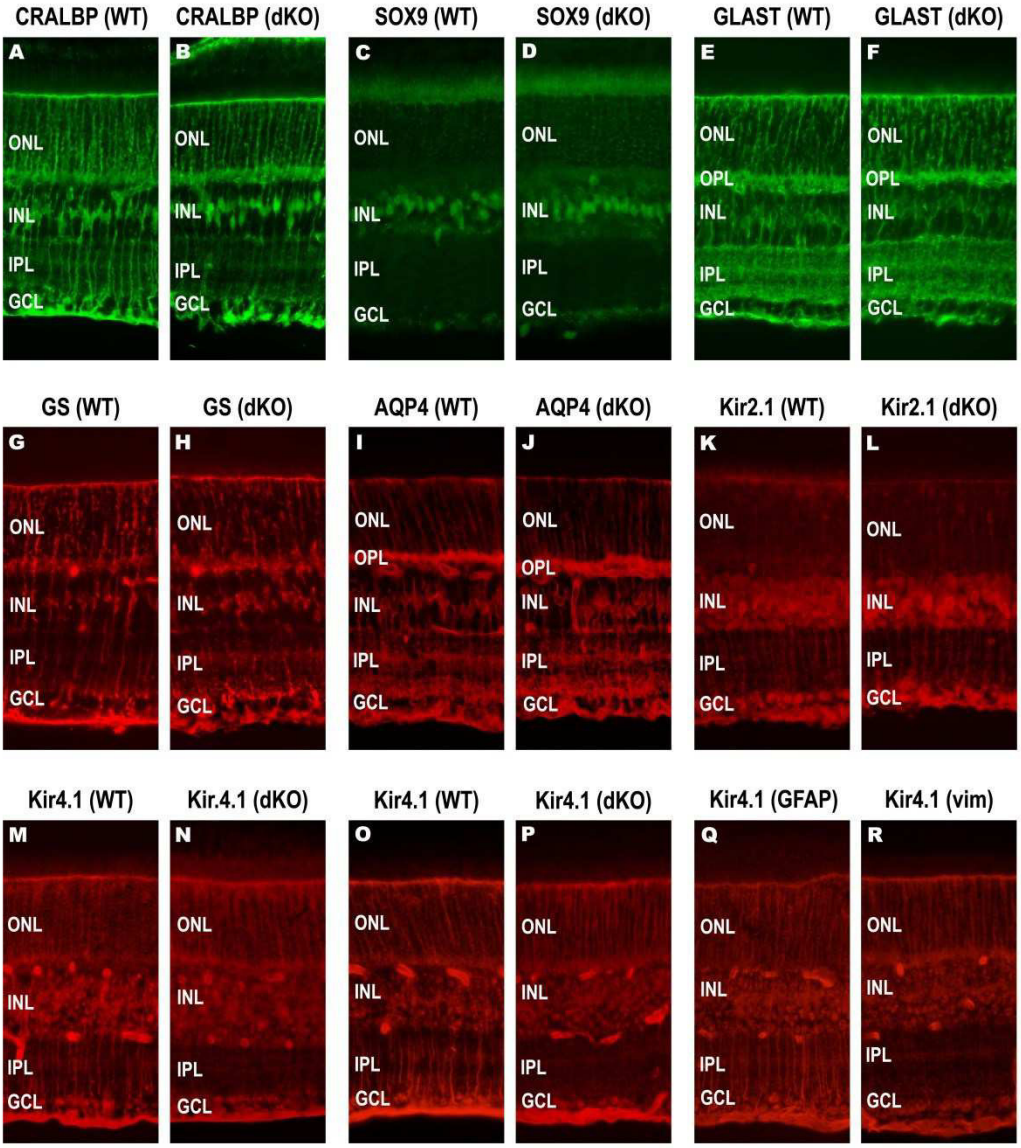
CRALBP (WT)
CRALBP (dKO)
SOX9 (WT)
SOX9 (dKO)
GLAST (WT)
GLAST (dKO)
A
B
C
D
E
F
ONL
OPL
INL
IPL
GCL
GS (WT)
GS (dKO)
AQP4 (WT)
AQP4 (dKO)
Kir2.1 (WT)
Kir2.1 (dKO)
G
H
I
J
K
L
Kir4.1 (WT)
Kir.4.1 (dKO)
Kir4.1 (WT)
Kir4.1 (dKO)
Kir4.1 (GFAP)
Kir4.1 (vim)
M
N
O
P
Q
R

Figure 4

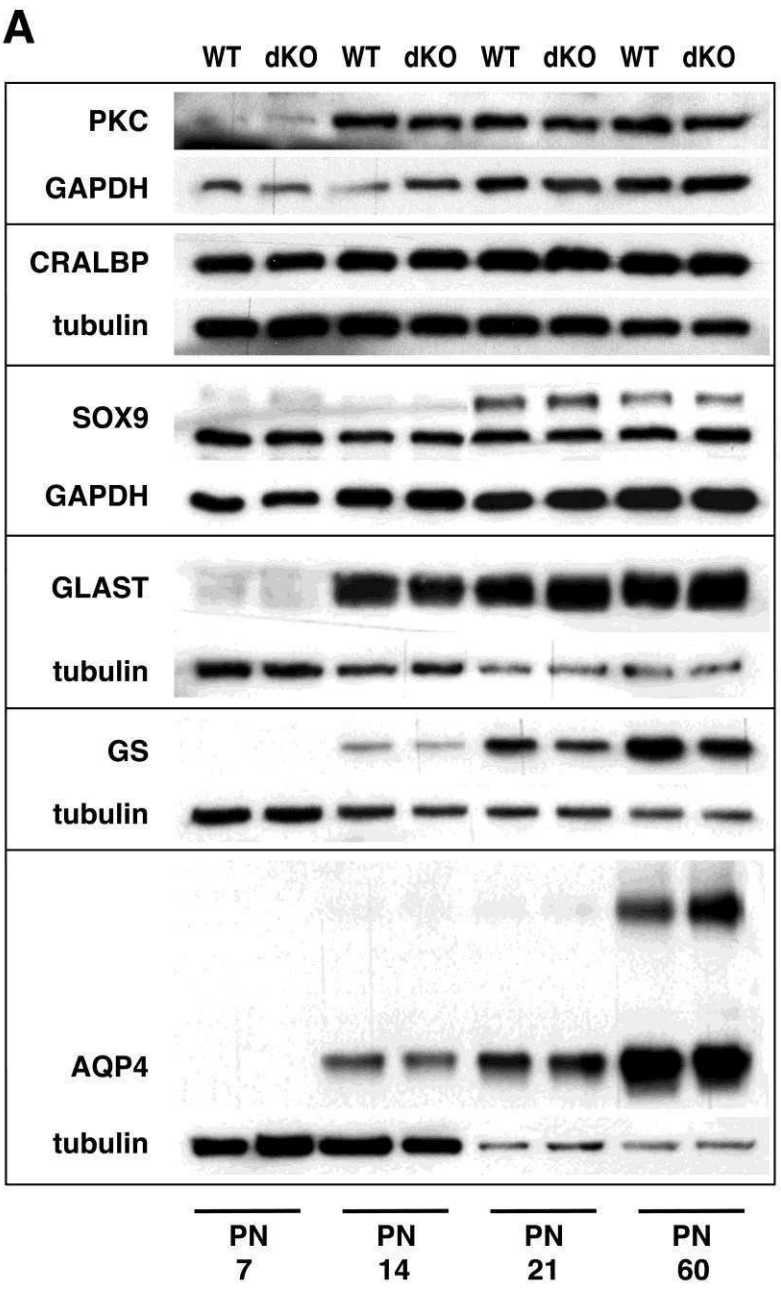
A
WT dKO WT dKO WT dKO WT dKO
PKC
GAPDH
CRALBP
tubulin
SOX9
GAPDH
GLAST
tubulin
GS
tubulin
AQP4
tubulin
PN 7
PN 14
PN 21
PN 60

Figure 5

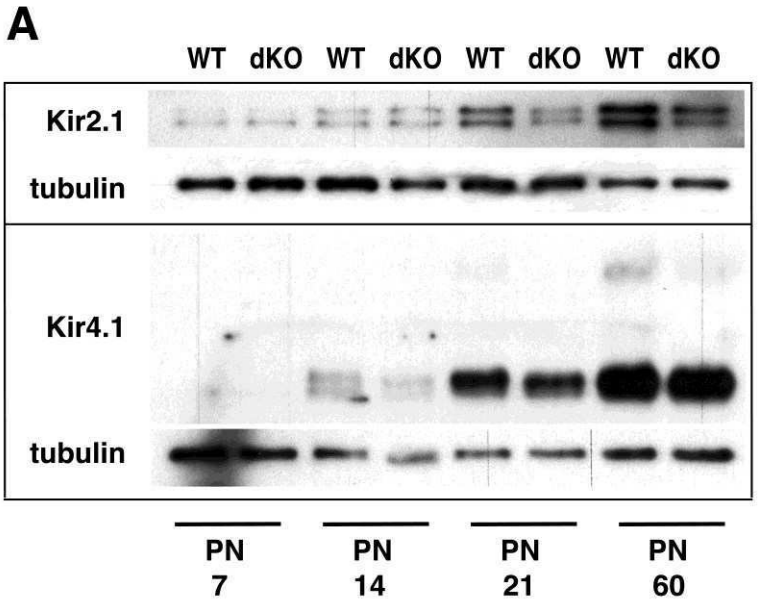
A
WT dKO WT dKO WT dKO WT dKO
Kir2.1
tubulin
Kir4.1
tubulin
PN 7
PN 14
PN 21
PN 60

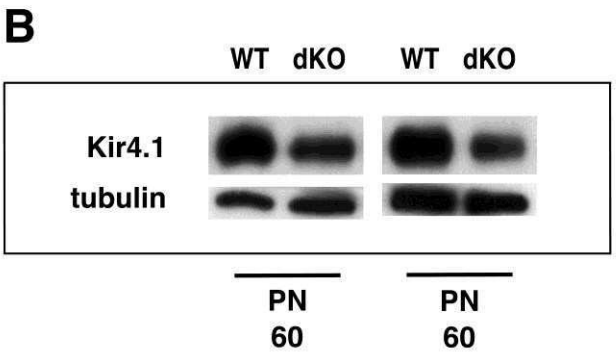
B
WT dKO WT dKO
Kir4.1
tubulin
PN 60
PN 60

4.2 The inability to produce glial fibrillary acidic protein (GFAP) and vimentin does not protect photoreceptors in a genetic model of degeneration

Manuscript

Summary

The inability of retinal glia to up-regulate the intermediate filament protein glial fibrillary acidic protein (GFAP) and vimentin has been shown to be beneficial for photoreceptor survival in a model of retinal detachment (Nakazawa et al., 2007)(Verardo et al., 2008). To investigate the role of GFAP and vimentin on the progression of inherited retinal degeneration in the *rd1* mouse, a model for retinitis pigmentosa, the retinal function of *rd1* mice lacking these intermediate filament proteins (*rd1, GFAP*$^{-/-}$*Vim*$^{-/-}$) was examined by electroretinography (ERG; performed by Naoyuki Tanimoto, Tübingen). Retinal morphology was evaluated with DAPI-stained retinal sections and the expression patterns of different photoreceptor and glial marker proteins were analyzed by the means of immunohistochemistry and western blot.

By postnatal day (PN) 21, the retinal responses to light stimuli were already weak, with non-distinguishable a-waves. Nevertheless, *rd1, GFAP*$^{-/-}$*Vim*$^{-/-}$ mice distinctly exhibited higher b-waves under dark- and light-adapted conditions, with prolonged implicit times, latencies, and delayed return to the baseline than the *rd1* control mice. By 5 weeks of age, no light responses were recordable, regardless of the genotype.

These results indicate that the lack of GFAP and vimentin could indeed have a small positive effect on photoreceptor survival.

To investigate whether the higher ERG responses reflect a beneficial effect on neuronal degeneration, the morphology of the retina, particularly that of the photoreceptor layer, was examined in more detail. The thickness of all retinal layers was comparable in *rd1, GFAP*$^{-/-}$ *Vim*$^{-/-}$ and *rd1, GFAP*$^{+/+}$*Vim*$^{+/+}$ mice, including the outer nuclear layer, which consisted of approximately one to two cell rows at the age of three weeks. Stainings with common cellular markers for rods (rhodopsin) and cones (peanut agglutinine, cone arrestin) revealed no differences in the number or distribution of photoreceptor cells in the two mouse lines.

Similar to what was described in chapter 4.1, the expression patterns of some essential glial proteins were evaluated. As in chapter 4.1, the number of Müller cells seemed to be similar in *rd1, GFAP*$^{-/-}$*Vim*$^{-/-}$ and *rd1, GFAP*$^{+/+}$*Vim*$^{+/+}$ mice, since the levels of SOX9 expression were comparable. GS expression was also reduced in mice lacking GFAP and vimentin, particularly at PN14 and PN21. In contrast to chapter 4.1, however, the levels of glutamate aspartate transporter (GLAST) were also reduced, as well as the levels of the water channel

aquaporin 4. Again, levels of the inwardly rectifying potassium channels Kir2.1 and Kir4.1 were lower in the animals lacking the intermediate filament proteins than in control mice. Kir4.1 expression was visibly lower in the proximal processes of the Müller cells.

No rescue effect on photoreceptors could be observed in this study. Furthermore, considering that chapter 4.1 revealed larger b-waves in *GFAP*$^{-/-}$*Vim*$^{-/-}$ animals even without photoreceptor degeneration, the apparently improved retinal function seems rather to be an effect of the altered glial physiology.

The inability to produce glial fibrillary acidic protein (GFAP) and vimentin does not protect photoreceptors in a genetic model of degeneration

KA Wunderlich[1,2,3], N Tanimoto[3], S Azadi[4], E Zrenner[3], MW Seeliger[3], MT Perez[1,5]

[1]Dept. of Ophthalmology, Clinical Sciences Lund, Lund University, Lund, Sweden
[2]Graduate School of Cellular & Molecular Neuroscience, Univ. of Tuebingen, Tuebingen, Germany
[3]Institute for Ophthalmic Research, University of Tuebingen, Tuebingen, Germany
[4]Dept. Of Cell Biology, University of Oklahoma Health Sciences Center, Oklahoma City, USA
[5]Dept. of Ophthalmology, Univ. of Copenhagen, Glostrup Hospital, Glostrup, Denmark

Short title: Retinal degeneration in GFAP- and vimentin-deficient mice

Key words: retina, photoreceptor, glia, GFAP, vimentin, electroretinogram, ERG, potassium channels, aquaporin, Kir4.1, mouse, knockout, intermediate filaments, *rd1*, retinal degeneration

Corresponding author:
Maria Thereza Perez
Inst. Clinical Sciences, Ophthalmology
Lund University
BMC B13, Klinikgatan 26
226 84 Lund, Sweden
tel. (+46) 46 2220772
fax (+46) 46 2220774
e-mail: maria_thereza.perez@med.lu.se

ABSTRACT

Purpose: Glial cell activation is characterized by proliferation and up-regulation of several molecules, including the intermediate filaments (IFs), glial fibrillary acidic protein (GFAP) and vimentin (Vim). Commonly used as markers for reactive gliosis, their function in the process has yet to be unraveled. The lack of GFAP and vimentin has been shown to be beneficial for photoreceptor survival after retinal detachment. In the present study, we have investigated whether the inability to produce these IFs might also affect the progression of inherited photoreceptor cell degeneration.

Methods: Two groups of animals were studied: mice with retinal degeneration (*Pde6b* mutation, *rd1*) expressing GFAP and Vim (*rd1, GFAP*$^{+/+}$*Vim*$^{+/+}$) and mice with retinal degeneration and lacking the IFs (*rd1, GFAP*$^{-/-}$*Vim*$^{-/-}$). Electroretinogram (ERG) analysis has been performed in animals of 3 and 5 weeks of age. Retinas from postnatal day 7 (PN7) to PN60 mice were processed for immunohistochemistry and Western Blot analysis of photoreceptor and glial cell markers.

Results: ERG recordings revealed slightly larger b-waves and longer latencies in *rd1* mice that do not express GFAP and vimentin compared to *rd1* mice expressing these IFs. No differences were noted in the distribution of rod and cone cell markers or in the thickness of the outer nuclear layer at a PN21 in the two groups of *rd1* mice. The number of Müller cells was also comparable in both genotypes. The expression of several astrocyte and Müller cell proteins, including the inwardly rectifying potassium channels Kir2.1 and Kir4.1, was altered in retinas lacking GFAP and vimentin.

Conclusions: Our findings do not support the idea that the inability to up-regulate GFAP and vimentin is beneficial for photoreceptor survival in the *rd1* mouse, an inherited model of retinal degeneration, or that it slows down the progression of the disease. The higher b-waves in the animals lacking glial IFs do not seem to be an effect of better preserved cone function and/or improved photoreceptor survival, but rather an effect of the altered glial physiology.

INTRODUCTION

With a prevalence of 1/3,500 to 1/4,000, retinitis pigmentosa (RP) is the most frequent hereditary retinal degeneration, named after the accumulation of subretinal cell debris, which is visible as a pigmented fundus. In fact, RP comprises a group of different diseases caused by many different mutations in primarily rod-specific genes (http://www.sph.uth.tmc.edu/Retnet/, RetNet is provided in the public domain by the University of Texas, Houston Health Science Center, Houston, TX, USA) that lead first to night blindness and tunnel vision due to rod cell death, but subsequently also to cone cell death, causing a total loss of vision (Daiger et al., 2007; Hamel, 2006; Hartong et al., 2006). Several transgenic (Flannery, 1999) and naturally occurring (Chang et al., 2002; Fauser et al., 2002) animal models for RP are available, such as the retinal degeneration 1 (*rd1*) mouse that has been examined in the present study. In the *rd1* mouse, a mutation in the β-subunit of the rod *cGMP-phosphodiesterase* gene (*Pde6b*) causes a rapid degeneration of rods within less than two weeks after eye opening (Bowes et al., 1990; Farber and Lolley, 1976) Although the mutation is rod-specific, cones also degenerate eventually (Carter-Dawson et al., 1978). The lack of protective survival factors provided by the rods might in part explain this secondary (cone) cell death (Sahel, 2005). Additionally, reactive changes, such as glial activation, may contribute to the disease progression.

There are two types of macroglia in the vascularized retina: astrocytes, which are largely restricted to the innermost layer of the vascularized retina, and the more prominent radial Müller glia cells, which span almost the entire thickness of the retina with their processes (reviewed in (Newman, 2009). Much like astrocytes in other parts of the central nervous system, the retinal glial cells are important for maintenance of ion-, water-, and neurotransmitter-homeostasis and support the neurons metabolically and structurally (Bringmann et al., 2006). Astrocytes in the normal adult mouse retina express detectable levels of the intermediate filament (IF) glial fibrillary acidic protein (GFAP), while Müller cells are mostly vimentin-positive under normal conditions (reviewed in Lewis and Fisher, 2003). Activation of astrocytes and Müller cells under pathologic conditions, including RP, is characterized by proliferation, hypertrophy, and increased expression of numerous growth factors and cytokines, as well as strong up-regulation of IFs (reviewed in Bringmann et al., 2006; Bringmann et al., 2009; Ekström et al., 1988; Lewis and Fisher, 2003; Luna et al., 2010; Sarthy and Egal, 1995). Despite the fact that these IFs are commonly used as early markers for reactive gliosis, their exact role in the pathologic processes has yet to be unraveled. It has been observed *in vitro* that neurons co-cultured with astrocytes lacking GFAP and vimentin have an improved survival and neurite outgrowth compared to co-cultures with normal astrocytes (Menet et al., 2001). *In vivo*, a better integration of neural

grafts transplanted next to retinas of GFAP- and vimentin-deficient mice has been observed (Kinouchi et al., 2003), possibly due to reduced hypertrophy of cell processes and limited scar formation (Pekny et al., 1999; Verardo et al., 2008; Wilhelmsson et al., 2004). Further, it has been shown that the lack of GFAP and vimentin results in an attenuation of the overall gliotic response (normally observed following detachment of the retina) and in better photoreceptor survival (Nakazawa et al., 2007; Verardo et al., 2008). These observations point to a role for GFAP and vimentin in the reactive state, and suggest that they may, directly or indirectly, contribute also to the degenerative process.

We have recently shown that the inability to produce GFAP and vimentin affects not only the reactive properties of the glial cells, but also normal retinal function (Wunderlich et al., submitted). Furthermore, we found that the expression of certain potassium channels was reduced in animals lacking these IFs (Wunderlich et al., submitted). In the present study, we have investigated whether the inability to produce GFAP and vimentin affects the rate of progression of photoreceptor cell degeneration in a mouse model of RP, the *rd1* mouse. A functional analysis was performed using electroretinography (ERG) along with tissue analysis in which the distribution and levels of expression of several neuronal and glial proteins were evaluated.

MATERIALS AND METHODS

Animals

Retinas from two groups of C57BL/129 mice were analyzed: mice with retinal degeneration (*Pde6b* mutation, *rd1*) expressing GFAP and vimentin (*rd1*, $GFAP^{+/+}Vim^{+/+}$) and mice lacking these IFs (*rd1*, $GFAP^{-/-}Vim^{-/-}$) (Eliasson et al., 1999; Pekny et al., 1995) with retinal degeneration. Polymerase chain reaction (PCR) genotyping confirmed the presence of the *rd1* allele (data not shown). Both male and female animals were used for the experiments. All experiments were conducted with the approval of the local animal experimentation ethics committee. The mice were handled in accordance to the guidelines set by the Government Committee on Animal Experimentation at the University of Lund and the ARVO Statement for the Use of Animals in Ophthalmic and Vision Research. The mice had free access to food and water and were kept on a 12-hour light-dark cycle.

Electroretinogram (ERG) analysis

Full-field electroretinographic (ERG) analysis was performed in *rd1*, $GFAP^{+/+}Vim^{+/+}$ (n=5) and *rd1*, $GFAP^{-/-}Vim^{-/-}$ (n=5) mice at postnatal day (PN) 21, as described previously (Seeliger et al., 2001; Tanimoto et al., 2009; Tanimoto et al., 2013). After dark-adaptation overnight, the

mice were anesthetized with ketamine (66.7 mg/kg body weight) and xylazine (11.7 mg/kg body weight) and the pupils were dilated. Single-flash ERG recordings were obtained under both scotopic (dark-adapted) and photopic (light-adapted for 10 min at 30 cd/m^2) conditions. Single-white-flash-stimulus intensities ranged from -4 to 1.5 log cd*s/m^2 under scotopic and from -2 to 1.5 log cd*s/m^2 under photopic conditions, in ten and eight steps, respectively. The ERG equipment consisted of a Ganzfeld bowl, a direct current amplifier, and a PC-based control and recording unit (Multiliner Vision; VIASYS Healthcare GmbH, Hoechberg, Germany).

Immunohistochemistry

Rd1, GFAP$^{+/+}$*Vim*$^{+/+}$ and *rd1*, *GFAP*$^{-/-}$*Vim*$^{-/-}$ mice (PN7 to PN60) were killed with carbon dioxide and eyes quickly enucleated. The eyes were fixed in 4% paraformaldehyde in Sørensen's buffer (0.1 M; pH 7.2) for 2 hours at 4°C, rinsed, cryoprotected with increasing concentrations of sucrose in the buffer, embedded in an albumin-gelatin medium, and frozen. Cryostat sections (12 µm) were stored at -20°C until further processing. Air-dried retinal sections were blocked with PBS (10 mM, pH = 7.2) containing Triton-X (0.25%), BSA (1%) (PBS-T-BSA), and the corresponding normal serum (5%) at room temperature for one hour and subsequently incubated with the primary serum (diluted in PBS-T-BSA containing 2% normal serum) at 4°C overnight. After thorough rinsing, the sections were incubated with the corresponding secondary antibodies diluted in PBS for 90 minutes at room temperature. Negative controls were included in which the primary antibody was omitted. Stained sections were mounted with an antifading medium, which, in some experiments, contained DAPI for visualization of the nuclei (VECTASHIELD®, Vector Laboratories, CA, USA), and were examined with a fluorescence microscope (Axiophot, Carl Zeiss Meditec, Inc., Oberkochen, Germany). Images were taken with a digital camera and accompanying software (Axiovision 4.2, Carl Zeiss Meditec) with the same settings for all sections with the same antibody. Brightness and contrast of the images were adjusted with Photoshop (Photoshop CS5v., Adobe). To facilitate direct comparisons between retinas of different age and/or genotype, the images were taken from approximately the same position near the optic nerve head.

Western blotting

Mice (PN7, PN14, PN21, and PN60) were killed with carbon dioxide and the eyes quickly enucleated. Three to five retinas were pooled and homogenized mechanically in sample buffer (2% sodium dodecyl sulphate, 10% glycerol, 0.0625 M Tris-HCl, pH 6.8). The protein concentrations were determined with a protein assay kit (DC Protein Assay kit, Bio-Rad, Hercules, CA, USA). 10 - 20 µg of protein were separated on 10-15% SDS-polyacrylamide

gels and semidry-blotted onto Immobilon polyvinylidene difluoride transfer membranes (Millipore, Billerica, MA, USA). After blocking with 5% non-fat dry milk in PBS with 0.1% Tween 20 for 2 hours, the membranes were incubated with primary antiserum at 4°C overnight and subsequently rinsed. Peroxidase-conjugated secondary antibodies were applied for 1 hour at room temperature followed by additional washing steps. The reaction was visualized with an enhanced chemiluminescence (ECL) Western Blotting kit and Hyperfilm (Amersham Biosciences, Sunnyvale, CA, USA). After a mild stripping in a solution containing 0.2 M glycine, 3.5 mM SDS, and 1% Tween 20 with the pH of 2.2, the membranes were incubated again to check for the expression of GAPDH as internal loading control.

Antibodies

Primary serum was applied in the following dilutions for immunohistochemistry (IHC) and western blot (WB) analysis, respectively: rabbit anti-aquaporin 4 (AQP4, 1:800 IHC/1:4,000 WB PN7+14, 1:6,000 WB PN21+60; Sigma-Aldrich, Saint Louis, MO, USA), rabbit anti-Kir2.1 (1:500 IHC/1:400 WB; Sigma-Aldrich, Saint Louis, MO, USA), rabbit anti-cone arrestin (1:1,000 IHC, kindly provided by Cheryl Craft, Univ Southern California, USA), guinea pig anti-glutamate-aspartate transporter (GLAST, 1:4,000 IHC/1:40000 WB), rabbit anti-glyceraldehyde-3-phosphate dehydrogenase (GAPDH, 1:2,000 WB, Abcam, Cambridge, UK), mouse anti-glutamine synthetase (GS, 1:2,000 IHC/1:25,000 WB, BD Biosciences, Franklin Lakes, NJ, USA), Kir4.1 (1:1,000 IHC/1:500 WB, Alomone Labs Ltd., Jerusalem, Israel), rhodopsin (clone RET-P1, 1:400 IHC, Millipore, Billerica, MA, USA), and Sox-9 (1:500-600 IHC/1:500 WB; Millipore, Billerica, MA, USA). Fluorescein-labeled Peanut agglutinin (PNA, 1:500, Vector Laboratories, Burlingame, CA, USA) was diluted in buffer containing 300 mM NaCl, 100 µM $CaCl_2$, and 10 mM HEPES (pH 7.5).

The following secondary antibodies were diluted 1:200 in PBS for IHC: goat anti-guinea pig (Sigma-Aldrich, Saint Louis, MO, USA), Alexa Fluor®594-conjugated goat anti-rabbit, Alexa Fluor®488-conjugated goat anti-mouse and goat anti-rabbit (Invitrogen Ltd., Paisley, UK), Texas Red®-conjugated donkey anti-mouse and donkey anti-rabbit (Jackson Immunoresearch, Westgrove, PA, USA). DyLight™549-conjugated donkey anti-mouse and DyLight™488-conjugated donkey anti-rabbit (Jackson Immunoresearch, Westgrove, PA, USA) were diluted 1:400. The following secondary antibodies for WB analyses were conjugated with horseradish peroxidase and raised in goat: anti-guinea pig (1:60,000), anti-mouse (1:40,000, Jackson Immunoresearch, Westgrove, PA, USA), anti-rabbit (1:30,000, Nordic BioSite, Täby, Sweden).

RESULTS

Electroretinographic Analysis

The *rd1* mouse is a well-characterized model for human retinitis pigmentosa (RP), including electrophysiological characterization of the disease progression (Gibson et al., 2013; Strettoi et al., 2003). Full-field electroretinography (ERG) is a widely used tool to assess the retinal function of humans in clinical diagnostics, but also of mice in vision research (Tanimoto et al., 2013). Stimulation with light flashes of different wavelengths, frequencies and intensities result in changes of the summed electrical potentials of the eye. The resulting ERG-waveforms generally consist of a cornea-negative deflection, the a-wave, which is produced by the hyperpolarizing photoreceptors, followed by the positive b-wave representing the activity of postsynaptic neurons. Small wavelets, the oscillatory potentials, are superimposed onto the b-wave. Altered latencies (time from stimulus onset to response onset), implicit times (time from light flash to response peak) and/or amplitudes are usually a characteristic measure of a pathological condition.

In the present study, we performed single-flash ERG recordings under dark- (scotopic) and light- (photopic) adapted conditions to assess and compare the degree of functional decline in retinas from *rd1, GFAP*$^{+/+}$*Vim*$^{+/+}$ and *rd1, GFAP*$^{-/-}$*Vim*$^{-/-}$ mice. Corresponding with the advanced photoreceptor degeneration at PN21, the typical ERG pattern was absent in both genotypes. The ERG curves were flat and almost indistinguishable from the baseline, lacking an a-wave and showing only a very subtle positively deflecting waveform at higher intensities that vaguely resembled the b-wave (Fig. 1). Nevertheless, under both scotopic and photopic conditions, the b-wave amplitudes were smaller in *rd1, GFAP*$^{+/+}$*Vim*$^{+/+}$ than in *rd1 GFAP*$^{-/-}$*Vim*$^{-/-}$ mice (Fig. 1A, 1B). Light-adapted *rd1, GFAP*$^{+/+}$*Vim*$^{+/+}$ seemed to have a lower sensitivity than *rd1, GFAP*$^{-/-}$*Vim*$^{-/-}$ mice, shown by the need of higher stimulus intensities to induce a response (Fig. 1B). Also, a clearly prolonged implicit time and delayed return to the baseline could be observed in *rd1, GFAP*$^{+/+}$*Vim*$^{+/+}$ compared to *rd1, GFAP*$^{-/-}$*Vim*$^{-/-}$ mice, especially when superimposing the scotopic recordings of both genotypes with a stretched (200%) Y-axis (Fig. 1A). The averaged b-wave latencies, plotted as a function of the logarithm of the stimulus intensity in figure 1B, show that there is a delay in the activation phase of *rd1, GFAP*$^{+/+}$*Vim*$^{+/+}$ in comparison to *rd1, GFAP*$^{-/-}$*Vim*$^{-/-}$ mice. At the age of 5 weeks, there were no recordable light responses (Fig. 1C).

Morphology/Photoreceptor distribution

In order to work out possible explanations for the slight electrophysiological differences, we compared the overall structure of PN21 retinas by the means of DAPI staining. The typical well organized retina-specific layering in three major nuclear layers (outer nuclear layer, inner

nuclear layer and ganglion cell layer) and the synaptical layers separating them – the outer plexiform layer and the inner plexiform layer – could be observed for both genotypes. The thickness of all layers was also comparable between *rd1, GFAP*$^{+/+}$*Vim*$^{+/+}$ and *rd1, GFAP*$^{-/-}$*Vim*$^{-/-}$ mice. One exception was the nerve fiber layer at the vitreous side of the retina, which had often sheared off in retinas lacking GFAP and vimentin. As a consequence of the advanced cell loss by three weeks of age, the outer nuclear layer consisted of only one to two remaining cell rows (Fig. 2, top panel). Despite small variations in outer nuclear layer thickness between *rd1, GFAP*$^{+/+}$*Vim*$^{+/+}$ and *rd1 GFAP*$^{-/-}$*Vim*$^{-/-}$ mice, deviations were observed also within the same group, such that no consistent differences could be found between the two genotypes. Accordingly, only a few cell bodies in the outer nuclear layer were immunostained with the rod photoreceptor-specific marker rhodopsin. No photoreceptor segments, where rhodopsin is located in healthy retinas, could be observed in either genotype (Fig. 2, second panel). The plant lectin peanut agglutinin (PNA), which binds to specific carbohydrates on the surface of cone photoreceptors (Blanks and Johnson, 1984), labeled synaptic pedicles in the outer plexiform layer, as well as some rudimental photoreceptor segments. The majority of all remaining photoreceptors at this stage of the disease are cones, although in the normal mouse retina, these cells are, by far, outnumbered by rods (Jeon et al., 1998). Yet again, we could not detect any differences between the two genotypes (Fig. 2, third panel) following immunostainings using an antibody against cone arrestin (Fig. 2, bottom panel). Taken together, these results indicate that there are no major morphological differences neither in the structure of the retina nor in the outer nuclear layer, in particular, that could explain the electrophysiological differences observed between the two genotypes.

Analysis of retinal glial proteins

Since the expression of intermediate filaments is strongly up-regulated in the *rd1* mouse retina from PN11 onwards (Ekström et al., 1988; Wunderlich et al., 2010), one could expect that the lack of GFAP and vimentin might have an impact on the levels of other molecules normally expressed in reactive Müller cells (and astrocytes) in the degenerating retina. We therefore examined the expression of several established glial cell markers and of proteins involved in fundamental functions of retinal glia cells, such as uptake and recycling of glutamate from the extracellular space and homeostasis of potassium and water.

Western blot analysis of retinal lysates from PN7, PN14, PN21, and PN60 mice for the SRY-box 9 (SOX9) protein resulted in an equally sized double band in both genotypes at all ages (Fig. 3). Immunohistological evaluation of this protein in retinal sections of PN21 *rd1,*

GFAP$^{+/+}$*Vim*$^{+/+}$ and *rd1, GFAP*$^{-/-}$*Vim*$^{-/-}$ mice revealed similar SOX9 expression in the nuclei of Müller cells (Fig. 4A, B) and in the retinal pigment epithelium (not shown) in both genotypes.

The levels of the glutamate aspartate transporter (GLAST) were low at PN7 and increased with age in both genotypes, but were slightly reduced in *rd1, GFAP*$^{-/-}$*Vim*$^{-/-}$ compared to *rd1, GFAP*$^{+/+}$*Vim*$^{+/+}$ mice. There was no glutamine synthetase (GS) expression detectable at PN7, but increasing levels were found from PN14 and onwards, with weaker bands for *rd1, GFAP*$^{-/-}$*Vim*$^{-/-}$ mice than for *rd1, GFAP*$^{+/+}$*Vim*$^{+/+}$ at PN14 and PN21 (Fig. 3). Immunolabeling showed strong glutamine synthetase (GS) staining in Müller cell bodies in the inner nuclear layer as well as their processes in all retinal layers (Fig. 4C, D). A slightly decreased staining intensity could be noted in PN21 *rd1, GFAP*$^{-/-}$*Vim*$^{-/-}$ mice, reflecting the reduced expression levels.

Expression of the inwardly rectifying potassium channel Kir2.1 was found in Müller cell-bodies and -processes of both genotypes at PN21, but the fluorescence intensity was overall stronger in the *rd1, GFAP*$^{+/+}$*Vim*$^{+/+}$ than in the *rd1, GFAP*$^{-/-}$*Vim*$^{-/-}$ (Fig. 4E, F). Indeed, the levels of Kir2.1 in Western blots were found to be lower in *rd1, GFAP*$^{-/-}$*Vim*$^{-/-}$ than in *rd1, GFAP*$^{+/+}$*Vim*$^{+/+}$ mice, which was especially prominent at the ages PN14 and PN21 (Fig. 3). Kir4.1 was not detectable at PN7 by western blotting, but double bands with increasing protein amounts with increasing age could be observed from PN14 onwards (Fig. 3). There was a lower Kir4.1 expression in mice lacking GFAP and vimentin, which could also be appreciated in the immunostainings; antiserum against Kir4.1 distinctively labeled Müller cell processes, most prominently in the region of the inner and outer limiting membranes, as well as in the proximity of blood vessels in both animal groups. However, the staining intensity was clearly reduced in the proximal Müller cell processes of *rd1, GFAP*$^{-/-}$*Vim*$^{-/-}$ mice (Fig. 4G, H).

The water channel aquaporin 4 (AQP4) was not detectable at PN7, but its levels increased significantly with age in both genotypes (Fig. 3). Slightly weaker AQP4-expression levels were observed in the *GFAP*$^{-/-}$*Vim*$^{-/-}$ mice at PN14 and PN21. Differences in staining intensities or distribution could, however, not be appreciated on immunohistological stainings. In both genotypes, AQP4-labeling showed a strong expression of the protein along the Müller cell processes. The signal was particularly intense at the Müller cell endfeet in the vitreal surface of the retina and around vessels (Fig. 4 I, J).

DISCUSSION

In the *rd1* mouse, a mutation in the *Pde6b* gene causes photoreceptor cell death (Bowes et al., 1990), which is, as in many other pathological conditions, affecting the retina, accompanied by glial activation. A common feature of this process of reactive gliosis is the

up-regulation of GFAP and vimentin (Ekström et al., 1988), and yet little is known about their exact function in the process. As mentioned above, the deficiency of GFAP and vimentin has been shown to increase neuronal survival following detachment of the mouse retina (Nakazawa et al., 2007; Verardo et al., 2008). In the present study, we have investigated which effect the inability to produce (and up-regulate) these IF proteins has on the more chronic condition of the *rd1* mouse model. For this purpose, we have compared electrophysiological function, distribution of photoreceptor cells, and the expression patterns of important glial proteins.

Predictably, ERG responses of the degenerating retinas were just above background noise by PN21. At this age, most rod photoreceptor cells are already lost and only one to two cell rows of mainly cones remain in the outer nuclear layer (Fig 2). Large scotopic responses cannot be expected even at younger ages due to the non-functional *Pde6b* in the *rd1*. Indeed, in earlier studies, rod responses were found to be completely absent in *rd1* mice at any age (Strettoi et al., 2003). Gibson et al., (2013), on the other hand, reported small rod-mediated b-waves until up to the age of PN16 and PN18, but no responses were detected at PN21. These differences could possibly be due to different experimental set-ups and/or the use of different mouse strains. We were still able to detect responses from dark-adapted animals at PN21, but only at higher intensities (above 0 log cd*s/m^2), which could also elicit cone responses. Slight differences between *rd1* mice expressing GFAP and vimentin and those lacking the IFs were detected (Fig. 1). Rod- and cone-driven responses to light stimuli were larger in amplitudes and faster with regards to response onset, implicit time and return to baseline in *rd1* $GFAP^{-/-}Vim^{-/-}$ mice compared to *rd1* $GFAP^{+/+}Vim^{+/+}$ mice. Delayed onset and return to baseline, as well as prolonged implicit times compared to normal mice, are known characteristics of the progression of the disease in the *rd1* mouse (Strettoi et al., 2003). Cones in the *rd1,* $GFAP^{-/-}Vim^{-/-}$ mouse retina seemed also slightly more sensitive to light than cones in *rd1,* $GFAP^{+/+}Vim^{+/+}$ retinas.

These results could indicate that the lack of GFAP and vimentin has a small but positive effect on photoreceptor cell survival. However, considering the generally very low responses seen at PN21, these results are to be taken with caution. Gibson et al., (2013) have shown that retinal function only reaches maturity at PN30 in wildtype mice. It is thus possible that the improved cone responses result from a developmental delay. Nonetheless, ERG responses could no longer be measured at five weeks of age, regardless of the genotype (Fig. 1C).

Our previous studies have revealed higher b-wave amplitudes in mice lacking GFAP and vimentin even without photoreceptor degeneration (Wunderlich et al., submitted). In that case, the alterations were assumed to involve the rod system, since no differences were

observed under photopic conditions. In the present study, we have therefore examined the retinal morphology and the subpopulation of photoreceptor cells in more detail. In DAPI-stained retinal sections, no obvious difference in the thickness of the nuclear layers was noted. The retinal organization was comparable between both genotypes with the exception that the innermost layers of the retinas often tended to shear off in GFAP/vimentin-deficient mice. This instability has been described before for *GFAP*$^{-/-}$*Vim*$^{-/-}$ mice without any retinal degeneration and is explained by lower resistance to mechanical stress during the handling of the tissue (Kinouchi et al., 2003; Lundkvist et al., 2004; Verardo et al., 2008; Wunderlich et al., submitted).

At PN21 in the *rd1* mouse retina, very few photoreceptors can be found, and most of those remaining correspond to cones. We found no indication that photoreceptors were protected in *GFAP*$^{+/+}$*Vim*$^{+/+}$ mice, as the retinas of both genotypes were comparable in terms of number and distribution of rods and cones (FIG. 2). Both groups of animals had only one to two cell rows remaining in the outer nuclear layer, consisting of a few rods and mostly cones. Rhodopsin, which is normally abundant in rod outer segments, was mislocalized to the cell body, which is a common feature of degenerating rods, in which the photoreceptor segments are affected first or do not develop properly altogether (Nir et al., 1989). PNA labeling of cones did not reveal any differences in cone cell number or distribution, neither did the immunostaining with an antibody against the cone specific arrestin. In conclusion, we found that the number and distribution of remaining photoreceptors are comparable between the two genotypes. The lack of GFAP and vimentin does not seem to affect rod and cone cell numbers, at least not to an extent that could explain the electrophysiological alterations.

The a-wave, reflecting the light-induced closure of sodium channels in photoreceptor outer segments, was too low to make out possible differences between the *rd1, GFAP*$^{+/+}$*Vim*$^{+/+}$ and the *rd1, GFAP*$^{-/-}$*Vim*$^{-/-}$ mouse. We can only assume that there was no difference, since there were no obvious morphological differences in photoreceptor distribution between the two genotypes. More in-depth analyses of the biophysical and biochemical properties of the photoreceptors would be necessary to conclude this more definitely.

GFAP and vimentin are cytoskeletal glial proteins, and the up-regulation of these IFs in Müller cells is a well-known reaction to many pathological conditions affecting the retina including the photoreceptor degeneration in the *rd1* mouse (Eberhardt et al., 2011; Ekström et al., 1988; Iandiev et al., 2008a; Lewis et al., 2010; Wunderlich et al., 2010). Even though it has been shown that Müller glia cells are not responsible for the generation of the b-wave (Lei and Perlman, 1999), it is still debated whether and how much they contribute to this response. In every case, Müller cells are important for the maintenance of the homeostasis

of extracellular ions and water, as well as for transmitter clearance and recycling (reviewed in Bringmann et al., 2006; Newman, 2009), and have thus at least a modulatory role. We have therefore investigated, whether the lack of GFAP and vimentin alters some of those properties.

The SRY-box 9 (SOX9) protein is expressed in Müller cell nuclei (Muto et al., 2009), and the fact that the expression level as well as the distribution was similar in *rd1, GFAP*$^{+/+}$*Vim*$^{+/+}$ and *rd1, GFAP*$^{-/-}$*Vim*$^{-/-}$ mice leads to the assumption that the lack of GFAP and vimentin did not affect the number of Müller cells. We have also examined two proteins that are involved in glutamate homeostasis, namely the glutamate aspartate transporter (GLAST) and glutamine synthetase (GS). Both proteins showed a slight reduction in protein expression in *rd1* mice lacking GFAP and vimentin, particularly at PN14 and PN21 and less so at PN60 (Fig. 1), concomitant with the transient GFAP up-regulation in normal *rd1* mice (Chua et al., 2013; Strettoi et al., 2002). GLAST is important for the clearing of glutamate from the extracellular space to prevent glutamate excitotoxicity and to ensure quick termination of neuronal signals (reviewed in e.g., Bringmann et al., 2009). Lower glutamate levels in the retina have been reported in *rd1* mice compared to age-matched wildtype controls, possibly simply because of decreased glutamate release and turnover in association with the photoreceptor cell loss (Gibson et al., 2013). Reduced GLAST expression could potentially result in higher extracellular glutamate levels and/or prolonged glutamate signaling. This could partly underlie the larger b-wave amplitudes and the prolonged response times in *rd1 GFAP*$^{-/-}$*Vim*$^{-/-}$ mice. However, in contrast to what was seen in the present study, we have previously found that GLAST levels were comparable, if not even slightly increased, in *GFAP*$^{-/-}$*Vim*$^{-/-}$ mice without a retinal degeneration phenotype, when compared to their wildtype controls (Wunderlich et al., submitted). It has been suggested earlier that the absence of GFAP impairs the accurate expression, trafficking, and anchoring of GLAST (Hughes et al., 2004; Sullivan et al., 2007). The knockout or knockdown of GLAST, on the other hand, has been shown to result in suppressed b-wave formation, which we could not observe here in *rd1, GFAP*$^{-/-}$*Vim*$^{-/-}$ mice, and prolonged latencies in healthy retinas (Barnett and Pow, 2000; Harada et al., 1998).

The pharmacological inhibition of GS has also been shown to cause a rapid decrease of the b-wave (Barnett et al., 2000). GS converts glutamate to glutamine in Müller glial cells. We have shown that GS levels are reduced in *rd1, GFAP*$^{-/-}$*Vim*$^{-/-}$ mice compared to *rd1, GFAP*$^{+/+}$*Vim*$^{+/+}$ (Fig. 3). Lower GS levels have also been reported in non-degenerating *GFAP*$^{-/-}$*Vim*$^{-/-}$ mouse retinas (Verardo et al., 2008; Wunderlich et al., submitted). A decreased glutamate uptake into Müller cells, due to lower GLAST levels, could be the reason for the

down-regulated expression of GS, as its expression is regulated by the availability of glutamate (Shen et al., 2004).

Glutamate uptake is also dependent on a potassium gradient between the intra- and the extracellular space, since GLAST counter-transports one K^+-ion with each glutamate molecule (Barbour et al., 1988; Sarantis and Attwell, 1990). Potassium siphoning by Müller cells is mainly carried out by inwardly rectifying potassium (Kir) channels (reviewed in e.g., Bringmann et al., 2009). We have previously found that the lack of GFAP and vimentin changes the electrophysiological responses of the healthy retina to light stimuli, possibly as a result of altered levels and distribution of Kir channels along the Müller cells (Wunderlich et al., submitted). Here, we show similar alterations in Kir channel expression in *rd1* mice lacking these IFs. The overall expression of both Kir2.1 and Kir4.1 is reduced in *rd1, GFAP*$^{-/-}$ *Vim*$^{-/-}$ mice compared to *rd1, GFAP*$^{+/+}$*Vim*$^{+/+}$ (Fig. 3). Kir4.1 is particularly weakly expressed in the proximal processes of Müller cells in the *rd1, GFAP*$^{-/-}$*Vim*$^{-/-}$ mice (Fig. 4H). This expression pattern has also been observed in *GFAP*$^{-/-}$*Vim*$^{-/-}$ mice without retinal degeneration (Wunderlich et al., submitted). Reduced levels and redistribution of Kir4.1 is characteristic for both immaturity and reactive gliosis (reviewed in Bringmann et al., 2000; Bringmann et al., 2006). Knockout of Kir4.1 has been reported to evoke increased b-wave amplitudes (Kofuji et al., 2000; Wu et al., 2004). Similarly augmented b-waves could be observed in experiments with intraocular barium injections, which almost completely block the potassium conductance in Müller cells (Sharma et al., 2005).

The water-channel aquaporin 4 (AQP4) is often co-localized with Kir4.1 (Connors and Kofuji, 2006; Fort et al., 2008). However, a direct functional coupling does not seem to exist (Ruiz-Ederra et al., 2007; Zhang and Verkman, 2008). In a recent study, we did not observe any functional coupling of Kir4.1 and AQP4, as the levels of Kir4.1, but not AQP4, were reduced in the intact *GFAP*$^{-/-}$*Vim*$^{-/-}$ mouse retinas compared to the wildtype controls (Wunderlich et al., submitted). The decreased AQP4 expression could therefore be a more direct effect of the inability to up-regulate GFAP and vimentin in response to photoreceptor cell death. Altered distribution of AQP4 has been observed following light-damage in the retina (Iandiev et al., 2008a; Iandiev et al., 2008b), but not the *rd1* mouse model (Roesch et al., 2012). AQP4 is supposedly involved in the hypertrophy of glia upon activation (Auguste et al., 2007; Saadoun et al., 2005) and the altered AQP4 expression could be associated with this, since Müller cells are less hypertrophic when they lack intermediate filaments (Wilhelmsson et al., 2004).

In conclusion, our findings do not support the idea that the inability to up-regulate GFAP and vimentin is beneficial for photoreceptor survival in the *rd1* mouse, an inherited model of retinal degeneration, or that it slows down the progression of the disease. The higher b-

waves in the animals lacking glial IFs do not seem to be an effect of better preserved cone function and/or improved photoreceptor survival, but rather an effect of the altered glial physiology. The exact mechanisms by which the ERG findings are connected to alterations in glutamate metabolism and potassium and/or water siphoning by Müller cells will have to be further evaluated.

Figure legends:

Figure 1. Electroretinographic (ERG) evaluation of retinal function in *rd1,* GFAP$^{+/+}$Vim$^{+/+}$ and *rd1,* GFAP$^{-/-}$Vim$^{-/-}$ mice. In **(A)**, selected single-flash ERGs from *rd1,* GFAP$^{+/+}$Vim$^{+/+}$ (green, left column, n=5) and *rd1,* GFAP$^{-/-}$Vim$^{-/-}$ (blue, middle column, n=5) mice of 3 weeks of age are shown with the overlay in the right column. The vertical lines are indicating the timing of the light flash. **(B)** Averaged b-wave amplitudes, measured from the minimum peak to the maximum peak following the light stimulation, are plotted against the logarithm of the stimulus intensity in the right panel. In the left panel, the averaged b-wave latencies are plotted against the stimulus intensity. Top: scotopic conditions, bottom: photopic conditions. Boxes indicate the 25% and 75% quantile range, whiskers indicate the 5% and 95% quantiles, and the asterisks indicate the median of the data. **(C)** Selected single-flash ERGs from 5-week-old *rd1,* GFAP$^{+/+}$Vim$^{+/+}$ (green, left column) and *rd1,* GFAP$^{-/-}$ Vim$^{-/-}$ (blue, right column) mice. The vertical lines indicate the timing of the light flash.

Figure 2. Comparable layering and distribution of photoreceptor cells in the retinas of three-week-old *rd1, GFAP$^{+/+}$Vim$^{+/+}$* and *rd1, GFAP$^{-/-}$Vim$^{-/-}$* mice. DAPI staining of retinal cell nuclei showed similarly organized layering into outer nuclear layer (ONL), inner nuclear layer (INL), and ganglion cell layer (GCL). The ONL consisted of one to two cell rows in *rd1,GFAP$^{+/+}$Vim$^{+/+}$* and *rd1*, *GFAP$^{-/-}$Vim$^{-/-}$* mice (top). Rod photoreceptors were stained with an antibody against rhodopsin (RHO; second panel). RHO expression was found in a few cell bodies in the ONL. Peanut agglutinin (PNA) staining showed comparably labeled synaptic pedicles and rudimental cone photoreceptor segments in both genotypes (third panel). Cone arrestin (CAR) expression was detected in cone cell bodies (bottom panel). The number and distribution of rods and cones were comparable in *rd1, GFAP$^{+/+}$Vim$^{+/+}$* and *rd1*, *GFAP$^{-/-}$Vim$^{-/-}$* mice. ONL, outer nuclear layer; INL, inner nuclear layer; GCL, ganglion cell layer. Scale bar, 20 µm.

Figure 3. Expression levels of glial proteins in the retinas of *rd1, GFAP$^{+/+}$Vim$^{+/+}$* and *rd1, GFAP$^{-/-}$Vim$^{-/-}$* mice of different ages. Western blot analyses of retina lysates were performed to compare the levels of the glial proteins SRY-box 9 (SOX9; ~65 kDa), glutamate aspartate transporter (GLAST; ~67 kDa), glutamine synthetase (GS; ~45 kDa), inwardly rectifying potassium channels Kir2.1 (~48 kDa) and Kir4.1 (~45 kDa), and aquaporin 4 (AQP4; ~32 kDa) in *rd1, GFAP$^{+/+}$Vim$^{+/+}$* and *rd1, GFAP$^{-/-}$Vim$^{-/-}$* mice of different ages: PN (postnatal day) 7, PN14, PN21, and PN60. The housekeeping proteins glyceraldehyde-3-phosphate dehydrogenase (GAPDH; ~36 kDa) was used as a loading control.

Figure 4. Localization of glial proteins in the retinas of three-week-old *rd1, GFAP$^{+/+}$Vim$^{+/+}$* and *rd1, GFAP$^{-/-}$Vim$^{-/-}$* mice. (A, B) Müller cell nuclei in the inner nuclear layer (INL) were stained with an antibody against the SRY-box 9 (SOX9) protein in both genotypes, and appeared to be slightly weaker in *rd1*, *GFAP$^{-/-}$Vim$^{-/-}$* mice. **(C, D)** Staining of Müller cell nuclei and radial processes for glutamine synthetase (GS) was weaker in *rd1*, *GFAP$^{-/-}$Vim$^{-/-}$* mice compared to the control group. **(E, F)** The inwardly rectifying potassium (Kir) channel Kir2.1 was found in Müller cell bodies and processes of both genotypes, but the fluorescence intensity was again overall stronger in the *rd1, GFAP$^{+/+}$Vim$^{+/+}$* than in the *rd1*, *GFAP$^{-/-}$Vim$^{-/-}$*. **(G, H)** A distinct Kir4.1 labeling of Müller cell processes was observed, which was very prominent in the region of the inner and outer limiting membranes, as well as in the proximity of blood vessels. A clearly decreased staining in the proximal radial processes was detected in *rd1*, *GFAP$^{-/-}$Vim$^{-/-}$* mice. **(I, J)** Aquaporin 4 (AQP4) showed a comparable distribution pattern along the Müller cell processes in both genotypes. The signal was particularly strong at the Müller cell endfeet in the ganglion cell layer (GCL) and around blood vessels. ONL, outer nuclear layer; INL, inner nuclear layer; GCL, ganglion cell layer. Scale bar, 20 µm.

Bibliography

Auguste, K.I., Jin, S., Uchida, K., Yan, D., Manley, G.T., Papadopoulos, M.C. and Verkman, A.S. (2007). Greatly impaired migration of implanted aquaporin-4-deficient astroglial cells in mouse brain toward a site of injury. FASEB J. *21*, 108-116.

Barbour, B., Brew, H. and Attwell, D. (1988). Electrogenic glutamate uptake in glial cells is activated by intracellular potassium. Nature *335*, 433-435.

Barnett, N.L. and Pow, D.V. (2000). Antisense knockdown of GLAST, a glial glutamate transporter, compromises retinal function. Invest. Ophthalmol. Vis. Sci. *41*, 585-591.

Barnett, N.L., Pow, D.V. and Robinson, S.R. (2000). Inhibition of Müller cell glutamine synthetase rapidly impairs the retinal response to light. Glia *30*, 64-73.

Blanks, J.C. and Johnson, L.V. (1984). Specific binding of peanut lectin to a class of retinal photoreceptor cells. A species comparison. Invest. Ophthalmol. Vis. Sci. *25*, 546-557.

Bowes, C., Li, T., Danciger, M., Baxter, L.C., Applebury, M.L. and Farber, D.B. (1990). Retinal degeneration in the rd mouse is caused by a defect in the beta subunit of rod cGMP-phosphodiesterase.. Nature *347*, 677-680.

Bringmann, A., Francke, M., Pannicke, T., Biedermann, B., Kodal, H., Faude, F., Reichelt, W. and Reichenbach, A. (2000). Role of glial K(+) channels in ontogeny and gliosis: a hypothesis based upon studies on Müller cells. Glia *29*, 35-44.

Bringmann, A., Pannicke, T., Biedermann, B., Francke, M., Iandiev, I., Grosche, J., Wiedemann, P., Albrecht, J. and Reichenbach, A. (2009). Role of retinal glial cells in neurotransmitter uptake and metabolism. Neurochem. Int. *54*, 143-160.

Bringmann, A., Pannicke, T., Grosche, J., Francke, M., Wiedemann, P., Skatchkov, S.N., Osborne, N.N. and Reichenbach, A. (2006). Müller cells in the healthy and diseased retina. Prog Retin Eye Res *25*, 397-424.

Carter-Dawson, L.D., LaVail, M.M. and Sidman, R.L. (1978). Differential effect of the rd mutation on rods and cones in the mouse retina.. Invest. Ophthalmol. Vis. Sci. *17*, 489-498.

Chang, B., Hawes, N.L., Hurd, R.E., Davisson, M.T., Nusinowitz, S. and Heckenlively, J.R. (2002). Retinal degeneration mutants in the mouse. Vision Res. *42*, 517-525.

Chua, J., Nivison-Smith, L., Fletcher, E.L., Trenholm, S., Awatramani, G.B. and Kalloniatis, M. (2013). Early remodeling of Müller cells in the rd/rd mouse model of retinal dystrophy. J. Comp. Neurol. *521*, 2439-2453.

Connors, N.C. and Kofuji, P. (2006). Potassium channel Kir4.1 macromolecular complex in retinal glial cells. Glia *53*, 124-131.

Daiger, S.P., Bowne, S.J. and Sullivan, L.S. (2007). Perspective on genes and mutations causing retinitis pigmentosa. Arch. Ophthalmol. *125*, 151-158.

Eberhardt, C., Amann, B., Feuchtinger, A., Hauck, S.M. and Deeg, C.A. (2011). Differential expression of inwardly rectifying K+ channels and aquaporins 4 and 5 in autoimmune uveitis indicates misbalance in Müller glial cell-dependent ion and water homeostasis. Glia *59*, 697-707.

Ekström, P., Sanyal, S., Narfström, K., Chader, G.J. and van Veen, T. (1988). Accumulation of glial fibrillary acidic protein in Müller radial glia during retinal degeneration. Invest. Ophthalmol. Vis. Sci. *29*, 1363-1371.

Eliasson, C., Sahlgren, C., Berthold, C.H., Stakeberg, J., Celis, J.E., Betsholtz, C., Eriksson, J.E. and Pekny, M. (1999). Intermediate filament protein partnership in astrocytes. J. Biol. Chem. *274*, 23996-24006.

Farber, D.B. and Lolley, R.N. (1976). Enzymic basis for cyclic GMP accumulation in degenerative photoreceptor cells of mouse retina. J Cyclic Nucleotide Res *2*, 139-148.

Fauser, S., Luberichs, J. and Schüttauf, F. (2002). Genetic animal models for retinal degeneration. Surv Ophthalmol *47*, 357-367.

Flannery, J.G. (1999). Transgenic Animal Models for the Study of Inherited Retinal Dystrophies. ILAR J *40*, 51-58.

Fort, P.E., Sene, A., Pannicke, T., Roux, M.J., Forster, V., Mornet, D., Nudel, U., Yaffe, D., Reichenbach, A., Sahel, J.A., et al. (2008). Kir4.1 and AQP4 associate with Dp71- and utrophin-DAPs complexes in specific and defined microdomains of Müller retinal glial cell membrane. Glia *56*, 597-610.

Gibson, R., Fletcher, E.L., Vingrys, A.J., Zhu, Y., Vessey, K.A. and Kalloniatis, M. (2013). Functional and neurochemical development in the normal and degenerating mouse retina. J. Comp. Neurol. *521*, 1251-1267.

Hamel, C. (2006). Retinitis pigmentosa.. Orphanet J Rare Dis *1*, 40.

Harada, T., Harada, C., Watanabe, M., Inoue, Y., Sakagawa, T., Nakayama, N., Sasaki, S., Okuyama, S., Watase, K., Wada, K., et al. (1998). Functions of the two glutamate transporters GLAST and GLT-1 in the retina. Proc. Natl. Acad. Sci. U.S.A. *95*, 4663-4666.

Hartong, D.T., Berson, E.L. and Dryja, T.P. (2006). Retinitis pigmentosa.. Lancet *368*, 1795-1809.

Hughes, E.G., Maguire, J.L., McMinn, M.T., Scholz, R.E. and Sutherland, M.L. (2004). Loss of glial fibrillary acidic protein results in decreased glutamate transport and inhibition of PKA-induced EAAT2 cell surface trafficking. Brain Res. Mol. Brain Res. *124*, 114-123.

Iandiev, I., Pannicke, T., Hollborn, M., Wiedemann, P., Reichenbach, A., Grimm, C., Remé, C.E. and Bringmann, A. (2008b). Localization of glial aquaporin-4 and Kir4.1 in the light-injured murine retina. Neurosci. Lett. *434*, 317-321.

Iandiev, I., Wurm, A., Hollborn, M., Wiedemann, P., Grimm, C., Remé, C.E., Reichenbach, A., Pannicke, T. and Bringmann, A. (2008a). Müller cell response to blue light injury of the rat retina. Invest. Ophthalmol. Vis. Sci. *49*, 3559-3567.

Jeon, C.J., Strettoi, E. and Masland, R.H. (1998). The major cell populations of the mouse retina. J. Neurosci. *18*, 8936-8946.

Kinouchi, R., Takeda, M., Yang, L., Wilhelmsson, U., Lundkvist, A., Pekny, M. and Chen, D.F. (2003). Robust neural integration from retinal transplants in mice deficient in GFAP and vimentin. Nat. Neurosci. *6*, 863-868.

Kofuji, P., Ceelen, P., Zahs, K.R., Surbeck, L.W., Lester, H.A. and Newman, E.A. (2000). Genetic inactivation of an inwardly rectifying potassium channel (Kir4.1 subunit) in mice: phenotypic impact in retina. J. Neurosci. *20*, 5733-5740.

Lei, B. and Perlman, I. (1999). The contributions of voltage- and time-dependent potassium conductances to the electroretinogram in rabbits. Vis. Neurosci. *16*, 743-754.

Lewis, G.P. and Fisher, S.K. (2003). Up-regulation of glial fibrillary acidic protein in response to retinal injury: its potential role in glial remodeling and a comparison to vimentin expression.. Int. Rev. Cytol. *230*, 263-290.

Lewis, G.P., Chapin, E.A., Luna, G., Linberg, K.A. and Fisher, S.K. (2010). The fate of Müller's glia following experimental retinal detachment: nuclear migration, cell division, and subretinal glial scar formation. Mol. Vis. *16*, 1361-1372.

Luna, G., Lewis, G.P., Banna, C.D., Skalli, O. and Fisher, S.K. (2010). Expression profiles of nestin and synemin in reactive astrocytes and Müller cells following retinal injury: a comparison with glial fibrillar acidic protein and vimentin. Mol. Vis. *16*, 2511-2523.

Lundkvist, A., Reichenbach, A., Betsholtz, C., Carmeliet, P., Wolburg, H. and Pekny, M. (2004). Under stress, the absence of intermediate filaments from Müller cells in the retina has structural and functional consequences. J. Cell. Sci. *117*, 3481-3488.

Menet, V., Giménez y Ribotta, M., Chauvet, N., Drian, M.J., Lannoy, J., Colucci-Guyon, E. and Privat, A. (2001). Inactivation of the glial fibrillary acidic protein gene, but not that of vimentin, improves neuronal survival and neurite growth by modifying adhesion molecule expression. J. Neurosci. *21*, 6147-6158.

Muto, A., Iida, A., Satoh, S. and Watanabe, S. (2009). The group E Sox genes Sox8 and Sox9 are regulated by Notch signaling and are required for Müller glial cell development in mouse retina. Exp. Eye Res. *89*, 549-558.

Nakazawa, T., Takeda, M., Lewis, G.P., Cho, K., Jiao, J., Wilhelmsson, U., Fisher, S.K., Pekny, M., Chen, D.F. and Miller, J.W. (2007). Attenuated glial reactions and photoreceptor degeneration after retinal detachment in mice deficient in glial fibrillary acidic protein and vimentin. Invest. Ophthalmol. Vis. Sci. *48*, 2760-2768.

Newman, E. (2009). Retinal glia, In Encyclopedia of Neuroscience, L. Squire, ed. (Oxford Academic Press), pp. 225-232.

Nir, I., Agarwal, N., Sagie, G. and Papermaster, D.S. (1989). Opsin distribution and synthesis in degenerating photoreceptors of rd mutant mice. Exp. Eye Res. *49*, 403-421.

Pekny, M., Johansson, C.B., Eliasson, C., Stakeberg, J., Wallén, A., Perlmann, T., Lendahl, U., Betsholtz, C., Berthold, C.H. and Frisén, J. (1999). Abnormal reaction to central nervous system injury in mice lacking glial fibrillary acidic protein and vimentin. J. Cell Biol. *145*, 503-514.

Pekny, M., Levéen, P., Pekna, M., Eliasson, C., Berthold, C.H., Westermark, B. and Betsholtz, C. (1995). Mice lacking glial fibrillary acidic protein display astrocytes devoid of intermediate filaments but develop and reproduce normally. EMBO J. *14*, 1590-1598.

Roesch, K., Stadler, M.B. and Cepko, C.L. (2012). Gene expression changes within Müller glial cells in retinitis pigmentosa. Mol. Vis. *18*, 1197-1214.

Ruiz-Ederra, J., Zhang, H. and Verkman, A.S. (2007). Evidence against functional interaction between aquaporin-4 water channels and Kir4.1 potassium channels in retinal Müller cells. J. Biol. Chem. *282*, 21866-21872.

Saadoun, S., Papadopoulos, M.C., Watanabe, H., Yan, D., Manley, G.T. and Verkman, A.S. (2005). Involvement of aquaporin-4 in astroglial cell migration and glial scar formation. J. Cell. Sci. *118*, 5691-5698.

Sahel, J. (2005). Saving cone cells in hereditary rod diseases: a possible role for rod-derived cone viability factor (RdCVF) therapy. Retina (Philadelphia, Pa.) *25*, S38-S39.

Sarantis, M. and Attwell, D. (1990). Glutamate uptake in mammalian retinal glia is voltage- and potassium-dependent. Brain Res. *516*, 322-325.

Sarthy, V. and Egal, H. (1995). Transient induction of the glial intermediate filament protein gene in Müller cells in the mouse retina. DNA Cell Biol. *14*, 313-320.

Seeliger, M.W., Grimm, C., Ståhlberg, F., Friedburg, C., Jaissle, G., Zrenner, E., Guo, H., Remé, C.E., Humphries, P., Hofmann, F., et al. (2001). New views on RPE65 deficiency: the rod system is the source of vision in a mouse model of Leber congenital amaurosis. Nat. Genet. *29*, 70-74.

Sharma, S., Ball, S.L. and Peachey, N.S. (2005). Pharmacological studies of the mouse cone electroretinogram. Vis. Neurosci. *22*, 631-636.

Shen, F., Chen, B., Danias, J., Lee, K.C., Lee, H., Su, Y., Podos, S.M. and Mittag, T.W. (2004). Glutamate-induced glutamine synthetase expression in retinal Muller cells after short-term ocular hypertension in the rat. Invest. Ophthalmol. Vis. Sci. *45*, 3107-3112.

Strettoi, E., Pignatelli, V., Rossi, C., Porciatti, V. and Falsini, B. (2003). Remodeling of second-order neurons in the retina of rd/rd mutant mice. Vision Res. *43*, 867-877.

Strettoi, E., Porciatti, V., Falsini, B., Pignatelli, V. and Rossi, C. (2002). Morphological and functional abnormalities in the inner retina of the rd/rd mouse. J. Neurosci. *22*, 5492-5504.

Sullivan, S.M., Lee, A., Björkman, S.T., Miller, S.M., Sullivan, R.K.P., Poronnik, P., Colditz, P.B. and Pow, D.V. (2007). Cytoskeletal anchoring of GLAST determines susceptibility to brain damage: an identified role for GFAP. J. Biol. Chem. *282*, 29414-29423.

Tanimoto, N., Muehlfriedel, R.L., Fischer, M.D., Fahl, E., Humphries, P., Biel, M. and Seeliger, M.W. (2009). Vision tests in the mouse: Functional phenotyping with electroretinography. Front. Biosci. *14*, 2730-2737.

Tanimoto, N., Sothilingam, V. and Seeliger, M.W. (2013). Functional phenotyping of mouse models with ERG. Methods Mol. Biol. *935*, 69-78.

Verardo, M.R., Lewis, G.P., Takeda, M., Linberg, K.A., Byun, J., Luna, G., Wilhelmsson, U., Pekny, M., Chen, D. and Fisher, S.K. (2008). Abnormal reactivity of muller cells after retinal detachment in mice deficient in GFAP and vimentin. Invest. Ophthalmol. Vis. Sci. *49*, 3659-3665.

Wilhelmsson, U., Li, L., Pekna, M., Berthold, C., Blom, S., Eliasson, C., Renner, O., Bushong, E., Ellisman, M., Morgan, T.E., et al. (2004). Absence of glial fibrillary acidic protein and vimentin prevents hypertrophy of astrocytic processes and improves post-traumatic regeneration. J. Neurosci. *24*, 5016-5021.

Wu, J., Marmorstein, A.D., Kofuji, P. and Peachey, N.S. (2004). Contribution of Kir4.1 to the mouse electroretinogram. Mol. Vis. *10*, 650-654.

Wunderlich, K.A., Leveillard, T., Penkowa, M., Zrenner, E. and Perez, M. (2010). Altered expression of metallothionein-I and -II and their receptor megalin in inherited photoreceptor degeneration. Invest. Ophthalmol. Vis. Sci. *51*, 4809-4820.

Zhang, H. and Verkman, A.S. (2008). Aquaporin-4 independent Kir4.1 K+ channel function in brain glial cells. Mol. Cell. Neurosci. *37*, 1-10.

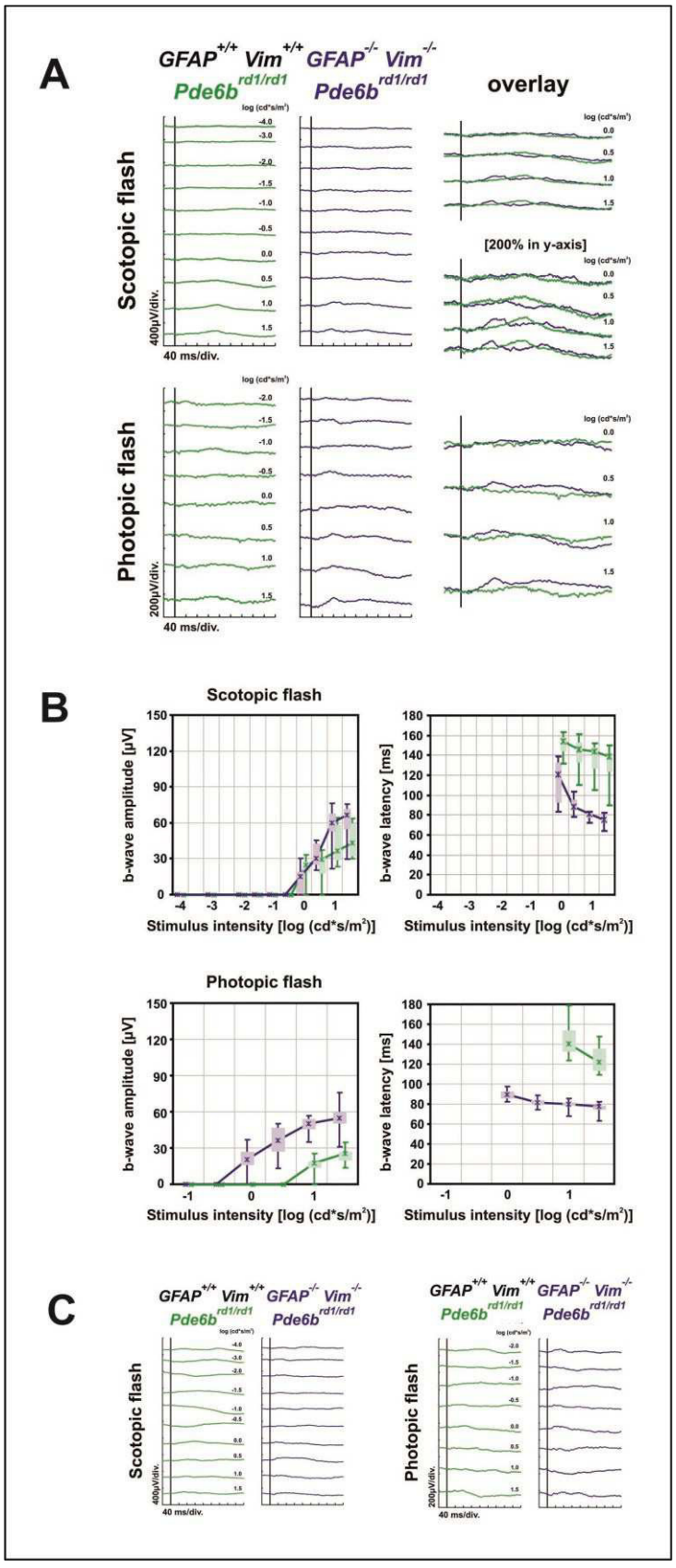
A
GFAP+/+ Vim+/+ Pde6brd1/rd1
GFAP-/- Vim-/- Pde6brd1/rd1
overlay
Scotopic flash
Photopic flash
log (cd*s/m²)
400µV/div.
200µV/div.
40 ms/div.
[200% in y-axis]
B
Scotopic flash
Photopic flash
b-wave amplitude [µV]
b-wave latency [ms]
Stimulus intensity [log (cd*s/m²)]
C

Figure 1

Figure 2

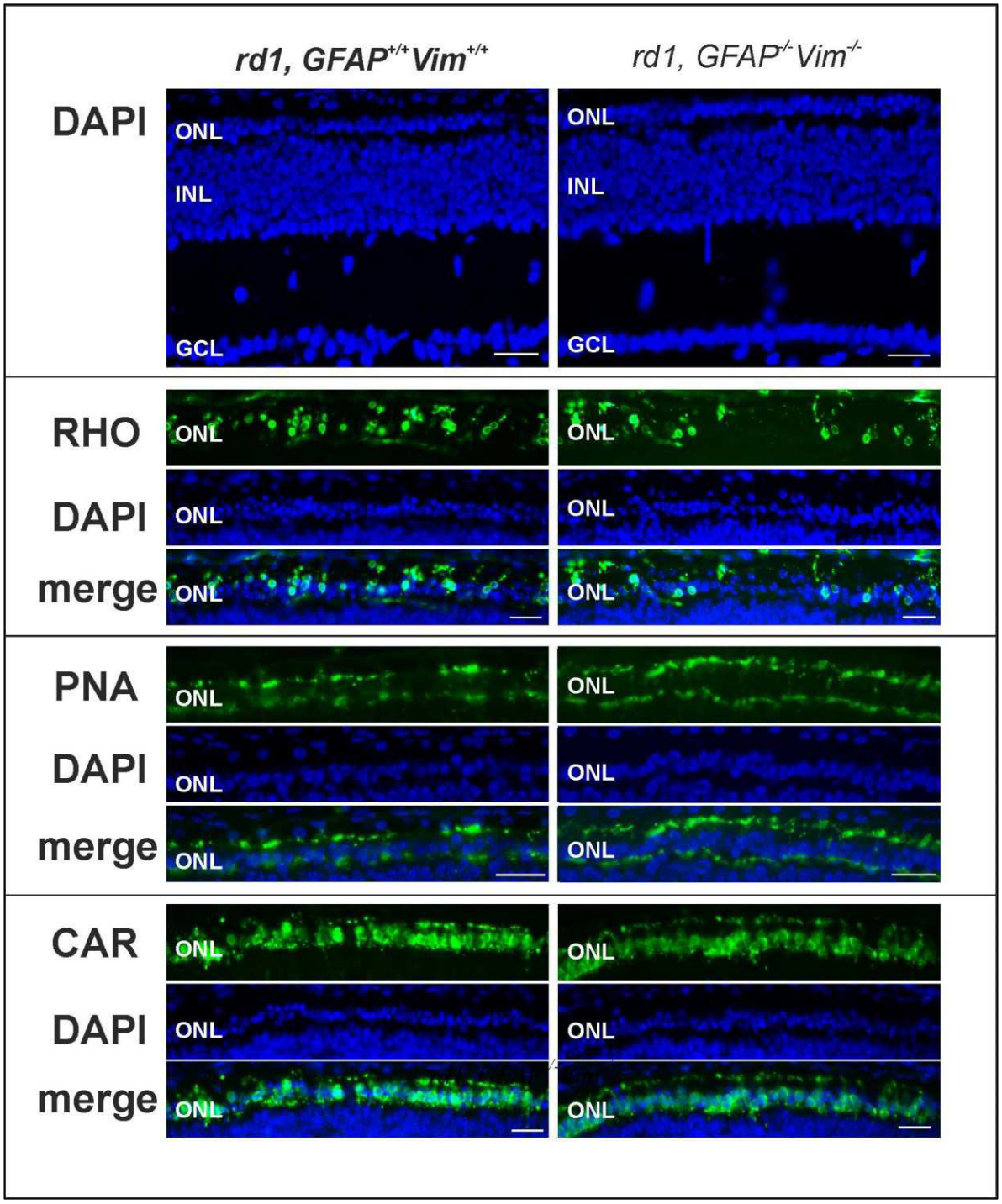
rd1, GFAP+/+Vim+/+
rd1, GFAP-/-Vim-/-
DAPI
RHO
DAPI
merge
PNA
DAPI
merge
CAR
DAPI
merge
ONL
INL
GCL

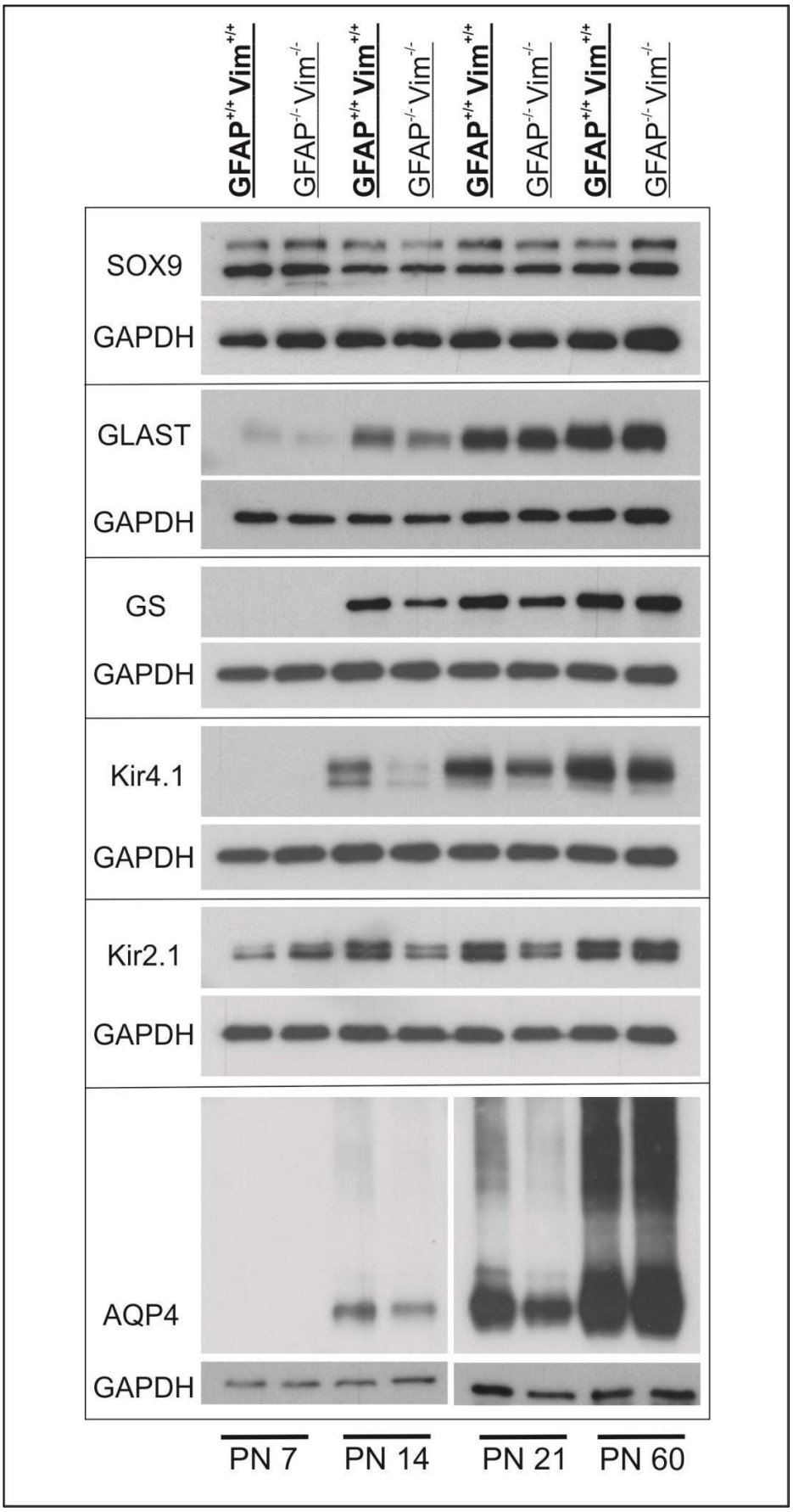
GFAP+/+ Vim+/+
GFAP-/- Vim-/-
GFAP+/+ Vim+/+
GFAP-/- Vim-/-
GFAP+/+ Vim+/+
GFAP-/- Vim-/-
GFAP+/+ Vim+/+
GFAP-/- Vim-/-
SOX9
GAPDH
GLAST
GAPDH
GS
GAPDH
Kir4.1
GAPDH
Kir2.1
GAPDH
AQP4
GAPDH
PN 7
PN 14
PN 21
PN 60

Figure 3

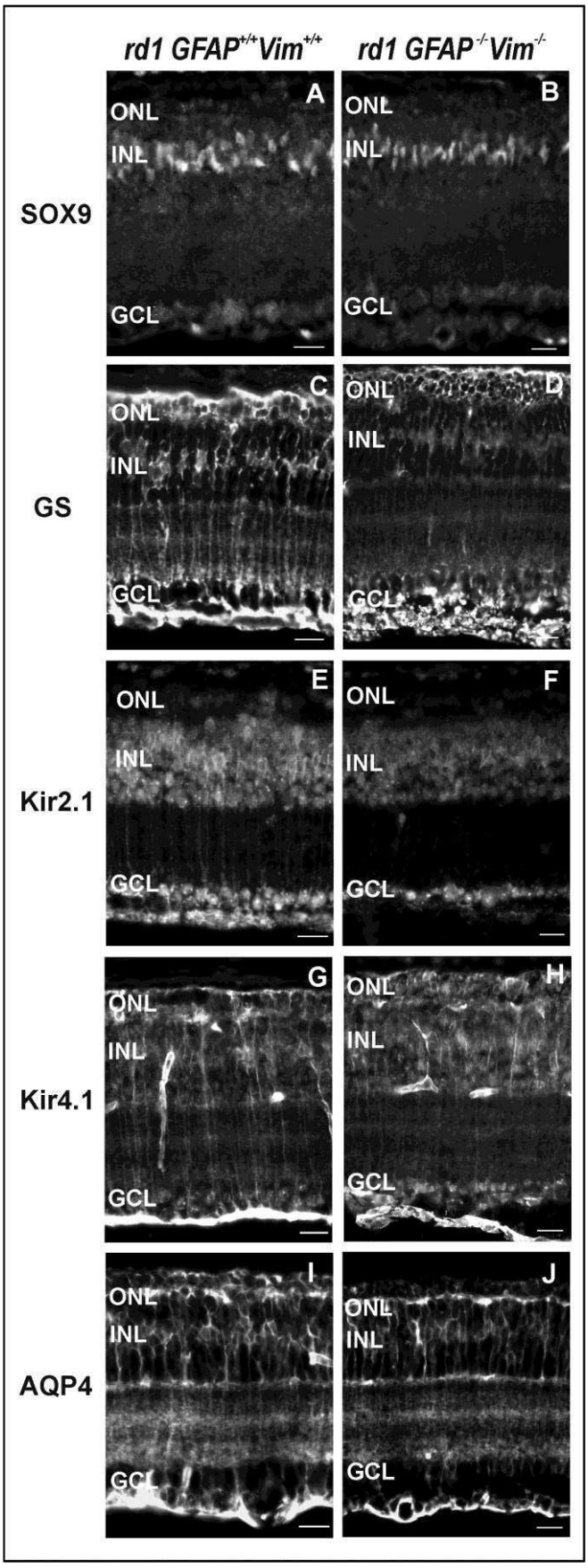
rd1 GFAP+/+Vim+/+
rd1 GFAP-/-Vim-/-
SOX9
GS
Kir2.1
Kir4.1
AQP4
A
B
C
D
E
F
G
H
I
J
ONL
INL
GCL

Figure 4

4.3 Altered expression of metallothionein-I and -II and their receptor megalin in inherited photoreceptor degeneration

Invest Ophthalmol Vis Sci. 2010 Sep;51(9):4809-20.

Summary

It has been shown that in different models of photoreceptor degeneration, activated Müller cells up-regulate the synthesis of several neuroprotective molecules (reviewed in Bringmann et al., 2006 and Bringmann et al., 2009). Metallothioneins, a superfamily of proteins with four major isoforms (metallothionein-I to metallothionein-IV) are presumable neuroprotectants (see above; reviewed in Chung et al., 2008 and West et al., 2008), and numerous insults have been shown to cause changes in their expression levels (Chen et al., 2004; Suemori et al., 2006; Thiersch et al., 2008; Vázquez-Chona et al., 2004). It has been found that metallothioneins can also be released by astrocytes and taken up by retinal ganglion cells mediated through the receptor megalin, where they promote neurite outgrowth and cell survival (Chung et al., 2008; Fitzgerald et al., 2007).

In chapter 4.3, the retinal expression patterns of metallothionein-I+II and megalin in two different mouse models of retinal degeneration (*rd1* and *rds*) and the RCS rat were compared with those of congenic controls by the means of microarray analyses (performed by Thierry Léveillard in Paris), semi-quantitative RT-PCR, immunohistochemistry, and proximity ligation assays. Metallothionein-I and II RNA levels slightly increased with age in normal mouse and rat retinas, and were significantly up-regulated in the course of the disease in all three models. Immunohistochemical analyses showed metallothionein-I+II protein expression in the RPE of all animals. A small number of metallothionein-I+II-positive microglia could be observed in the inner retinas of wildtype mice and of mice with photoreceptor degeneration mice between postnatal (PN) 7 and PN11, which was confirmed by co-labeling with the microglial markers CD11b and isolectin B4. Additional metallothionein-I+II-stained microglia were located in the outer nuclear layer of degenerating mouse retinas during the peak of cell death.

Metallothionein-I+II was strongly expressed in Müller cell bodies and processes of degenerating retinas, which was verified by co-stainings with the Müller cell specific markers CRALBP and GFAP. GFAP is commonly used to detect Müller cell activation, and the first time point when metallothionein-I+II-protein expression was observed in the two mouse models coincided with the onset of GFAP expression, some days after signs of oxidative

damage and cell death could first be detected by avidin staining and TUNEL assay, respectively. In RCS rats, however, oxidative damage and cell death were detected by PN12. GFAP staining indicated first Müller cell activation already by PN21, but metallothionein-I+II-positive Müller cells were not observed before PN32. Metallothionein expression in Müller cells was still present at later ages (PN150 in *rd1*, PN270 in *rds*, PN449 in RCS), when most photoreceptors have already been lost, but mainly in the cell bodies of Müller cells (*rds*) and mainly in the far periphery (*rd1*). Metallothionein-I+IIexpression does not seem thus to be a response to cell death per se, but to changes in one or several factors accompanying glial cell activation, where the type and degree of change might determine the onset.

Megalin expression could be detected in the nerve fiber layer and the photoreceptor segments of normal mice. By PN13, megalin expression was more prominent over the photoreceptor inner segments, whereas in older animals staining was strongest over the outer segments. Additional megalin staining was noted in astrocytes and/or Müller cell endfeet and their ascending processes. In *rd1* mice, strong staining of the inner retina was noted at earlier ages than in wildtype mice. Initially, labeling of the photoreceptor segments was also detected, but was significantly reduced by PN15 and absent at PN25. In *rds* mouse retinas, megalin expression was still observed at PN14 but no longer visible at later ages, whereas sporadic Müller cell processes appeared labeled. In rats, megalin expression was found in the nerve fiber layer, the subretinal space, and in younger animals also in the plexiform layers. As opposed to the mouse retinas, positively labeled Müller cell processes could not be observed even in older animals (PN202). In retinas of RCS rats, megalin staining was initially undistinguishable from that in normal rats, but disappeared completely in the photoreceptor segments with age. Co-localization of metallothionein-I+II and megalin in retinal sections was assessed by *in situ* PLA, an assay that only results in positive, punctate signal when the two proteins are in close proximity to each other (max. 30-40 nm). In normal mouse and rat retinas, a distinct and consistent signal was observed over the photoreceptor inner and outer segments, in the ganglion cell layer, and in the nerve fiber layer at the examined ages (PN13 to PN40). In the three degeneration models, the same distribution was observed in younger animals, while at older ages, signal in the outer retina was absent or reduced to a narrow band next to the retinal pigment epithelium. The fact that megalin expression is lost in the outer retina during the course of the degeneration is likely to limit any potential protective effect of endogenous metallothionein-I+II despite its marked up-regulation. Moreover, it is possible that increased metallothionein-I+II expression supports the various events mediated by glial cells, secondary to photoreceptor degeneration and/or supports the glial cells themselves.

Altered Expression of Metallothionein-I and -II and Their Receptor Megalin in Inherited Photoreceptor Degeneration

Kirsten A. Wunderlich,[1,2,3] *Thierry Leveillard,*[4] *Milena Penkowa,*[5] *Eberhart Zrenner,*[3] *and Maria-Thereza Perez*[1,6]

Purpose. To examine in rodent models of retinitis pigmentosa (RP) the expression of the neuroprotectants metallothionein-I and -II and of megalin, an endocytic receptor that mediates their transport into neurons.

Methods. Gene and protein expression were analyzed in retinas of *rd1* and *rds* mice and in those of RCS (Royal College of Surgeons) rats of various ages. Glial cell markers (cellular retinaldehyde binding protein, CRALBP; glial fibrillary acidic protein, GFAP; CD11b; and isolectin B4) were used to establish the identity of the cells.

Results. Metallothionein-I and -II gene expression increased with age in normal and degenerating retinas and was significantly greater in the latter. Protein expression, corresponding to metallothionein-I+II, was first observed in *rd1* mice in Müller cells at postnatal day (P)12 and in *rds* mice at P16, coinciding with the onset of GFAP expression in these cells. In RCS rats, the same distribution was observed, but not until P32, long after the onset of GFAP expression. Metallothionein-I+II was observed also in a small number of microglial cells. Megalin was expressed in the nerve fiber layer and in the region of the inner and outer segments in normal animals, but expression in the outer retina was lost with age in degenerating retinas.

Conclusions. Induction of metallothionein-I and -II occurs in the RP models studied and correlates with glial activation. The progressive loss of megalin suggests that transport of metallothionein-I+II into the degenerating photoreceptors (from e.g., Müller cells), could be impaired, potentially limiting the actions of these metallothioneins. (*Invest Ophthalmol Vis Sci.* 2010;51:4809–4820) DOI:10.1167/iovs.09-5073

Development and maintenance of the retina require that sufficient levels of survival factors be continuously synthesized and secreted. Predictably, even higher levels are necessary after mutations or injury, and a number of studies have shown that acute and chronic retinal cell damage triggers distinct endogenous protective mechanisms. In retinitis pigmentosa (RP), a progressive and irreversible loss of photoreceptor cells occurs as a result of mutations in primarily rod-specific genes (http://www.sph.uth.tmc.edu/Retnet/ RetNet is provided in the public domain by the University of Texas Houston Health Science Center, Houston, TX). Over time, cone cells also die, leading eventually to total loss of vision.[1,2] In the course of the disease, prosurvival signaling cascades are activated in the dysfunctional photoreceptor cells themselves and in support cells. Numerous endogenous protective molecules are upregulated, such as growth factors, cytokines, and antioxidants, some of which have also been shown to extend, at least temporarily, the lifespan of photoreceptors when applied exogenously.[3–7]

In the present study, we have examined the expression of metallothionein-I and -II in three rodent models of RP. Metallothioneins constitute a class of low-molecular-mass (6–7 kDa), cysteine-rich proteins and exist in four major isoforms. Metallothionein-I and -II are ubiquitously expressed in most tissues, whereas metallothionein-III and -IV are rather restricted to a few specific tissues. Metallothionein-I and -II are structurally and functionally analogous and are often referred to as a single entity (metallothionein-I+II in the present study). In the rodent CNS, they are regulated and induced together by various pathogenic factors, including metals, hormones, proinflammatory cytokines, and reactive oxygen species (ROS).[8–15]

Because of the high abundance of thiol groups, metallothioneins bind and release both essential (e.g., zinc) and toxic metals, serving thereby as intracellular regulating factors of metal ions during physiological and pathologic conditions.[9,14–16] The redox properties of metallothionein, in addition, enable its own oxidation even by mild oxidants, allowing zinc to be transferred from metallothionein to other proteins to subserve numerous cellular functions. Via the metal thiolates, metallothioneins also exchange zinc with ROS that are scavenged during cellular oxidative stress.[9,14,16–19]

Metallothionein-I and -II are expressed in the retina and in the retinal pigment epithelium (RPE),[20–25] and significantly higher levels have been observed after intraocular application

From the [1]Department of Ophthalmology, Clinical Sciences Lund, Lund University, Lund, Sweden; the [2]Graduate School of Cellular and Molecular Neuroscience, University of Tübingen, Tübingen, Germany; [3]Pathophysiology of Vision, University Eye Hospital Tübingen, Tübingen, Germany; [4]Department of Genetics, Institut de la Vision, Institut National de la Santé et de la Recherche Médicale (INSERM), UPMC (University Pierre et Marie Curie) University of Paris 06, UMR-S (Unité Mixte de Recherche en Santé) 968, CNRS (Centre National de la Recherche Scientifique) 7210, Paris, France; the [5]Section of Neuroprotection, Department of Neuroscience and Pharmacology, Faculty of Health Sciences, University of Copenhagen, Copenhagen, Denmark; and the [6]Department of Ophthalmology, University of Copenhagen, Glostrup Hospital, Glostrup, Denmark.

Supported by European Union Grants LSHG-CT-2005-512036 and MEST-CT-2005-020235, Foundation Fighting Blindness, Swedish Medical Research Council Grant 12209, Crown Princess Margareta's Committee for the Blind, Stiftelse för Synskadade i f.d. Malmöhus Län, Crafoordska Stiftelsen, Torsten och Ragnar Söderbergs Stiftelser, and Thorsten och Elsa Segerfalks Stiftelse (M-TP); Institut National de Santé et de Recherche Médicale, Agence Nationale pour la Recherche, and the European Commission (TL); and Kerstan-Stiftung (KAW).

Submitted for publication December 15, 2009; revised March 1, 2010; accepted March 17, 2010.

Disclosure: **K.A. Wunderlich**, None; **T. Leveillard**, None; **M. Penkowa**, None; **E. Zrenner**, None; **M.-T. Perez**, None

Corresponding author: Maria-Thereza Perez, Department of Ophthalmology, Clinical Sciences Lund, Lund University, BMC B13, SE-221 84, Lund, Sweden; maria_thereza.perez@med.lu.se.

of *N*-methyl-D-aspartate (NMDA),[26] phototoxic insult,[27] mechanical damage,[28] and hypoxic preconditioning.[29] Cell loss is increased after NMDA application in metallothionein-I+II-deficient mice,[26] and a correlation has been suggested between low levels of metallothionein in retinal pigment epithelial cells and macular degeneration.[22,30–32] Accordingly, induction of metallothionein in the RPE directly, by plasmid transfection, and indirectly, by reduction of the adaptor protein p66Shc, has been shown to contribute to protect these cells against oxidative damage.[31,32]

More recently, a report showed that metallothionein-I+II can also function in a paracrine manner, being secreted by astrocytes and thus regulating survival and regeneration of retinal ganglion cell axons.[33,34] This effect is mediated through interaction with megalin, a member of the low-density lipoprotein receptor (LDLR) receptor family, which binds and takes up, not only lipoproteins, but also a range of other ligands, including metallothionein-I+II.[35–37] In this article, we examine the expression patterns of megalin and of metallothionein-I+II in normal and degenerating retinas.

Materials and Methods

Animals

All experiments were approved by the local committee for animal experimentation and ethics. Handling of animals was in accordance with the ARVO Statement for the Use of Animals in Ophthalmic and Vision Research. The animals were kept on a 12-hour light–dark cycle, with no limitation of food or water.

The examined animals included *rd1* mice, *rds* mice, and wild-type (wt) mice (own colonies, homozygous, and C3H/HeA background), as well as pink-eyed, tan-hooded Royal College of Surgeon rats (RCS; *rdy/rdy*; own colony), and congenic wt RCS-*rdy*$^{+}$ rats (kindly provided by Olaf Strauss, Freie Universität, Berlin, Germany). Wild-type Sprague-Dawley (SD) rats were purchased from B&K Universal (Uppsala, Sweden) and Scanbur (Stockholm, Sweden).

In the *rd1* mouse, a mutation in the β subunit of the rod cGMP-phosphodiesterase gene (*Pde6b*) leads to a fast degeneration of rods during the first 3 weeks after birth.[38] Homozygous retinal degeneration slow (*rds*) mice lack rod and cone outer segments because of a null mutation in the *Prph2* gene (*Prph2*^{Rd2}) encoding peripherin, and photoreceptors are lost over a period of several months.[39] In RCS rats, a mutation in the *Mertk* gene expressed in retinal pigment epithelial cells leads to the accumulation of photoreceptor outer segment debris in the subretinal space.[40] Although the primary defect is not in a photoreceptor-specific gene, photoreceptors die within the first 3 months after birth.

Microarray: Sample Isolation Procedures

Neural retinas from wt control and *rd1* mice (number of replicates: wt/*rd1*),[41] were dissected at postnatal days (P) 5 (2/2), 6 (2/2), 7 (3/3), 8 (3/3), 9 (3/3), 11 (3/3), 12 (3/3), 13 (3/3), 15 (3/3), 21 (2/2), 28 (2/2), and 35 (2/2), resulting in 24 experimental conditions (12 time points × 2 strains). Total RNA was purified by sedimentation through cesium chloride.[42] Double-stranded cDNA was synthesized from 5 μg total RNA (Superscript Choice System; Invitrogen, Carlsbad, CA). The cDNA was then transcribed in vitro with an RNA transcript labeling kit (ENZO Diagnostics, Farmingdale, NY), to form biotin-labeled cRNA.

GeneChip Hybridization and Scan

The labeled RNA was hybridized to mouse gene microarrays (MG 430 2.0 GeneChips; Affymetrix, Santa Clara, CA) using standard protocols.[43] Quality control reports were generated as published elsewhere.[44,45] The data were uploaded into Retinobase.[46]

q-RT-PCR

Retinas of three to five animals per age group were isolated through a cut in the cornea, snap-frozen separately in liquid nitrogen, and stored at −80°C until further processing. The following ages were examined (the number of specimen per age appears in parentheses): *rd1* mice at P7 (4), 11 (4), 14 (5), 21 (4), 28 (5), 60 (4), 120 (3) (total $n = 29$); *rds* mice at P7 (3), 14 (3), 17 (3), 21 (4), 28 (3), 60 (3), 120 (4), 280 (4) (total $n = 27$); wt mice at P7 (4), 11 (4), 14 (4), 17 (3), 21 (4), 28 (4), 60 (5), 120 (4), 280 (3) (total $n = 35$); RCS rats at P8 (3), 15 (3), 22 (4) 28 (4), 35 (4), 43 (4), 60 (4) (total $n = 26$); and SD rats at P8 (3), 15 (3), 22 (4), 28 (4), 35 (3), 43 (3), 60 (3) (total $n = 23$).

After homogenization of the retinas, RNA was isolated (RNeasy MiniKit; Qiagen, Hilden, Germany), including a DNase treatment step to remove any contamination of genomic DNA, according to the manufacturer's instructions (RNase-Free DNase Set; Qiagen). RNA concentration was spectrophotometrically measured and its purity confirmed with 260-nm/280-nm absorbance ratios. RNA was reverse transcribed with a kit (QuantiTect Reverse Transcription Kit; Qiagen).

Equal amounts of cDNA were applied for PCR amplification in triplicate in a thermocycler (LightCycler; Roche, Mannheim, Germany), using SYBR green master-mix (SYBR Green JumpStart *Taq* ReadyMix for qPCR Capillary Formulation; Sigma-Aldrich, Stockholm, Sweden) with a total reaction volume of 10 μL in each glass capillary (LightCycler Capillaries; Roche). The primers indicated in Table 1 were used in a final concentration of 0.25 μM. PCR conditions were set to 95°C for 10 minutes' initialization, followed by 45 cycles of 5 seconds' denaturation at 95°C, 8 seconds' annealing at 62°C, and 4 to 12 seconds' elongation at 72°C. Fluorescence from the SYBR green that binds to double-stranded DNA was measured at the end of each extension period. A calibrator sample, produced by mixing samples of different genotypes and ages from either mouse or rat tissue, provided a constant calibration point for all samples within and between runs. A software program (LightCycler Relative Quantification Software, ver. 1.01; Roche) automatically calculated ratios between calibrator-normalized target and reference. To verify the absence of genomic DNA contamination, control samples were run in which no reverse transcriptase was included. Also, controls without cDNA but only water were included in some experiments. Specificity of the PCR template was verified by melting-curve analysis. Subsequent gel electrophoresis assured amplification of only one PCR product of the expected size. A spreadsheet (Excel; Microsoft, Redmond, WA) was used for further data analysis and graphical visualization. Statistical evaluation was performed online (two-sample *t*-tests, *F*-test, one-way ANOVA, Tukey's HSD procedure for independent samples, http://faculty.vassar.edu/lowry/VassarStats.html).

Table 1. Primers Used to Amplify Mouse and Rat Metallothionein-I and -II, and β-Actin

Gene	Forward (5′–3′)	Reverse (5′–3′)	Size (bp)
β-Actin[47]	CAACGGCTCCGGCATGTGC	CTCTTGCTCTGGGCCTCG	153
Mouse metallothionein-I[47]	GAATGGACCCCAACTGCTC	GCAGCAGCTCTTCTTGCAG	104
Mouse metallothionein-II[47]	TGTACTTCCTGCAAGAAAAGCTG	ACTTGTCGGAAGCCTCTTTG	94
Rat metallothionein-I[48]	GCTGTGTCTGCAAAGGTGC	ATTTACACCTGAGGGCAGCA	82
Rat metallothionein-II (adapted from Ref.[47])	GAATGGACCCCAACTGCTC	GCATTTGCAGTTCTTGCAG	94

Tissue Staining

Eyes were quickly enucleated and fixed with Bouin's solution (Sigma-Aldrich, St. Louis, MO) at 4°C overnight and thereafter washed several times with ethanol of increasing concentrations. After a last dehydration step in xylene, the eyes were embedded in paraffin. Sections (4–5 μm) were stained with hematoxylin and eosin.

Some eyes were fixed with 4% paraformaldehyde in Sørensen's buffer for 2 hours at 4°C. The tissue was rinsed several times with the same buffer and thereafter cryoprotected by increasing concentrations of sucrose in the buffer. The eyes were embedded in an albumin-gelatin medium and frozen. Twelve-micrometer cryostat sections were collected on gelatin/chrome alum-coated glass slides and air-dried before storage at −20°C.

Immunohistochemistry

Cryosections from one to seven animals of the following ages were used in the immunohistochemical studies: *rd1* mice, P2 to P150 (total $n = 53$); *rds* mice, P2 to P274 (total $n = 29$); wt mice, P2 to P150 (total $n = 37$); RCS rats, P2 to P449 (total $n = 50$); RCS-*rdy*$^+$, P13 to P202 (total $n = 4$); and SD rats embryonic day (E)19 to P60 (total $n = 15$).

The sections were preincubated for 60 to 90 minutes at room temperature in PBS-TBN: phosphate-buffered saline (PBS) containing 0.25% Triton X-100 (T), 1% bovine serum albumin (BSA), and 2% to 5% goat and/or donkey normal serum (N). Incubation with primary antibodies was performed overnight at 4°C and included an antibody that recognizes both metallothionein-I+II (monoclonal mouse anti-metallothionein E9, 1:50; Dako, Glostrup, Denmark); a polyclonal rabbit anti-glial fibrillary acidic protein (GFAP, 1:1500; Dako); or a polyclonal rabbit anti-megalin (1:50; Santa Cruz Biotechnology Inc., Santa Cruz, CA), all diluted in PBS-TBN. For colocalization studies, the metallothionein-I+II antibody was applied in combination with rabbit anti-cellular retinaldehyde binding protein (CRALBP, 1:5000 in PBS-TBN; kind gift from John C. Saari, University of Washington, Seattle, WA), monoclonal rat anti-mouse CD11b (1:75 in Tris-buffered saline [TBS] containing TBN; R&D Systems, Abingdon, UK), Alexa Fluor 594-conjugated isolectin B4 (IB4, 1:50; Molecular Probes, Eugene, OR) in buffer containing 300 mM NaCl, 100 μM $CaCl_2$, and 10 mM HEPES (pH 7.5), or tomato lectin (1:50 in PBS-TBN; Sigma-Aldrich).

The sections were washed three times with PBS or TBS and incubated for 90 minutes with the corresponding secondary antibody at 1:200: biotinylated rabbit anti-rat (Vector Laboratories, Burlingame, CA) followed by streptavidin Cy3 (Jackson ImmunoResearch Laboratories, West Chester, PA); Texas red sulfonyl chloride-conjugated donkey anti-mouse (Jackson ImmunoResearch Laboratories); Alexa fluorescein isothiocyanate- or Alexa Fluor-conjugated goat anti-mouse or anti-rabbit (Molecular Probes).

The specificity of the labeling was verified by preadsorbing the metallothionein-I+II antiserum with purified rabbit metallothionein protein (1:5 molar ratio for 4 hours; Sigma-Aldrich) before application to the sections. A secondary antibody control was also performed on some sections.

TUNEL Assay

Dying cells were detected with a terminal deoxynucleotidyl transferase dUTP nick end- labeling (TUNEL) assay (TMR red In Situ Cell Death Detection Kit; Roche). Briefly, the enzyme solution was diluted 1:9 and the labeling solution 1:4 in PBS. The two components were mixed 1:4.44 immediately before application to the sections for 45 minutes at 37°C. The reaction was stopped by several washes with cold PBS before mounting.

Oxidative Stress and Damage Assay

Oxidatively damaged DNA was detected by incubating retinal sections for 1 hour at room temperature with Texas red- or Alexa Fluor 488-conjugated avidin (10 μg/mL in PBS-TB, Molecular Probes Inc.).[49,50]

In Situ Proximity Ligation Assay

The proximity ligation assay (PLA; Olink AB, Uppsala, Sweden) was applied to visualize the co-localization of metallothionein-I+II and megalin. In this assay, a signal is produced only when the oligonucleotide-labeled secondary antibodies (PLA probes) that have been applied bind to the corresponding primary antibodies (in the present case, metallothionein-I+II and megalin) in close proximity.[51] The PLA was performed according to the manufacturer's protocol, with the reagents provided. All incubation steps were performed in a humidity chamber at 37°C, except for the incubation with primary antibodies, which was done at 4°C. Briefly, the sections were blocked for 30 minutes before incubation with both primary antibodies (each 1:50) overnight. The slides were washed three times for 5 minutes each time with TBS-T before incubating with the secondary anti-mouse and anti-rabbit antibodies conjugated to unique oligonucleotides for 2 hours. A hybridization and a ligation step followed for 15 minutes each, with brief and careful washes between. The rolling-circle DNA amplification was applied for 90 minutes, and the product was labeled with a complementary DNA linker conjugated to a Tex613 fluorophore for 1 hour. The slides were washed with decreasing concentrations of SSC buffer (2×, 1×, 0.2×, 0.02×) and finally with 70% ethanol before being air-dried and mounted with the provided antifade medium.

Other stained sections were mounted with antifade medium (Vectashield; Vector Laboratories) and examined with a fluorescence microscope (Axiophot; Carl Zeiss Meditec, Inc., Oberkochen, Germany). Images were taken with a digital camera and accompanying software (Axiovision 4.2; Carl Zeiss Meditec).

Results

Gene Expression

A microarray analysis performed on samples from wt mouse retinas (P5–P35) showed a modest upregulation particularly of metallothionein-I with age, noted from P11. In *rd1* mouse retinas, increased expression was observed from P12 to P13 and onward, peaking at ~P21 for both genes (Fig. 1A).

Gene induction was also verified by q-RT-PCR in retinas of different ages (Figs. 1B–D). This analysis confirmed that in wt animals, metallothionein-I and -II levels increase slightly with age. Significantly higher levels of metallothionein-I were noted in P21 and older mice than in P7 to P11 animals ($P < 0.01$); for metallothionein-II, a significant difference was seen between P7 and P11 and in animals P28 and older ($P < 0.05$). Levels of both metallothionein-I and -II were significantly higher in P43 and older normal rats than in younger animals (P8–P15; $P < 0.05$).

The analysis showed also that in the two mouse models, metallothionein-I and -II gene levels increased relatively rapidly, whereas in RCS rats, an upregulation was not observed until weeks after the onset of photoreceptor degeneration, suggesting that cell death per se is not what triggered metallothionein-I and -II. In *rd1* mouse retinas, significantly higher levels were found between P14 and P60, but not in older animals (Fig. 1B). In *rds* mice, altered expression was found from P14 (metallothionein-II) and P17 (metallothionein-I; Fig. 1C). At P280, the last time point examined, gene levels were still several times higher in *rds* retinas than in their wt counterparts (Fig. 1C). In RCS rats, an upregulation of metallothionein-I and -II was first observed in the fourth week of age (Fig. 1D).

It should be noted that the method used to isolate the retina for gene analysis, although ensuring a quick dissection, does not control for the amount of RPE contamination in the sample, and therefore, the increases observed may not correspond only to stimulated expression in the retina. The immunohistochemical analysis did not allow us to conclusively establish whether metallothionein-I+II protein levels changed in the epithelium, but clearly indicated that they increase substantially with age in the degenerating neural retina.

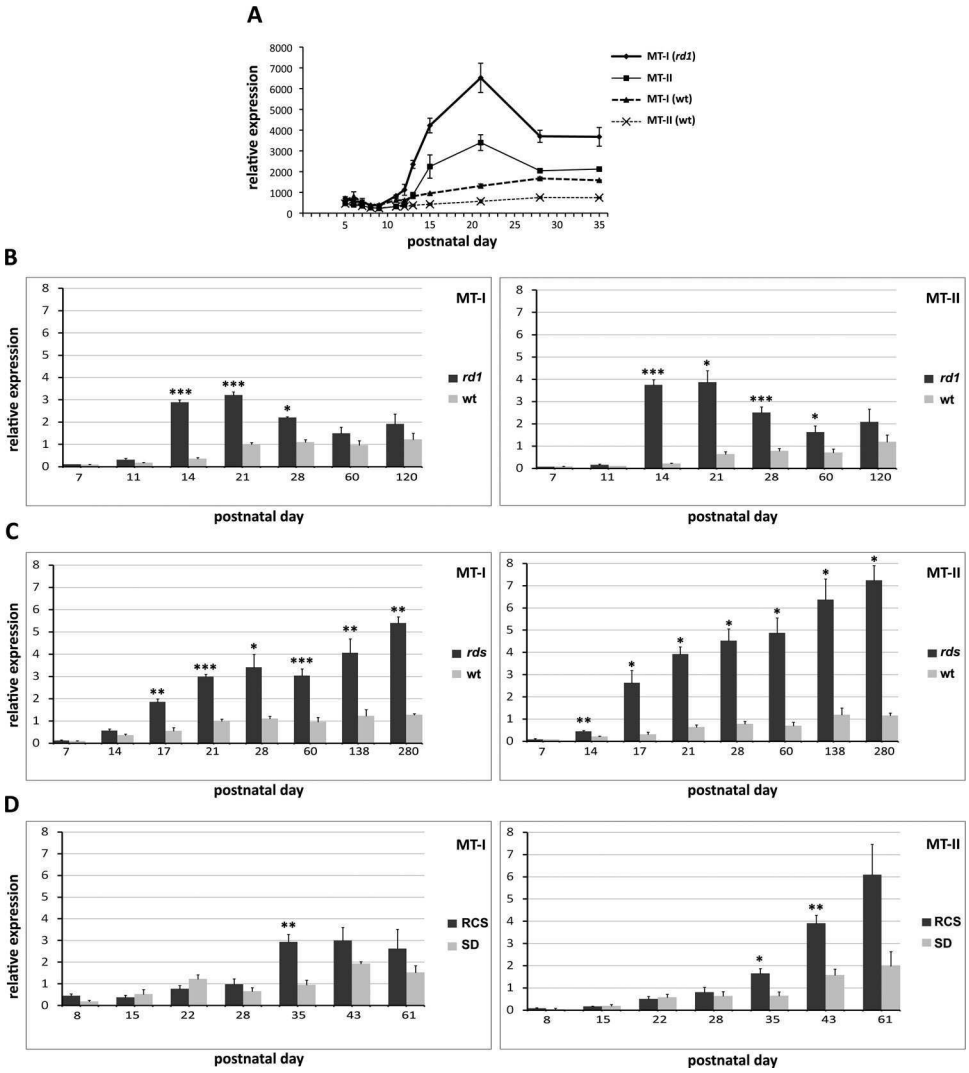

FIGURE 1. Metallothionein-I and -II gene expression by microarray analysis (**A**) and q-RT-PCR (**B–D**). (**A**) Expression profiles of wt and degenerating homozygous *rd1* retinas of corresponding ages. Bars represent mean ± SD. (**B–D**) q-RT-PCR analysis of metallothionein-I and -II expression at different ages in normal animals (wt mice, SD rats), in *rd1* and *rds* mice, and in RCS rats. The bars represent the mean ± SEM of ratios created by comparing, at different ages, the expression of metallothionein-I and -II with that of β-actin in control and in degenerating retinas. Ratios of a calibrator sample were set to 1. Statistically significant differences between control and degenerating retinas for each age: $^{*}P < 0.05$; $^{**}P < 0.01$; $^{***}P < 0.001$. Differences between ages for each genotype are given in the text.

Avidin, TUNEL, GFAP, and Metallothionein-I+II

Wild-Type Mice. In wt mouse retinas, no avidin staining was noted in the outer nuclear layer (ONL) at any of the time points examined. A small number of TUNEL-positive cells were seen in the ONL in the younger ages examined (P7 and P13), but none at P21 or onward. GFAP labeling was found along the vitreal margin of the retina and weakly in radial Müller cell processes in the far periphery (not shown).

Immunolocalization of metallothionein-I+II resulted in positive staining in the RPE, in the inner plexiform layer (IPL), in sporadic cells with a morphology characteristic of microglia, and in retinal vessels (Fig. 2F). After preadsorption of the antiserum, labeling persisted in vessels. The latter were stained also after incubation of sections with secondary antibodies alone, so a specific staining could not be verified nor excluded.

***rd1* Mice.** The number of avidin- and TUNEL-stained cells detected in the ONL was higher in *rd1* retinas than in wt controls at P8 to P10, mainly in the central areas (Table 2). By P12 and P13, positive cells were found in all eccentricities (Figs. 2B, 2C) and at P14, the number of photoreceptor cell rows was reduced to less than half in the midperiphery (Fig. 2E) compared with age-matched wt controls (Fig. 2A). GFAP staining of radial Müller cell processes was noted throughout the retina from P11 onward (Table 2, Fig. 2D).

Metallothionein-I+II-positive staining was observed also in the *rd1* mouse in the RPE at all ages examined. Additional metallothionein-I+II expression was noted in Müller cell bodies and processes in the central retina, near the optic nerve head at P11 to P12 (Table 2, Fig. 2G). Cellular profiles resembling microglia were also found in the inner retina between P7 and P11 and in the ONL between P11 and P15 (Fig. 2H). Co-labeling with microglial cell markers, confirmed the identity of some of these metallothionein-I+II-positive cells (see Figs. 5G–I).

Between P12 and P17, an increasing number of metallothionein-I+II-labeled Müller cells was observed toward the periphery (Fig. 2I). Staining was observed also in the innermost retina and could therefore correspond to Müller cell endfeet and/or astrocytes.

By P21, the strongest signal was observed in Müller cell bodies and processes in the far periphery (Fig. 2J) and more weakly and in fewer numbers in the midperiphery and central retina. At later ages (P46, P150), only a few labeled Müller cells could still be observed, mainly in the far periphery and close to the optic nerve head (not shown).

***rds* Mice.** Avidin-stained cells were observed in the ONL in *rds* mice from P14 to P16 and TUNEL-positive cells from P12 to P14 (Table 2). The number of stained cells declined between the peak at P16 to P18 (Figs. 3B, 3C) and at P270, at which point three to five rows of photoreceptor cells were still found (Fig. 3A). Uniform GFAP labeling of Müller cell radial processes throughout the retina was observed also at P18 and onward (Fig. 3D).

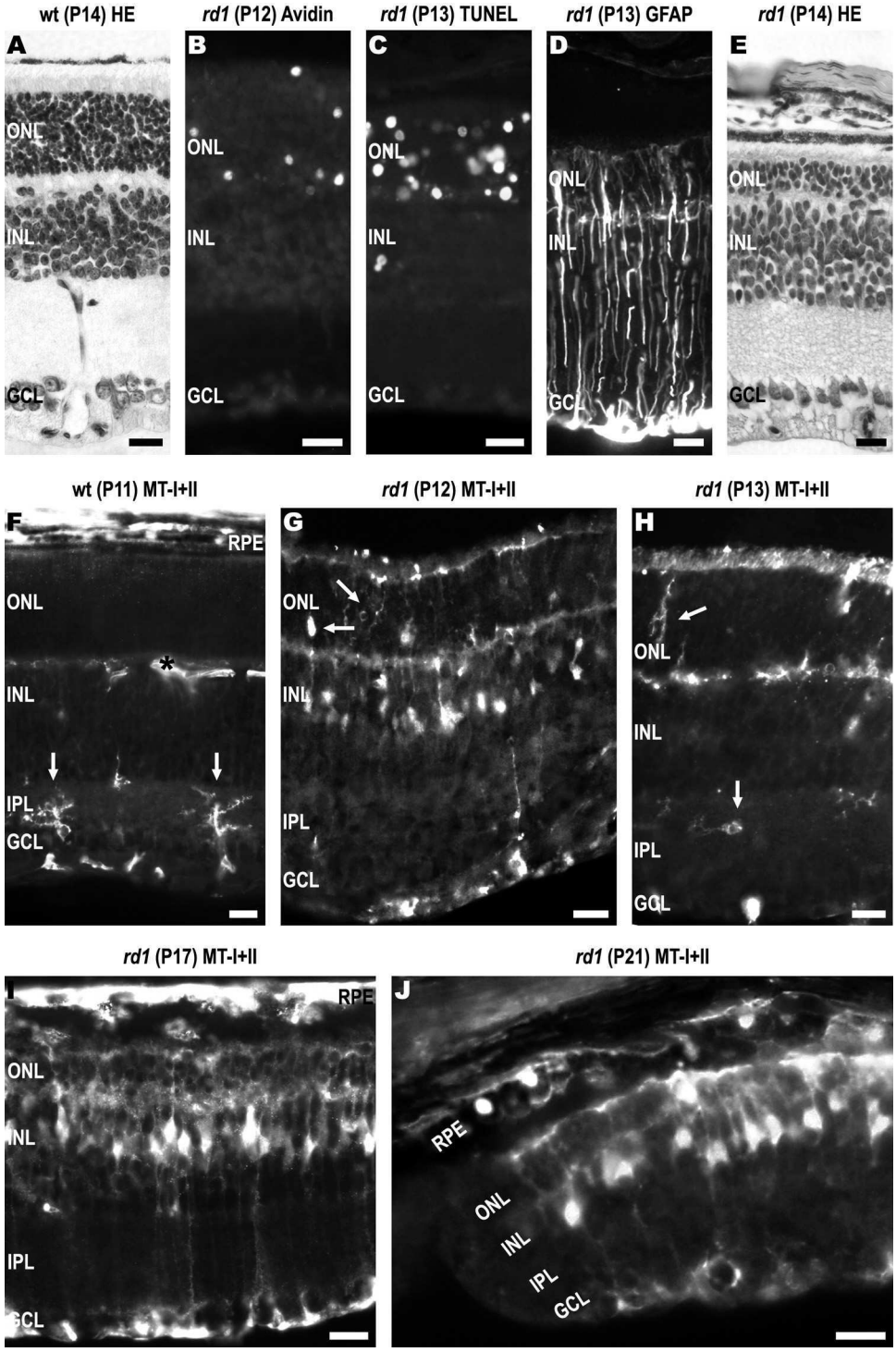

FIGURE 2. Localization of various markers in wt (**A**, **F**) and *rd1* (**B–E**, **G–J**) mouse retinas: All markers were detected in the *rd1* retina at P12 to P13, when about half of the photoreceptor cells remain (**E**). Specific metallothionein-I+II immunoreactivity was observed in the RPE (**F**, **I**, **J**) and in microglia in the IPL (**F**, **H**, *arrows*). In *rd1* retinas, labeling was also present in Müller cells as well as microglia (*arrows*) located in the ONL: (**G**) P12, central retina; (**H**) P13, midperiphery; (**I**) P17, midperiphery; (**J**) P21, far periphery. Labeling of vessels (**F**, ✱). HE, hematoxylin-eosin; MT, metallothionein. Scale bars, 20 μm.

Metallothionein-I+II expression was observed in the RPE in *rds* mouse retinas at all ages examined. In addition, labeled Müller cells were noted in *rds* mouse retinas, but not until P16 (Table 2). Yet, by P18, expression could already be observed throughout the whole retina in Müller cell bodies and processes (Fig. 3E). This distribution was still observed in older animals (Fig. 3F), although in 9-month-old animals, labeling was restricted to the cell bodies only (Fig. 3G). A few microglial cells appeared also labeled in the younger ages (not shown).

Normal Rats and RCS Rats. Retinas obtained from SD and from congenic RCS-*rdy*$^+$ rats processed for the avidin and TUNEL assays showed no specific labeling of photoreceptor cells. GFAP staining was limited also in these specimens to the innermost retina (not shown). Avidin- and TUNEL-stained cells were observed in the ONL in RCS rats from P12 onward (Table 2, Figs. 3I, 3J). GFAP labeling of Müller cell radial processes was observed from ~P21 onward (Table 2, Fig. 3K).

Metallothionein-I+II expression was found in control rat retinas in the RPE and in vessels, as seen with normal mouse retinas (not shown). In RCS rats, labeling of Müller cells and processes was also observed, but not until P32 (Table 2). At this age, less than half of the photoreceptor layer remains (Fig. 3H). Within a few days, staining was seen throughout the retina with labeled processes extending beyond the outer limiting membrane, into

TABLE 2. Ages at Which the Various Markers Were First Detected

	Avidin	TUNEL	GFAP	Metallothionein-I+II
rd1	P8–P10	P8–P10	P11–P12	P11–P12
rds	P14–P16	P12–P14	P16–P18	P16–P18
RCS	P12–P14	P12–P14	P21–P25	P32–P35

Avidin and TUNEL were detected in the ONL and GFAP and metallothionein-I+II in Müller cells and processes. The time periods indicated reflect individual differences and do not necessarily correspond to the time point when the markers were uniformly distributed throughout the retina.

the subretinal space (Figs. 3L, 3M). In older animals (P145, P449), expression of metallothionein-I+II was still observed but only in a few sporadic cells, with accumulation of labeling also in the subretinal space in some places (Fig. 3N).

Megalin Expression

In younger normal mouse retinas (P6–P40), megalin staining revealed labeling in the subretinal space and in the nerve fiber layer (NFL). By P13, expression in the outer retina was still more prominent over the photoreceptor inner segments (IS; not shown), whereas at P29 and P40, strong staining was noted also over the outer segments (OS; Fig. 4A). In older animals, staining was strongest over the OS and was in addition observed in astrocytes and/or Müller cell endfeet and their ascending processes (Fig. 4B).

In *rd1* mice, staining of photoreceptor segments was initially detected, but was significantly reduced by P15 and absent at P25 (Fig. 4C). Strong staining was noted also in the inner retina, but at earlier ages than in normal retinas (Fig. 4C), and at P46 labeling of proximal Müller cell processes was already very prominent (Fig. 4D). In *rds* mouse retinas, labeling of IS was still detectable at P14, accompanied by distinct labeling in the innermost retina (Fig. 4E). At later ages, staining in the outer retina was no longer visible, whereas sporadic Müller cell processes appeared labeled (Fig. 4F).

In young normal rat retinas (SD and rdy^{+}), megalin expression was found in the subretinal space, in the NFL, and in the plexiform layers (not shown), but decreased in the latter with age (Fig. 4G). As opposed to normal mouse retinas, staining of Müller cell processes was not observed in older animals up to P202. In retinas of RCS rats, megalin labeling was initially undistinguishable from that in normal rats. With age, staining over the photoreceptor segments disappeared completely (Figs. 4H, 4I).

Co-localization

Most cell bodies and processes expressing metallothionein-I+II within the retina were also CRALBP positive (Figs. 5A–C). Co-labeling with the two markers was also observed in the RPE in all retinas analyzed (Figs. 5D–F).

Processing of mouse retinas with CD11b, isolectin IB4, or tomato lectin resulted in labeling of vessels (Figs. 5G–I). In addition, co-staining with these markers showed that metallothionein-I+II labeled structures in the ONL of *rd1* and *rds* mouse retinas corresponded to microglial cells (Figs. 5G–I). Metallothionein-I+II labeling of cells resembling microglial cells was also noted in the IPL in normal (Fig. 2F) and degenerating (Fig. 2H) mouse retinas.

Co-localization of metallothionein-I+II and megalin was assessed in retinal samples using the in situ PLA assay. A distinct and consistent signal was observed in normal mouse and rat retinas in the subretinal space, over the photoreceptor IS and OS and in the ganglion cell layer (GCL) and NFL at the ages examined (P13–40; Fig. 5J). This distribution was observed in all three models of degeneration in younger ages (Figs. 5K, 5M), but in older animals, signal in the outer retina was absent or reduced to a narrow band next to the RPE (Figs. 5L, 5N).

DISCUSSION

The present study confirmed previous reports showing that metallothioneins are expressed in mouse and rat retinas and pigment epithelium,[20,24,26–29,32] and showed in addition: (1) that adult expression levels of metallothionein-I and -II are not reached in normal retinas until around P21 or later; (2) that metallothionein-I+II are induced in glial cells in the three models of hereditary photoreceptor degeneration studied; and (3) that the receptor megalin is expressed not only in the inner retina, as previously shown,[34] but also in the outer retina, and that this latter expression is lost in degenerating retinas.

A small but significant increase in metallothionein-I and -II gene expression levels was observed during the first postnatal weeks both in mice and rats, which could correlate with the structural and functional maturation of the retina that takes place during this period. Expression of these metallothioneins is tightly regulated by levels of, for example, growth factors and cytokines, many of which are notably active during early postnatal retinal development. Increases in expression could also reflect an increased availability of free zinc. Metallothioneins are induced not only to protect cells against potentially toxic high zinc levels, but seem to be expressed also in association with increases in physiological zinc. Chelatable zinc and zinc transporters are observed in association with glutamatergic synapses[52] and co-release of vesicular zinc with glutamate has been shown to occur from photoreceptor terminals at the level of the outer plexiform layer (OPL).[53,54] In addition, high levels of zinc have been noted around the photoreceptor IS in light-adapted retina.[54,55] Full maturation of both these retinal regions occurs around the second postnatal week in a center-to-periphery gradient,[56] thus correlating with the increasing levels of metallothionein-I and -II detected, and in agreement with observations made in the brain.[57] However, no differences were noted in the present study in the expression of metallothionein-I+II in developing retinas. There is the possibility that small increases in protein levels escaped detection with the antibody used. Alternatively, the increase could correspond to expression in retinal vessels, which also develop in rodents during the same period,[58] as it has been shown that endothelial and smooth muscle cells also express metallothionein.[59] The specificity of metallothionein-I+II labeling in the retinal vessels structures could not be verified in the present study and needs therefore to be examined further.

A marked increase in both gene and protein expression was seen, however, in the three models of photoreceptor degeneration. The microarray and q-RT-PCR analyses showed that levels of metallothionein-I and -II are significantly upregulated in *rd1* mice at P12, and that protein expression can also be observed at this stage in the central retina in these mice. The increase in expression followed the center-to-periphery pattern of progression normally ob-

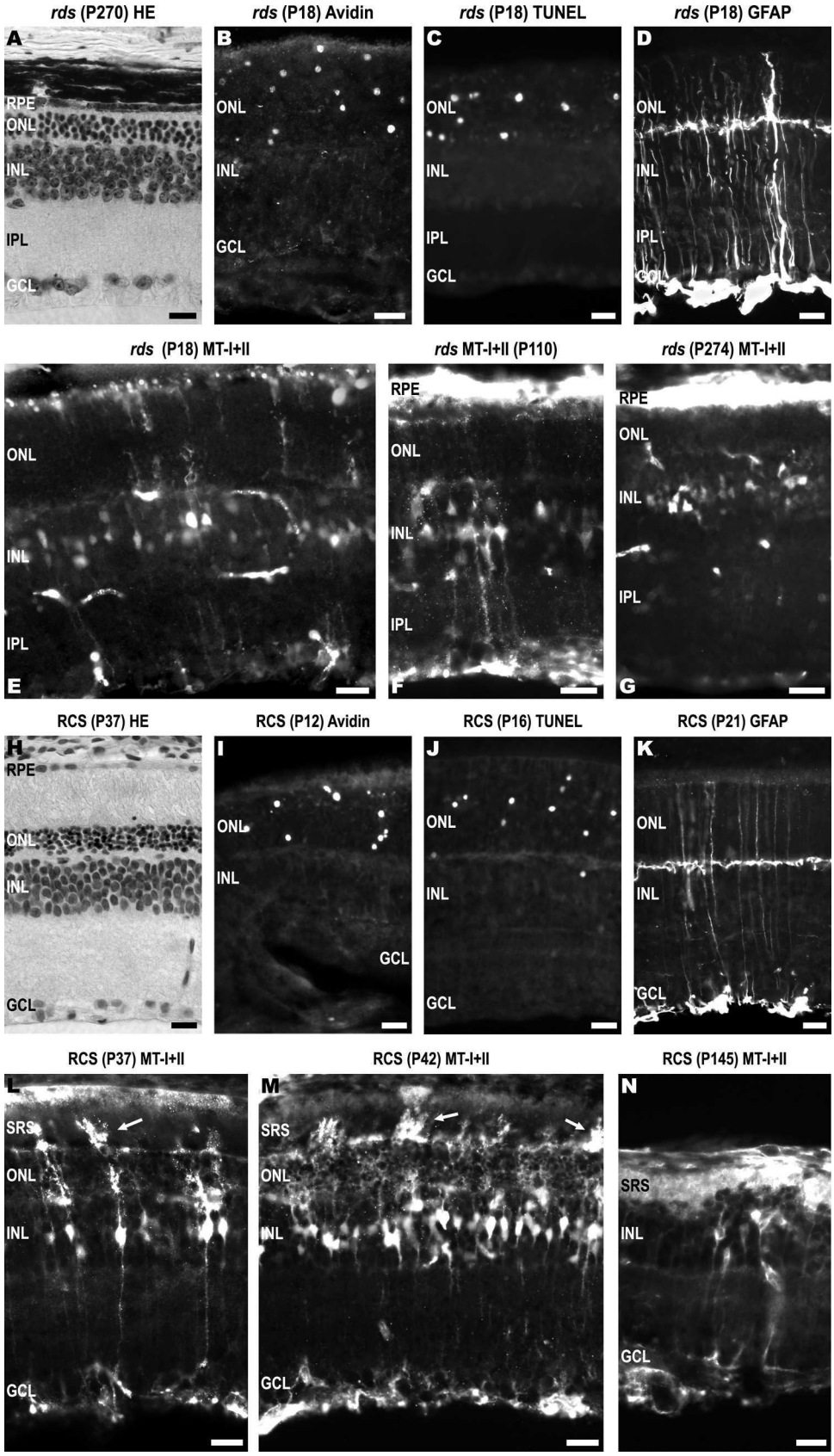

FIGURE 3. Localization of various markers in *rds* mouse (**A–G**) and RCS rat (**H–N**) retinas. At P270 in *rds* mice, about half of the photoreceptor cells remained (**A**), although all markers analyzed were already detected throughout the *rds* retina in the first postnatal weeks (**B–E**). Metallothionein-I+II staining was observed in the RPE and in Müller cell bodies and processes (**E–F**). In older animals, staining in Müller cells was restricted to the cell bodies (**G**). In RCS rats, about half of the ONL was lost by the first month of age (**H**). Avidin and TUNEL staining were observed relatively early (**I**, **J**), followed by GFAP (**K**) and metallothionein-I+II (**L**, **M**). The latter was initially observed in sporadic Müller cell bodies and processes (**L**) and in a large number of cells within a few days (**M**). Occasionally, staining was observed in the subretinal space (*arrows*; **L**, **M**). Metallothionein-I+II staining was observed also in older animals in a small number of Müller cells (**N**). HE, hematoxylin-eosin; MT, metallothionein; SRS, subretinal space. Scale bars, 20 μm.

served in this model, but increased protein expression was still seen in retinas of P46 and P150 animals, when only a few degenerating cones remained.[60,61] The upregulation of metallothionein-I+II appears to correlate with glial activation rather than with the onset of photoreceptor cell death as such, as the latter was detectable by TUNEL staining as

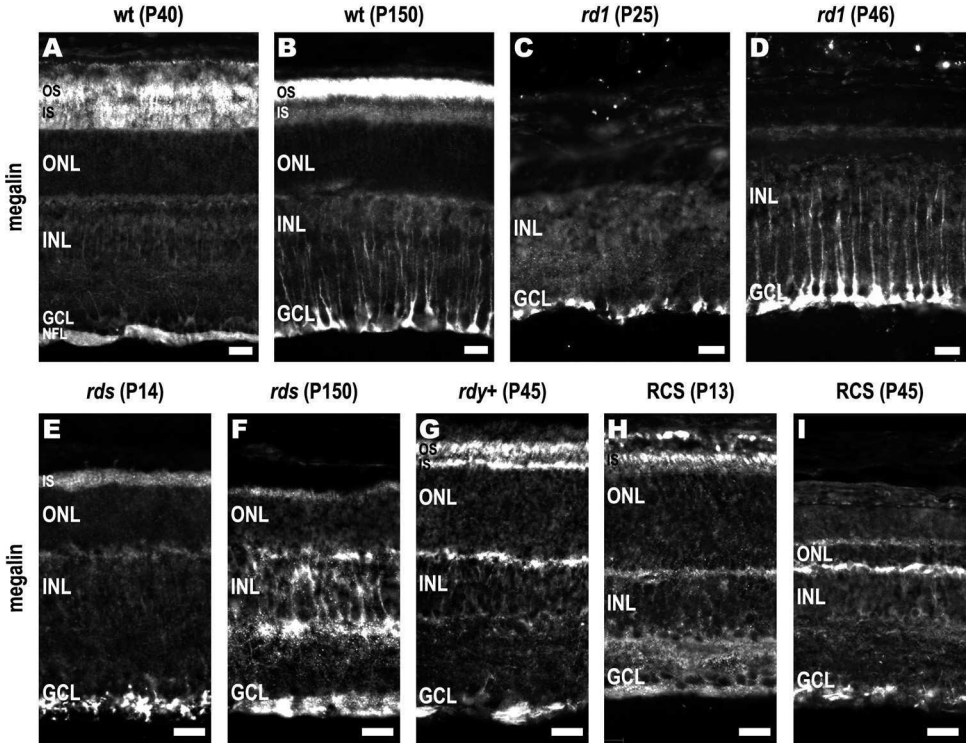

Figure 4. Localization of megalin immunoreactivity in normal and degenerating retinas. In the young normal mouse retina (**A**), megalin immunoreactivity was most prominent in the subretinal space and becomes more concentrated over the photoreceptor outer segments with age (**B**). In older animals, the most proximal processes of Müller cells were also labeled (**B**). In *rd1* and *rds* mice, staining in the outer retina was initially weaker and, at older ages, was absent (**C**–**F**). In the latter, Müller cell processes were also labeled (**D**, **F**). In normal rat retinas (*rdy*$^{+}$), megalin expression was also detected over the photoreceptor inner and outer segments (**G**). In RCS rats, labeling in the outer retina was lost with age (**H**, **I**). OS, outer segments; IS, inner segments. Scale bars, 20 μm.

early as P9. Further, metallothionein-I+II expression was induced mainly in Müller cells and coincided with the onset of GFAP expression, one of the earlier indicators of activation of these cells.[62] Such a distribution corresponds to what has been observed after neuronal damage in various models of CNS injury, where it is seen that metallothionein-I+II accumulate mainly in activated astrocytes, the main source of these metallothioneins in the brain (see recent reviews in Refs. 19 and 34).

The accumulation of metallothionein-I+II observed here in Müller cells does not, however, fully correspond to observations made with a model of light-induced damage.[27] In the latter, an upregulation of metallothionein-I+II was noted in the RPE and in the plexiform layers immediately after a 7-hour exposure to bright light, in the ONL and GCL after 8 hours, and only in the inner retina 28 hours after exposure,[27] with no obvious expression in the Müller cells. Bright light exposure causes massive, immediate damage to photoreceptors, which involves, at some point, elevated intracellular calcium levels and an accumulation of reactive oxygen species, which contribute to oxidative damage.[63] Most photoreceptors die relatively fast in *rd1* mice, compared with those in *rds* mice or RCS rats. In *rd1* retinas, impaired cGMP-phosphodiesterase activity,[38] supposedly also leads to deregulated Ca^{2+} homeostasis, as suggested by observations that activation of calpain is increased in these retinas[64,65] and that application of a Ca^{2+} blocker confers protection.[66] Others and we in this study have found evidence that the *rd1* mouse photoreceptors also undergo oxidative damage.[50,61] Nonetheless, no accumulation of metallothionein-I+II was seen in the present study in photoreceptors in *rd1* mice, as reported to occur after light damage.

As mentioned earlier, metallothionein-I+II are primarily of glial origin, and accumulation in photoreceptors would therefore require that the metallothioneins be transferred to the latter. Transport of glial-derived metallothionein into retinal ganglion cells has recently been shown to occur, where it was found to modulate axonal regeneration.[34] It is possible, thus, that the events initiated in *rd1* mouse photoreceptors are still not sufficient to induce significant metallothionein synthesis and accumulation in these cells or that they actually die before detectable amounts of metallothionein can be found.

However, as found in the present study, metallothionein-I+II also did not accumulate in photoreceptors of homozygous *rds* mice. In these animals, a mutation of the gene encoding peripherin leads to the absence of rod photoreceptor disc membranes and the development of abnormal cone outer segments.[39,67] As a result, the normal compartmentalization of proteins involved in phototransduction does not occur, altering expression of at least some genes.[68] The inner segments appear to develop normally but are immediately adjacent to the microvilli of the RPE.[39] We found the first TUNEL-stained cells in *rds* retinas at P12 and P14, with the largest number seen at ~ P16 and P18, which agrees with previous reports.[69,70] Despite this early peak of cell death, complete loss of photoreceptors was seen only at ~12 months of age.[39] Yet, no metallothionein-I+II was detected in photoreceptors in this slow-progressing model, but was seen to correlate rather with some stage of glial activation, as indicated by concomitant accumulation of GFAP in the Müller cells.

In RCS rat retinas, overexpression of metallothionein-I+II was similarly seen in Müller cells. Yet, it was not detected until ~10 days after the onset of GFAP accumulation in these cells. In RCS rats, phagocytosis of shed outer segments is not performed due to a mutation in the *Mertk* gene expressed by retinal epithelial cells.[40] As a consequence, membrane debris accumulate in the subretinal space, eventually leading to secondary photoreceptor cell death, which was first detectable by TUNEL staining at ~P12 in the present study. We found that upregulation of mRNA levels of metallothionein-I and -II was also delayed in RCS rat retinas, indicating that the late expression of metallothionein-I+II is not due to slow protein synthesis.

The present study thus shows that metallothionein-I and -II are induced in the three models of degeneration. The upregulation did not coincide with the onset of photoreceptor cell loss, but rather with the widespread accumulation of GFAP in

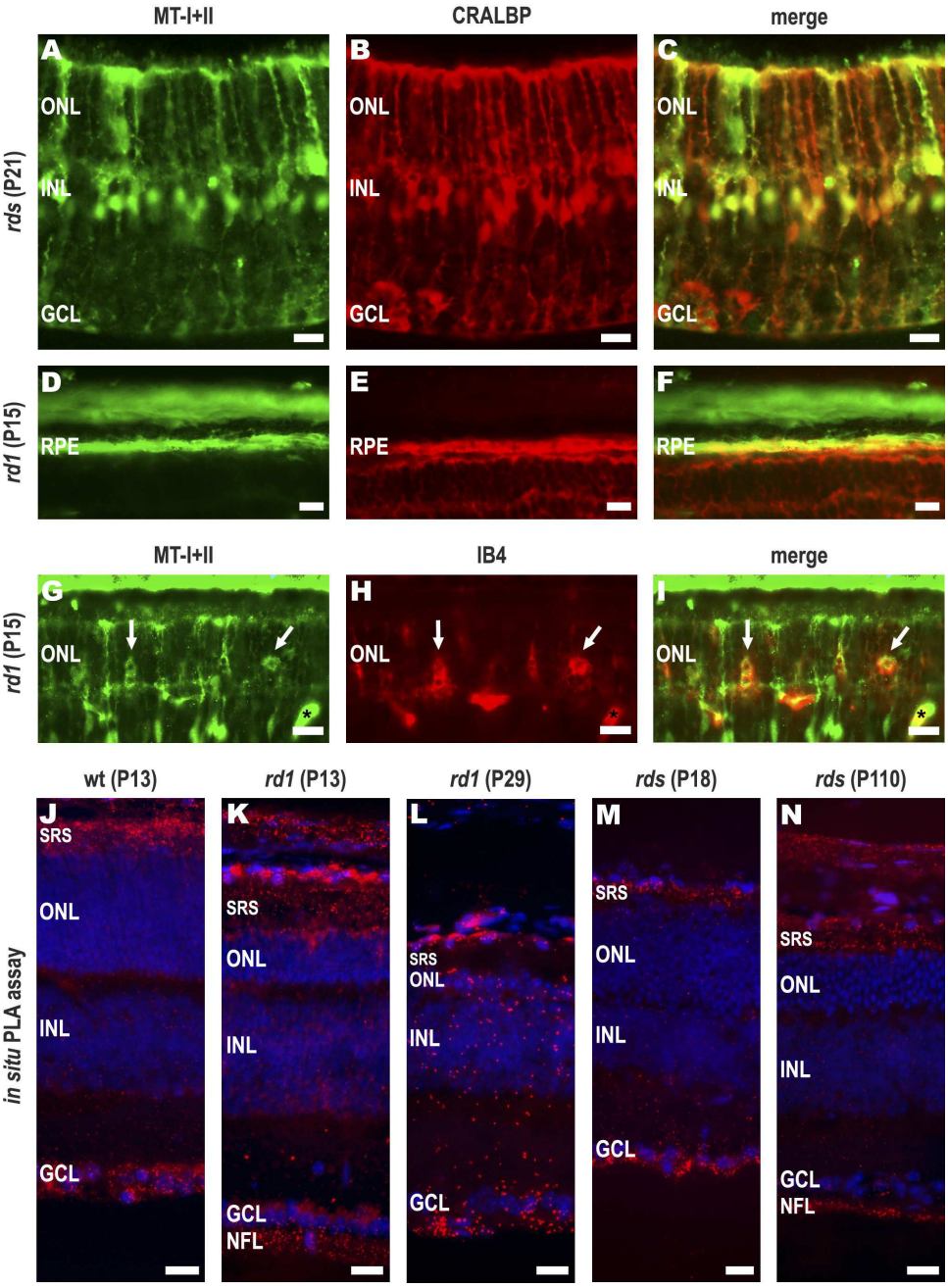

FIGURE 5. Colocalization of various markers (**A–I**) and in situ PLA assay (**J–N**). (**A**) Metallothionein-I+II staining, *rds* mouse, P21; (**B**) CRALBP staining, *rds* mouse, P21; (**C**) merged image showing metallothionein-I+II accumulation in Müller cells and processes; (**D**) metallothionein-I+II staining, *rd1* mouse, P15; (**E**) CRALBP staining, *rd1* mouse, P15; (**F**) merged image showing metallothionein-I+II accumulation in the RPE; (**G**) metallothionein-I+II staining, *rd1* mouse, P15; (**H**) IB4 staining, *rd1* mouse, P15; (**I**) merged image showing metallothionein-I+II accumulation in microglial cells in the ONL (*arrows*); accumulation of IB4 in vessels co-localizes with unspecific metallothionein-I+II staining (✱); (**J–N**) In situ PLA assay including DAPI nuclear staining (*blue*). Dots represent putative sites of megalin/metallothionein-I+II interaction (*red*): (**J**) wt mouse, P13: signal in the inner retina and in the subretinal space, over the photoreceptor inner and outer segment region; (**K**) *rd1* mouse, P13: signal in the nerve fiber layer and reduced signal in the subretinal space; (**L**) *rd1* mouse, P29: reduction of signal both in the inner and outer retina; (**M**) *rds* mouse, P18: signal in the inner retina and in a thin band in the subretinal space; (**N**) *rds* mouse, P110: signal in the inner retina and diffusely distributed in the subretinal space. MT, metallothionein; CRALBP, cellular retinaldehyde binding protein; IB4, isolectin B4; SRS, subretinal space. Scale bars, 20 μm.

Müller cells, at least in *rd1* and *rds* mice. In RCS rats, it was considerably delayed in relation to expression of GFAP. Accumulation of the GFAP is normally associated with the process of Müller glia activation,[62,71] although it may not necessarily reflect the time when activation is initiated. We showed, for instance, in previous studies that glial-derived molecules accumulate in RCS rat retinas long before GFAP upregulation can be detected and even before signs of photoreceptor cell death.[72] Further, although GFAP accumulation occurred in Müller cells in the three models, previous studies have shown, for instance, that the downregulation of inwardly rectifying K^+ (Kir) currents displayed by Müller cells and which normally accompanies fast neuronal degeneration is not observed in RCS rats or *rds* mice.[73,74] Upregulation of metallothionein-I+II, as other features of Müller cell activation, may therefore not correlate always with the same specific events triggered in these cells.

Furthermore, like other glial-derived factors, metallothionein-I+II levels can be stimulated without neuronal cell death. It is therefore possible that upregulation is not a response to cell death, but to changes in one or several factors accompanying or even preceding cell death, where the type and degree of change determine the onset of metallothionein-I+II expression. Previous studies have shown that the levels of free glutamate are increased as photoreceptors degenerate and that uptake and metabolism of glutamate by Müller cells is impaired, at least in some cases.[75,76] As mentioned, zinc is co-released with glutamate in several neuronal structures, including photoreceptor terminals.[77,78] Detectable levels of zinc have in fact been found, not only in the terminal region, but throughout the rod photoreceptor cell.[77] It could thus be speculated that zinc leaking from dysfunctional/dying photoreceptors is one of the initial triggers of metallothionein-I and -II expression. Zinc transporters (ZnT) are localized through-

out the retina, including the photoreceptor inner segment region and the apical processes of Müller cells.[79–81] An upregulation of ZnT was not seen by microarray analysis in *rd1* mouse retinas in young ages (P11–P15, P21), when some layers of photoreceptor cells remain (not shown). Yet, at older ages (P28, P35), no reduction in expression was observed, despite the almost complete loss of the photoreceptor cell layer, suggesting that there may indeed be a relative increase over time in the number of zinc transporters expressed by Müller cells and/or other cells in the inner portions of the retina. This would correlate with our observation that increased metallothionein-I+II expression was still observed in retinas of *rd1* mice and RCS rats long after most photoreceptors had been lost. Moreover, it is possible that accumulation of other metals, in addition to zinc, may induce increases in metallothionein-I+II expression. In RCS rats, the concentrations of iron and copper are also increased in the outer retina.[82,83] Although it is not clear how these increases are produced, their accumulation in the subretinal space could contribute to the triggering of metallothionein-I+II upregulation in Müller cells.

A critical question is also whether the increases noted in endogenous metallothionein-I+II levels actually contribute to prolonged photoreceptor survival in the course of degeneration and how protection would be mediated. The endocytic receptor megalin has been recently shown to mediate the internalization of exogenous and glial-derived metallothionein-I+II into neurons, including retinal ganglion cells.[34] The present study confirmed that megalin is expressed in normal retinas in the NFL and showed that it is also expressed in the IS and OS region of the retina at all ages analyzed. This distribution correlates well with the sites of metallothionein-I+II expression and the concept that the latter mediates its functions, at least in part, through interactions with megalin.[33,34] Of note, the pattern of megalin expression changed with age in the normal retina, and accumulation was eventually observed also in Müller cells, at least in mouse retinas. As megalin mediates the transport of not only metallothioneins but of several other ligands,[35,36] this could explain its localization in Müller cells in the normal retina, even in the absence of metallothionein-I+II.

The expression of megalin observed in the outer retina in normal mice and rats was lost very early in degenerating retinas (confirmed by a lack of signal in this region using the PLA assay) and was probably due to the loss of the outer and inner segments as photoreceptors degenerate. In the degenerating mouse retinas, megalin expression was instead seen in the processes of Müller cells at younger ages than in normal animals. This expression did not correlate with the increases in metallothionein-I+II expression in Müller cells and may instead be a consequence of the loss of megalin expression in the subretinal space region. Cubulin, another multiligand endocytic receptor is found to be co-expressed with megalin in epithelial cells where they mediate the reabsorption of retinol-binding proteins, for example.[84] Defects of chloride channels/transporters have been shown to cause retinal degeneration,[85,86] possibly involving alterations in megalin and cubilin function. Metallothionein-I+II could thus be transported by either megalin or cubilin receptors in the outer retina.[87] However, the activity of cubilin has been shown to depend on the presence and activity of megalin.[88] It appears thus that if metallothionein-I+II were to exert a protective effect on photoreceptors, it would not involve megalin- or cubilin-mediated transport of metallothioneins in the outer retina, which could also explain why we found no metallothionein-I+II labeling in the photoreceptors.

Inability to produce endogenous metallothionein-I+II has been shown to exacerbate ganglion cell loss after intraocular injections of *N*-methyl-D-aspartate,[26] but not the loss of photoreceptors induced by hyperbaric oxygen exposure,[89] suggesting that the dependence on metallothionein for survival varies with the type of insult and/or the type of cell affected. Moreover, it is possible that increases in metallothionein-I+II levels occur, not to protect photoreceptors, but to support the various events mediated by glial cells, secondary to photoreceptor degeneration and/or to support the glial cells themselves. The activity and function of Müller cells is regulated by several factors, including cytokines such as IL-6, acting through signal transducer and activator of transcription 3 (STAT3).[90] The latter targets several genes, including metallothionein-I and -II,[91,92] suggesting that upregulation of these metallothioneins is both a cause and an effect of glial activation. The same may apply to RPE and microglial cells, which we found also to express metallothionein-I+II and which react to damage and injury by upregulating various cytokines.[93,94]

In summary, although the initial triggers of photoreceptor dysfunction differ in the three models studied, common processes are eventually activated, including an upregulation of metallothionein-I+II. The onset of their expression did not coincide with that of cell death (nor of glial activation in RCS rats), suggesting that stimulation of these metallothioneins is controlled, at least in part, by different events in the three diseases. As to the role of metallothionein-I+II in photoreceptor degeneration, one might argue that cell loss progresses in the three models studied despite upregulation of metallothioneins and of several other neuroprotective factors. However, whether endogenous metallothioneins actually protects photoreceptors would have to be verified in genetic experiments.

Acknowledgments

The authors thank Markus Thiersch, Marijana Samardzija (Department of Ophthalmology, University of Zurich, Switzerland), and Kenneth Beri Ploug (Department of Neurology and Danish Headache Center, Glostrup, Denmark) for help with the q-RT-PCR protocols; Hodan Abdalle for technical support; and Karin Arnér and Birgitta Klefbohm for assistance with the animal colonies.

References

1. Hartong DT, Berson EL, Dryja TP. Retinitis pigmentosa. *Lancet.* 2006;368:1795–1809.
2. Hamel C. Retinitis pigmentosa. *Orphanet J Rare Dis.* 2006;1:40.
3. LaVail MM, Yasumura D, Matthes MT, et al. Protection of mouse photoreceptors by survival factors in retinal degenerations. *Invest Ophthalmol Vis Sci.* 1998;39:592–602.
4. Sieving PA, Caruso RC, Tao W, et al. Ciliary neurotrophic factor (CNTF) for human retinal degeneration: phase I trial of CNTF delivered by encapsulated cell intraocular implants. *Proc Natl Acad Sci U S A.* 2006;103:3896–3901.
5. Ahuja P, Caffé AR, Holmqvist I, et al. Lens epithelium-derived growth factor (LEDGF) delays photoreceptor degeneration in explants of rd/rd mouse retina. *Neuroreport.* 2001;12:2951–2955.
6. Delyfer MN, Simonutti M, Neveux N, Léveillard T, Sahel JA. Does GDNF exert its neuroprotective effects on photoreceptors in the rd1 retina through the glial glutamate transporter GLAST? *Mol Vis.* 2005;11:677–687.
7. Azadi S, Johnson LE, Paquet-Durand F, et al. CNTF+BDNF treatment and neuroprotective pathways in the rd1 mouse retina. *Brain Res.* 2007;1129:116–129.
8. Palmiter RD. The elusive function of metallothioneins. *Proc Natl Acad Sci U S A.* 1998;95:8428–8430.
9. Hidalgo J, Aschner M, Zatta P, Vasák M. Roles of the metallothionein family of proteins in the central nervous system. *Brain Res Bull.* 2001;55:133–145.
10. Coyle P, Philcox JC, Carey LC, Rofe AM. Metallothionein: the multipurpose protein. *Cell Mol Life Sci.* 2002;59:627–647.
11. Haq F, Mahoney M, Koropatnick J. Signaling events for metallothionein induction. *Mutat Res.* 2003;533:211–226.

12. Penkowa M. Metallothioneins are multipurpose neuroprotectants during brain pathology. *FEBS Lett J.* 2006;273:1857–1870.
13. Nielsen AE, Bohr A, Penkowa M. The balance between life and death of cells: roles of metallothioneins. *Biomark Insights.* 2007; 1:99–111.
14. Hidalgo J, Chung R, Penkowa M, Vasák M. Structure and functions of vertebrate metallothioneins. In: Sigel A, Sigel H, Sigel RKO, eds. *Metal Ions in Life Sciences: Metallothioneins and Related Chelators.* Vol. 5. Cambridge, UK: The Royal Society of Chemistry. 2009:279–317.
15. Pedersen MØ, Larsen A, Stoltenberg M, Penkowa M. Cell death in the injured brain: roles of metallothioneins. *Prog Histochem Cytochem.* 2009;44:1–27.
16. Maret W, Vallee BL. Thiolate ligands in metallothionein confer redox activity on zinc clusters. *Proc Natl Acad Sci U S A.* 1998; 95:3478–3482.
17. Sato M, Kondoh M. Recent studies on metallothionein: protection against toxicity of heavy metals and oxygen free radicals. *Tohoku J Exp Med.* 2002;196:9–22.
18. Stankovic RK, Chung RS, Penkowa M. Metallothioneins I and II: neuroprotective significance during CNS pathology. *Int J Biochem Cell Biol.* 2007;39:484–489.
19. Pedersen MØ, Jensen R, Pedersen DS, et al. Metallothionein-I+II in neuroprotection. *Biofactors.* 2009;35:315–325.
20. Nishimura H, Nishimura N, Kobayashi S, Tohyama C. Immunohistochemical localization of metallothionein in the eye of rats. *Histochemistry.* 1991;95:535–539.
21. Oliver PD, Tate DJ, Newsome DA. Metallothionein in human retinal pigment epithelial cells: expression, induction and zinc uptake. *Curr Eye Res.* 1992;11:183–188.
22. Tate DJ, Newsome DA, Oliver PD. Metallothionein shows an age-related decrease in human macular retinal pigment epithelium. *Invest Ophthalmol Vis Sci.* 1993;34:2348–2351.
23. Tate DJ, Miceli MV, Newsome DA, Alcock NW, Oliver PD. Influence of zinc on selected cellular functions of cultured human retinal pigment epithelium. *Curr Eye Res.* 1995;14:897–903.
24. Chen W, Hunt DM, Lu H, Hunt RC. Expression of antioxidant protective proteins in the rat retina during prenatal and postnatal development. *Invest Ophthalmol Vis Sci.* 1999;40:744–751.
25. Tate DJ, Miceli MV, Newsome DA. Expression of metallothionein isoforms in human chorioretinal complex. *Curr Eye Res.* 2002;24: 12–25.
26. Suemori S, Shimazawa M, Kawase K, et al. Metallothionein, an endogenous antioxidant, protects against retinal neuron damage in mice. *Invest Ophthalmol Vis Sci.* 2006;47:3975–3982.
27. Chen L, Wu W, Dentchev T, Wong R, Dunaief JL. Increased metallothionein in light damaged mouse retinas. *Exp Eye Res.* 2004;79:287–293.
28. Vázquez-Chona F, Song BK, Geisert EE. Temporal changes in gene expression after injury in the rat retina. *Invest Ophthalmol Vis Sci.* 2004;45:2737–2746.
29. Thiersch M, Raffelsberger W, Frigg R, et al. Analysis of the retinal gene expression profile after hypoxic preconditioning identifies candidate genes for neuroprotection. *BMC Genomics.* 2008;9:73.
30. Nicolas MG, Fujiki K, Murayama K, et al. Studies on the mechanism of early onset macular degeneration in cynomolgus monkeys. II. Suppression of metallothionein synthesis in the retina in oxidative stress. *Exp Eye Res.* 1996;62:399–408.
31. Lu H, Hunt DM, Ganti R, et al. Metallothionein protects retinal pigment epithelial cells against apoptosis and oxidative stress. *Exp Eye Res.* 2002;74:83–92.
32. Wu Z, Rogers B, Kachi S, Hackett SF, Sick A, Campochiaro PA. Reduction of p66Shc suppresses oxidative damage in retinal pigmented epithelial cells and retina. *J Cell Physiol.* 2006;209:996–1005.
33. Fitzgerald M, Nairn P, Bartlett CA, Chung RS, West AK, Beazley LD. Metallothionein-IIA promotes neurite growth via the megalin receptor. *Exp Brain Res.* 2007;183:171–180.
34. Chung RS, Penkowa M, Dittmann J, et al. Redefining the role of metallothionein within the injured brain: extracellular metallothioneins play an important role in the astrocyte-neuron response to injury. *J Biol Chem.* 2008;283:15349–15358.
35. Christensen EI, Birn H. Megalin and cubilin: multifunctional endocytic receptors. *Nat Rev Mol Cell Biol.* 2002;3:256–266.
36. May P, Herz J, Bock HH. Molecular mechanisms of lipoprotein receptor signalling. *Cell Mol Life Sci.* 2005;62:2325–2338.
37. Ambjørn M, Asmussen JW, Lindstam M, et al. Metallothionein and a peptide modeled after metallothionein, EmtinB, induce neuronal differentiation and survival through binding to receptors of the low-density lipoprotein receptor family. *J Neurochem.* 2008;104: 21–37.
38. Bowes C, Li T, Danciger M, Baxter LC, Applebury ML, Farber DB. Retinal degeneration in the rd mouse is caused by a defect in the beta subunit of rod cGMP-phosphodiesterase. *Nature.* 1990;347: 677–680.
39. Sanyal S, Jansen HG. Absence of receptor outer segments in the retina of rds mutant mice. *Neurosci Lett.* 1981;21:23–26.
40. D'Cruz PM, Yasumura D, Weir J, et al. Mutation of the receptor tyrosine kinase gene Mertk in the retinal dystrophic RCS rat. *Hum Mol Genet.* 2000;9:645–651.
41. Viczian A, Sanyal S, Toffenetti J, Chader GJ, Farber DB. Photoreceptor-specific mRNAs in mice carrying different allelic combinations at the rd and rds loci. *Exp Eye Res.* 1992;54:853–860.
42. Chirgwin J, Przybyla AE, MacDonald RJ, Rutter WJ. Isolation of biologically active ribonucleic acid from sources enriched in ribonuclease. *Biochemistry.* 1979;18:5294–5299.
43. Lockhart DJ, Dong H, Byrne MC, et al. Expression monitoring by hybridization to high-density oligonucleotide arrays. *Nat Biotechnol.* 1996;14:1675–1680.
44. Wilson CL, Miller CJ. Simpleaffy: a BioConductor package for Affymetrix Quality Control and data analysis. *Bioinformatics.* 2005;21:3683–3685.
45. Raffelsberger W, Krause Y, Moulinier L, et al. RReportGenerator: automatic reports from routine statistical analysis using R. *Bioinformatics.* 2008;24:276–278.
46. Kalathur RK, Gagniere N, Bertommier G, et al. RETINOBASE: a web database, data mining and analysis platform for gene expression data on retina. *BMC Genomics.* 2008;9:208.
47. Thiersch M, Lange C, Joly S, et al. Retinal neuroprotection by hypoxic preconditioning is independent of hypoxia-inducible factor-1 alpha expression in photoreceptors. *Eur J Neurosci.* 2009; 29:2291–2302.
48. Dohi Y, Shimaoka H, Ikeuchi M, Ohgushi H, Yonemasu K, Minami T. Role of metallothionein isoforms in bone formation processes in rat marrow mesenchymal stem cells in culture. *Biol Trace Elem Res.* 2005;104:57–70.
49. Struthers L, Patel R, Clark J, Thomas S. Direct detection of 8–oxodeoxyguanosine and 8-oxoguanine by avidin and its analogues. *Anal Biochem.* 1998;255:20–31.
50. Sanz MM, Johnson LE, Ahuja S, Ekström PA, Romero J, van Veen T. Significant photoreceptor rescue by treatment with a combination of antioxidants in an animal model for retinal degeneration. *Neuroscience.* 2007;145:1120–1129.
51. Söderberg O, Leuchowius KJ, Gullberg M, et al. Characterizing proteins and their interactions in cells and tissues using the in situ proximity ligation assay. *Methods.* 2008;45:227–232.
52. Palmiter RD, Cole TB, Quaife CJ, Findley SD. ZnT-3, a putative transporter of zinc into synaptic vesicles. *Proc Natl Acad Sci U S A.* 1996;93:14934–14939.
53. Wu SM, Qiao X, Noebels JL, Yang XL. Localization and modulatory actions of zinc in vertebrate retina. *Vision Res.* 1993;33:2611–2616.
54. Redenti S, Chappell RL. Neuroimaging of zinc released by depolarization of rat retinal cells. *Vision Res.* 2005;45:3520–3525.
55. Ugarte M, Osborne NN. The localization of free zinc varies in rat photoreceptors during light and dark adaptation. *Exp Eye Res.* 1999;69:459–461.
56. Hack I, Koulen P, Peichl L, Brandstätter JH. Development of glutamatergic synapses in the rat retina: the postnatal expression of ionotropic glutamate receptor subunits. *Vis Neurosci.* 2002;19: 1–13.
57. Penkowa M, Nielsen H, Hidalgo J, Bernth N, Moos T. Distribution of metallothionein I + II and vesicular zinc in the developing central nervous system: correlative study in the rat. *J Comp Neurol.* 1999;41:303–318.

58. Stone J, Itin A, Alon T, et al. Development of retinal vasculature is mediated by hypoxia-induced vascular endothelial growth factor (VEGF) expression by neuroglia. *J Neurosci.* 1995;15:4738–4747.
59. Kaji T, Yamamoto C, Suzuki M, et al. Induction of metallothionein by thrombin in cultured vascular endothelial and smooth muscle cells. *Biol Pharm Bull.* 1995;18:1272–1274.
60. Carter-Dawson LD, LaVail MM, Sidman RL. Differential effect of the rd mutation on rods and cones in the mouse retina. *Invest Ophthalmol Vis Sci.* 1978;17:489–498.
61. Komeima K, Rogers BS, Lu L, Campochiaro PA. Antioxidants reduce cone cell death in a model of retinitis pigmentosa. *Proc Natl Acad Sci U S A.* 2006;103:11300–11305.
62. Bringmann A, Pannicke T, Grosche J, et al. Müller cells in the healthy and diseased retina. *Prog Retin Eye Res.* 2006;25:397–424.
63. Wenzel A, Grimm C, Samardzija M, Remé C. Molecular mechanisms of light-induced photoreceptor apoptosis and neuroprotection for retinal degeneration. *Prog Retin Eye Res.* 2005;24:275–306.
64. Paquet-Durand F, Azadi S, Hauck SM, Ueffing M, van Veen T, Ekström P. Calpain is activated in degenerating photoreceptors in the rd1 mouse. *J Neurochem.* 2006;96:802–814.
65. Sanges D, Comitato A, Tammaro R, Marigo V. Apoptosis in retinal degeneration involves cross-talk between apoptosis-inducing factor (AIF) and caspase-12 and is blocked by calpain inhibitors. *Proc Natl Acad Sci U S A.* 2006;103:17366–17371.
66. Frasson M, Sahel JA, Fabre M, Simonutti M, Dreyfus H, Picaud S. Retinitis pigmentosa: rod photoreceptor rescue by a calcium-channel blocker in the rd mouse. *Nat Med.* 1999;5:1183–1187.
67. Farjo R, Skaggs JS, Nagel BA, et al. Retention of function without normal disc morphogenesis occurs in cone but not rod photoreceptors. *J Cell Biol.* 2006;173:59–68.
68. Agarwal N, Nir I, Papermaster DS. Loss of diurnal arrestin gene expression in rds mutant mouse retinas. *Exp Eye Res.* 1994;58:1–8.
69. Chang GQ, Hao Y, Wong F. Apoptosis: final common pathway of photoreceptor death in rd, rds, and rhodopsin mutant mice. *Neuron.* 1993;11:595–605.
70. Portera-Cailliau C, Sung CH, Nathans J, Adler R. Apoptotic photoreceptor cell death in mouse models of retinitis pigmentosa. *Proc Natl Acad Sci U S A.* 1994;91:974–978.
71. Lewis GP, Fisher SK. Up-regulation of glial fibrillary acidic protein in response to retinal injury: its potential role in glial remodeling and a comparison to vimentin expression. *Int Rev Cytol.* 2003;230:263–290.
72. Zhang Y, Rauch U, Perez MT. Accumulation of neurocan, a brain chondroitin sulfate proteoglycan, in association with the retinal vasculature in RCS rats. *Invest Ophthalmol Vis Sci.* 2003;44:1252–1261.
73. Felmy F, Pannicke T, Richt JA, Reichenbach A, Guenther E. Electrophysiological properties of rat retinal Müller (glial) cells in postnatally developing and in pathologically altered retinae. *Glia.* 2001;34:190–199.
74. Iandiev I, Biedermann B, Bringmann A, Reichel MB, Reichenbach A, Pannicke T. Atypical gliosis in Müller cells of the slowly degenerating rds mutant mouse retina. *Exp Eye Res.* 2006;82:449–457.
75. Fletcher EL, Kalloniatis M. Neurochemical architecture of the normal and degenerating rat retina. *J Comp Neurol.* 1996;376:343–360.
76. Delyfer MN, Forster V, Neveux N, Picaud S, Léveillard T, Sahel JA. Evidence for glutamate-mediated excitotoxic mechanisms during photoreceptor degeneration in the rd1 mouse retina. *Mol Vis.* 2005;11:688–696.
77. Redenti S, Ripps H, Chappell RL. Zinc release at the synaptic terminals of rod photoreceptors. *Exp Eye Res.* 2007;85:580–584.
78. Chappell RL, Anastassov I, Lugo P, Ripps H. Zinc-mediated feedback at the synaptic terminals of vertebrate photoreceptors. *Exp Eye Res.* 2008;87:394–397.
79. Redenti S, Chappell RL. Localization of zinc transporter-3 (ZnT-3) in mouse retina. *Vision Res.* 2004;44:3317–3321.
80. Wang X, Wang ZY, Gao HL, Danscher G, Huang L. Localization of ZnT7 and zinc ions in mouse retina: immunohistochemistry and selenium autometallography. *Brain Res Bull.* 2006;71:91–96.
81. Redenti S, Chappell RL. Müller cell zinc transporter-3 labeling suggests a role in outer retina zinc homeostasis. *Mol Med.* 2007;13:376–379.
82. Sergeant C, Gouget B, Llabador Y, et al. Iron and other elements (Cu, Zn, Ca) contents in retina of rats during development and hereditary retinal degeneration. *Nucl Instr Methods Phys Res B.* 2001;181:533–538.
83. Yefimova MG, Jeanny JC, Keller N, et al. Impaired retinal iron homeostasis associated with defective phagocytosis in Royal College of Surgeons rats. *Invest Ophthalmol Vis Sci.* 2002;43:537–545.
84. Verroust PJ, Christensen EI. Megalin and cubilin: the story of two multipurpose receptors unfolds. *Nephrol Dial Transplant.* 2002;17:1867–1871.
85. Bösl MR, Stein V, Hübner C, et al. Male germ cells and photoreceptors, both dependent on close cell-cell interactions, degenerate upon ClC-2 Cl(−) channel disruption. *EMBO J.* 2001;20:1289–1299.
86. Kornak U, Kasper D, Bösl MR, et al. Loss of the ClC-7 chloride channel leads to osteopetrosis in mice and man. *Cell.* 2001;104:205–215.
87. Assémat E, Châtelet F, Chandellier J, et al. Overlapping expression patterns of the multiligand endocytic receptors cubilin and megalin in the CNS, sensory organs and developing epithelia of the rodent embryo. *Gene Expr Patterns.* 2005;6:69–78.
88. Christensen EI, Devuyst O, Dom G, et al. Loss of chloride channel ClC-5 impairs endocytosis by defective trafficking of megalin and cubilin in kidney proximal tubules. *Proc Natl Acad Sci U S A.* 2003;100:8472–8477.
89. Nachman-Clewner M, Giblin FJ, Dorey CK, et al. Selective degeneration of central photoreceptors after hyperbaric oxygen in normal and metallothionein-knockout mice. *Invest Ophthalmol Vis Sci.* 2008;49:3207–3215.
90. Samardzija M, Wenzel A, Aufenberg S, Thiersch T, Remé C, Grimm C. Differential role of Jak-STAT signaling in retinal degenerations. *FASEB J.* 2006;20:2411–2413.
91. Lee DK, Carrasco J, Hidalgo J, Andrews GK. Identification of a signal transducer and activator of transcription (STAT) binding site in the mouse metallothionein-I promoter involved in interleukin-6-induced gene expression. *Biochem J.* 1999;337:59–65.
92. Penkowa M, Giralt M, Lago N, et al. Astrocyte-targeted expression of IL-6 protects the CNS against a focal brain injury. *Exp Neurol.* 2003;181:130–148.
93. Holtkamp GM, Kijlstra A, Peek R, de Vos AF. Retinal pigment epithelium-immune system interactions: cytokine production and cytokine-induced changes. *Prog Retin Eye Res.* 2001;20:29–48.
94. Langmann T. Microglia activation in retinal degeneration. *J Leukoc Biol.* 2007;81:1345–1351.

4.4 Sialoadhesin expression in intact degenerating retinas and following transplantation

Invest Ophthalmol Vis Sci. 2008 Dec;49(12):5602-10.

Summary

There is increasing evidence that the immune system is implicated in the pathogenesis and progression of retinal diseases such as age-related macular degeneration (AMD), glaucoma and diabetic retinopathy (Hageman et al., 2005)(Joussen et al., 2004). It is still unknown whether or not immune responses contribute to the progression of retinal cell loss in Retinitis Pigmentosa, but it is very likely that they have an effect on the outcome of cell-based therapies. Sialoadhesin, a macrophage-restricted cell adhesion molecule, has been shown to support immunoregulating functions influencing T-cell behavior in a pro-inflammatory manner (Wu et al., 2009), and participates in the recognition and discrimination of pathogens versus 'self' (reviewed in Klaas and Crocker, 2012). It is usually expressed in secondary lymphatic tissues. Although normally not present in the central nervous system, retinal microglia/macrophages were found to express sialoadhesin in the course of the disease in the retinal degeneration slow (*rds*) mouse (Hughes et al., 2003), suggesting a breakdown of the blood-retina barrier. In chapter 4.4, the expression of sialoadhesin was examined in the *rd1* mouse, an established model for human Retinitis Pigmentosa, as well as after subretinal transplantation of neonatal retinal tissue.

During the course of the retinal degeneration in *rds* and *rd1* mice, microglia that were positive for the microglia marker protein CD11b invaded the outer nuclear layer. Still, no sialoadhesin expression was detected at any time point. However, after transplantation of neonatal retinal cells, derived from PN2 GFP mice, to both, normal and degenerating (*rd1*) eyes, sialoadhesin positive cells could be observed within the graft, at the graft-host interphase and in the subretinal space. Due to the size and the anatomy of the mouse eye, the graft needed to be delivered through the sclera, which could disrupt the cellular and molecular base of the immune-privilege normally observed in mouse eyes (Al-Amro et al., 1999; Jiang et al., 1993; Lund et al., 2003). It is thus not absolutely certain whether the expression of sialoadhesin is a reaction to the transplant or to the combination of the transplant with tissue damage. Since most sialoadhesin positive cells were not GFP positive, they most likely derived from the host. Even if sialoadhesin-mediated immune responses do not seem to participate in the disease progression in *rd1* and *rds* mice, the occurrence of its expression could be of significance for the integration and long-term survival of retinal grafts.

Sialoadhesin Expression in Intact Degenerating Retinas and Following Transplantation

Javier Sancho-Pelluz,[1,2,3] *Kirsten A. Wunderlich,*[1] *Uwe Rauch,*[4] *F. Javier Romero,*[2] *Theo van Veen,*[1,3] *G. Astrid Limb,*[5,6] *Paul R. Crocker,*[7] *and Maria-Thereza Perez*[1,8]

Purpose. Resident microglial cells normally do not express sialoadhesin (Sn; a sialic acid–binding receptor), whereas recruited inflammatory macrophages have been shown to do so. The expression of Sn was examined in the course of photoreceptor cell degeneration and after transplantation.

Methods. Sn expression was analyzed in retinas of *rd1* and *rds* mice. For transplantation studies, neonatal (P2) retinal cells derived from GFP mice were injected intraocularly in adult *rd1* mice and control mice. Antibodies recognizing different Sn epitopes, CD11b, and MHC-II were used to identify activated microglial cells in intact retinas and 21 days after transplantation.

Results. In *rd1* mice, a few CD11b-positive cells were observed in the outer nuclear layer in the central retina at postnatal day (P)11 and in increasing numbers between P12 to P21. In *rds* mice, CD11b-expressing cells were found from P16 onward. No Sn-expressing cells were observed within the *rd1* or *rds* mouse retinas at any of the ages examined (up to P150). Specific staining was observed only in cells found in the vitreous margin of the retina and in surrounding tissues (sclera, cornea, ciliary body, choroid). After transplantation to normal and *rd1* mice, a variable number of Sn-positive cells were detected within the grafts, in the graft–host interface, and in the subretinal space.

Conclusions. The significant activation of microglia/macrophages observed in the various stages of degeneration in *rd1* and *rds* mouse retinas is not accompanied by Sn expression. However, Sn-expressing cells are observed after transplantation. The occurrence of such cells could be of significance for the integration and long-term survival of retinal grafts, as the expression of Sn could facilitate other phagocytic receptors.

(*Invest Ophthalmol Vis Sci.* 2008;49:5602–5610) DOI:10.1167/iovs.08-2117

Retinitis pigmentosa (RP) is a genetically and phenotypically heterogeneous family of inherited blinding diseases, with a prevalence of 1:3500 to 1:4000.[1,2] It develops as a result of defects in genes responsible for the structural and/or functional integrity of photoreceptor cells (http://www.sph.uth.tmc.edu/Retnet/ RetNet is provided in the public domain by the University of Texas Houston Health Science Center, Houston, TX). The progressive loss of these cells leads to characteristic alterations, such as a reduced ability to dark adapt (night blindness), gradual constriction of the visual field (tunnel vision), accumulation of intraretinal pigment deposits, and eventually loss of central vision.[3]

Earlier studies have established that the primary rod photoreceptor cell loss, observed in most forms of RP, occurs by apoptosis,[4–6] although it appears, at least in some cases, to involve activation of effectors other than caspases.[7] A fundamental question is why cone photoreceptor cells invariably degenerate when mutations occur in rod-specific genes. A lack of rods is likely to lead not only to a lack of rod-derived structural and paracrine support,[8–10] but also to alterations in, for example, retinal oxygen metabolism, as well as to disruption of glutamate and calcium homeostasis, which also affects the rest of the retina.[7,11–13] Accordingly, numerous reports have shown that secondary pathologic changes, such as reactive gliosis, neuronal remodeling, retinal pigment epithelium (RPE) cell proliferation and migration, vascular attenuation, and neovascularization, occur in retinas of several RP animal models and in patients.[11,14–16] It is therefore important to consider that responses elicited in the other retinal cells (neuronal and nonneuronal) are very likely to affect the progression of the disease and ultimately also the outcome of potential treatments.

There is strong evidence that the immune system may play a central role in the pathogenesis of another group of photoreceptor degenerative diseases, age-related macular degeneration (AMD).[17] Several studies have implicated inflammation and immune system activation in the progression of retinal cell loss in other prevalent ocular diseases, as well, such as diabetic retinopathy and glaucoma.[18–21] Although whether inflammation and other immune responses contribute to the progression of photoreceptor cell loss in human retinitis pigmentosa and animal models is still unresolved, it is likely that they play a role in the outcome of cell-based therapies designed to treat photoreceptor degeneration. Several studies have explored the use of various cell types (e.g., neuroretinal cells, retinal pigment epithelial cells, brain and retinal precursors, and Schwann cells) in retinal transplantation approaches aimed at slowing down the progression of the degenerative process or reconstructing the degenerating retina.[22–26] Although intraocular grafts are seen to thrive for relatively long periods, it is clear that host immune responses are triggered,[27–29] ultimately limiting the survival and function of the grafts.

Sialoadhesin (Sn), also known as CD169 or Siglec-1, is the prototypic member of the Siglec (sialic acid binding Ig-like

From the [1]Department of Ophthalmology and [4]Vessel Wall Biology Group, Lund University, Lund, Sweden; the [2]Fundación Oftalmológica del Mediterráneo (FOM) and Universidad Cardenal Herrera-CEU, Valencia, Spain; [3]Experimental Ophthalmology, University Eye Hospital, Tübingen, Germany; the Divisions of [5]Pathology and [6]Cell Biology, UCL Institute of Ophthalmology, London, United Kingdom; the [7]Wellcome Trust Biocentre, University of Dundee, Dundee, United Kingdom; and the [8]Department of Ophthalmology, University of Copenhagen, Glostrup Hospital, Glostrup, Denmark.

Supported by European Union Grant LSHG-CT-2005-512036 and MEST-CT-2005-020235; The Foundation Fighting Blindness; Swedish Medical Research Council Grant MTP12209; Crown Princess Margareta's Committee for the Blind; Stiftelse för Synskadade i f.d. Malmöhus Län; Crafoordska Stiftelsen; and Thorsten och Elsa Segerfalks Stiftelse.

Submitted for publication April 2, 2008; revised June 1, 2008; accepted October 22, 2008.

Disclosure: **J. Sancho-Pelluz**, None; **K.A. Wunderlich**, None; **U. Rauch**, None; **F.J. Romero**, None; **T. van Veen**, None; **G.A. Limb**, None; **P.R. Crocker**, None; **M.-T. Perez**, None

The publication costs of this article were defrayed in part by page charge payment. This article must therefore be marked "*advertisement*" in accordance with 18 U.S.C. §1734 solely to indicate this fact.

Corresponding author: Maria-Thereza Perez, Department of Ophthalmology, Lund University, BMC B13, S-221 84, Lund, Sweden; maria_thereza.perez@med.lu.se.

lectin) family of cellular interaction molecules. Sn is a cell surface adhesion receptor that binds preferentially to a particular subpopulation of sialic acids, negatively charged carbohydrate residues that are found on the cell surfaces and glycoproteins.[30–32] It is constitutively expressed at high levels by subsets of macrophages, for example, in the perifollicular zones of lymphoid tissues and in the inner marginal zone of the spleen, but can be expressed also by inflammatory macrophages, promoting their adhesion to T cells, to neutrophils, or to other activated macrophages.[33] It has been shown to be expressed by macrophages in the eye after experimental autoimmune uveoretinitis and to contribute to the inflammatory response elicited in this model.[34,35] It has also been reported to be expressed in retinal microglia/macrophages in a model of photoreceptor degeneration, the retina degeneration slow (*rds*) mouse.[36]

The present studies were conducted with the purpose of examining the distribution of Sn in the *rd1* mouse model of human RP,[37,38] a model extensively used to elucidate the mechanisms of photoreceptor cell death, and after transplantation of retinal cells in this same model. Sn expression was examined with several monoclonal antibodies recognizing the different epitopes of Sn.

Materials and Methods

Animals

The experiments were conducted with the approval of the local animal experimentation and ethics committee. Animals were handled according to the guidelines on care and use of experimental animals set forth by the Government Committee on Animal Experimentation at the University of Lund and the ARVO Statement for the Use of Animals in Ophthalmic and Vision Research.

Retinal degeneration 1 (*rd1*), *rds*, and corresponding control wild-type (wt) mice were used for studies on the expression of retinal CD11b, Sn, and MHC. Animals were bred on a homozygous background (*rd1:* C3H/HeA or C57BL6/129; *rds*: C3H/HeA; and wt: C3H/HeA or C57BL6/129; own colonies), and maintained on a 12-hour light-dark cycle, with free access to food and water. They were killed with carbon dioxide at different ages (*rd1:* postnatal days (P)7–P150, $n = 24$; *rds:* P8–P30, $n = 16$; and wt: P11–P150, $n = 8$). Eyes were thereafter quickly enucleated and immersed in a solution of 4% paraformaldehyde (PFA) in Sørensen's buffer (pH 7.4) for 2 hours at 4°C. The tissue was subsequently rinsed, cryoprotected in the same buffer containing increasing concentrations of sucrose, embedded in an albumin-gelatin medium, frozen, and stored at −20°C. The sections were obtained on a cryostat (12 μm), collected on gelatin/chrome alum-coated glass slides, air-dried, and stored at −20°C until further processing. Some eyes from all groups were enucleated, quickly frozen without prior fixation ($n = 8$), and stored at −80°C. Retinas from wild-type control mice were also dissected from the pigment epithelium under cold Sørensen's buffer and transferred to a 3-μm pore filter (Millipore AB, Solna, Sweden) with the photoreceptor side down. The attached flattened retinas were fixed for 5 minutes with 4% PFA and rinsed thereafter with Sørensen's buffer.

Transplantation

For the transplantation studies, neonatal (P2) retinal tissue derived from transgenic mice expressing green fluorescent protein (GFP, C57BL6) was injected intraocularly in adult (P55 to P70) *rd1* mice and in wild-type control animals (C57BL6/129), as previously described.[39–40] Briefly, the eyes were enucleated from GFP mouse pups and the neural retinas carefully dissected (without RPE or the optic nerve head region). The retinal pieces were kept for up to 20 minutes in Ames' medium (Sigma-Aldrich, St. Louis, MO) at 4°C until transplanted. The recipients were anesthetized with an intraperitoneal injection of xylazine (100 mg/kg; Rompun; Bayer AG, Göteborg, Sweden) and ketamine (100 mg/kg; Ketalar; Parke, Davis & Co., Morris Plains, NJ) and locally anesthetized with 1% amethocaine hydrochloride. Donor tissue was drawn into a plastic (polyethylene) pipette tip (GELoader Tip, Eppendorf, Hamburg, Germany) connected to a precision microsyringe, and injected (1.0 μL total volume) through the sclera into the superior subretinal or epiretinal space of recipients. Twenty-one days after transplantation, the recipients were killed with carbon dioxide and the surgically altered eyes (*rd1*, $n = 7$; wt, $n = 8$) were enucleated and processed as just described. A group of animals received a subretinal injection of 1.0 μL of Ames' medium alone (sham surgery; *rd1*, $n = 3$; wt, $n = 4$). No immunosuppression was used.

Immunohistochemistry

Retinal sections were thawed and air dried before preincubation for 60 to 90 minutes at room temperature in Tris-buffered saline (TBS; pH 7.2) containing 0.25% Triton X-100 (TBS-T), 1% bovine serum albumin (BSA), 50% fetal bovine serum, and 20% normal serum (goat or rabbit). Immunohistochemistry was performed overnight at 4°C, with rat anti-mouse monoclonal antibodies (Abs) that recognize different Sn epitopes: CD169 (four different batches of clone 3D6.112; 1:75; Serotec, Oxford, UK) and SER-4 (1:20; provided by author PRC).[41] MOMA-1 (rat anti-mouse metallophilic macrophage antibody), which has been recently shown to recognize Sn[42] was also used (1:75; BMA Biomedical, Augst, Switzerland). To identify microglia/macrophages, CD11b (monoclonal rat anti-mouse; 1:75; R&D Systems, Abingdon, UK) was used. In addition, a rat anti-mouse I-A/I-E monoclonal antibody (clone M5/114.15.2; Alexa Fluor 647–conjugated; 1:100; BioLegend, San Diego, CA) was used to detect major histocompatibility complex (MHC)-II–expressing cells. All primary antibodies were diluted in TBS-T containing 5% goat or donkey normal serum. The tissue was subsequently rinsed and incubated for 90 minutes with one of the following secondary antibodies: Alexa 594 goat anti-rat, Alexa 488 goat anti-rat (1:200; Invitrogen-Molecular Probes, Leiden, The Netherlands), Texas-red donkey anti-rat (1:200; Jackson ImmunoResearch Laboratories, West Grove, PA), or biotinylated rabbit anti-rat IgG (H+L, 1:200; Vector Laboratories, Burlingame, CA), followed by anti-biotin streptoavidin-cy3 (1:400; Jackson ImmunoResearch Laboratories). The sections were rinsed and mounted (Vectashield; Vector Laboratories). Flat-mounted retinas were processed in a similar manner, except that incubation with the primary antibody was performed for 48 hours at 4°C.

In addition to testing different antibodies recognizing Sn, a series of further control experiments were performed by including the following: (1) sections obtained from the spleen of adult normal mice (C3H and C56BL6/129; $n = 2$). Pieces of the spleens were either fixed, cryoprotected, and sectioned as described earlier ($n = 2$) or frozen without prior fixation ($n = 2$); (2) eyes and spleens from Sn-deficient mice[42] (C56BL6; $n = 2$); (3) sections from fresh-frozen retinas ($n = 9$). The sections were thawed, air-dried, fixed in cold acetone for 10 minutes, rinsed and further processed for immunohistochemistry. Immunodetection was also performed with the avidin-biotin complex (ABC) method. Retinal sections were incubated with the primary antibodies as described earlier, followed by a biotinylated rabbit anti-rat secondary antibody (1:75; Vector Laboratories) for 45 minutes. Staining was performed using ABC and diaminobenzidine (DAB) substrate kits (Vectastain ABC Elite; Vector Laboratories), according to the manufacturer's protocol ($n = 3$). Sections were washed, dehydrated, and mounted. An additional control was also performed by omitting the primary antibody and incubating ocular and spleen sections with secondary antibodies alone. Epifluorescence and confocal microscopes were used to examine the sections (Carl Zeiss Meditec, Inc., Oberkochen, Germany). Images were captured with digital cameras and software (Axiovision 4.2 and LSM5 Pascal, respectively; Carl Zeiss Meditec). Image-analysis software (Photoshop; Adobe, San Jose, CA) was used for contrast and brightness adjustment of images.

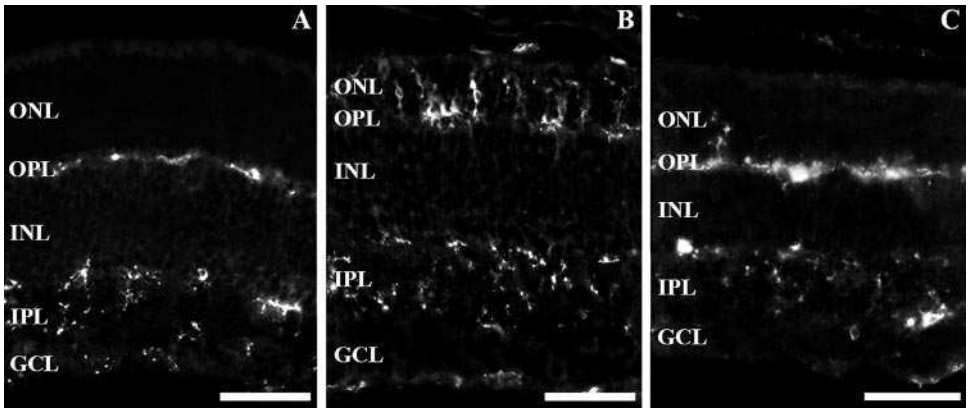

FIGURE 1. CD11b expression. (**A**) Wild-type control mouse retina at P13: labeled cells were seen in the inner retina over the IPL and at the level of the OPL. (**B**) *Rd1* mouse retina at P14: numerous labeled cells were also seen in the ONL and in the subretinal space. (**C**) *Rds* mouse retina at P21: CD11b-positive cells were seen in the inner retina, in the OPL, and in small numbers in the ONL. Scale bars, 50 μm.

RESULTS

Microglial Cell Activation in Intact Retinas

In wild-type control mice, CD11b-positive cells were found mostly in the inner retina, over the inner plexiform (IPL) and ganglion cell (GCL) layers, and at the level of the outer plexiform layer (OPL). The labeled cells exhibited a typical ramified morphology and were observed in both the central and the peripheral retina (Fig. 1A). The morphology and localization of these CD11b-expressing cells indicate that they correspond to microglial cells.

In the *rd1* mouse retina, a large number of labeled cells were also noted in the outer nuclear layer (ONL; Fig. 1B). The first cells were observed in this layer at postnatal day (P11) in the central areas of the retina, but were seen in the whole retina as early as P17 to P18. From P21 onward, when the ONL consists of only about one cell row, it was no longer possible to determine the exact localization of the labeled cells in the outer retina. Most labeled cells were then observed in the OPL and occasionally also in the subretinal space. The same distribution of CD11b-positive cells was seen in all *rd1* mouse retinas, irrespective of the strain examined (C3H/HeA or C57Bl6/129). In the *rds* mouse retina, a few CD11b-positive cells were also observed over the ONL both in the central and peripheral retina from P16 onward (Fig. 1C).

Sn in Intact Retinas

In this study, it was essential to verify the specificity of the Sn-recognizing antibodies, and this was accomplished with several assays. Staining of spleen sections obtained from normal animals revealed the presence of immunoreactive macrophages in the inner marginal zone with all batches of anti-CD169 antibodies examined (Fig. 2A), whereas no specific staining was observed with any of the batches in Sn-deficient mice (Fig. 2B). The same was observed after staining with MOMA-1 (Fig. 2C) and SER-4 (Fig. 2D). No labeling was noted in the ocular tissues of Sn-deficient animals with two of the batches of anti-CD169 tested (hereafter referred to as CD169-specific; Fig. 2E), whereas staining with the two other batches resulted in labeling of some cells in the peripheral retina and choroid (Fig. 2F) and within the degenerating retina (see below). These batches of anti-CD169 are hereafter referred to as nonspecific. The observations were consistent whether using unfixed or fixed spleen and ocular tissues and irrespective of the detection method used.

With the specific CD-169 antibodies, no labeled cells were observed in the retina of wild-type control mice at any of the examined ages (Figs. 3A, 3B). Labeled cells were, however, observed in the ciliary body (Figs. 3C, 3D), in the sclera (Fig. 3E), and between the lens and the retina. Many of the latter appeared to adhere to the vitreous–retinal surface (Fig. 3A). In Sn-deficient mice, no labeled cells were noted in these ocular tissues when the specific CD169 antibodies were used (Fig.

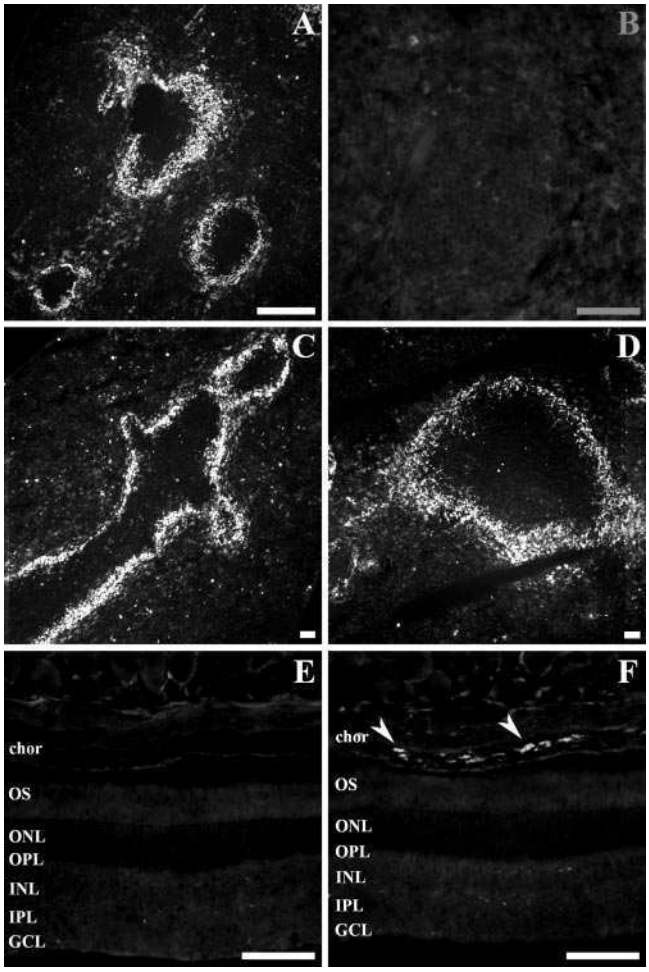

FIGURE 2. Sn expression in the spleen and retina with different antibodies. (**A**) Wild-type mouse spleen: characteristic localization of CD169-labeled macrophages in the marginal zone with all antibodies tested. (**B**) No specific signal was observed in the spleen of Sn-deficient mice. (**C**, **D**) The same distribution of labeled macrophages was seen in the spleen of wild-type mice with MOMA-1 (**C**) and SER-4 (**D**). (**E**) No labeling was observed in ocular tissues in Sn-deficient mice with CD-169 specific antibodies. (**F**) CD-169-positive cells (*arrowheads*) were seen in the choroid in Sn-deficient mice with the nonspecific antibodies. chor, choroid; OS, outer segments. Scale bars, 50 μm.

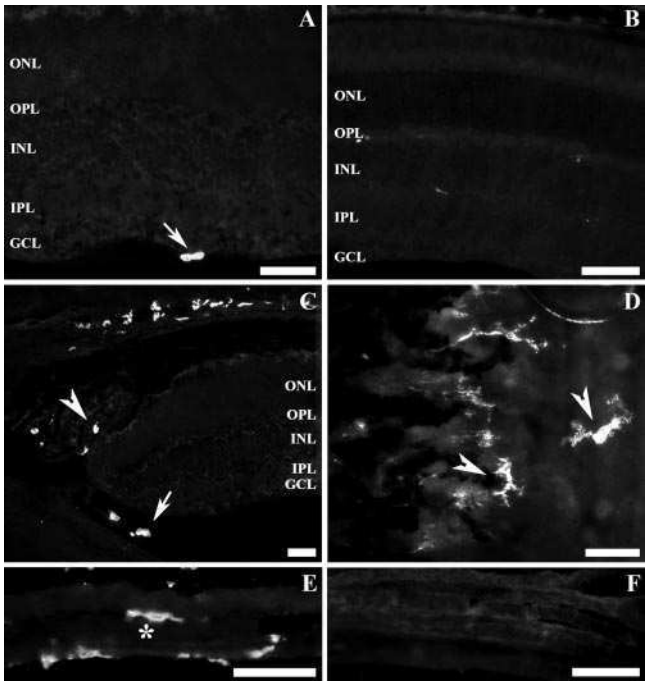

FIGURE 3. Sn expression in the eye detected by specific CD169 antibodies. (**A**, **B**) Wild-type mouse retina at P13 (**A**) and P150 (**B**): staining was not observed within the retina, with occasional labeled cells seen only along the vitreous margin of the retina (*arrow*). (**C–E**) CD169-positive cells are observed in wild-type animals also in the ciliary body and retinal margin (*arrowheads*), in the intravitreous space (*arrow*), and in the sclera (✻). No specific labeling was observed in the sclera of Sn-deficient animals (**F**). The image in (**D**) was taken from a flat-mounted retina. Scale bars, 50 μm.

3F). These antibodies and MOMA-1 and SER-4 antibodies also produced no signal in *rd1* or *rds* mouse degenerating retinas at any of the ages examined (Figs. 4B–J) and detected only occasional cells in the other ocular tissues (Figs. 4D, 4G, 4J).

With the nonspecific CD169 antibody batches, however, several stained cells were noted over the ONL and in the subretinal space in *rd1* mice (Fig. 4A) and in *rds* mice (not shown).

Sn after Transplantation

After subretinal transplantation in wild-type control mice, GFP-positive cells were noted within the ONL, where many of them assumed the position and morphology of photoreceptor cells (Figs. 5A, 6B). Little or no migration of graft cells was noted in transplantation to *rd1* mice (Figs. 5C, 5E, 5G, 5I, 5K).

Transplantation resulted in a variable number of Sn expressing cells within the grafts and at the graft-host interface, both in transplantation into wild-type (Fig. 5B) and *rd1* mice (Figs. 5D, 5F). In addition, labeled cells were found in the subretinal space in the vicinity of the grafts, even after intravitreous grafting (Figs. 5F, 5H). The same observations were made with the specific CD169 antibodies, MOMA-1, and Ser-4. The extent of the detachment produced in the host retina by the surgery and the size of the grafts varied considerably between the different specimens, precluding a reliable quantitative analysis. However, there was no indication that the number of Sn-expressing cells was higher in transplantation into *rd1* mice than in transplantation into wild-type mice.

MHC-II Expression

No MHC-II-labeled cells were detected within the retina of unoperated, normal or *rd1* mice. However, a highly variable number of MHC-II-expressing cells were observed in both

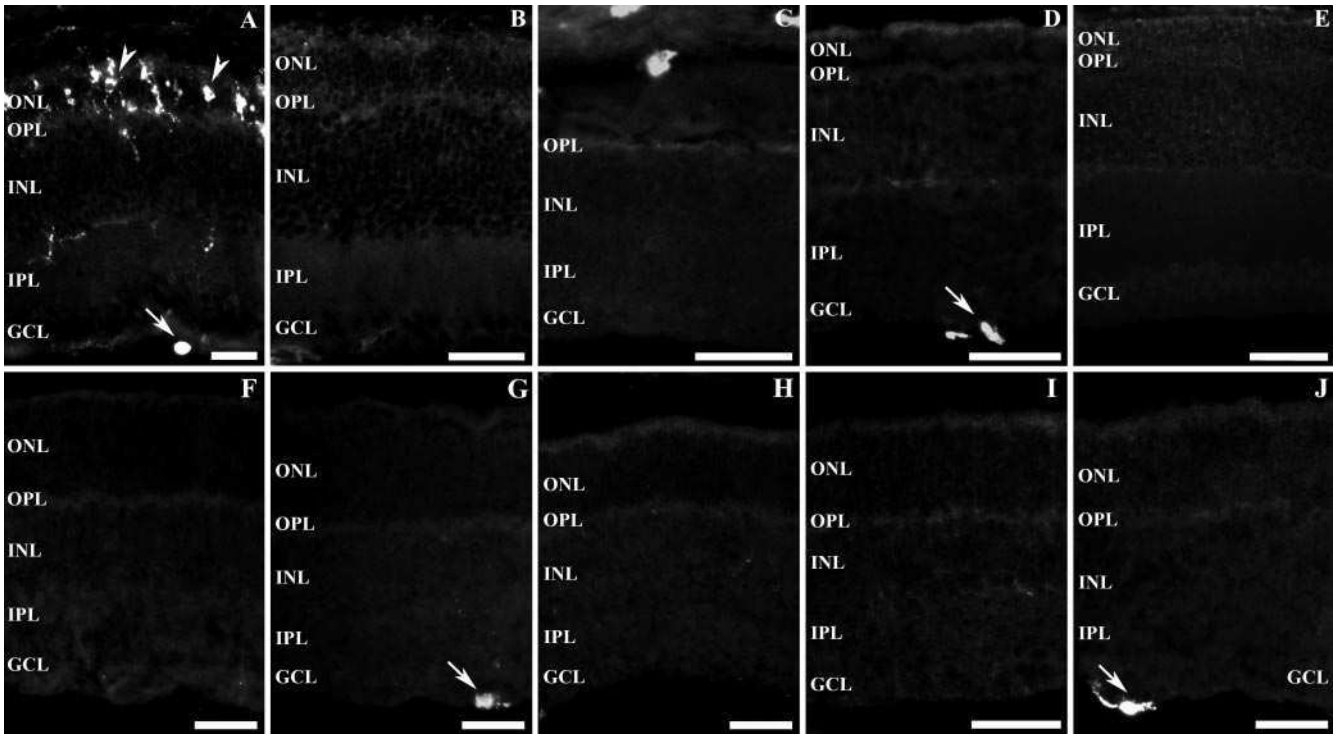

FIGURE 4. Sn expression in the retina of *rd1* (**A–E**) and *rds* (**F–J**) mouse retinas. (**A**) A large number of stained cells (*arrowheads*) over the ONL in *rd1* mouse retina at P14 detected by a nonspecific CD169 antibody. No staining was observed within the retina with specific antibodies at P14 (**B**; CD169), P150 (**C**, CD169), P15 (**D**, MOMA-1), or P15 (**E**, Ser-4). The same was observed in *rds* mouse retinas with specific CD169 antibodies: P8 (**F**), P16 (**G**), P18 (**H**), P21 (**I**), and P30 (**J**). A few cells found next to the vitreous margin of the retina were labeled with all antibodies (**A**, **D**, **G**, **J**, *arrows*). Scale bars, 50 μm.

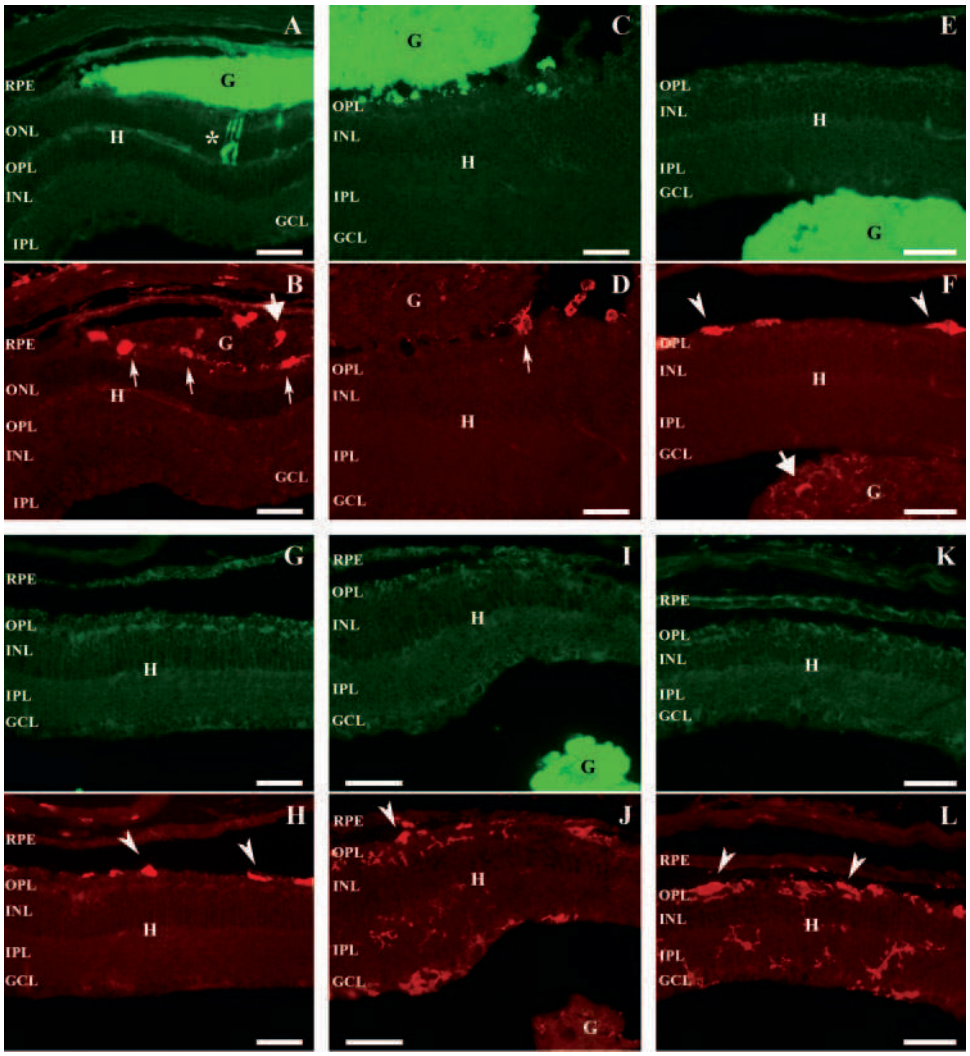

FIGURE 5. Transplantation to normal (**A**, **B**) and *rd1* mice (**C**–**L**). Subretinal (**A**–**D**) and epiretinal (**E**, **F**, **I**, **J**) grafts (G) are shown: (**A**) GFP-expressing cells were observed within the ONL of the host (H) wild-type mouse retina (✻). (**B, D, F, H**) Sn-expressing cells were seen in the graft–host interface (**B**, **D**, *arrows*) and within the grafts (**B**, **F**, *short arrows*). Labeled cells (*arrowheads*) were also found in the subretinal space near (**F**) and away (**H**) from the grafts. (**J**, **L**). The localization of CD11b-positive cells within the host retina and in the subretinal space (*arrowheads*) near an epiretinal graft (**I**, **J**) and away from a subretinal graft (**K**, **L**). Scale bars, 50 μm.

groups after transplantation. Positive cells were mostly found within the grafts and in the graft–host interface (Figs. 6A, 6C), but were occasionally observed also in the subretinal space. In three cases (of nine), a large number of labeled dendriform cells were seen near the host ciliary body (Figs. 6D, 6F). These cells were observed after transplantation in both *rd1* ($n = 2$) and wild-type ($n = 1$) mice. As observed with Sn, most MHC-II-positive cells did not coexpress GFP (Figs. 6C, 6F), suggesting that some of them should be of host origin. No Sn or MHC-II expression was noted within the retina or subretinal space in sham-surgery animals (wild type and *rd1* mice; not shown).

DISCUSSION

The present study confirms previous reports showing microglial cell activation in different models of photoreceptor degeneration.[43–49] CD11b-positive cells were visible in the ONL in *rd1* and *rds* mouse retinas in the early stages of degeneration, which corresponds to observations made using this and other markers.[36,47–50]

Sn and Degenerating Retinas

Sn is expressed by activated microglia and macrophages within the parenchyma in brain tissue only after exposure to plasma proteins, which occurs as a consequence of damage to the blood–brain barrier.[51] In experimental autoimmune uveoretinitis (EAU), a marked increase in the number of Sn-expressing cells has been observed in the retina and in other inflammatory areas in the eye.[34,35] It was found in this model that Sn-expressing cells constitute a subset of activated macrophages that do not coexpress CD11b or MHC class II, and it was suggested that they are not involved in antigen presentation, but correspond rather to phagocytic macrophages.

A slow, but constant migration of blood-borne monocytes into the retina has been shown to occur even under physiological conditions.[52] In addition, changes associated with the vasculature, such as vascular attenuation and neovascularization, and blood–retina barrier breakdown are observed in the course of photoreceptor degeneration in several animal models and in patients.[14,15,53–55] Such changes are generally considered to be relatively late events, although we have also detected an alteration of the matrix composition surrounding the intraretinal vessels in another model of photoreceptor degeneration, the Royal College of Surgeons (RCS) rat, at a very early stage of degeneration.[56] In the *rd1* mouse retina, increased levels of monocyte chemoattractant protein (MCP)-1, MCP-3, macrophage inflammatory protein (MIP)-1α, MIP-1β, regulated on activation normal *t*-cell expressed and **s**ecreted (RANTES), and TNF-α have been detected as photoreceptor cell loss progresses.[48,57,58] The expression of aquaporin-4, essential for the maturation and maintenance of the blood–brain barrier,[59]

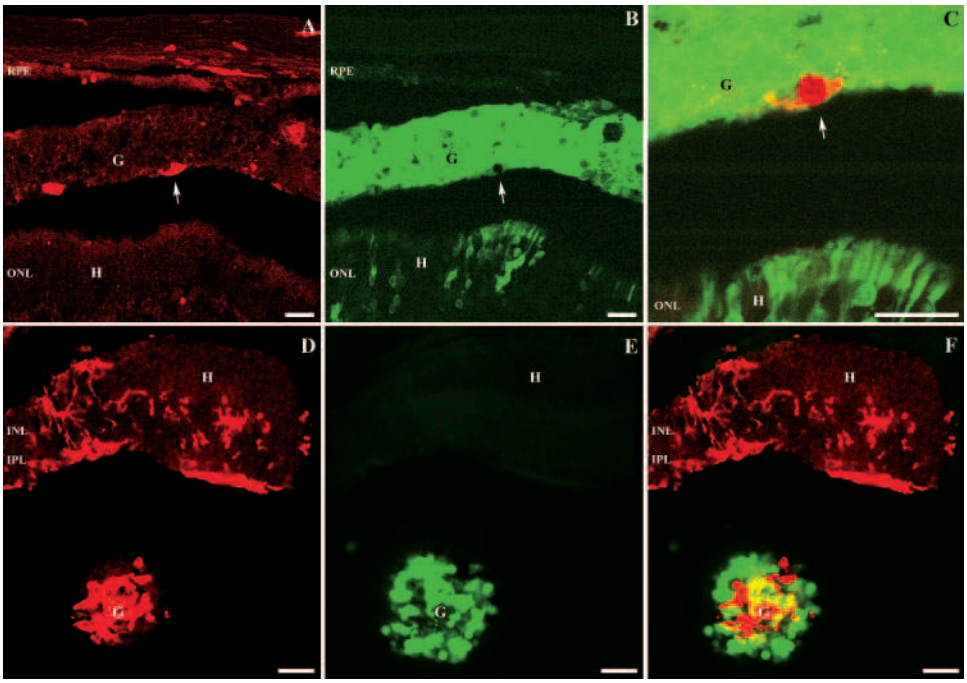

FIGURE 6. Transplantation in normal (**A–C**) and *rd1* mice (**D–F**). Subretinal (**A–C**) and epiretinal (**D–F**) grafts (G) are shown: (**A**) MHC-II-expressing cells were seen in the graft–host interface (*arrow*) and within the graft. (**C**) Merged image, showing in higher magnification the GFP-expressing cells seen in (**B**), within the graft and within the ONL of the host retina (H), and a cell expressing MHC-II (*red, arrow*). A large number of MHC-expressing cells were seen in the host *rd1* mouse retina (**D**), exhibiting a dendritic shape. Numerous MHC-II-positive cells (also GFP-negative) were observed within the epiretinal graft (**D–F**). Scale bars, 20 μm.

is also elevated in older *rd1* mouse retinas.[58] It is therefore reasonable to assume that activated blood-borne macrophages may be recruited in the process of photoreceptor cell loss, at least in some types of degeneration.

Yet, our results showed that no Sn expression could be observed in the *rd1* mouse retina in areas of microglial activation at any stage of the degeneration (0–7 weeks old) or at 5 months of age, when significant vascular alterations are normally observed.[15] It was also not possible to confirm the observations made previously in *rds* mouse retinas.[36]

The observations made in the present study were obtained with antibodies recognizing different Sn epitopes: clone 3D6.112 (four batches available through Serotec), SER-4, and MOMA-1. Two batches of 3D6.112 produced distinct labeling of microglia/macrophages over the ONL in *rd1* mice and of occasional cells in the subretinal space in *rds* mouse retinas. On the other hand, none of the remaining four batches of monoclonal antibodies was seen to produce a specific signal in the retina of any of these animals. The *rds* mice examined in the previous study[36] were on a different genetic background (CBA). However, the possibility that strain differences or method of tissue fixation account for the lack of signal in retinal macrophages in *rd1* and *rds* mouse retinas in the present study appears unlikely. Specific signal was obtained in the present study with the four remaining antibody preparations in spleens of all mice tested irrespective of the strain or method of fixation and was absent in spleens and eyes of Sn-deficient mice.

Using the specific antibodies, signal was detected in the present study in subpopulations of macrophages located in other ocular tissues, as previously found in different mouse strains.[34,60,61] Sn-positive cells exhibiting an elongated or spherical shape were also observed near the optic nerve head and scattered in the vitreous cavity, sometimes next to the inner surface of the retina. In addition, labeling was seen in some large cells with irregular shape in the retinal margin, next to and within the ciliary body. Many, if not all of these cells found in the vitreous and in association with the ciliary body are likely to correspond to hyalocytes, which also belong to the monocyte/macrophage lineage.[62,63]

Retinal Transplantation

The transplantation model used in the present study is well established and has been used in studies on graft–host integration.[39,64] Limited graft–host integration was observed, with only a few cells and fibers bridging the graft–host interface, also confirming previous observations.[39,40] After subretinal transplantation to normal animals, most of the cells that migrated into the host retina assumed the morphology and position of photoreceptor cells. This observation agrees with what has been recently shown in transplantation of dissociated retinal cells obtained from GFP donor mice of the same age as used in the present study.[24] A certain degree of graft–host integration was also observed after subretinal transplantation in *rd1* mice and in epiretinal transplantation in both wild-type and *rd1* mice. In *rd1* mice, most host photoreceptors had degenerated at the time of transplantation, reducing the ONL to a thin layer of sporadic cones. Cells with typical photoreceptor morphology were no longer identifiable, and integrated cells were occasionally seen in the inner host layers (not shown).

Sn and Retinal Transplantation

A highly variable number of Sn-positive cells were observed after intraocular grafting of retinal cells in both wild-type and *rd1* mice. Overall, only a relatively small number of labeled cells were seen after transplantation, and these were most often seen in the graft–host interface and in the subretinal space in the vicinity of the grafts, indicating that Sn induction was a localized response. In transplantation to the *rd1* mice, which was performed on adult animals, one would have expected elevated levels of at least some immune-related genes to be present at the time of transplantation, due to the ongoing degeneration. Induction of Sn was not observed during the process of photoreceptor degeneration as such (the present study), which may explain why we could not detect any obvious differences between transplantation to normal and *rd1* mice.

The subretinal and epiretinal spaces have been considered to be immune privileged sites, although this appears not to be

absolute.[65,66] An intrinsic problem associated with sub- and epiretinal transplantation in rodents stems from the fact that grafts need to be delivered through the sclera due to the size and anatomy of the rodent eye. It has been argued that this transscleral approach may disrupt the cellular and molecular bases of immune privilege.[66,67] Furthermore, subretinal transplantation induces a localized, permanent detachment of the host retina, a condition that has been shown to lead to microglial activation and to increased levels of several cytokines and chemokines.[19,68] We observed an increase in the number of Sn-positive cells after transplantation of tissue, but not after sham operations. It is not possible to determine in transplantation to the mouse eye, whether Sn expression would have been triggered without the damage to the choroid and associated structures. It is clear, however, that the surgical trauma alone is not sufficient to elicit expression of Sn, as it was observed only in specimens containing a graft. The latter (perhaps in conjunction with the trauma) is in some way capable of triggering or exacerbating a localized immune response.

Allogeneic neuroretinal transplants can survive for several months without immunosuppression.[69,70] However, upregulation of MHC class II expression on donor microglial cells[27,28] and induction of potent T-cell responses to donor antigens[29] have been observed. We observed MHC-II expression on transplantation, but neither after sham surgery nor within the intact retinas of wild-type and *rd1* mice. It was not possible to establish the origin of all the MHC-II-expressing cells found within the grafts (subretinal or epiretinal), but those found in the subretinal space did not coexpress GFP, indicating that they are most likely derived from the host. The same was observed for Sn-expressing cells.

The donor neuroretina, even if derived from neonatal stages, is considered to be an only partially immune privileged tissue.[27,71] A small population of dendritic cells constitutively expressing MHC class II has been observed in normal, intact mice in the retinal margin and in the juxtapapillary region.[72] Strain differences were noted, but these cells were clearly identifiable in C57BL/6 mice. Such cells were not observed until 2 weeks of age,[72] and should thus not have been included in our donor tissue (obtained from 2-day-old C57BL/6 mice), unless the cells are present at P2 but only mature enough to express MHC II at approximately 2 weeks. Microglial cells are also observed in the normal mouse retina as early as embryonic day (E)11.5, and although their density is reduced after E18.5, a significant number of cells are found also in the neonatal retina.[73] Further, although attempts were made in the present study to dissect the donor neuroretina from the RPE, grafts may contain a small but variable number of these potential antigen-presenting cells. We can therefore not exclude the possibility that a fraction of MHC-II (and perhaps also some Sn)-positive cells were derived from the donor.

It should be noted also that in some specimens, in which the grafts were placed near the ciliary body, a very large number of MHC-II-positive cells of host origin were seen in the peripheral retina and within the graft itself. The proximity to the peripheral retina, where subpopulations of dendritic cells have been shown to express MHC-II even in normal retinas,[72] may have facilitated the infiltration of these cells into the host and the graft. These observations point to the fact that the level of expression of MHC-II, and possibly also that of Sn, is determined not only by the presence of a graft, but also by the position of the graft.

It was not determined in the present study whether and to what extent Sn and MHC-II were expressed in the same cells after transplantation. However, there seemed to be no direct correlation between the number of Sn- and MHC-II-expressing cells after retinal transplantation. Moreover, in a model of EAU, it was shown that MHC class II/Cd11b and Sn are in fact expressed in different subsets of activated macrophages.[34]

In conclusion, the present study showed that Sn is expressed by host-activated microglia/macrophages after retinal transplantation in the mouse. Cotransplantation of neonatal retinal cells with host-strain–derived immature dendritic cells, which can induce immune tolerance, was recently shown to lead to a lower number of activated $CD8^+$ T cells and to a better graft survival rate.[74] Thus, although allogeneic grafts are seen to thrive, expression of Sn (and of MHC-II) by donor- and host-derived macrophages potentially facilitate other phagocytic receptors, making the grafts susceptible to long-term immune responses. Whether transplantation-induced Sn expression occurs in other species and what implications it might have must be verified.

The study also shows that Sn is not expressed in *rd1* (or *rds*) mouse retinas and that its expression is also not significantly altered in the other ocular tissues in these models. It appears that cross-reactivity with an unknown protein may have produced the positive labeling observed with two of the batches of 3D6.112 tested in this study, which may also explain the results previously obtained in the *rds* mouse retina.[36] It has been shown in genetic studies that lack of functional B and T cells or of complement factor C1qα has no impact on the progression of photoreceptor cell loss in *rd1* mice, suggesting that the classic complement system of innate immunity and acquired immune responses may not be implicated.[75] Yet, these observations and the fact that Sn is not expressed in retinal macrophages in the two models studied should not be taken as definitive indication that immune-related events do not contribute to photoreceptor cell loss.

Acknowledgments

The authors thank Karin Arnér, Birgitta Klefbohm, and Hodan Abdalle for excellent technical support.

References

1. Kennan A, Aherne A, Humphries P. Light in retinitis pigmentosa. *Trends Genet.* 2005;21(2):103–110.
2. Daiger SP, Bowne SJ, Sullivan LS. Perspective on genes and mutations causing retinitis pigmentosa. *Arch Ophthalmol.* 2007;125(2):151–158.
3. Hartong DT, Berson EL, Dryja TP. Retinitis pigmentosa. *Lancet.* 2006;368(9549):1795–1809.
4. Chang GQ, Hao Y, Wong F. Apoptosis: final common pathway of photoreceptor death in rd, rds, and rhodopsin mutant mice. *Neuron.* 1993;11(4):595–605.
5. Portera-Cailliau C, Sung CH, Nathans J, Adler R. Apoptotic photoreceptor cell death in mouse models of retinitis pigmentosa. *Proc Natl Acad Sci U S A.* 1994;91:974–978.
6. Xu GZ, Li WW, Tso MO. Apoptosis in human retinal degenerations. *Trans Am Ophthalmol Soc.* 1996;94:411–430.
7. Sanges D, Comitato A, Tammaro R, Marigo V. Apoptosis in retinal degeneration involves cross-talk between apoptosis-inducing factor (AIF) and caspase-12 and is blocked by calpain inhibitors. *Proc Natl Acad Sci U S A.* 2006;103(46):17366–17371.
8. Huang PC, Gaitan AE, Hao Y, Petters RM, Wong F. Cellular interactions implicated in the mechanism of photoreceptor degeneration in transgenic mice expressing a mutant rhodopsin gene. *Proc Natl Acad Sci U S A.* 1993;90(18):8484–8488.
9. Adler R, Curcio C, Hicks D, Price D, Wong F. Cell death in ARMD. *Mol Vis.* 1999;5:31–42.
10. Sahel JA, Mohand-Said S, Leveillard T, Hicks D, Picaud S, Dreyfus H. Rod–cone interdependence: implications for therapy of photoreceptor cell diseases. *Prog Brain Res.* 2001;131:649–661.
11. Jones BW, Marc RE. Retinal remodeling during retinal degeneration. *Exp Eye Res.* 2005;81(2):123–137.
12. Delyfer MN, Forster V, Neveux N, Picaud S, Leveillard T, Sahel JA. Evidence for glutamate-mediated excitotoxic mechanisms during

photoreceptor degeneration in the rd1 mouse retina. *Mol Vis.* 2005;11:688–696.
13. Yu DY, Cringle SJ. Retinal degeneration and local oxygen metabolism. *Exp Eye Res.* 2005;80(6):745–751.
14. Milam AH, Li ZY, Fariss RN. Histopathology of the human retina in retinitis pigmentosa. *Prog Retin Eye Res.* 1998;17(2):175–205.
15. Wang S, Villegas-Perez MP, Vidal-Sanz M, Lund RD. Progressive optic axon dystrophy and vascular changes in rd mice. *Invest Ophthalmol Vis Sci.* 2000;41(2):537–545.
16. Bringmann A, Pannicke T, Grosche J, et al. Muller cells in the healthy and diseased retina. *Prog Retin Eye Res.* 2006;25(4):397–424.
17. Gehrs KM, Anderson DH, Johnson LV, Hageman GS. Age-related macular degeneration: emerging pathogenetic and therapeutic concepts. *Ann Med.* 2006;38(7):450–471.
18. Joussen AM, Poulaki V, Le ML, et al. A central role for inflammation in the pathogenesis of diabetic retinopathy. *FASEB J.* 2004;18(12):1450–1452.
19. Nakazawa T, Matsubara A, Noda K, et al. Characterization of cytokine responses to retinal detachment in rats. *Mol Vis.* 2006;12:867–878.
20. Tezel G, Yang X, Luo C, Peng Y, Sun SL, Sun D. Mechanisms of immune system activation in glaucoma: oxidative stress-stimulated antigen presentation by the retina and optic nerve head glia. *Invest Ophthalmol Vis Sci.* 2007;48(2):705–714.
21. Langmann T. Microglia activation in retinal degeneration. *J Leukoc Biol.* 2007;81(6):1345–1351.
22. Aramant RB, Seiler MJ. Progress in retinal sheet transplantation. *Prog Retin Eye Res.* 2004;23(5):475–494.
23. Limb GA, Daniels JT, Cambrey AD, et al. Current prospects for adult stem cell-based therapies in ocular repair and regeneration. *Curr Eye Res.* 2006;31(5):381–390.
24. MacLaren RE, Pearson RA, MacNeil A, et al. Retinal repair by transplantation of photoreceptor precursors. *Nature.* 2006;444(7116):203–207.
25. Canola K, Angénieux B, Tekaya M, et al. Retinal stem cells transplanted into models of late stages of retinitis pigmentosa preferentially adopt a glial or a retinal ganglion cell fate. *Invest Ophthalmol Vis Sci.* 2007;48(1):446–454.
26. McGill TJ, Lund RD, Douglas RM, et al. Syngeneic Schwann cell transplantation preserves vision in RCS rat without immunosuppression. *Invest Ophthalmol Vis Sci.* 2007;48(4):1906–1912.
27. Ma N, Streilein JW. Contribution of microglia as passenger leukocytes to the fate of intraocular neuronal retinal grafts. *Invest Ophthalmol Vis Sci.* 1998;39(12):2384–2393.
28. Larsson J, Juliusson B, Holmdahl R, Ehinger B. MHC expression in syngeneic and allogeneic retinal cell transplants in the rat. *Graefes Arch Clin Exp Ophthalmol.* 1999;237(1):82–85.
29. Anosova NG, Illigens B, Boisgérault F, Fedoseyeva EV, Young MJ, Benichou G. Antigenicity and immunogenicity of allogeneic retinal transplants. *J Clin Invest.* 2001;108(8):1175–1183.
30. Crocker PR, Gordon S. Properties and distribution of a lectin-like hemagglutinin differentially expressed by murine stromal tissue macrophages. *J Exp Med.* 1986;164:1862–1875.
31. Crocker PR, Kelm S, Dubois C, et al. Purification and properties of sialoadhesin, a sialic acid-binding receptor of murine tissue macrophages. *EMBO J.* 1991;10(7):1661–1669.
32. Crocker PR, Paulson JC, Varki A. Siglecs and their roles in the immune system. *Nat Rev Immunol.* 2007;7(4):255–266.
33. Crocker PR, Freeman S, Gordon S, Kelm S. Sialoadhesin binds preferentially to cells of the granulocytic lineage. *J Clin Invest.* 1995;95(2):635–643.
34. Jiang HR, Lumsden L, Forrester JV. Macrophages and dendritic cells in IRBP-induced experimental autoimmune uveoretinitis in B10RIII mice. *Invest Ophthalmol Vis Sci.* 1999;40(13):3177–3185.
35. Jiang HR, Hwenda L, Makinen K, Oetke C, Crocker PR, Forrester JV. Sialoadhesin promotes the inflammatory response in experimental autoimmune uveoretinitis. *J Immunol.* 2006;177(4):2258–2264.
36. Hughes EH, Schlichtenbrede FC, Murphy CC, et al. Generation of activated sialoadhesin-positive microglia during retinal degeneration. *Invest Ophthalmol Vis Sci.* 2003;44(5):2229–2234.
37. Farber DB, Lolley RN. Enzymic basis for cyclic GMP accumulation in degenerative photoreceptor cells of mouse retina. *J Cyclic Nucleotide Res.* 1976;2(3):139–148.
38. Bowes C, Li T, Danciger M, Baxter LC, Applebury ML, Farber DB. Retinal degeneration in the rd mouse is caused by a defect in the beta subunit of rod cGMP-phosphodiesterase. *Nature.* 1990;347:677–680.
39. Zhang Y, Kardaszewska AK, van Veen T, Rauch U, Perez MT. Integration between abutting retinas: role of glial structures and associated molecules at the interface. *Invest Ophthalmol Vis Sci.* 2004;45(12):4440–4449.
40. Zhang Y, Klassen HJ, Tucker BA, Perez MT, Young MJ. CNS progenitor cells promote a permissive environment for neurite outgrowth via a matrix metalloproteinase-2-dependent mechanism. *J Neurosci.* 2007;27(17):4499–4506.
41. Crocker PR, Gordon S. Mouse macrophage hemagglutinin (sheep erythrocyte receptor) with specificity for sialylated glycoconjugates characterized by a monoclonal antibody. *J Exp Med.* 1989;169(4):1333–1346.
42. Oetke C, Kraal G, Crocker PR. The antigen recognized by MOMA-I is sialoadhesin. *Immunol Lett.* 2006;106(1):96–98.
43. Thanos S. Sick photoreceptors attract activated microglia from the ganglion cell layer: a model to study the inflammatory cascades in rats with inherited retinal dystrophy. *Brain Res.* 1992;588(1):21–28.
44. Thanos S, Richter W. The migratory potential of vitally labelled microglial cells within the retina of rats with hereditary photoreceptor dystrophy. *Int J Dev Neurosci.* 1993;11(5):671–680.
45. Ng TF, Streilein JW. Light-induced migration of retinal microglia into the subretinal space. *Invest Ophthalmol Vis Sci.* 2001;42(13):3301–3310.
46. Hughes EH, Schlichtenbrede FC, Murphy CC, et al. Minocycline delays photoreceptor death in the rds mouse through a microglia independent mechanism. *Exp Eye Res.* 2004;78(6):1077–1084.
47. Zeiss CJ, Johnson EA. Proliferation of microglia, but not photoreceptors, in the outer nuclear layer of the rd-1 mouse. *Invest Ophthalmol Vis Sci.* 2004;45(3):971–976.
48. Zeng HY, Zhu XA, Zhang C, Yang LP, Wu LM, Tso MO. Identification of sequential events and factors associated with microglial activation, migration, and cytotoxicity in retinal degeneration in rd mice. *Invest Ophthalmol Vis Sci.* 2005;46(8):2992–2999.
49. Yang LP, Zhu XA, Tso MO. A possible mechanism of microglia-photoreceptor crosstalk. *Mol Vis.* 2007;13:2048–2057.
50. Yang LP, Li Y, Zhu XA, Tso MO. Minocycline delayed photoreceptor death in rds mice through iNOS-dependent mechanism. *Mol Vis.* 2007;13:1073–1082.
51. Perry VH, Crocker PR, Gordon S. The blood-brain barrier regulates the expression of a macrophage sialic acid-binding receptor on microglia. *J Cell Sci.* 1992;101:201–207.
52. Xu H, Chen M, Mayer EJ, Forrester JV, Dick AD. Turnover of resident retinal microglia in the normal adult mouse. *Glia.* 2007;55(11):1189–1198.
53. Blanks JC, Johnson LV. Vascular atrophy in the retinal degenerative rd mouse. *J Comp Neurol.* 1986;254(4):543–553.
54. Fitzgerald ME, Slapnick SM, Caldwell RB. Alterations in lectin binding accompany increased permeability in the dystrophic rat model for proliferative retinopathy. *Prog Clin Biol Res.* 1989;314:409–425.
55. Vinores SA, Küchle M, Derevjanik NL, et al. Blood-retinal barrier breakdown in retinitis pigmentosa: light and electron microscopic immunolocalization. *Histol Histopathol.* 1995;10(4):913–923.
56. Zhang Y, Rauch U, Perez MT. Accumulation of neurocan, a brain chondroitin sulfate proteoglycan, in association with the retinal vasculature in RCS rats. *Invest Ophthalmol Vis Sci.* 2003;44(3):1252–1261.
57. Hackam AS, Strom R, Liu D, et al. Identification of gene expression changes associated with the progression of retinal degeneration in the rd1 mouse. *Invest Ophthalmol Vis Sci.* 2004;45(9):2929–2942.
58. Rohrer B, Pinto FR, Hulse KE, Lohr HR, Zhang L, Almeida JS. Multidestructive pathways triggered in photoreceptor cell death of the rd mouse as determined through gene expression profiling. *J Biol Chem.* 2004;279(40):41903–41910.

59. Nicchia GP, Nico B, Camassa LM, et al. The role of aquaporin-4 in the blood-brain barrier development and integrity: studies in animal and cell culture models. *Neuroscience.* 2004;129(4):935–945.
60. McMenamin PG. Dendritic cells and macrophages in the uveal tract of the normal mouse eye. *Br J Ophthalmol.* 1999;83(5):598–604.
61. Chinnery HR, Ruitenberg MJ, Plant GW, Pearlman E, Jung S, McMenamin PG. The chemokine receptor CX3CR1 mediates homing of MHC class II-positive cells to the normal mouse corneal epithelium. *Invest Ophthalmol Vis Sci.* 2007;48(4):1568–1574.
62. Lazarus HS, Hageman GS. In situ characterization of the human hyalocyte. *Arch Ophthalmol.* 1994;112(10):1356–1362.
63. Qiao H, Hisatomi T, Sonoda KH, et al. The characterisation of hyalocytes: the origin, phenotype, and turnover. *Br J Ophthalmol.* 2005;89(4):513–517.
64. Zhang Y, Arnér K, Ehinger B, Perez MT. Limitation of anatomical integration between subretinal transplants and the host retina. *Invest Ophthalmol Vis Sci.* 2003;44(1):324–331.
65. Jiang LQ, Jorquera M, Streilein JW. Subretinal space and vitreous cavity as immunologically privileged sites for retinal allografts. *Invest Ophthalmol Vis Sci.* 1993;34(12):3347–3354.
66. Lund RD, Ono SJ, Keegan DJ, Lawrence JM. Retinal transplantation: progress and problems in clinical application. *J Leukoc Biol.* 2003;74(2):151–160.
67. Al-Amro S, Tang L, Kaplan HJ. Limitations in the study of immune privilege in the subretinal space of the rodent. *Invest Ophthalmol Vis Sci.* 1999;40(12):3067–3069.
68. Lewis GP, Sethi CS, Carter KM, Charteris DG, Fisher SK. Microglial cell activation following retinal detachment: a comparison between species. *Mol Vis.* 2005;11:491–500.
69. Sharma RK, Bergström A, Zucker CL, Adolph AR, Ehinger B. Survival of long-term retinal cell transplants. *Acta Ophthalmol Scand.* 2000;78(4):396–402.
70. Gouras P, Tanabe T. Survival and integration of neural retinal transplants in rd mice. *Graefes Arch Clin Exp Ophthalmol.* 2003;241(5):403–409.
71. Streilein JW, Ma N, Wenkel H, Ng TF, Zamiri P. Immunobiology and privilege of neuronal retina and pigment epithelium transplants. *Vision Res.* 2002;42(4):487–495.
72. Xu H, Dawson R, Forrester JV, Liversidge J. Identification of novel dendritic cell populations in normal mouse retina. *Invest Ophthalmol Vis Sci.* 2007;48(4):1701–1710.
73. Santos AM, Calvente R, Tassi M, et al. Embryonic and postnatal development of microglial cells in the mouse retina. *J Comp Neurol.* 2008;506(2):224–239.
74. Oishi A, Nagai T, Mandai M, Takahashi M, Yoshimura N. The effect of dendritic cells on the retinal cell transplantation. *Biochem Biophys Res Commun.* 2007;363(2):292–296.
75. Rohrer B, Demos C, Frigg R, Grimm C. Classical complement activation and acquired immune response pathways are not essential for retinal degeneration in the rd1 mouse. *Exp Eye Res.* 2007;84(1):82–91.

5. General discussion and future perspectives

When I look at a staining of glial cells, I do not (in the first instance) think about, how important they are, or even only how interesting all their functions may be, but I find them amazingly beautiful. A beauty that many people will never be able to appreciate (again). Blinding diseases can be devastating, as vision is probably the most important sense for people, and it is very difficult to lead an autonomous life without it.

Despite all the knowledge about the genetic backgrounds and disease mechanisms, there is until today no adequate treatment of retinal degenerations available. The large heterogeneity challenges the otherwise promising approaches of gene therapy immensely. And since different complementary pathways of cell death have been found (for example, once caspase-driven apoptosis is blocked, necroptosis pathways are initiated; Sato et al., 2013), it has become clear that anti-apoptotic and neuroprotective treatments will not reach the goal either, unless probably in multiple combinations.

The major focus of research lies on the dying neurons. This might be understandable, but it is important to be aware of secondary reactive changes in neighboring cells and to find out more about their effects on normal physiology, disease progression and treatment outcome. In chapter 4.1, it was shown that even in the non-reactive state, the intermediate filament proteins GFAP and vimentin play an important role in normal physiology. Some of the features disclosed in $GFAP^{-/-}Vim^{-/-}$ mice, such as mislocalized potassium channels along Müller cells or down-regulated proteins involved in glutamate homeostasis, are known from immature as well as gliotic Müller cells (reviewed in Bringmann 2006, 2009), so the outcome of these two stages is probably rather similar: impaired neuronal functionality. The up-regulation of GFAP and vimentin during retinal pathology has generally been regarded as negative, not at least by inhibiting neuronal regeneration through glial scars. Neuronal survival and regeneration was shown to be much higher in $GFAP^{-/-}Vim^{-/-}$ than in wildtype mice, e.g., after retinal detachment (Nakazawa et al., 2007). In chapter 4.2, we could not find any beneficial (nor negative) effect of GFAP and vimentin deficiency on the inherited retinal degeneration in the *rd1* mouse. The actions of GFAP and vimentin might differ between different models, possibly reacting differently to chronic insults than to acute damage.

Müller cells are also known to exhibit neuroprotective functions. Once activated, they secrete numerous growth factors, neurotrophic factors and cytokines (reviewed in Bringmann et al., 2009). One potential neuroprotective protein that is upregulated during glial reactivity is metallothionein. Leung et al. (2009) observed that metallothionein that was exogenously applied induced GFAP up-regulation as well as other typical gliotic changes in cultured

astrocytes. Yet, the metallothionein-induced gliosis was permissive to neurite outgrowth and pro-regenerative. These positive actions were regulated via JAK/STAT and Rho signaling pathways rather than via the classical, growth-inhibiting MAPK signaling pathway.

It seems thus, that reactive gliosis has two faces one needs to be aware of. In future therapeutic attempts, blocking or initiating certain glial reactions, such as up-regulation of intermediate filament proteins, is probably not desirable but instead modulating molecules like metallothioneins.

Sometimes, secondary reactive changes might not even be part of the disease process, but be triggered by treatment approaches themselves. Sialoadhesin expression in retinal microglia following transplantation could be such a case. In chapter 4.4, no sialoadhesin expression was observed at any time during retinal degeneration. But after transplantation of neonatal cells, the macrophage-restricted cell-adhesion molecule was expressed by microglia/macrophages in the retina. The occurrence of such cells could be of significance for the integration and long-term survival of retinal grafts in the otherwise immune-privileged retina, as sialoadhesin is known to participate in the recognition and discrimination of pathogens versus 'self' (reviewed in Klaas and Crocker, 2012), and to influence T-cell behavior in a pro-inflammatory manner (Wu et al., 2009).

The studies of the present thesis revealed differential functions and secondary effects of glial cells in retinal degeneration itself and after treatment approaches. Therefore, the better understanding of glial physiology might not only be valuable for putative treatments, but also for improvement of diagnostics and their interpretations (e.g. of ERG). Most importantly, it will lead to a broader knowledge of the interconnections between different cells that make up one functional tissue.

6. Summary

The retina is highly specialized and, due to its unique physiology, at the same time a very vulnerable neural tissue. Numerous mutations are known today that lead to photoreceptor degeneration, and the exact mechanisms causing cell death are still not completely understood. However, photoreceptor cell death is not a stand-alone event, but triggers secondary reactive changes in other neurons as well as non-neuronal cells. The key goal of this thesis was to elucidate some of the dynamics of reactive changes and how these affect the progression of photoreceptor cell loss in several models of human retinal degeneration.

Up-regulation of the intermediate filament proteins, glial fibrilary acidic protein (GFAP) and vimentin, in astrocytes and Müller cells is a feature of gliotic stress responses in the retina. The inability to produce these filament proteins has been shown to alter the reactivity of glial cells to numerous insults. For the present study, mice deficient for GFAP and vimentin (*GFAP*$^{-/-}$*Vim*$^{-/-}$ mice) were characterized with regards to their retinal function. The electroretinography measurements (ERG, experiments performed by N. Tanimoto) revealed alterations of the scotopic responses of post-photoreceptor neurons. While immunohistochemical and western blot analysis could show that the number of neurons and glia was comparable, the expression of glutamine synthetase (GS) and inwardly rectifying potassium (Kir) channels was markedly reduced in *GFAP*$^{-/-}$*Vim*$^{-/-}$ and *Vim*$^{-/-}$, but not *GFAP*$^{-/-}$ mice. The Kir4.1 channel was also observed to mislocalize along the Müller cells, which could possibly underlie the electrophysiological phenotype.

Similar results were obtained from *GFAP*$^{-/-}$*Vim*$^{-/-}$ mice on the *rd1* (retinal degeneration 1) background. Levels of GS, Kir2.1, Kir4.1, and the water channel aquaporin 4 were lower in *rd1* mice lacking GFAP and vimentin than in *rd1* mice expressing these proteins. According to immunohistochemical results, no alteration of the cell death progression could be detected although the ERG analysis revealed a small improvement of retinal function.

Müller cells up-regulate also neuroprotective substances upon activation. In chapter 4.3, the spatio-temporal expression changes of the putative neuroprotective metal-binding proteins metallothioneins were evaluated at RNA and protein levels in the *rd1* and the *rds* (retinal degeneration slow) mouse models as well as in the RCS rat. During the course of the disease, the expression of metallothioneins was up-regulated in Müller cells and microglia. With the proximity ligation assay, a putative interaction with the endocytic receptor megalin that mediates the transport of metallothioneins into neurons could be visualized *in situ* in the

inner and outer photoreceptor segments but was lost at later stages of the retinal degeneration.

The *rd1* and *rds* mouse models were also employed to evaluate the microglial reactivity during retinal degeneration. In association with photoreceptor cell death, microglia migrated into the outer nuclear layer and the subretinal space. The macrophage-restricted cell adhesion molecule sialoadhesin, which has been shown to support immunoregulating functions influencing T-cell behavior in a pro-inflammatory manner, had been reported to be present in activated microglia in the *rds* mouse retina. This fact could not be reproduced with the present study, nor were any sialoadhesin-positive cells found in the *rd1* model. However, after intraocular transplantation of neonatal cells to wildtype and *rd1* mice, sialoadhesin-positive cells were observed in association with the graft and in the subretinal space.

These results add to the evidence that retinal glial cells are important both under physiological and pathological conditions.

7. Authors' contributions

Concerning the study titled "**Retinal functional alterations in mice lacking the intermediate filament proteins glial fibrillary acidic protein (GFAP) and vimentin**" by *KA Wunderlich, N Tanimoto, M Pekny, E Zrenner, MW Seeliger, MT Perez* (manuscript 1).
The single contributions of the co-authors are listed below:

- Kirsten A. Wunderlich and Maria-Thereza Perez conceived and designed the study.
- Maria-Thereza Perez and Eberhart Zrenner supervised the study.
- Naoyuki Tanimoto and Mathias W. Seeliger designed the ERG experiments.
- Naoyuki Tanimoto performed the ERG experiments and analyzed the ERG data.
- Kirsten A. Wunderlich performed IHC and WB experiments, and Kirsten A. Wunderlich and Maria-Thereza Perez analyzed the IHC and WB data.
- Kirsten A. Wunderlich, Naoyuki Tanimoto, and Maria-Thereza Perez interpreted the results.
- Milos Pekny, Mathias W. Seeliger, Maria-Thereza Perez contributed reagents/materials/animals/analysis tools.
- Kirsten A. Wunderlich, Naoyuki Tanimoto, Milos Pekny, and Maria-Thereza Perez wrote the paper.
- All authors discussed, revised, and approved the manuscript.

Concerning the study titled "**The inability to produce glial fibrillary acidic protein (GFAP) and vimentin does not protect photoreceptors in a genetic model of degeneration**" by *KA Wunderlich, N Tanimoto, S Azadi, E Zrenner, MW Seeliger, MT Perez* (manuscript 2).
The single contributions of the co-authors are listed below:

- Kirsten A. Wunderlich and Maria-Thereza Perez conceived and designed the study.
- Maria-Thereza Perez and Eberhart Zrenner supervised the study.
- Naoyuki Tanimoto and Mathias W. Seeliger designed the ERG experiments.
- Naoyuki Tanimoto performed the ERG experiments and analyzed the ERG data.
- Seifollah Azadi performed the genotyping.
- Kirsten A. Wunderlich performed IHC and WB experiments, and Kirsten A. Wunderlich and Maria-Thereza Perez analyzed the IHC and WB data.
- Kirsten A. Wunderlich, Naoyuki Tanimoto, and Maria-Thereza Perez interpreted the results.
- Mathias W. Seeliger, Maria-Thereza Perez contributed reagents/materials/animals/ analysis tools.
- Kirsten A. Wunderlich, Naoyuki Tanimoto, and Maria-Thereza Perez wrote the paper.
- All authors discussed, revised, and approved the manuscript.

Concerning the study titled "**Altered expression of metallothionein-I and -II and their receptor megalin in inherited photoreceptor degeneration**" by *KA Wunderlich, T Leveillard, M Penkowa, E Zrenner, and MT Perez* (Invest Ophthalmol Vis Sci. 2010 Sep;51(9):4809-4820). The single contributions of the co-authors are listed below:

- Maria-Thereza Perez conceived and designed the study.
- Maria-Thereza Perez supervised the study.
- Thierry Léveillard performed and analyzed the microarray experiments.
- Kirsten A. Wunderlich performed the q-RT-PCR and TUNEL assays, IHC and WB experiments, and proximity ligation assays.
- Kirsten A. Wunderlich, Thierry Léveillard and Maria-Thereza Perez analyzed the data and interpreted the results.
- Thierry Léveillard, Milena Penkowa and Maria-Thereza Perez contributed reagents/ materials/animals/analysis tools.
- Kirsten A. Wunderlich, Thierry Léveillard, and Maria-Thereza Perez wrote the paper.
- All authors discussed, revised, and approved the manuscript.
- The Association for Research in Vision and Ophthalmology is the copyright holder.

Concerning the study titled "**Sialoadhesin Expression in Intact Degenerating Retinas and Following Transplantation"** by J Sancho-Pelluz, KA Wunderlich, U Rauch, FJ Romero, T van Veen, GA Limb, P Crocker, and MT Perez (Invest Ophthalmol Vis Sci. 2008 Dec;49(12):5602-10). The single contributions of the co-authors are listed below:

- Maria-Thereza Perez conceived and designed the study.
- Maria-Thereza Perez supervised the study.
- Javier Sancho-Pelluz, Kirsten A. Wunderlich, Uwe Rauch, and Maria-Thereza Perez performed and analyzed experiments.
- Javier Sancho-Pelluz, Kirsten A. Wunderlich, Uwe Rauch, and Maria-Thereza Perez analyzed the data and interpreted the results.
- Paul Crocker, Uwe Rauch, and Maria-Thereza Perez contributed reagents/materials/ animals/analysis tools.
- Javier Sancho-Pelluz, Kirsten A. Wunderlich, G. Astrid Limb, Paul Crocker, and Maria-Thereza Perez wrote the paper.
- All authors discussed, revised, and approved the manuscript.
- The Association for Research in Vision and Ophthalmology is the copyright holder.

8. Acknowledgements

Many people have supported and inspired me during my PhD time, both professionally and emotionally, and have helped me to finally finish my studies and publish them in this thesis. I am grateful to all of them and hope they know that. Some of these people I would like to mention here and thereby thank them individually:

My deepest gratitude belongs to **Maithe Perez**; my supervisor, boss, advisor, colleague, chauffeur, mother, sister, friend… . Whatever accomplishment I have received with this book, it was only because of her. I have learned a lot from her and could always rely on her, both in science and personal life. Her honesty, curiosity, passion, and thoroughness will always guide me through my future career. And her warmth, openness, understanding, and tolerance will hopefully lead me when dealing with others. I could fill a whole thesis with happy memories, joyful thoughts and words of thankfulness. But I hope she will, as always, understand me and what I am trying to express here without words.

I want to thank Prof. Dr. **Eberhart Zrenner** for giving me the opportunity to complete this thesis, for his kindness and patience. It motivates me to see that it is possible to combine research and clinic, scientific curiosity and dedication to his patients.

I also would like to thank Prof. Dr. **Bernd Wissinger** for helping out on short notice and reviewing my dissertation. I know it is always time- and energy-consuming, and I appreciate it very much that he agreed to do it anyway.

I want to thank the Graduate School team, specifically **Tina Lampe**, who very professionally, patiently and friendly guided me through the jungle of the necessary rules and regulations, bureaucracy and forms with clear and quick advises.

Likewise, I thank **Thomas Wheeler-Schilling** and his team for all the efforts that everything could go smoothly in our Neurotrain programme. I am thankful that I could be part of this program, which provided the chance for scientific education and professional net-working, but mainly that it gave me the opportunity to get to know a bunch of amazing people, all very special and individual in their own way but at the same time keeping up a fantastic team spirit. I hope, we stay in touch from time to time.

I am very thankful for the financial support from the Marie Curie Early Stage Research training (EST) network Neurotrain, as well as the Tistou & Charlotte Kerstan Foundation.

A great deal of my work would have been impossible without my colleagues in Lund: I thank **Birgitta "Gitt" Klefbohm** for her help with the animals and in the lab; I enjoyed our common work a lot. But most of all, I thank her for her friendship: for laughing with me, when time was fun; for holding me, when I was down; for letting me stay in her home and getting to know a warmhearted artist whom I admire a lot. I thank **Hodan Abdshill** for all her support in the lab and for a wonderful summer in her flat, including cooking and eating the most fantastic Ramadan food. I thank **Katarzyna Said Hilmersson**, the cutting Kat, for all the help and joyful laughter in the lab. I miss that. I thank **Karin Arnér** for her help and advices (and I am still waiting for my elk poo!). I thank **Theo van Veen** for his helpfulness, for his understanding, for his friendliness, for his advices. I thank **Anitha "Nitten" Bruun** for being the soul of the lab and helping with so many things. I thank **Ingela Liljeqvist Soltic** for her usual good sprit that brightened most days. I thank **Francois Paquet-Durand** for pointing out the free position in Lund to me and his hospitality during my first stay for the interview. I

thank **Sten Andréasson** for his steady interest in my work and his kind support, whenever it was needed. I thank **Javier Sancho-Pelluz** for all our joint team work, for **s**itting in an office with me, and for quite some party invitations. I thank **Pietro Farinelli** for his help with my western blots and for sharing his thoughts and experiences. I wish, I could work as orderly, focused and disciplined as he does. I thank **Per Ekström** for his help and advice whenever needed. His polite kindness and calm professionalism could always calm me down and give me confidence. I thank **Satpal Ahuja** for many interesting conversations and his humor and his gently smiling eyes. I thank **José Silva** and **Julianne McCall** for their company, both in the lab and at home, when they would share some nice food with me at 3:00 o'clock at night. I thank **Michael "Micke" Kindler**, **Jeppe Stridh** and **Susanne Geres** and the rest of the animal house team for excellent work and nice chats in the hallway. And I thank every former, temporary and current group member for all their support, advices, laughter etc., even when I do not name everybody. I very much enjoyed my time in Lund, not at least because of all of them.

I also thank the flies and the frogs, especially **Hooi Min** for her friendship and **Shirui** with whom I shared the flat, the food, the sofa, and thoughts and views about people, work and life.

I also thank **Leif Johnson** for being such good company in Lund, Glostrup and inbetween. I very much enjoyed all our talks, be it about work or other themes.

At this place, I would also like to thank the people in Glostrup who have helped me with my projects and spent their lunchtime with me. Especially I'd like to thank **Kenneth Beri Plough** for all his time and effort to introduce me into the work with the light-cycler and for sharing all his knowledge and expertise in the qPCR technique with me.

A big thankyou belongs also to **Marijana Samardzija**, who patiently and extensively has taught me the miracles of work with RNA /qPCR via email, and **Markus Thiersch** for all his time when I was in Zürich and also later by email, as well as everybody in the lab of Christian Grimm for their help and hospitality.

I also thank the lab of Shomi Bhattacharya, especially **Kinga** for her hospitality and **Ciara** for all her efforts to bring genetics a little closer to me, and for being such a cheerful and amazing person. Pity, that we live so far apart.

I want to thank my new lab, the Wolfrum group, especially **Uwe** for his patient understanding and **Kerstin** and **Nasrin** for revising parts of my thesis and their constant encouragement.

I would like to thank all my friends who always showed interest in my life (including the progress of my work) and stood by me during low times. And I still owe a big thanks to **Sabine**; without her I would never have been able to even start my work.

I thank **Mario**, my greatest critic, for revising my thesis one last time, but most of all for bearing with me all this time, for being with me, challenging and forming me, and for grounding me in a life outside the lab.

Last but not least, I wish to thank my family for their love and support in so many ways, which gave me the freedom and security to take the chances that life has offered me.

Thank you! Danke! Tack så mycket!

9. References

Ahuja, P., Caffé, A.R., Ahuja, S., Ekström, P. and van Veen, T. (2005). Decreased glutathione transferase levels in rd1/rd1 mouse retina: replenishment protects photoreceptors in retinal explants. Neuroscience *131*, 935-943.

Ahuja-Jensen, P., Johnsen-Soriano, S., Ahuja, S., Bosch-Morell, F., Sancho-Tello, M., Romero, F.J., Abrahamson, M. and Veen, T.V. (2007). Low glutathione peroxidase in rd1 mouse retina increases oxidative stress and proteases.. Neuroreport *18*, 797-801.

Al-Amro, S., Tang, L. and Kaplan, H.J. (1999). Limitations in the study of immune privilege in the subretinal space of the rodent. Invest. Ophthalmol. Vis. Sci. *40*, 3067-3069.

Aleman, T.S., Cideciyan, A.V., Volpe, N.J., Stevanin, G., Brice, A. and Jacobson, S.G. (2002). Spinocerebellar ataxia type 7 (SCA7) shows a cone-rod dystrophy phenotype. Exp. Eye Res. *74*, 737-745.

Ambjörn, M., Asmussen, J.W., Lindstam, M., Gotfryd, K., Jacobsen, C., Kiselyov, V.V., Moestrup, S.K., Penkowa, M., Bock, E. and Berezin, V. (2008). Metallothionein and a peptide modeled after metallothionein, EmtinB, induce neuronal differentiation and survival through binding to receptors of the low-density lipoprotein receptor family.. J. Neurochem. *104*, 21-37.

Antonetti, D.A., Klein, R. and Gardner, T.W. (2012). Diabetic retinopathy. N. Engl. J. Med. *366*, 1227-1239.

Archibald, N.K., Clarke, M.P., Mosimann, U.P. and Burn, D.J. (2009). The retina in Parkinson's disease. Brain *132*, 1128-1145.

Athanasiou, D., Aguilà, M., Bevilacqua, D., Novoselov, S.S., Parfitt, D.A. and Cheetham, M.E. (2013). The cell stress machinery and retinal degeneration. FEBS Lett. *587*, 2008-2017.

Bova, L.M., Wood, A.M., Jamie, J.F. and Truscott, R.J. (1999). UV filter compounds in human lenses: the origin of 4-(2-amino-3-hydroxyphenyl)-4-oxobutanoic acid O-beta-D-glucoside. Invest. Ophthalmol. Vis. Sci. *40*, 3237-3244.

Bowes, C., Li, T., Danciger, M., Baxter, L.C., Applebury, M.L. and Farber, D.B. (1990). Retinal degeneration in the rd mouse is caused by a defect in the beta subunit of rod cGMP-phosphodiesterase.. Nature *347*, 677-680.

Bringmann, A., Pannicke, T., Biedermann, B., Francke, M., Iandiev, I., Grosche, J., Wiedemann, P., Albrecht, J. and Reichenbach, A. (2009). Role of retinal glial cells in neurotransmitter uptake and metabolism. Neurochem. Int. *54*, 143-160.

Bringmann, A., Pannicke, T., Grosche, J., Francke, M., Wiedemann, P., Skatchkov, S.N., Osborne, N.N. and Reichenbach, A. (2006). Müller cells in the healthy and diseased retina. Prog Retin Eye Res *25*, 397-424.

Caicedo, A., Espinosa-Heidmann, D.G., Piña, Y., Hernandez, E.P. and Cousins, S.W. (2005). Blood-derived macrophages infiltrate the retina and activate Muller glial cells under experimental choroidal neovascularization. Exp. Eye Res. *81*, 38-47.

Capetanaki, Y., Smith, S. and Heath, J.P. (1989). Overexpression of the vimentin gene in transgenic mice inhibits normal lens cell differentiation. J. Cell Biol. *109*, 1653-1664.

Caprioli, J. and Varma, R. (2011). Intraocular pressure: modulation as treatment for glaucoma. Am. J. Ophthalmol. *152*, 340-344.e2.

Chang, B., Hawes, N.L., Hurd, R.E., Davisson, M.T., Nusinowitz, S. and Heckenlively, J.R. (2002). Retinal degeneration mutants in the mouse. Vision Res. *42*, 517-525.

Chen, L., Wu, W., Dentchev, T., Wong, R. and Dunaief, J.L. (2004). Increased metallothionein in light damaged mouse retinas.. Exp. Eye Res. *79*, 287-293.

Chen, L., Wu, W., Dentchev, T., Zeng, Y., Wang, J., Tsui, I., Tobias, J.W., Bennett, J., Baldwin, D. and Dunaief, J.L. (2004). Light damage induced changes in mouse retinal gene expression.. Exp. Eye Res. *79*, 239-247.

Chen, L., Yang, P. and Kijlstra, A. (2002). Distribution, markers, and functions of retinal microglia. Ocul. Immunol. Inflamm. *10*, 27-39.

Cheung, N., Mitchell, P. and Wong, T.Y. (2010). Diabetic retinopathy. Lancet *376*, 124-136.

Chiu, K., Chan, T., Wu, A., Leung, I.Y., So, K. and Chang, R.C. (2012). Neurodegeneration of the retina in mouse models of Alzheimer's disease: what can we learn from the retina?. Age (Dordr) *34*, 633-649.

Chung, D.C. and Traboulsi, E.I. (2009). Leber congenital amaurosis: clinical correlations with genotypes, gene therapy trials update, and future directions. J AAPOS *13*, 587-592.

Chung, R.S., Hidalgo, J. and West, A.K. (2008). New insight into the molecular pathways of metallothionein-mediated neuroprotection and regeneration.. J. Neurochem. *104*, 14-20.

Chung, R.S., Penkowa, M., Dittmann, J., King, C.E., Bartlett, C., Asmussen, J.W., Hidalgo, J., Carrasco, J., Leung, Y.K.J., Walker, A.K., et al. (2008). Redefining the role of metallothionein within the injured brain: extracellular metallothioneins play an important role in the astrocyte-neuron response to injury.. J. Biol. Chem. *283*, 15349-15358.

Coleman, H.R., Chan, C., Ferris, F.L.3. and Chew, E.Y. (2008). Age-related macular degeneration. Lancet *372*, 1835-1845.

Colucci-Guyon, E., Giménez Y Ribotta, M., Maurice, T., Babinet, C. and Privat, A. (1999). Cerebellar defect and impaired motor coordination in mice lacking vimentin. Glia *25*, 33-43.

Colucci-Guyon, E., Portier, M.M., Dunia, I., Paulin, D., Pournin, S. and Babinet, C. (1994). Mice lacking vimentin develop and reproduce without an obvious phenotype. Cell *79*, 679-694.

Coyle, P., Philcox, J.C., Carey, L.C. and Rofe, A.M. (2002). Metallothionein: the multipurpose protein.. Cell. Mol. Life Sci. *59*, 627-647.

Crocker, P., Hill, M. and Gordon, S. (1988). Regulation of a murine macrophage haemagglutinin (sheep erythrocyte receptor) by a species-restricted serum factor. Immunology *65(4)*, 515-522.

Crocker, P.R. and Gordon, S. (1986). Properties and distribution of a lectin-like hemagglutinin differentially expressed by murine stromal tissue macrophages. J. Exp. Med. *164*, 1862-1875.

Crocker, P.R., Freeman, S., Gordon, S. and Kelm, S. (1995). Sialoadhesin binds preferentially to cells of the granulocytic lineage. J. Clin. Invest. *95*, 635-643.

D'Cruz, P.M., Yasumura, D., Weir, J., Matthes, M.T., Abderrahim, H., LaVail, M.M. and Vollrath, D. (2000). Mutation of the receptor tyrosine kinase gene Mertk in the retinal dystrophic RCS rat.. Hum. Mol. Genet. *9*, 645-651.

D'Orazio, T.J. and Niederkorn, J.Y. (1998). A novel role for TGF-beta and IL-10 in the induction of immune privilege. J. Immunol. *160*, 2089-2098.

Delyfer, M., Léveillard, T., Mohand-Saïd, S., Hicks, D., Picaud, S. and Sahel, J. (2004). Inherited retinal degenerations: therapeutic prospects. Biol. Cell *96*, 261-269.

Detrick, B. and Hooks, J.J. (2010). Immune regulation in the retina. Immunol. Res. *47*, 153-161.

Dizhoor, A.M., Ray, S., Kumar, S., Niemi, G., Spencer, M., Brolley, D., Walsh, K.A., Philipov, P.P., Hurley, J.B. and Stryer, L. (1991). Recoverin: a calcium sensitive activator of retinal rod guanylate cyclase. Science *251*, 915-918.

Doonan, F., Donovan, M. and Cotter, T.G. (2003). Caspase-independent photoreceptor apoptosis in mouse models of retinal degeneration. J. Neurosci. *23*, 5723-5731.

Ekström, P., Sanyal, S., Narfström, K., Chader, G.J. and van Veen, T. (1988). Accumulation of glial fibrillary acidic protein in Müller radial glia during retinal degeneration. Invest. Ophthalmol. Vis. Sci. *29*, 1363-1371.

Eliasson, C., Sahlgren, C., Berthold, C.H., Stakeberg, J., Celis, J.E., Betsholtz, C., Eriksson, J.E. and Pekny, M. (1999). Intermediate filament protein partnership in astrocytes. J. Biol. Chem. *274*, 23996-24006.

Eng, L.F., Lee, Y.L., Kwan, H., Brenner, M. and Messing, A. (1998). Astrocytes cultured from transgenic mice carrying the added human glial fibrillary acidic protein gene contain Rosenthal fibers. J. Neurosci. Res. *53*, 353-360.

Estrada-Cuzcano, A., Roepman, R., Cremers, F.P.M., den Hollander, A.I. and Mans, D.A. (2012). Non-syndromic retinal ciliopathies: translating gene discovery into therapy. Hum. Mol. Genet. *21*, R111-24.

Faktorovich, E.G., Steinberg, R.H., Yasumura, D., Matthes, M.T. and LaVail, M.M. (1990). Photoreceptor degeneration in inherited retinal dystrophy delayed by basic fibroblast growth factor. Nature *347*, 83-86.

Fitzgerald, M., Nairn, P., Bartlett, C.A., Chung, R.S., West, A.K. and Beazley, L.D. (2007). Metallothionein-IIA promotes neurite growth via the megalin receptor.. Exp Brain Res *183*, 171-180.

Fletcher, E., Jobling, A., Vessey, K., Luu, C., Guymer, R. and Baird, P. (2011). Progress in molecular biology and translational science. Volume 100. Animal models of retinal disease., Vol , edn (Elsevir Inc.).

Franze, K., Grosche, J., Skatchkov, S.N., Schinkinger, S., Foja, C., Schild, D., Uckermann, O., Travis, K., Reichenbach, A. and Guck, J. (2007). Muller cells are living optical fibers in the vertebrate retina. Proc. Natl. Acad. Sci. U.S.A. *104*, 8287-8292.

Frishman, L. (2006). Origins of the electroretinogram, In Principles and practice of clinical electrophysiology of vision, 2nd edn., J. Heckenlively and G. Arden, ed. (Massachusetts: The MIT press.), pp. 139-183.

Gal, A., Li, Y., Thompson, D.A., Weir, J., Orth, U., Jacobson, S.G., Apfelstedt-Sylla, E. and Vollrath, D. (2000). Mutations in MERTK, the human orthologue of the RCS rat retinal dystrophy gene, cause retinitis pigmentosa. Nat. Genet. *26*, 270-271.

Galou, M., Gao, J., Humbert, J., Mericskay, M., Li, Z., Paulin, D. and Vicart, P. (1997). The importance of intermediate filaments in the adaptation of tissues to mechanical stress: evidence from gene knockout studies. Biol. Cell *89*, 85-97.

Gao, H. and Hollyfield, J.G. (1992). Aging of the human retina. Differential loss of neurons and retinal pigment epithelial cells. Invest. Ophthalmol. Vis. Sci. *33*, 1-17.

Gargini, C., Terzibasi, E., Mazzoni, F. and Strettoi, E. (2007). Retinal organization in the retinal degeneration 10 (rd10) mutant mouse: a morphological and ERG study. J. Comp. Neurol. *500*, 222-238.

Gerhardinger, C., Costa, M.B., Coulombe, M.C., Toth, I., Hoehn, T. and Grosu, P. (2005). Expression of acute-phase response proteins in retinal Müller cells in diabetes. Invest. Ophthalmol. Vis. Sci. *46*, 349-357.

Giménez Y Ribotta, M., Langa, F., Menet, V. and Privat, A. (2000). Comparative anatomy of the cerebellar cortex in mice lacking vimentin, GFAP, and both vimentin and GFAP. Glia *31*, 69-83.

Gomi, H., Yokoyama, T., Fujimoto, K., Ikeda, T., Katoh, A., Itoh, T. and Itohara, S. (1995). Mice devoid of the glial fibrillary acidic protein develop normally and are susceptible to scrapie prions. Neuron *14*, 29-41.

Gouras, P. and Ekesten, B. (2004). Why do mice have ultra-violet vision?. Exp. Eye Res. *79*, 887-892.

Grasl-Kraupp, B., Ruttkay-Nedecky, B., Koudelka, H., Bukowska, K., Bursch, W. and Schulte-Hermann, R. (1995). In situ detection of fragmented DNA (TUNEL assay) fails to discriminate among apoptosis, necrosis, and autolytic cell death: a cautionary note. Hepatology *21*, 1465-1468.

Guo, L., Duggan, J. and Cordeiro, M.F. (2010). Alzheimer's disease and retinal neurodegeneration. Curr Alzheimer Res *7*, 3-14.

Hageman, G.S., Anderson, D.H., Johnson, L.V., Hancox, L.S., Taiber, A.J., Hardisty, L.I., Hageman, J.L., Stockman, H.A., Borchardt, J.D., Gehrs, K.M., et al. (2005). A common haplotype in the complement regulatory gene factor H (HF1/CFH) predisposes individuals to age-related macular degeneration. Proc. Natl. Acad. Sci. U.S.A. *102*, 7227-7232.

Haines, J.L., Hauser, M.A., Schmidt, S., Scott, W.K., Olson, L.M., Gallins, P., Spencer, K.L., Kwan, S.Y., Noureddine, M., Gilbert, J.R., et al. (2005). Complement factor H variant increases the risk of age-related macular degeneration. Science *308*, 419-421.

Hamel, C. (2006). Retinitis pigmentosa.. Orphanet J Rare Dis *1*, 40.

Hamel, C.P. (2007). Cone rod dystrophies. Orphanet J Rare Dis *2*, 7.

Haq, F., Mahoney, M. and Koropatnick, J. (2003). Signaling events for metallothionein induction.. Mutat. Res. *533*, 211-226.

Hartong, D.T., Berson, E.L. and Dryja, T.P. (2006). Retinitis pigmentosa.. Lancet *368*, 1795-1809.

Hartveit, E. and Veruki, M.L. (2012). Electrical synapses between AII amacrine cells in the retina: Function and modulation. Brain Res. *1487*, 160-172.

Hattar, S., Liao, H.W., Takao, M., Berson, D.M. and Yau, K.W. (2002). Melanopsin-containing retinal ganglion cells: architecture, projections, and intrinsic photosensitivity. Science *295*, 1065-1070.

Haverkamp, S. and Wässle, H. (2000). Immunocytochemical analysis of the mouse retina. J. Comp. Neurol. *424*, 1-23.

Haynes, C.M., Titus, E.A. and Cooper, A.A. (2004). Degradation of misfolded proteins prevents ER-derived oxidative stress and cell death. Mol. Cell *15*, 767-776.

Helmlinger, D., Yvert, G., Picaud, S., Merienne, K., Sahel, J., Mandel, J. and Devys, D. (2002). Progressive retinal degeneration and dysfunction in R6 Huntington's disease mice. Hum. Mol. Genet. *11*, 3351-3359.

Heng, L.Z., Comyn, O., Peto, T., Tadros, C., Ng, E., Sivaprasad, S. and Hykin, P.G. (2013). Diabetic retinopathy: pathogenesis, clinical grading, management and future developments. Diabet. Med. *30*, 640-650.

Henriksson, J.T., Bergmanson, J.P.G. and Walsh, J.E. (2010). Ultraviolet radiation transmittance of the mouse eye and its individual media components. Exp. Eye Res. *90*, 382-387.

Hewitt, A.T., Lindsey, J.D., Carbott, D. and Adler, R. (1990). Photoreceptor survival-promoting activity in interphotoreceptor matrix preparations: characterization and partial purification. Exp. Eye Res. *50*, 79-88.

Hicks, D. and Barnstable, C.J. (1987). Different rhodopsin monoclonal antibodies reveal different binding patterns on developing and adult rat retina. J. Histochem. Cytochem. *35*, 1317-1328.

Hicks, D. and Molday, R.S. (1986). Differential immunogold-dextran labeling of bovine and frog rod and cone cells using monoclonal antibodies against bovine rhodopsin. Exp. Eye Res. *42*, 55-71.

Hiscott, P., Sheridan, C., Magee, R.M. and Grierson, I. (1999). Matrix and the retinal pigment epithelium in proliferative retinal disease. Prog Retin Eye Res *18*, 167-190.

Honke, N., Shaabani, N., Cadeddu, G., Sorg, U.R., Zhang, D., Trilling, M., Klingel, K., Sauter, M., Kandolf, R., Gailus, N., et al. (2012). Enforced viral replication activates adaptive immunity and is essential for the control of a cytopathic virus. Nat. Immunol. *13*, 51-57.

Hughes, E.H., Schlichtenbrede, F.C., Murphy, C.C., Sarra, G., Luthert, P.J., Ali, R.R. and Dick, A.D. (2003). Generation of activated sialoadhesin-positive microglia during retinal degeneration. Invest. Ophthalmol. Vis. Sci. *44*, 2229-2234.

Hugosson, T., Gränse, L., Ponjavic, V. and Andréasson, S. (2009). Macular dysfunction and morphology in spinocerebellar ataxia type 7 (SCA 7). Ophthalmic Genet. *30*, 1-6.

Ito, M. and Yoshioka, M. (1999). Regression of the hyaloid vessels and pupillary membrane of the mouse. Anat. Embryol. *200*, 403-411.

Jackson, G.R. and Barber, A.J. (2010). Visual dysfunction associated with diabetic retinopathy. Curr. Diab. Rep. *10*, 380-384.

Jacobs, G.H., Neitz, J. and Deegan, J.F. (1991). Retinal receptors in rodents maximally sensitive to ultraviolet light. Nature. 353, 655-656

Jacobs, G.H., Williams, G.A. and Fenwick, J.A. (2004). Influence of cone pigment coexpression on spectral sensitivity and color vision in the mouse. Vision Res. *44*, 1615-1622.

Jeon, C.J., Strettoi, E. and Masland, R.H. (1998). The major cell populations of the mouse retina. J. Neurosci. *18*, 8936-8946.

Jiang, H., Hwenda, L., Makinen, K., Oetke, C., Crocker, P.R. and Forrester, J.V. (2006). Sialoadhesin promotes the inflammatory response in experimental autoimmune uveoretinitis. J. Immunol. *177*, 2258-2264.

Jiang, H.R., Lumsden, L. and Forrester, J.V. (1999). Macrophages and dendritic cells in IRBP-induced experimental autoimmune uveoretinitis in B10RIII mice. Invest. Ophthalmol. Vis. Sci. *40*, 3177-3185.

Jiang, L.Q., Jorquera, M. and Streilein, J.W. (1993). Subretinal space and vitreous cavity as immunologically privileged sites for retinal allografts. Invest. Ophthalmol. Vis. Sci. *34*, 3347-3354.

Jing, G., Wang, J.J. and Zhang, S.X. (2012). ER stress and apoptosis: a new mechanism for retinal cell death. Exp Diabetes Res *2012*, 589589.

Johnson, L.E., Larsen, M. and Perez, M. (2013). Retinal adaptation to changing glycemic levels in a rat model of type 2 diabetes. PLoS ONE *8*, e55456.

Joussen, A.M. and Bornfeld, N. (2009). The treatment of wet age-related macular degeneration. Dtsch Arztebl Int *106*, 312-317.

Joussen, A.M., Poulaki, V., Le, M.L., Koizumi, K., Esser, C., Janicki, H., Schraermeyer, U., Kociok, N., Fauser, S., Kirchhof, B., et al. (2004). A central role for inflammation in the pathogenesis of diabetic retinopathy. FASEB J. *18*, 1450-1452.

Karlstetter, M., Ebert, S. and Langmann, T. (2010). Microglia in the healthy and degenerating retina: insights from novel mouse models. Immunobiology *215*, 685-691.

Katta, S., Kaur, I. and Chakrabarti, S. (2009). The molecular genetic basis of age-related macular degeneration: an overview. J. Genet. *88*, 425-449.

Klaas, M. and Crocker, P.R. (2012). Sialoadhesin in recognition of self and non-self. Semin Immunopathol *34*, 353-364.

Klein, R., Peto, T., Bird, A. and Vannewkirk, M.R. (2004). The epidemiology of age-related macular degeneration. Am. J. Ophthalmol. *137*, 486-495.

Kofuji, P., Biedermann, B., Siddharthan, V., Raap, M., Iandiev, I., Milenkovic, I., Thomzig, A., Veh, R.W., Bringmann, A. and Reichenbach, A. (2002). Kir potassium channel subunit expression in retinal glial cells: implications for spatial potassium buffering. Glia *39*, 292-303.

Kofuji, P., Ceelen, P., Zahs, K.R., Surbeck, L.W., Lester, H.A. and Newman, E.A. (2000). Genetic inactivation of an inwardly rectifying potassium channel (Kir4.1 subunit) in mice: phenotypic impact in retina. J. Neurosci. *20*, 5733-5740.

Kolb, H., Nelson, R., Ahnelt, P. and Cuenca, N. (2001). Cellular organization of the vertebrate retina. Prog. Brain Res. *131*, 3-26.

Kollias, A.N. and Ulbig, M.W. (2010). Diabetic retinopathy: Early diagnosis and effective treatment. Dtsch Arztebl Int *107*, 75-83; quiz 84.

Komeima, K., Rogers, B.S., Lu, L. and Campochiaro, P.A. (2006). Antioxidants reduce cone cell death in a model of retinitis pigmentosa.. Proc. Natl. Acad. Sci. U.S.A. *103*, 11300-11305.

Kur, J., Newman, E.A. and Chan-Ling, T. (2012). Cellular and physiological mechanisms underlying blood flow regulation in the retina and choroid in health and disease. Prog Retin Eye Res *31*, 377-406.

Langmann, T. (2007). Microglia activation in retinal degeneration.. J. Leukoc. Biol. *81*, 1345-1351.

Lei, B. and Perlman, I. (1999). The contributions of voltage- and time-dependent potassium conductances to the electroretinogram in rabbits. Vis. Neurosci. *16*, 743-754.

Leist, M. and Jäättelä, M. (2001). Four deaths and a funeral: from caspases to alternative mechanisms. Nat. Rev. Mol. Cell Biol. *2*, 589-598.

Leung, J.Y.K., Bennett, W.R., Herbert, R.P., West, A.K., Lee, P.R., Wake, H., Fields, R.D., Chuah, M.I. and Chung, R.S. (2012). Metallothionein promotes regenerative axonal sprouting of dorsal root ganglion neurons after physical axotomy. Cell. Mol. Life Sci. *69*, 809-817.

Lewis, S.A., Balcarek, J.M., Krek, V., Shelanski, M. and Cowan, N.J. (1984). Sequence of a cDNA clone encoding mouse glial fibrillary acidic protein: structural conservation of intermediate filaments. Proc. Natl. Acad. Sci. U.S.A. *81*, 2743-2746.

Li, R., Maminishkis, A., Wang, F.E. and Miller, S.S. (2007). PDGF-C and -D induced proliferation/migration of human RPE is abolished by inflammatory cytokines. Invest. Ophthalmol. Vis. Sci. *48*, 5722-5732.

Liedtke, W., Edelmann, W., Bieri, P.L., Chiu, F.C., Cowan, N.J., Kucherlapati, R. and Raine, C.S. (1996). GFAP is necessary for the integrity of CNS white matter architecture and long-term maintenance of myelination. Neuron *17*, 607-615.

Lohr, H.R., Kuntchithapautham, K., Sharma, A.K. and Rohrer, B. (2006). Multiple, parallel cellular suicide mechanisms participate in photoreceptor cell death. Exp. Eye Res. *83*, 380-389.

Lu, H., Hunt, D.M., Ganti, R., Davis, A., Dutt, K., Alam, J. and Hunt, R.C. (2002). Metallothionein protects retinal pigment epithelial cells against apoptosis and oxidative stress.. Exp. Eye Res. *74*, 83-92.

Lund, R.D., Ono, S.J., Keegan, D.J. and Lawrence, J.M. (2003). Retinal transplantation: progress and problems in clinical application. J. Leukoc. Biol. *74*, 151-160.

Lynes, M.A., Zaffuto, K., Unfricht, D.W., Marusov, G., Samson, J.S. and Yin, X. (2006). The physiological roles of extracellular metallothionein.. Exp. Biol. Med. (Maywood) *231*, 1548-1554.

Lyubarsky, A.L., Falsini, B., Pennesi, M.E., Valentini, P. and Pugh, E.N.J. (1999). UV- and midwave-sensitive cone-driven retinal responses of the mouse: a possible phenotype for coexpression of cone photopigments. J. Neurosci. *19*, 442-455.

Léveillard, T., Mohand-Saïd, S., Lorentz, O., Hicks, D., Fintz, A., Clérin, E., Simonutti, M., Forster, V., Cavusoglu, N., Chalmel, F., et al. (2004). Identification and characterization of rod-derived cone viability factor. Nat. Genet. *36*, 755-759.

Martin, S. and Henry, C. (2013). Distinguishing between apoptosis, necrosis, necroptosis and other cell death modalities.. Methods *1;61(2)*, 87-89.

Martinez-Pomares, L. and Gordon, S. (2012). CD169+ macrophages at the crossroads of antigen presentation. Trends Immunol. *33*, 66-70.

Masland, R.H. (2012). The neuronal organization of the retina. Neuron *76*, 266-280.

Masland, R.H. (2012). The tasks of amacrine cells. Vis. Neurosci. *29*, 3-9.

Matsui, K., Hosoi, N. and Tachibana, M. (1999). Active role of glutamate uptake in the synaptic transmission from retinal nonspiking neurons. J. Neurosci. *19*, 6755-6766.

McCall, M.A., Gregg, R.G., Behringer, R.R., Brenner, M., Delaney, C.L., Galbreath, E.J., Zhang, C.L., Pearce, R.A., Chiu, S.Y. and Messing, A. (1996). Targeted deletion in astrocyte intermediate filament (Gfap) alters neuronal physiology. Proc. Natl. Acad. Sci. U.S.A. *93*, 6361-6366.

McLaughlin, M.E., Ehrhart, T.L., Berson, E.L. and Dryja, T.P. (1995). Mutation spectrum of the gene encoding the beta subunit of rod phosphodiesterase among patients with autosomal recessive retinitis pigmentosa. Proc. Natl. Acad. Sci. U.S.A. *92*, 3249-3253.

Menet, V., Giménez y Ribotta, M., Chauvet, N., Drian, M.J., Lannoy, J., Colucci-Guyon, E. and Privat, A. (2001). Inactivation of the glial fibrillary acidic protein gene, but not that of vimentin, improves neuronal survival and neurite growth by modifying adhesion molecule expression. J. Neurosci. *21*, 6147-6158.

Messing, A., Head, M.W., Galles, K., Galbreath, E.J., Goldman, J.E. and Brenner, M. (1998). Fatal encephalopathy with astrocyte inclusions in GFAP transgenic mice. Am. J. Pathol. *152*, 391-398.

Michalik, A., Martin, J. and Van Broeckhoven, C. (2004). Spinocerebellar ataxia type 7 associated with pigmentary retinal dystrophy. Eur. J. Hum. Genet. *12*, 2-15.

Mignot, C., Boespflug-Tanguy, O., Gelot, A., Dautigny, A., Pham-Dinh, D. and Rodriguez, D. (2004). Alexander disease: putative mechanisms of an astrocytic encephalopathy. Cell. Mol. Life Sci. *61*, 369-385.

Milam, A.H., Dacey, D.M. and Dizhoor, A.M. (1993). Recoverin immunoreactivity in mammalian cone bipolar cells. Vis. Neurosci. *10*, 1-12.

Miller, H., Miller, B. and Ryan, S.J. (1986). The role of retinal pigment epithelium in the involution of subretinal neovascularization. Invest. Ophthalmol. Vis. Sci. *27*, 1644-1652.

Murakami, Y., Miller, J.W. and Vavvas, D.G. (2011). RIP kinase-mediated necrosis as an alternative mechanisms of photoreceptor death. Oncotarget *2*, 497-509.

Murakami, Y., Notomi, S., Hisatomi, T., Nakazawa, T., Ishibashi, T., Miller, J.W. and Vavvas, D.G. (2013). Photoreceptor cell death and rescue in retinal detachment and degenerations. Prog Retin Eye Res *37*, 114-140.

Müller, H. (1851). Zur Histologie der Netzhaut.. Z. Wiss. Zool. *3*, 234-237.

Müller, M., Bhattacharya, S.S., Moore, T., Prescott, Q., Wedig, T., Herrmann, H. and Magin, T.M. (2009). Dominant cataract formation in association with a vimentin assembly disrupting mutation. Hum. Mol. Genet. *18*, 1052-1057.

Nakazawa, T., Matsubara, A., Noda, K., Hisatomi, T., She, H., Skondra, D., Miyahara, S., Sobrin, L., Thomas, K.L., Chen, D.F., et al. (2006). Characterization of cytokine responses to retinal detachment in rats. Mol. Vis. *12*, 867-878.

Nakazawa, T., Takeda, M., Lewis, G.P., Cho, K., Jiao, J., Wilhelmsson, U., Fisher, S.K., Pekny, M., Chen, D.F. and Miller, J.W. (2007). Attenuated glial reactions and photoreceptor degeneration after retinal detachment in mice deficient in glial fibrillary acidic protein and vimentin. Invest. Ophthalmol. Vis. Sci. *48*, 2760-2768.

Newman, E. (2009). Retinal glia, In Encyclopedia of Neuroscience, L. Squire, ed. (Oxford Academic Press), pp. 225-232.

Newman, E.A. (1993). Inward-rectifying potassium channels in retinal glial (Müller) cells. J. Neurosci. *13*, 3333-3345.

Newman, E.A. and Zahs, K.R. (1998). Modulation of neuronal activity by glial cells in the retina. J. Neurosci. *18*, 4022-4028.

Nickla, D.L. and Wallman, J. (2010). The multifunctional choroid. Prog Retin Eye Res *29*, 144-168.

Nicolas, M.G., Fujiki, K., Murayama, K., Suzuki, M.T., Shindo, N., Hotta, Y., Iwata, F., Fujimura, T., Yoshikawa, Y., Cho, F., et al. (1996). Studies on the mechanism of early onset macular degeneration in cynomolgus monkeys. II. Suppression of metallothionein synthesis in the retina in oxidative stress.. Exp. Eye Res. *62*, 399-408.

O'Donnell, B.F., Blekher, T.M., Weaver, M., White, K.M., Marshall, J., Beristain, X., Stout, J.C., Gray, J., Wojcieszek, J.M. and Foroud, T.M. (2008). Visual perception in prediagnostic and early stage Huntington's disease. J Int Neuropsychol Soc *14*, 446-453.

Oliver, P.D., Tate, D.J. and Newsome, D.A. (1992). Metallothionein in human retinal pigment epithelial cells: expression, induction and zinc uptake.. Curr. Eye Res. *11*, 183-188.

Paglinawan, R., Malipiero, U., Schlapbach, R., Frei, K., Reith, W. and Fontana, A. (2003). TGFbeta directs gene expression of activated microglia to an anti-inflammatory phenotype strongly focusing on chemokine genes and cell migratory genes. Glia *44*, 219-231.

Paulus, W., Schwarz, G., Werner, A., Lange, H., Bayer, A., Hofschuster, M., Müller, N. and Zrenner, E. (1993). Impairment of retinal increment thresholds in Huntington's disease. Ann. Neurol. *34*, 574-578.

Pekny, M. and Lane, E.B. (2007). Intermediate filaments and stress. Exp. Cell Res. *313*, 2244-2254.

Pekny, M., Johansson, C.B., Eliasson, C., Stakeberg, J., Wallén, A., Perlmann, T., Lendahl, U., Betsholtz, C., Berthold, C.H. and Frisén, J. (1999). Abnormal reaction to central nervous

system injury in mice lacking glial fibrillary acidic protein and vimentin. J. Cell Biol. *145*, 503-514.

Pekny, M., Levéen, P., Pekna, M., Eliasson, C., Berthold, C.H., Westermark, B. and Betsholtz, C. (1995). Mice lacking glial fibrillary acidic protein display astrocytes devoid of intermediate filaments but develop and reproduce normally. EMBO J. *14*, 1590-1598.

Perry, V.H., Crocker, P.R. and Gordon, S. (1992). The blood-brain barrier regulates the expression of a macrophage sialic acid-binding receptor on microglia. J. Cell. Sci. *101 (Pt 1)*, 201-207.

Petrasch-Parwez, E., Saft, C., Schlichting, A., Andrich, J., Napirei, M., Arning, L., Wieczorek, S., Dermietzel, R. and Epplen, J.T. (2005). Is the retina affected in Huntington disease?. Acta Neuropathol *110*, 523-525.

Poitry, S., Poitry-Yamate, C., Ueberfeld, J., MacLeish, P.R. and Tsacopoulos, M. (2000). Mechanisms of glutamate metabolic signaling in retinal glial (Müller) cells. J. Neurosci. *20*, 1809-1821.

Poitry-Yamate, C.L., Poitry, S. and Tsacopoulos, M. (1995). Lactate released by Müller glial cells is metabolized by photoreceptors from mammalian retina. J. Neurosci. *15*, 5179-5191.

Provencio, I., Rodriguez, I.R., Jiang, G., Hayes, W.P., Moreira, E.F. and Rollag, M.D. (2000). A novel human opsin in the inner retina. J. Neurosci. *20*, 600-605.

Przedborski, S., Vila, M. and Jackson-Lewis, V. (2003). Neurodegeneration: what is it and where are we?. J. Clin. Invest. *111*, 3-10.

Quinlan, R.A., Brenner, M., Goldman, J.E. and Messing, A. (2007). GFAP and its role in Alexander disease. Exp. Cell Res. *313*, 2077-2087.

Resnikoff, S., Pascolini, D., Etya'ale, D., Kocur, I., Pararajasegaram, R., Pokharel, G.P. and Mariotti, S.P. (2004). Global data on visual impairment in the year 2002. Bull. World Health Organ. *82*, 844-851.

Rieck, J. (2013). The pathogenesis of glaucoma in the interplay with the immune system. Invest. Ophthalmol. Vis. Sci. *54*, 2393-2409.

Riva, C., Alm, A. and Pournaras, C. (2011). Ocular circulation. In Adler's Physiology of the Eye., Vol , edn (Elsevier Health Sciences,).

Roque, R.S., Imperial, C.J. and Caldwell, R.B. (1996). Microglial cells invade the outer retina as photoreceptors degenerate in Royal College of Surgeons rats. Invest. Ophthalmol. Vis. Sci. *37*, 196-203.

Roque, R.S., Rosales, A.A., Jingjing, L., Agarwal, N. and Al-Ubaidi, M.R. (1999). Retina-derived microglial cells induce photoreceptor cell death in vitro. Brain Res. *836*, 110-119.

Ruether, K., Feigenspan, A., Pirngruber, J., Leitges, M., Baehr, W. and Strauss, O. (2010). PKC{alpha} is essential for the proper activation and termination of rod bipolar cell response. Invest. Ophthalmol. Vis. Sci. *51*, 6051-6058.

Ruttkay-Nedecky, B., Nejdl, L., Gumulec, J., Zitka, O., Masarik, M., Eckschlager, T., Stiborova, M., Adam, V. and Kizek, R. (2013). The role of metallothionein in oxidative stress. Int J Mol Sci *14*, 6044-6066.

Saari, J.C. (2012). Vitamin A metabolism in rod and cone visual cycles. Annu. Rev. Nutr. *32*, 125-145.

Saint-Geniez, M. and D'Amore, P.A. (2004). Development and pathology of the hyaloid, choroidal and retinal vasculature. Int. J. Dev. Biol. *48*, 1045-1058.

Sancho-Pelluz, J., Arango-Gonzalez, B., Kustermann, S., Romero, F.J., van Veen, T., Zrenner, E., Ekström, P. and Paquet-Durand, F. (2008). Photoreceptor cell death mechanisms in inherited retinal degeneration. Mol. Neurobiol. *38*, 253-269.

Sanyal, S. and Jansen, H.G. (1981). Absence of receptor outer segments in the retina of rds mutant mice. Neurosci. Lett. *21*, 23-26.

Sanz, M.M., Johnson, L.E., Ahuja, S., Ekström, P.A.R., Romero, J. and van Veen, T. (2007). Significant photoreceptor rescue by treatment with a combination of antioxidants in an animal model for retinal degeneration. Neuroscience *145*, 1120-1129.

Sato, M., Abe, T. and Tamai, M. (2000). Analysis of the metallothionein gene in age-related macular degeneration. Jpn. J. Ophthalmol. *44*, 115-121.

Schraermeyer, U. and Heimann, K. (1999). Current understanding on the role of retinal pigment epithelium and its pigmentation. Pigment Cell Res. *12*, 219-236.

Schubert, U., Antón, L.C., Gibbs, J., Norbury, C.C., Yewdell, J.W. and Bennink, J.R. (2000). Rapid degradation of a large fraction of newly synthesized proteins by proteasomes. Nature *404*, 770-774.

Shen, J., Yang, X., Dong, A., Petters, R.M., Peng, Y., Wong, F. and Campochiaro, P.A. (2005). Oxidative damage is a potential cause of cone cell death in retinitis pigmentosa. J. Cell. Physiol. *203*, 457-464.

Shi, G., Maminishkis, A., Banzon, T., Jalickee, S., Li, R., Hammer, J. and Miller, S.S. (2008). Control of chemokine gradients by the retinal pigment epithelium. Invest. Ophthalmol. Vis. Sci. *49*, 4620-4630.

Smith, C.U. (2008). Biology of Sensory Systems., Vol , edn (Wiley-Blackwell).

Strauss, O. (2005). The retinal pigment epithelium in visual function. Physiol. Rev. *85*, 845-881.

Strettoi, E., Porciatti, V., Falsini, B., Pignatelli, V. and Rossi, C. (2002). Morphological and functional abnormalities in the inner retina of the rd/rd mouse. J. Neurosci. *22*, 5492-5504.

Suemori, S., Shimazawa, M., Kawase, K., Satoh, M., Nagase, H., Yamamoto, T. and Hara, H. (2006). Metallothionein, an endogenous antioxidant, protects against retinal neuron damage in mice. Invest. Ophthalmol. Vis. Sci. *47*, 3975-3982.

Sun, H. and Nathans, J. (2001). ABCR, the ATP-binding cassette transporter responsible for Stargardt macular dystrophy, is an efficient target of all-trans-retinal-mediated photooxidative damage in vitro. Implications for retinal disease. J. Biol. Chem. *276*, 11766-11774.

Szeverenyi, I., Cassidy, A.J., Chung, C.W., Lee, B.T.K., Common, J.E.A., Ogg, S.C., Chen, H., Sim, S.Y., Goh, W.L.P., Ng, K.W., et al. (2008). The Human Intermediate Filament Database: comprehensive information on a gene family involved in many human diseases. Hum. Mutat. *29*, 351-360.

Thiersch, M., Raffelsberger, W., Frigg, R., Samardzija, M., Wenzel, A., Poch, O. and Grimm, C. (2008). Analysis of the retinal gene expression profile after hypoxic preconditioning identifies candidate genes for neuroprotection. BMC Genomics *9*, 73.

Trifunović, D., Sahaboglu, A., Kaur, J., Mencl, S., Zrenner, E., Ueffing, M., Arango-Gonzalez, B. and Paquet-Durand, F. (2012). Neuroprotective strategies for the treatment of inherited photoreceptor degeneration. Curr. Mol. Med. *12*, 598-612.

Valko, M., Leibfritz, D., Moncol, J., Cronin, M.T.D., Mazur, M. and Telser, J. (2007). Free radicals and antioxidants in normal physiological functions and human disease. Int. J. Biochem. Cell Biol. *39*, 44-84.

Verardo, M.R., Lewis, G.P., Takeda, M., Linberg, K.A., Byun, J., Luna, G., Wilhelmsson, U., Pekny, M., Chen, D. and Fisher, S.K. (2008). Abnormal reactivity of muller cells after retinal detachment in mice deficient in GFAP and vimentin. Invest. Ophthalmol. Vis. Sci. *49*, 3659-3665.

Vázquez-Chona, F., Song, B.K. and Geisert, E.E.J. (2004). Temporal changes in gene expression after injury in the rat retina. Invest. Ophthalmol. Vis. Sci. *45*, 2737-2746.

Wahlin, K.J., Campochiaro, P.A., Zack, D.J. and Adler, R. (2000). Neurotrophic factors cause activation of intracellular signaling pathways in Müller cells and other cells of the inner retina, but not photoreceptors. Invest. Ophthalmol. Vis. Sci. *41*, 927-936.

Wang, J. and Kefalov, V.J. (2009). An alternative pathway mediates the mouse and human cone visual cycle. Curr. Biol. *19*, 1665-1669.

Wang, J. and Kefalov, V.J. (2011). The cone-specific visual cycle. Prog Retin Eye Res *30*, 115-128.

Weidemann, A., Krohne, T.U., Aguilar, E., Kurihara, T., Takeda, N., Dorrell, M.I., Simon, M.C., Haase, V.H., Friedlander, M. and Johnson, R.S. (2010). Astrocyte hypoxic response is essential for pathological but not developmental angiogenesis of the retina. Glia *58*, 1177-1185.

West, A.K., Hidalgo, J., Eddins, D., Levin, E.D. and Aschner, M. (2008). Metallothionein in the central nervous system: Roles in protection, regeneration and cognition. Neurotoxicology *29*, 489-503.

Wilhelmsson, U., Li, L., Pekna, M., Berthold, C., Blom, S., Eliasson, C., Renner, O., Bushong, E., Ellisman, M., Morgan, T.E., et al. (2004). Absence of glial fibrillary acidic

protein and vimentin prevents hypertrophy of astrocytic processes and improves post-traumatic regeneration. J. Neurosci. *24*, 5016-5021.

Wolfrum, U. (2011). Protein networks related to the Usher syndrome gain insights in the molecular basis of the disease. In Usher Syndrome: Pathogenesis, Diagnosis and Therapy, Vol , edn (Nova Science Publishers, Inc).

Wood, L., Theriault, N. and Vogeli, G. (1989). Vimentin cDNA clones covering the complete intermediate-filament protein are found in an EHS tumor cDNA library. Gene *76*, 171-175.

Wormstone, I.M. and Wride, M.A. (2011). The ocular lens: a classic model for development, physiology and disease. Philos. Trans. R. Soc. Lond., B, Biol. Sci. *366*, 1190-1192.

Wright, A.F., Chakarova, C.F., Abd El-Aziz, M.M. and Bhattacharya, S.S. (2010). Photoreceptor degeneration: genetic and mechanistic dissection of a complex trait. Nat. Rev. Genet. *11*, 273-284.

Wu, C., Rauch, U., Korpos, E., Song, J., Loser, K., Crocker, P.R. and Sorokin, L.M. (2009). Sialoadhesin-positive macrophages bind regulatory T cells, negatively controlling their expansion and autoimmune disease progression. J. Immunol. *182*, 6508-6516.

Wu, J., Marmorstein, A.D., Kofuji, P. and Peachey, N.S. (2004). Contribution of Kir4.1 to the mouse electroretinogram. Mol. Vis. *10*, 650-654.

Wunderlich, K.A., Leveillard, T., Penkowa, M., Zrenner, E. and Perez, M. (2010). Altered expression of metallothionein-I and -II and their receptor megalin in inherited photoreceptor degeneration. Invest. Ophthalmol. Vis. Sci. *51*, 4809-4820.

Wässle, H. (2004). Parallel processing in the mammalian retina. Nat. Rev. Neurosci. *5*, 747-757.

Wässle, H. and Boycott, B.B. (1991). Functional architecture of the mammalian retina. Physiol. Rev. *71*, 447-480.

Wässle, H., Grünert, U., Chun, M.H. and Boycott, B.B. (1995). The rod pathway of the macaque monkey retina: identification of AII-amacrine cells with antibodies against calretinin. J. Comp. Neurol. *361*, 537-551.

Zeiss, C.J. and Johnson, E.A. (2004). Proliferation of microglia, but not photoreceptors, in the outer nuclear layer of the rd-1 mouse. Invest. Ophthalmol. Vis. Sci. *45*, 971-976.

van Leeuwen, R., Klaver, C.C.W., Vingerling, J.R., Hofman, A. and de Jong, P.T.V.M. (2003). Epidemiology of age-related maculopathy: a review. Eur. J. Epidemiol. *18*, 845-854.